HIGH FREQUENCY GENETIC VARIATION AND OSMOTIC STRESS SURVIVAL IN THE SUCCESS OF THE HUMAN PATHOGEN *CAMPYLOBACTER JEJUNI*

by

Andrew Cameron

B.Sc., The University of British Columbia, 2009

A THESIS SUBMITTED IN PARTIAL FULFILLMENT OF

THE REQUIREMENTS FOR THE DEGREE OF

DOCTOR OF PHILOSOPHY

in

THE FACULTY OF GRADUATE AND POSTDOCTORAL STUDIES

(Microbiology and Immunology)

THE UNIVERSITY OF BRITISH COLUMBIA

(Vancouver)

August 2015

ABSTRACT

Campylobacter jejuni is the leading bacterial cause of severe infectious diarrhea worldwide, and prior infection with the pathogen is highly correlated with the acute neuromuscular paralysis of Guillain-Barré Syndrome. As a zoonotic bacterium, *C. jejuni* successfully colonizes multiple host animal species harmlessly, survives transmission in the natural environment, and as a widespread food-borne pathogen, causes gastroenteritis in humans. Stress survival mechanisms are important to understand because they enable this success, and may lead to new food safety strategies and interventions to eliminate the harm caused by *C. jejuni*. Here, the global response of *C. jejuni* to hyperosmotic stress—which is encountered in hosts, the environment, and food processing—was characterized by whole-genome transcriptional profiling. This identified important physiological responses to hyperosmotic stress, and in particular, identified the importance of cross-induction of heat shock and oxidative stress response proteins. Single-cell and single-colony comparisons also identified prevalent stress phenotypic heterogeneity within the population. Contributing to the phenotypic variation, high frequency multifarious mutations in two purine biosynthesis genes were identified via whole-genome sequencing of colonial isolates. These mutations differentially affected tolerance to a variety of stresses, and different mutations were important for enhanced intracellular survival in epithelial cells, which is correlated with virulence in humans. This genetic variation in the population also contributed to enhanced biofilm formation, and conferred differential niche-preference behavior to individual mutation-bearing bacteria. Together, these high frequency mutations contributed to novel adaptive properties of *C. jejuni*, and thus a mechanism of success was identified. A hyperosmotic stress-upregulated gene, *cj1533c*, was also recognized as a novel determinant of hyperosmotic and oxidative stress resistance. Preliminary characterizations of *cj1533c* via mutational and proteomic analyses suggested a critical role for Cj1533c, a putative ATPase, in

the coordination of multiple stress-related cellular pathways. Lastly, new genetics tools, fluorescent probes, and proteomics techniques were adapted for used in future *C. jejuni* research. Collectively, a number of unique *C. jejuni* success mechanisms were identified via their importance for hyperosmotic stress tolerance.

PREFACE

All CHAPTERS are based on research designed by Andrew Cameron, Dr. Sarah L. Svensson, Dr. Emilisa Frirdich and Dr. Erin C. Gaynor, with scientific contributions from Dr. Craig T. Parker, Dr. Robert E. W. Hancock, Dr. William W. Mohn and Dr. James W. Kronstad. Unless otherwise stated, experiments were performed by Andrew Cameron in the laboratory of Dr. Erin C. Gaynor, Department of Microbiology and Immunology, UBC, Vancouver, BC. Research was performed under the UBC Research Ethics Board Biosafety Committee Certificate of Approval #B10-0061.

A version of CHAPTER TWO has been published (**Cameron A, Frirdich E, Huynh S, Parker CT, Gaynor EC.** 2012. Hyperosmotic stress response of *Campylobacter jejuni*. J Bacteriol **194:**6116-6130.) (1). DNA microarray whole-genome transcriptional profiling was carried out in the laboratory of Dr. Craig T. Parker at the Agricultural Research Service of the <u>U</u>nited <u>S</u>tates <u>D</u>epartment of <u>A</u>griculture (USDA). The Δ*kpsM* mutant was obtained from the laboratory of Dr. Patricia Guerry, Naval Medical Research Centre, Bethesda, MD.

A version of CHAPTER THREE has been prepared for publication (High frequency genetic variation of purine biosynthesis genes is a mechanism of success in *Campylobacter jejuni*). Samples for whole-genome and amplicon-based sequencing were prepared by Andrew Cameron and sequenced/analyzed in the laboratory of Dr. Craig T. Parker at the Agricultural Research Service of the USDA, Albany, CA. DNA-protein affinity chromatography was performed by Andrew Cameron. The Δ*argH* SILAC arginine auxotroph strain was constructed by Dr. Dmitry Apel, Department of Microbiology and Immunology, UBC, Vancouver, BC. SILAC-based proteomic LC-MS analyses were performed by Dr. Nichollas E. Scott in the laboratory of Dr. Leonard J. Foster, Department of Biochemistry and Molecular Biology, UBC, Vancouver, BC.

A version of CHAPTER FOUR has been prepared for publication (Genetic heterogeneity enhances *Campylobacter jejuni* biofilm formation). Samples for amplicon-based sequencing were prepared by Andrew Cameron and sequenced/analyzed in the laboratory of Dr. Craig T. Parker at the Agricultural Research Service of the USDA, Albany, CA.

Research described in CHAPTER FIVE is ongoing. DNA microarray analyses were performed by Andrew Cameron in the laboratory of Dr. Craig T. Parker at the Agricultural Research Service of the USDA, Albany, CA. Protein expression and protein-protein interaction screening was carried out by Andrew Cameron. SILAC-based proteomics were performed by Dr. Nichollas E. Scott in the laboratory of Dr. Leonard J. Foster, Department of Biochemistry and Molecular Biology, UBC, Vancouver, BC.

A version of CHAPTER SIX has been published (**Cameron A, Gaynor EC.** 2014. Hygromycin B and apramycin antibiotic resistance cassettes for use in *Campylobacter jejuni*. PloS one **9:**e95084.) (2). The pMV261.hyg and p261comp.apra plasmids were obtained from Jan Burian in the laboratory of Dr. Charles Thompson, Department of Microbiology and Immunology, UBC, Vancouver, BC.

TABLE OF CONTENTS

LIST OF TABLES

LIST OF FIGURES

LIST OF ABBREVIATIONS

α	Alpha or anti
β	Beta
γ	Gamma
Δ	Delta or deletion
ε	Epsilon
μ	Micro
σ	Sigma
^{32}P	Phosphorus-32
6XHIS	Hexahistidine tag
81-176	Virulent *C. jejuni*
AAA+	ATPases associated with various cellular activities
AIDS	Acquired immuno-deficiency syndrome
AMP	Adenosine monophosphate
ANOVA	Analysis of variance
apr^R	Apramycin resistant
APS	Adenosine 5'-phosphosulfate
Apt	Adenine phosporibosyltransferase
ArgC	Arginine proteinase
asRNA	antisense RNA
astA	Arylsulfatase
AT	Adenine and thymine
ATP	Adenosine triphosphate
bioID	Proximity-dependent biotin identification
°C	Celsius
C	Molar concentration of solute
cat	Chloramphenicol acetyltransferase
CCD	Charged-couple device
CCV	*Campylobacter*-containing vacuole

cDNA	Complementary DNA
CFU	Colony forming unit
Cm	Chloramphenicol
Cm^R	Chloramphenicol resistant
CpG	Cytosine-guanine dinucleotide
CPS	Capsular polysaccharide
Ct	Threshold cycle
cv	Coefficient of variation
Cy3	Cyanine fluorescent dye
Cy5	Cyanine fluorescent dye
D-ala	D-alanine amino acid
DAPI	4',6-diamino-2-phenylindol
del	Deletion
delins	Deletion-insertion
DIG	Dioxygenin
DMEM	Dulbecco's modified Eagle medium
DNA	Deoxyribonucleic acid
Dps	DNA protection from starvation
DTT	Dithiothreitol
ERK	Extracellular-signal-regulated kinases
FACS	Fluorescence-assisted cell sorting
$FADH_2$	Flavin adenine dinucleotide
Fe-S	Iron-sulfur containing protein
GC	Guanine and cytosine
GFP	Green fluorescent protein
GM1	Monosialotetrahexosylganglioside
GMP	Guanosine monophosphate
GTP	Guanosine triphosphate
Hyg^R	Hygromycin resistant

IMP	Inosine monophosphate
INT407	Intestinal epithelial cells
K^+	Potassium ion
Kan^R	Kanamycin resistant
kDa	Kilo Daltons
Kan	Kanamycin
LC-MS	Liquid chromatography mass spectrometry
LOS	Lipooligosaccharide
Mbp	Mega base-pairs
MH	Mueller-Hinton agar/broth
MIC	Minimum inhibitory concentration
ml	Millilitres
mM	Millimolar
MMR	Mismatch repair
MOPS	3-[N-morpholino]propanesulfonic acid
mRNA	Messenger RNA
NaCl	Sodium chloride
NADH	Nicotinamide adenine dinucleotide
NCBI	National Center for Biotechnology Information
NFκB	Nuclear factor kappa enhancer of activated B cells
Ni-NTA	Nickel-nitrilotriacetic acid
N-linked	Nitrogen-linked (amide of asparagine)
nm	Nanometer
OD	Optical density
O-linked	Oxygen-linked
ORF	Open reading frame
osmol L^{-1}	Osmotic concentration
P	Probability
PAGE	Polyacrylamide gel electrophoresis

PAPS	3'-phosphoadenosine-5'-phosphosulfate
PBS	Phosphate-buffered saline
PCR	Polymerase chain reaction
pH	Hydrogen ion activity
PI	Propidium iodide fluorescent dye
P-loop	Phosphate loop
ppGpp	Guanosine tetraphosphate
pppGpp	Guanosine pentaphosphate
PRPP	5-phospho-α-D-ribose-1-diphosphate
PurF	amidophosphoribosyl transferase
R	antibiotic resistance
RBS	Ribosome binding site (Shine-Dalgarno sequence)
RFP	Red fluorescent protein
RGD	Arg-Gly-Asp tripeptide
RNA	Ribonucleic acid
ROS	Reactive oxygen species
rpm	Revolutions per minute
rRNA	Ribosomal RNA
RT	Room temperature
RT-PCR	Reverse-transcription PCR
RTqPCR	Quantitative reverse-transcription PCR
SDS	Sodium dodecyl sulfate
SEM	Standard error of the mean
SILAC	Stable isotope labeling of amino acids
SNP	Single nucleotide polymorphism
spp.	Species
ssDNA	Single-stranded DNA
sRNA	Small regulatory RNA
SSB	Single-stranded DNA-binding protein

SSM	Slip-strand mispairing
Syto-9	Green fluorescent nucleic acid stain
TAE	Tris-acetate-EDTA buffer
TCA	Tricarboxylic acid cycle
TEG	Triethyleneglycol
TLR	Toll-like receptor
tRNA	Transfer RNA
USDA	United States Department of Agriculture
UV	Ultraviolet
Vanco-FL	Fluorescent vancomycin conjugate
VBNC	Viable-but-non-culturable
w/v	Percentage solution
x g	Acceleration due to gravity
XS	5-bromo-4-chloro-3-indolyl sulfate potassium salt

ACKNOWLEDGEMENTS

I would like to thank my supervisor Dr. Erin C. Gaynor for giving me the opportunity to work on a fascinating microbe in her laboratory. My scientific development has been aided by her encouragement, and her support has given me incredible opportunities for conducting basic research.

I have also been extremely fortunate to receive experimental advice and recommendations from a fantastic Ph.D. committee during my time at UBC. I thank Dr. Robert E. W. Hancock, Dr. William W. Mohn and Dr. James W. Kronstad for their encouragement and support over the years. I would also like to thank Dr. Craig Parker and Steven Huynh at the USDA for their support in conducting multiple experiments.

I have also been fortunate to have great mentors and friends within the Gaynor laboratory, and within the Department of Microbiology and Immunology. I would like to thank the following people, who include graduate students and post-doctoral fellows alike, for their friendship and assistance (in no particular order):

- Dr. Sarah L. Svensson, for thoughtful support and experience.
- Dr. Emilisa Frirdich, for scientific advice, experimental scrutiny, and a great sense of humour.
- Dr. Nichollas E. Scott, for enthusiasm and new ideas.
- Dr. Dmitry Apel, a great microbiologist.
- Dr. Mizue Naito, for introducing me to reality television.
- Dr. Ann E. Lin, for motivational friendship.
- Dr. Jan Burian IV, for scientific advice and home-brewed alcoholic beverages.

DEDICATION

I would like to thank my family for their support and encouragement, and firm commitment to never asking questions about my research.

"You can't *B. cereus*"
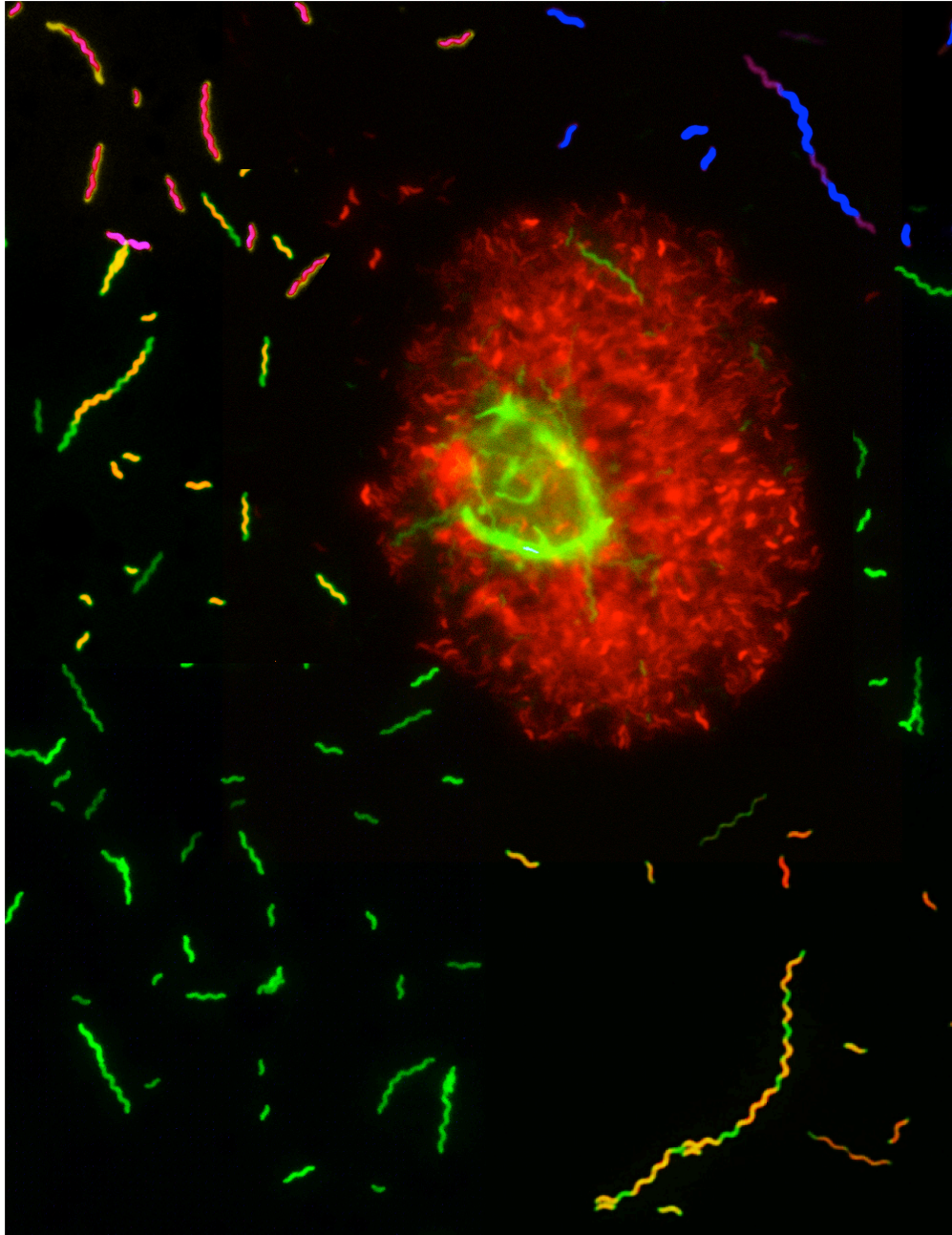
CHAPTER ONE: Introduction

1.1 THE TWISTED HISTORY OF *CAMPYLOBACTER JEJUNI*

1.1.1 Importance as a human diarrheal pathogen

Campylobacter jejuni is a prevalent bacterial pathogen most known as a prominent cause of acute self-limiting gastroenteritis (3, 4). It is a helical, Gram-negative bacillus, and represents a major genus in the ε-proteobacteria, which also includes the related gastric oncopathogen *Helicobacter pylori* (5). As an enteropathogen, *C. jejuni* is responsible for a range of human diseases, including asymptomatic carriage, ferocious gastroenteritis, septicemia, myocarditis, and dermatitis in hosts of differential susceptibility (6-11). However, human infection with *C. jejuni* most often results in inflammatory, sometimes bloody diarrhea, accompanied by vomiting and fever (12). Death by *C. jejuni* is known, but is extremely rare, and most often occurs in infants and the very old, while unusual manifestations occur in individuals with underlying immunodeficiencies, such as AIDS patients or individuals with gammaglobinanemia genetic disorders (8, 13, 14). The first individual to putatively observe a *Campylobacter* was the famed pediatrician Theodor Escherich—discoverer of *Escherichia coli*—who in 1886 described a non-culturable colon-tropic "spirilla" occurring in cases of cholera-like disease in neonates or "cholera infantum", and which was mucous-associated in diarrheal stool specimens (15). In 1968, *C. jejuni* was first isolated from a human patient (16), and *Campylobacter spp.* have since been increasingly characterized, and recognized for their importance in human and animal diseases (17, 18).

Despite the importance of *C. jejuni* in human disease, specific virulence mechanisms have proven difficult to identify and characterize. The first *C. jejuni* genome sequence, published in 2000, was for strain NCTC11168 (19). Since then, over 30 other *C. jejuni* genomes have been sequenced (20-25). The circular genomes of *C. jejuni* are typically ~1.7 Mbp, and are AT-rich (~30% GC content), and genomic comparisons have revealed substantial diversity between otherwise closely related strains. These genomic differences are thought to account for the differential virulence of *C. jejuni* isolates. Despite this, *C. jejuni* genomes are typically devoid of pathogenicity-associated genomic islands and insertion sequences, and many widely conserved stress regulators are absent (19, 22, 26). However, genomics has revealed the importance of hypervariable polynucleotide tracts in genes that encode proteins with various roles in the biogenesis of surface structures. These tracts facilitate the DNA replication phenomenon of phase variation, in which high frequency lengthening/shortening of the tracts results in "ON-OFF" transcription or premature truncation of a translated protein (19, 26). Flagella, divergent metabolism, and surface polysaccharides have been shown to be important pathogenesis factors (22, 27-29). Interestingly, the associated loci are frequently phase variable, and the highest genetic diversity between *C. jejuni* strains is often found in those gene clusters (23, 24). These attributes are also thought to enable human immunoevasion. During infection, *C. jejuni* evades the sentinel flagellin-activated **T**oll-**l**ike **r**eceptor (TLR)-5 via primary structure modifications to flagellin (30), and AT-rich DNA does not stimulate the CpG-dinucleotide-sensing TLR-9 (31, 32). In addition, highly variable surface structures are thought to confound antibody-mediated human immune defenses. *C. jejuni* strain 81-176, the strain primarily used in the current studies, was acquired from a diarrheal patient whose infection was linked to the consumption of non-pasteurized raw milk (33). Strain 81-176 has enhanced invasiveness in epithelial cell culture (34), which is associated with virulence in humans (35). Metabolic diversity in strain 81-176 also enables greater tissue tropism in infected hosts (22, 29), and the enhanced virulence of

this strain has been demonstrated in both macaque monkeys (36), and humans (37).

1.1.2 Epidemiology of *C. jejuni* - the summer complaint

Campylobacter spp. are the most common cause of bacterial diarrheal disease in many countries (38). Worldwide, there are an estimated 400 million cases of campylobacteriosis per year, such that *C. jejuni* infections outnumber infections with pathogenic *E. coli*, *Salmonella* and *Shigella* (39-41). Infection of humans can occur with as few as 500 bacteria, which is followed by a 2-5 day incubation period before the onset of diarrhea (3, 4, 13, 36-38, 40, 41). Symptoms are typically self-resolving, but may last for up to two weeks (37). Infected food and water are thought to be the primary vehicle for transmission to humans, and are responsible for sporadic and major outbreaks (4, 41, 42). As a zoonotic pathogen, *C. jejuni* is a commensal—or is minimally harmful (43)—in many animal species, and has been cultured from common farm animal species, pet animals, and from the abiotic environment, where *C. jejuni* may thrive in biofilms (4, 41, 44). Contamination of the food chain is implicated in most outbreaks, and unpasteurized milk is a frequent infection culprit (4, 45, 46). Viable *Campylobacter* are frequently isolated from commercial poultry products, which are often ubiquitously contaminated (47, 48). Seasonality in infection rates shows that *C. jejuni* infections are more frequent during the summer months in either hemisphere (13, 49). Symptomatic infections with *C. jejuni* are endemic in developing countries and primarily affect young children (41). Epidemiological surveillance of symptomatic infections indicates that *C. jejuni* is predominantly isolated from gastrointestinal niches (99.7% of all cases) (49). *Campylobacter*-related deaths occur infrequently (0.008% of all cases), and these are primarily in individuals > 60 years old (49). Interestingly, infections in men are 30% more prevalent across all age groups (49).

1.1.3 Treatment of infection and major post-infectious complications

A rare (~0.1% of all infections), but costly and serious complication of *C. jejuni* infection is the autoimmune demyelinating neuropathy Guillain-Barré syndrome, the most common acute flaccid paralysis since the eradication of polio (50, 51). *C. jejuni* is also frequently associated with the autoimmune disorders reactive arthritis and Miller-Fisher syndrome (52, 53). In more than 25% of Guillain-Barré cases, *C. jejuni* is cultured from patients at the onset of neurological symptoms (50, 54). Consequently, the high economic costs of *C. jejuni* infection come from both the high frequency of food poisoning, and the severity of post-infectious autoimmune complications. Although *C. jejuni* infection is predominantly self-resolving, and mediated by innate immunity, antibiotic therapy is indicated in more severe or systemic infections. The potent inflammatory response to *C. jejuni* is normally protective, but can also be damaging (36). Otherwise, treatment solely involves fluid and electrolyte replacement. The macrolide erythromycin, and the fluoroquinolone ciprofloxacin, are the most common antibiotics prescribed, although high rates of resistance to the fluoroquinolones and other antibiotics are prevalent among *C. jejuni* isolates (55, 56). A number of vaccines have been developed, but their efficacy is limited due to the complexity and variability of *C. jejuni* surface antigens and multiple serotypes (57), which is consistent with roles in immune avoidance (58). Immunity can be acquired post-exposure, and can protect against future infections, but can also wane or be ineffective against different *C. jejuni* isolates (59, 60). Variation in lipooligosaccharides also results in strains with surface structures that are mimics of human peripheral neuronal gangliosides, such as GM1 in myelin (53, 61, 62). Therefore, in autoimmunity, antibodies produced against these lipooligosaccharides cross-react with, and damage, the axonal myelin sheath, and acute paralysis results from inhibited signal transduction. These post-infectious complications cannot be treated with antibiotics.

1.2 BACTERIAL CHARACTERISTICS AND ESSENTIALS OF PATHOGENICITY

1.2.1 *C. jejuni* nutrient acquisition and metabolism

C. jejuni is an obligate microaerophile, and cannot grow under strict anaerobic conditions. The bacterium has stringent growth requirements in the laboratory, and requires an elevated CO_2 atmosphere (12% O_2 6% CO_2) (63). Despite this, *C. jejuni* has multifaceted respiration, and a highly branched electron transport chain enables the utilization of numerous electron donors (22, 29, 64). Energy sources are diverse, and may be microbiota-derived in host animals (64). *C. jejuni* electron donors include H_2, formate, acetate, lactate, succinate, sulfite (SO_3^{2-}), nitrate (NO_3^-), nitrite (NO_2^-), NADH, and $FADH_2$ (64, 65). Electron acceptors include O_2, nitrite (NO_2^-) and fumarate. *C. jejuni* is primarily asaccharolytic and cannot catabolize glucose—although certain strains can metabolize L-fucose (64, 66). Glycolysis is non-functional because *C. jejuni* lacks the prominent glycolytic enzyme 6-phosphofructokinase (66). Thus, major carbon and nitrogen sources are amino acids, which are utilized sequentially in preferential order beginning with L-aspartate, L-serine and L-glutamate, which all promote high growth rates in comparison to less-favored amino acids (29, 64, 66). *C. jejuni* 81-176 encodes a γ-glutamyltranspeptidase that facilitates the metabolism of glutamine and glutathione (67), and strain 81-176 also harbors a L-asparaginase for asparagine catabolism (29). Correspondingly, the genome encodes multiple amino acid transporters, many of which are known for multi-functional roles in metabolism, cell adhesion and pathogenesis (68). The genome encodes both the biosynthetic machinery for all amino acids, and the entirety of the **tric**arboxylic **a**cid cycle (TCA cycle) (19, 22, 66). Interestingly, L-aspartate, L-glutamate, L-serine, formate, L-fucose, and pyruvate are effective chemoattractants for *C. jejuni*, whereas L-arginine, and L-lysine are potent chemorepellants (69-71). Thus, the metabolism of *C. jejuni* is strikingly versatile,

and integrated with motility.

1.2.2 Flagella-mediated motility

C. jejuni is a highly motile organism and this is mediated by two polar flagella that enable movement through the environment and within hosts (72). The flagella are vital for many facets of *C. jejuni* biology, and are required for cell invasion, host colonization, and biofilm formation (72, 73). The flagella complex is also involved in protein secretion (74). The coordination of flagellar motility is complex, and requires organization of > 40 proteins to assemble the functional flagella structure (75). The flagellar hook-basal body complex is comprised of a flagellar type III secretion system, while the filament is constructed with two different flagellin subunits, FlaA (major component required for motility) and FlaB (minor component) (76). Rotation of the flagella is controlled by > 10 signal-specific methyl-accepting chemotaxis proteins that enable favorable movements in chemical gradients (69-71, 77). Energy taxis is coordinated via the flagella and the bipartite CetAB energy taxis/aerotaxis system (77, 78). A regulatory hierarchy between the two flagella-gene σ-factors, σ^{28} and σ^{54}, and the phase variable FlgRS two-component system controls flagellar gene expression (72, 75, 79, 80). *C. jejuni* flagella must be glycosylated for filament biogenesis, and changes in glycosylation affect the virulence potential of the bacterium (81, 82).

1.2.3 Lipooligosaccharides, capsular polysaccharides, and glycosylation

C. jejuni encodes two protein glycosylation systems. The *O*-linked glycosylation system modifies serine/threonine residues on flagellin, and the *N*-linked glycosylation system (the *pgl* system) modifies protein asparagine residues (83). Before the discovery of the *N*-linked-modification system in *C. jejuni*, *N*-linked glycosylation had been only been observed in eukaryotes (26, 84,

6

85). In strain 81-176, the pseudaminic acid *O*-linked glycosylation is necessary for flagella filament formation, affecting all flagella-mediated biology (82). Notwithstanding, *N*-linked glycosylation *pgl* deletion mutants are also defective for host cell invasion, and animal colonization (81, 82, 84-86). *C. jejuni* also harbors genes for the biosynthesis of other important carbohydrates (19, 26). These include the <u>c</u>apsular <u>p</u>oly<u>s</u>accharide (CPS) and the <u>l</u>ip<u>oo</u>ligo<u>s</u>accharide (LOS) gene clusters. The greatest genetic variation between *C. jejuni* strains is found in these carbohydrate biosynthesis loci, and many of the genes are phase variable (27, 58, 87, 88). Thus, extensive variation in both the capsule and LOS structures has been attributed to multiple mechanisms, and may have roles in *C. jejuni* host immune evasion. The Penner serotyping scheme for *C. jejuni* strains is based on these differential capsular polysaccharide structures (89). The capsule is important for many aspects of *C. jejuni* biology, including epithelial cell adherence and invasion, colonization of chicks, and serum resistance (27, 58). The phase variable LOS of *C. jejuni*, aside from known roles in Guillain-Barré syndrome autoimmunity, also has important roles in antimicrobial peptide resistance, intracellular survival, and host colonization (62, 85, 87, 90-92). The LOS is comprised of a hydrophobic lipid A attached to an oligosaccharide, which has a conserved inner core, and a variable outer core (88).

1.2.4 Host-cell interactions and colonization

C. jejuni is primarily an extracellular pathogen, and it harmlessly colonizes the gastrointestinal tract of many species as a commensal organism (21, 43, 93, 94). The ability to invade epithelial cells is correlated with virulence in susceptible hosts, and in humans, *C. jejuni*-host cell interactions result in inflammation, disruption of epithelial tissue, and damage to the mucosa (36, 37, 95). In avians, high loads of *C. jejuni* are carried in the cecum with minimal consequences (43, 96). For colonization and/or invasion, attachment to the epithelium is mediated by motility—for movement through the mucosa towards

host cells—and adherence mechanisms, which includes adhesins such as FlaA flagellin, JlpA lipoprotein, the autotransporter CapA, Peb1 (periplasmic ABC transporter/adhesin), and the RGD integrin binding motif-containing CadF (**C**ampylobacter **a**dhesion to **f**ibronectin) (26, 72, 86, 97-100). Outer membrane endotoxic LOS and CPS are also required for adhesion to host cells, and differential polysaccharide structures can modulate the host immune response (58, 93, 101, 102). After adhesion, invasion/uptake may occur via caveolae- and microtubule-dependent processes, potentially mediated by adherence-initiated signaling events that cause membrane ruffling (34, 103). The specific internalization mechanisms are presently unclear, and the intracellular fate of *C. jejuni* is also ambiguous (26). *C. jejuni* is rapidly annihilated post-phagocytosis in C57BL/6 bone marrow-derived and human peripheral monocyte-derived macrophages (104, 105). In epithelial cells, *C. jejuni* does not replicate, but may reside in a membrane-bound **C**ampylobacter-**c**ontaining **v**acuole (CCV) that is divergently trafficked from the early endocytic pathway to the Golgi apparatus (26, 34, 35, 103). Intracellular survival is mediated by prevention of CCV fusion with the lysosome (103), and also differential expression of *C. jejuni* survival genes. Infected epithelial cells activate a number of signaling cascades, including NFκB transcription and ERK kinase signaling (22, 74, 103), which lead primarily to expression of pro-inflammatory cytokines, including IL-8 and TNFα (95, 104, 106, 107). IL-8 recruits other host immune cells, and in particular, massive neutrophil recruitment exaggerates the mucosal inflammatory response, which may damage the epithelium, and create diarrheal symptoms (36, 37). These actions may aid translocation of *C. jejuni* across the epithelium to the baso-lateral lamina propria, further provoking inflammation, and increasing the potential for systemic dissemination (26, 108). Success in the host requires stress survival genes and the ability to acquire host nutrients, and as a consequence, so-called *C. jejuni* pathogenesis/virulence traits include stress tolerance mechanisms and differential metabolic capabilities (26, 29, 64, 98, 109-112).

1.2.5 Stress tolerance during transmission and within hosts

Although *C. jejuni* is difficult to grow in the laboratory, persistence in the natural environment and in hosts is attributed to lifestyle-specific stress tolerance and adaptation mechanisms (3, 4, 26, 113-116). For success as a zoonotic pathogen, *C. jejuni* must adapt to differential conditions, which include variances in nutrient availability, temperature, oxygen tension, and hyperosmotic concentration. Under nutrient deprivation, *C. jejuni* activates the stringent response, in which amino acid deprivation results in uncharged tRNAs that are thought to stall protein synthesis at the ribosome (117, 118). In *C. jejuni,* this results in activation of SpoT, which catalyzes the synthesis of guanosine pentaphosphate (pppGpp), and also the phosphoanhydride bond hydrolysis of pppGpp to ppGpp (117). In turn, binding of ppGpp to the RNA polymerase is thought to affect promoter specificity for alteration of stress-adaptation gene expression (117-119). The *C. jejuni* SpoT-mediated stringent response is essential for stationary phase survival, and tolerance to high O_2 atmospheres (117, 120). Furthermore, the phosphoanhydride bond-containing molecule polyphosphate is also important for stationary phase survival, and is required for intracellular survival and chick colonization, and tolerance to nutrient deprivation, aerobic and hyperosmotic stress (109, 121-123). Polyphosphate is synthesized by two kinases, Ppk1/Ppk2, and homeostasis of polyphosphate is maintained by several exophosphatases (Ppx) (110, 120, 121, 124).

C. jejuni is a thermophilic bacterium that cannot replicate below 30°C, but grows preferentially between 37°C and 42°C optimums (26, 64, 113). Respectively, these reflect the average body temperatures of humans and avians. *C. jejuni* encodes several heat shock proteins that are induced during the thermal stress response, and *in vivo* during chicken colonization (94, 125). Major

C. jejuni heat shock proteins include the chaperones GroES and GroEL, the Lon and ClpB proteases, the endoprotease/acyltransferase HtrA/HtrB, the HslU protease/ATPase, and also the heat shock chaperones DnaK, DnaJ, and GrpE. Many of the heat shock genes in *C. jejuni* are harbored in regulons that are controlled by the HrcA and HspR thermo-responsive transcription factors (126-128). In addition, exposure to a variety of other stresses is known to stimulate heat shock protein expression both in *C. jejuni* and other enteropathogens (115, 128-134).

As a microaerophilic bacterium, *C. jejuni* requires oxygen and is non-fermentative (135). The aerobic respiration of *C. jejuni* produces **r**eactive **o**xygen **s**pecies (ROS), which are also produced within hosts, and within epithelial/macrophage cells, where defensive ROS include superoxides and hydrogen peroxide (H_2O_2) (67, 113, 116, 136-138). In oxidative stress, *C. jejuni* expresses the alkyhydroperoxidase AhpC, the superoxidedismutase SodB, and the catalase KatA (131, 139-143). The HtrA/HtrB protease/chaperone heat shock proteins and the SpoT-mediated stringent response are important for aerobic tolerance (117, 129). Despite expression of these oxidative stress tolerance mechanisms, the bacteria cannot grow at atmospheric levels of O_2 (135). Furthermore, the expression of oxidative stress response proteins is coordinated with iron homeostasis (139, 144). The iron-sequestering activities of the bacterioferritin Dps are activated by ROS, which alleviates the effects of the Fenton reaction, in which iron and O_2 react to form oxidative radicals; thus, iron regulation contributes to oxidative stress tolerance (144-150).

Despite harboring prototypical nutrient deprivation, thermotolerance and oxidative stress response systems, no *C. jejuni* species encodes for known osmoadaptive regulators, and all lack the elaborate osmoadaptive mechanisms of other enteric bacterial species (22, 26). Thus, *C. jejuni* appears to have minimal or uncharacterized osmoadaptive machinery. Known osmotic tolerance factors

include polyphosphate (synthesized by the *ppk*-encoded kinases), the glutamate/glutamine transporter PaqPQ, and the *C. jejuni*-specific two-component regulatory system CprRS, which influences biofilm formation and chick colonization by modulation of metabolic, oxidative stress response (AhpC, KatA and SodB), and cell envelope proteins (68, 91, 121, 151). The importance of osmotic stress tolerance is obvious during *C. jejuni* host colonization, disease, and transmission, but is also relevant for food processing, where the antimicrobial activity of many food preservatives is based on hyperosmotic properties that inhibit bacterial growth (113, 152). In addition, many enteric pathogens differentially express virulence traits in hyperosmotic stress, and those hyperosmotic conditions may approximate lifestyle niches within hosts (153-157). Despite this, the osmoadaptive capabilities/mechanisms of *C. jejuni* have not previously been fully characterized (4, 158-160)—however, *C. jejuni* is known to exhibit reduced osmotic stress tolerance compared to other niche-relevant bacterial species (130).

1.3 HYPOTHESIS

Despite the importance of osmotolerance during *C. jejuni* transmission and host colonization, no further characterization had previously been enacted, either with respect to general stress responses, or targeted identification of specific factors conferring stress tolerance. *C. jejuni* species do not harbor known osmoadaptive regulators or readily identifiable tolerance mechanisms.

Thus, <u>we hypothesized that *C. jejuni* possesses novel molecular mechanisms to counter hyperosmotic stress</u>, and that these mechanisms are also important in human disease, stress survival, and transmission.

CHAPTER TWO: The hyperosmotic stress response of *Campylobacter jejuni*

2.1 SYNOPSIS

Campylobacter jejuni and other gastrointestinal bacteria encounter changes in osmolarity in the environment, through exposure to food processing, or upon entering host organisms, where osmotic adaptation can be associated with virulence. In this study, growth profiles, transcriptomics, and phenotypic, mutant, and single-cell analyses were used to explore the effects of hyperosmotic stress exposure on *C. jejuni*. Increased growth inhibition correlated with increased osmotic concentration, with both ionic and non-ionic stressors inhibiting growth at 0.620 total osmol L^{-1}. *C. jejuni* adaptation to a range of osmotic stressors and concentrations was accompanied by severe chaining in subpopulations, with microscopy indicating septum formation and phenotypic diversity between individual cells in a filament. Population heterogeneity was also exemplified by the bifurcation of colony morphology into small and large variants on salt stress plates. Flow cytometry of *C. jejuni* harboring GFP fused to the ATP synthase promoter likewise revealed bimodal subpopulations under hyperosmotic stress. We also identified frequent hyperosmotic stress-sensitive variants within the clonal wild-type population propagated on standard laboratory medium. Microarray analysis following hyperosmotic upshift revealed enhanced expression of heat shock genes, genes encoding enzymes for synthesis of potential osmoprotectants, and cross-protective induction of oxidative stress genes. The capsule export gene *kpsM* was also upregulated, and an acapsular mutant was defective for growth under hyperosmotic stress. For *C. jejuni*, an organism lacking most conventional osmotic response factors, these data suggest an unusual hyperosmotic stress response, including likely 'bet-hedging' survival strategies relying on the presence of stress-fit individuals in a heterogeneous population.

2.2 INTRODUCTION

The majority of human infections with *Campylobacter jejuni* occur through consumption of undercooked poultry, or cross-contamination of other food with raw poultry juice. Most well-characterized gastrointestinal pathogens are robust and relatively halotolerant, attributes necessary for transmission through the environment, for survival within host organisms, and for endurance in the unfavorable conditions encountered in food processing. In the intestine, *C. jejuni* is faced with numerous stresses, including antimicrobial bile salts, resident flora, human immune defenses and significant changes in osmolarity (161, 162). *C. jejuni* also encounters osmotic stress in food products, where preservatives such as sodium chloride (NaCl) and sucrose dehydrate food-borne microorganisms (116). NaCl is one of the most important agents in food preservation, known since ancient times to be a potent microbial inhibitor. More recent studies show that NaCl and osmotic stress affect virulence factor expression in numerous bacterial species such as *Salmonella* spp., *Escherichia coli* and *Helicobacter pylori* (154, 163, 164).

Adaptation to changing osmotic environments is essential for homeostasis, ensuring that the bacterial cytoplasm remains hydrated and that solutes necessary for normal biological functions are available. Consequently, the genetic and physiological responses to hyperosmotic shock have been studied extensively in bacteria and higher-level organisms. For *C. jejuni*, our current understanding of osmotolerance mechanisms is limited, although it has been shown that *C. jejuni* is more sensitive to NaCl and high osmolarity than most gastrointestinal pathogens (130, 165). Osmolarity or osmotic concentration (in osmol L^{-1}) is a measure of solute concentration; i.e., moles of solute particles rather than moles of solute (molarity). Other enteric pathogens like *E. coli* can adapt to and grow in osmolarities up to $1.7 - 2.0$ osmol L^{-1} and can even survive for long periods exposed to 30% NaCl (10.2 osmol L^{-1}) (166). In contrast, *C. jejuni*

is incapable of survival when standard Mueller-Hinton (MH) growth medium [0.31 osmol L^{-1} (167)] is supplemented with 2.0% NaCl (+0.68 osmol L^{-1}; sum total of 0.99 osmol L^{-1}) (130). The host niche of *C. jejuni* is the chicken cecum, which has an osmolarity of ~0.7 osmol L^{-1} (168). In comparison, the osmotic concentration in the human intestine approximates MH broth at ~0.3 osmol L^{-1}, but can vary widely with ingested food (161). A comparison of relevant *in vivo* and experimental osmotic conditions for *C. jejuni* is presented in FIGURE 2.1A.

Studies of model bacteria have shown that upon exposure to hyperosmotic upshock or stress, physiological changes occur that are triggered by the rapid flux of cellular water along the osmotic gradient (169-172). As water leaves the bacteria, dehydration of the cytoplasm occurs, and turgor (the hydrostatic pressure exerted against the cell membrane from within) is reduced. Bacteria must sense, reverse or adapt to these changes in order to continue growing. This reaction is known as osmoadaptation and occurs in distinct phases, resulting in immediate and long-term responses. The transient short-term response restores hydration by active accumulation of high concentrations of intracellular ions, notably K^+, which contributes to a high internal ionic strength incompatible with growth. In *E. coli,* rapid K^+ influx is counterbalanced with endogenously synthesized glutamate (170), which amasses at a slower rate. Long-term osmoadaptive responses are designed for the maintenance of turgor in sustained adverse conditions and frequently results from the synthesis or import of compatible solutes. These solutes comprise a limited number of structurally diverse, small, neutral, polar and osmotically active substances that are 'compatible' with cellular functions. In most microorganisms, compatible solutes include proline, glycine betaine and the disaccharide trehalose (152, 171). The capacity to synthesize or uptake compatible solutes is often correlated with hyperosmotic stress tolerance (169).

Several well-annotated *Campylobacter* genome sequences (19) indicate

little in the way of known or predicted osmoadaptive machinery, perhaps unsurprising given the apparent sensitivity of *C. jejuni* to osmotic stress. *C. jejuni* does not appear to have functioning potassium (K^+) transporters, encoding only pseudogenes or truncated ORFs of the *kdp* operon, which in *E. coli* is an osmotic stress-induced high affinity K^+ transport system (172). The *C. jejuni* genome also lacks homologues of the *trk* genes, which code for low affinity K^+ transporters. *C. jejuni* possesses an orthologue of ProP, a low affinity proline/glycine betaine transporter, but does not appear to encode any previously characterized high affinity transporters for glycine betaine, such as ProU. It does encode the highly specific proline transport system PutP, but in other bacteria this is thought to be important for transport of this metabolite when used as a carbon or nitrogen source. In addition, *C. jejuni* does not appear to have the capacity for endogenous synthesis of the major compatible solutes, lacking glycine betaine (*bet*) and trehalose (*ots*) biosynthetic pathways. Despite these limitations, *C. jejuni* is a successful zoonotic organism and must therefore rely on other mechanisms to survive hyperosmotic environments.

What methods can *C. jejuni*, apparently devoid of typical osmoadaptive systems, use to overcome osmotic stress and optimize chances of survival? In this study, our goals were to characterize the hyperosmotic stress response and reveal genes important for hyperosmotic tolerance and adaptation in *C. jejuni*. During the course of this work we also noted that the *C. jejuni* population does not respond to hyperosmotic stress in a uniform manner. This was in agreement with a previous study showing that a small fraction of the total *C. jejuni* population can withstand extreme stress conditions, such as exposure to NaCl, sodium deoxycholate and methyl viologen (an oxidative stressor) (43). This suggested the existence of heterogeneous subpopulations of cells with genetic changes that favored survival. Clonal populations can quickly diverge by simple point mutations or by switching events such as phase variation due to slip-strand mispairing during DNA replication and/or chromosomal inversion in

certain genes or promoters (173). For example, *C. jejuni* contains hypervariable homopolymeric nucleotide tracts in several genes, especially those involved in the biosynthesis or modification of surface structures (19, 26, 27). These genes are called contingency loci because the resulting population heterogeneity protects against future events that cannot be predicted. Work in other bacteria has shown that epigenetic mechanisms can also create stable, but easily reversible variation. Epigenetic noise (stochasticity or randomness) is typically a product of the random fluctuations in the synthesis or degradation of mRNA and protein (173-175). Sometimes, this noise can result in co-existing and phenotypically distinct populations of genetically identical cells. This is known as bistability and yields populations with bimodal characteristics (58). Bistability has been most studied in *Bacillus subtilis* spore formation and competence, and is also exemplified in *E. coli* by persister cells (dormant, non-growing cells unresponsive to antibiotics) (173).

This study represents the first comprehensive report on the physiology of *C. jejuni* under hyperosmotic stress. Survival profiles and minimum inhibitory concentrations for a number of hyperosmotic stressors are identified, as is the whole-genome transcriptional response to hyperosmotic stress. We also uncovered physiological responses such as induction of population heterogeneity, cell division defects in subpopulations of bacteria, and both cross-protective and detrimental effects of hyperosmotic shock on other key stress responses. Evidence for the importance of both variability within a clonal population and bistable response mechanisms for hyperosmotic stress survival is also provided.

2.3 METHODS AND MATERIALS

2.3.1 Bacterial strains and growth conditions

Studies were performed using the *C. jejuni* wild-type strain 81-176, originally isolated from an outbreak of campylobacteriosis following consumption of unpasteurized milk (33). A site-insertional KpsM (capsule export protein) mutant (kanamycin resistance) was acquired from P. Guerry (27); DNA was purified and the mutation re-introduced into wild-type strain 81-176 by natural transformation and selection with kanamycin. A *cj0561c* mutant was generated based on the procedures of Guo *et al.* (176) (see TABLE A.1.1 for a full list of bacterial strains and plasmids). All *C. jejuni* strains were grown at 38°C on Mueller-Hinton (MH) agar or broth (Oxoid) supplemented with vancomycin (10 µg ml^{-1}) and trimethoprim (5 µg mL^{-1}) under microaerobic and increased CO_2 conditions (6% O_2, 12% CO_2) in a Sanyo tri-gas incubator (solid media) or generated using the Oxoid CampyGen system (shaken broth cultures). Unless otherwise stated, all *C. jejuni* analyses were conducted in these standard conditions. When necessary, media were supplemented with kanamycin (Kan, 50 µg/ml, Sigma). Hyperosmotic media were prepared by supplementation with various concentrations of NaCl, KCl, $MgCl_2$, sucrose or glucose (Sigma). For osmolarity calculations, the sum of the concentrations of osmotically active solutes in solution was given by the formula: osmol L^{-1} = $\Sigma C_i n_i$, where C is the molar concentration of the solute and n gives the number of particles into which the solute dissociates.

2.3.2 Examination of growth and stress tolerance

C. jejuni strains were grown in MH broth overnight to mid-log phase then diluted to an OD_{600} of 0.005 in the appropriate pre-warmed media. Cultures were incubated under standard *C. jejuni* growth conditions at 38°C with shaking

17

at 200 rpm. Growth and culturability were assessed at various times post-dilution by measuring the OD_{600} and plating serial 10-fold dilutions for CFU on MH agar. For osmotic sensitivity comparisons between strains, a spot method was used. Strains were standardized to an OD_{600} of 0.05, and 5 μl of serial 10-fold dilutions was spotted on MH or hyperosmotic media (in most cases MH + 0.8% NaCl). Minimum inhibitory concentrations (MIC_{90}) of select osmotic stressors were determined using a microtiter broth dilution method (177) in MH broth and an initial inoculum of approximately 10^6 bacteria ml^{-1} from mid-log-phase cultures. Polypropylene microtiter plates containing bacterial strains with various compounds were incubated for 48 hours, then dilutions were spotted on MH plates to enumerate CFU or plates were read for optical density (OD_{600}). MIC_{90} was established as the concentration at which 90% (based on OD_{600}) of bacterial growth was inhibited. For heat shock and oxidative stress tolerance studies, an OD_{600} equivalent of 0.1 was taken from cultures exposed to MH broth and MH broth + 1.0% NaCl for 2 hours. The bacteria were washed in PBS and then re-suspended in either PBS (Invitrogen) or PBS + 5 mM H_2O_2 (Sigma), or subjected to a heat stress of 45°C. 10-fold dilutions were plated on standard MH medium and CFU enumerated. Heat shock and oxidative stress studies were carried out in room atmosphere.

2.3.3 Examination of clonal isolates for frequency and heritability of hyperosmotic stress sensitivity and resistance

To quantify and explore the frequency and phenotypic stability of salt sensitive bacteria existing within the wild-type population, *C. jejuni* 81-176 was plated for single colonies on MH agar. 200 clonal isolates were selected and tested for salt sensitivity by patching on MH (control/passage) and MH + 0.8% NaCl agar plates (test condition) with a glass probe. Plates were incubated for 48 hours and growth on the test condition was categorized either as 1 (sensitive), 2 (wild-type-like) or 3 (enhanced growth). Each patch was rated in this manner

18

three times. For heatmap visualizations, the rating for each clone was averaged and heatmaps generated by Matrix2png (178). Next, 5 progeny of the original population were selected from each category if initially rated unambiguously as 1, 2 or 3. Although growth on MH + 0.8% NaCl was used to establish salt sensitivity rankings, all bacteria for further analyses were obtained from the corresponding MH (control/passage) plate, ensuring that any changes occurring were not due to exposure to NaCl stress. The 15 strains were then passed daily for 2 days on MH agar plates, and 200 clones from each were re-tested in the manner above. For CFU enumerations of sensitive isolates, overnight cultures (in MH) were standardized to an OD_{600} of 0.1, and 10-fold dilutions were plated for CFU on MH, MH + 0.8% NaCl and MH + 1.0% NaCl agar plates. Capsule immunoblotting was carried out as described in (27).

2.3.4 Brightfield and fluorescence microscopy and imaging

For brightfield microscopy, bacteria from various samples were planted on 1.0% agarose pads and overlaid with a coverslip. Cells were imaged with a Nikon TE 2000-U microscope equipped with an argon-ion laser (EXFO X-Cite), 100× oil-immersion objective and Hamamatsu CCD camera controlled by NIS Elements (Nikon). Bacteria were counted and measured for length using the threshold function of this software. Bacterial colony area was measured with ImageJ (179). Fluorescence in GFP-expressing bacteria was detected using an excitation filter for GFP at 485 nm and emission at 520 nm wavelengths. For propidium iodide and syto-9 staining, cells were prepared as per the instructions of the LIVE/DEAD BacLight® Bacterial Viability Kit (Invitrogen) and fixed by agarose implantation. Vancomycin binding sites were detected with 1 µg/ml BODIPY® FL vancomycin (Vanco-FL, Invitrogen). Specific images were obtained with fixed exposure times and fluorescence distributions calculated with ImageJ (179). Microscopy data are representative of three or more fields-of-view from independent experiments.

2.3.5 RNA extraction

Bacteria from log phase overnight cultures were diluted to OD_{600} 0.2 in MH and inoculated into an equal volume of MH or MH + 2.0% NaCl (final starting OD_{600} of 0.1, and final NaCl concentration of 1.0%). At indicated time points, bacteria were removed into a 1/10 volume of 10X Stop solution (5% buffer-saturated phenol in 95% ethanol), collected by centrifugation at 10,000 x *g* for 5 min at room temperature, flash frozen in a dry ice/ethanol bath, and stored at -80°C. Total RNA was extracted from growth curve time points based on methods described (174). RNA concentration was quantified using a ND-1000 spectrophotometer (NanoDrop, Wilmington, DE), and RNA quality was assessed by electrophoresis on 1.0% agarose TAE gels. Absence of genomic DNA within RNA samples was confirmed by PCR.

2.3.6 Construction of the *C. jejuni* DNA microarray, sample hybridization, and analysis

Construction of the DNA microarray was performed essentially as previously described (180). In addition, open reading frames specific to strain 81-176 were included on the array using oligonucleotides (Operon Technologies) designed with ArrayDesigner 2.0 (Premier Biosoft). An indirect comparison of gene expression was performed in which the expression profiles of *C. jejuni* 81-176 cultured in the presence and absence of + 1.0% NaCl were determined separately on different slides (180). Cy3-labeled test cDNA (*C. jejuni* +/- NaCl) was mixed with Cy5-labeled reference genomic DNA from strain *C. jejuni* 81-176 and hybridized to the *Campylobacter* cDNA array. Arrays were scanned using an Axon GenePix 4000B microarray laser scanner (Axon Instruments). The array experiment was repeated two times (biological replicate) with two technical replicate arrays and two replicate features per array for each of the five time

points studied. Spot and background intensity data were processed with GenePix 4.0 software, and data normalization was performed to compensate for differences in the amount of template amount or unequal Cy3 or Cy5 dye incorporation as previously described (180). Normalized data was analyzed with GeneSpring 7.3 software (Silicon Genetics). A parametric statistical t test was used to determine the significance of the centered data at a P value of <0.05, adjusting the individual P value with the Benjamini-Hochberg false discovery rate multiple test correction in the GeneSpring analysis package.

2.3.7 RTqPCR validation of select microarray data

To validate the temporal expression of *dnaK* and *groEL*, real-time quantitative PCR (RTqPCR) was performed on the RNA isolated for the transcriptome profile. Total RNA was used to generate cDNA using SSII enzyme (Invitrogen) and cleaned with the Qiaquick® PCR purification kit (Qiagen). RTqPCR reactions were performed with iQ SYBR® Green (Bio-Rad, Hercules, CA) chemistry as per the manufacturer's instructions. Briefly, RTqPCR amplification of 7 μL of cDNA (20 ng μL^{-1}) was added to a reaction mix containing 7.5 μL 2x SYBR® Green master mix, 0.3 μL of 10 μM mix of forward and reverse primers and 0.2 μL H$_2$O. Amplification was performed using Opticon 2 thermocycler (Bio-Rad) and the comparative threshold cycle ($\Delta\Delta$Ct) method was used to calculate fold change where samples were normalized to *gyrA* (181). Reactions were performed in duplicate, and two biological replicates were performed for each sample. Oligonucleotide sequences are shown in TABLE A.2.1.

2.3.8 Fluorescence-activated cell sorting

Flow cytometry and sorting were conducted on a LSRII flow cytometer (BD) and data analyzed using FlowJo analysis software (Tree Star). Sample

preparations are as follows: log-phase cultures of *C. jejuni* 81-176 harboring p*atpF'*-GFP were grown in standard conditions overnight. The plasmid is derived from pMW10 (182) and harbors the *atpF'* promoter fused to a stable GFP reporter (p*atpF'*-GFP). Mid-log phase cultures were diluted to an OD_{600} of 0.005 in MHKan or MHKan + 1.0% NaCl and sampled at various time points. Samples were standardized to OD_{600} of 0.1 in 1 mL, washed with PBS, then diluted 10-fold and immediately analyzed by flow cytometry. For FACS, 100,000 events were sorted from each gated population (shown in FIGURE 2.6B) into pre-warmed MHKan. Samples were then centrifuged, washed with MHKan and assessed by plating 10-fold dilutions.
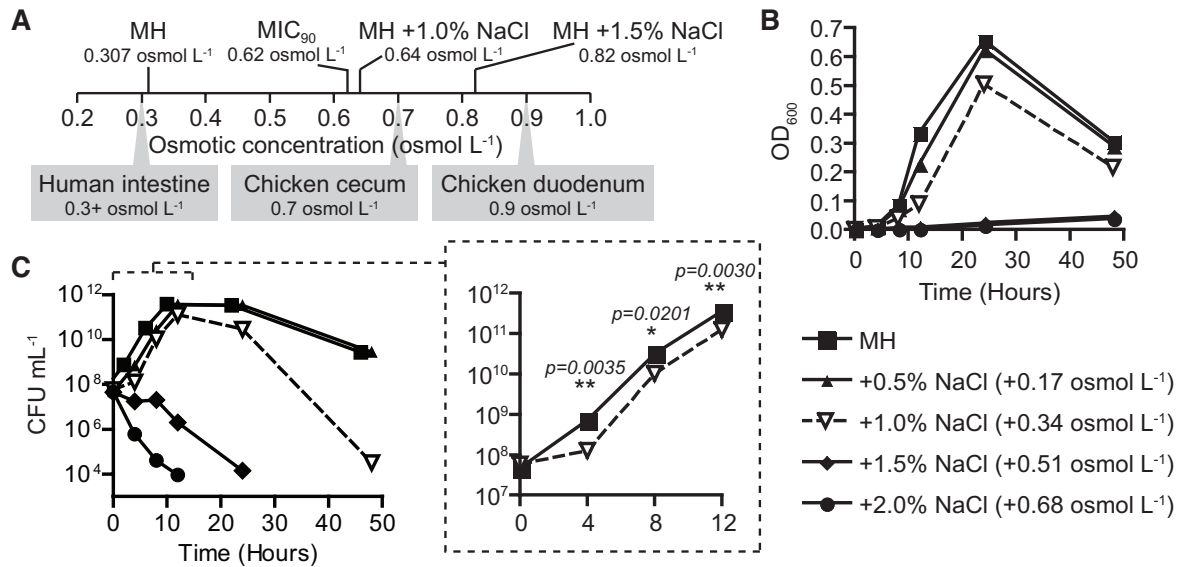
FIGURE 2.1 Growth and survival of *C. jejuni* 81-176 in broth cultures containing increasing concentrations of NaCl in Mueller-Hinton (MH) medium.
(A) Comparison of biologically relevant osmolarities and the conditions used in this experiment. (B and C) Optical density (OD) readings (B) and CFU ml^{-1} counts (C) demonstrated that growth and survivability are inhibited at osmolarities exceeding 1.5% NaCl. Initial adaptation under the 1.0% NaCl condition (open triangles) was followed by logarithmic growth and late-stage growth defects; the dashed bracket and box in panel C show an expanded view of the 0- to 12-h time points for 1.0% NaCl versus unsupplemented medium. The MH + 0.5% NaCl CFU ml^{-1} curve is identical to the MH curve but has been offset to enable viewing. The experiment is representative of three biological replicates; error bars for three technical replicates are present but in most cases are too small to see; *, $P \leq 0.05$; **, $P \leq 0.01$.

2.4 RESULTS

2.4.1 Increasing the osmotic concentration inhibits growth of *C. jejuni*

Previous reports have noted that *Campylobacter* spp. are highly intolerant to osmotic stress compared to other bacterial food-borne pathogens and are incapable of growing in media preparations containing 2.0% NaCl (0.68 osmol L^{-1}) (130). To establish the temporal response of *C. jejuni* strain 81-176 to various osmolarities and an appropriate hyperosmotic upshock concentration for further experiments, *C. jejuni* strain 81-176 was grown in MH supplemented with a range of physiologically relevant NaCl concentrations (FIGURE 2.1A), and bacterial culturability was assessed over a 48 hour period (FIGURE 2.1B and C). In MH media supplemented with equal to or greater than 1.5% (0.51 osmol L^{-1}) NaCl, logarithmic growth was prevented, and a severe decrease in CFU counts was observed. In contrast, *C. jejuni* 81-176 grown in MH media supplemented with 1.0% NaCl (0.34 osmol L^{-1}) exhibited a brief initial lag/adaptation phase (0 to 4 hours), a period of log-phase growth (4 to 12 hours), and finally a decline in late stage culturability (12 hours onwards). Supplementation with 0.5% NaCl (+0.17 osmol L^{-1}) resulted in growth and survival characteristics similar to those seen in unsupplemented MH medium.

2.4.2 Hyperosmotically stressed *C. jejuni* exhibit chaining and population length heterogeneity

Loss of culturability, aging, and exposure to stresses such as low nutrient and hypoosmotic conditions are associated with conversion into a viable-but-non-culturable (VBNC) state, often represented by a coccoid morphology in *Campylobacter* spp. (159, 183, 184). *C. jejuni* exposed to hyperosmotic conditions were observed by light microscopy to determine if late-stage growth defects correlated with increased coccoid formation. An increase in coccoid formation

23

was not observed in any hyperosmotic condition tested. However, chaining—often referred to as filamentation in the literature—did occur in a proportion of the bacterial population grown in the presence of 1.0% and 1.5% NaCl (FIGURE 2.2A). Visual inspection (FIGURE 2.2A) and single cell analyses (FIGURE 2.2B and C) showed that the degree of chaining increased with both osmotic concentration (FIGURE 2.2B; 12 hours is shown as representative) and over time until later growth stages (FIGURE 2.2C; 1.0% NaCl is shown as representative). In the 2.0% NaCl condition, no chaining was observed, and the population was non-motile. In contrast, chains and normal length bacteria in the 1.0% and 1.5% NaCl conditions were motile (i.e., alive), although longer chains swam less efficiently than shorter cells. Chain length was heterogeneous, with some exceeding 25 μm in length (not shown).
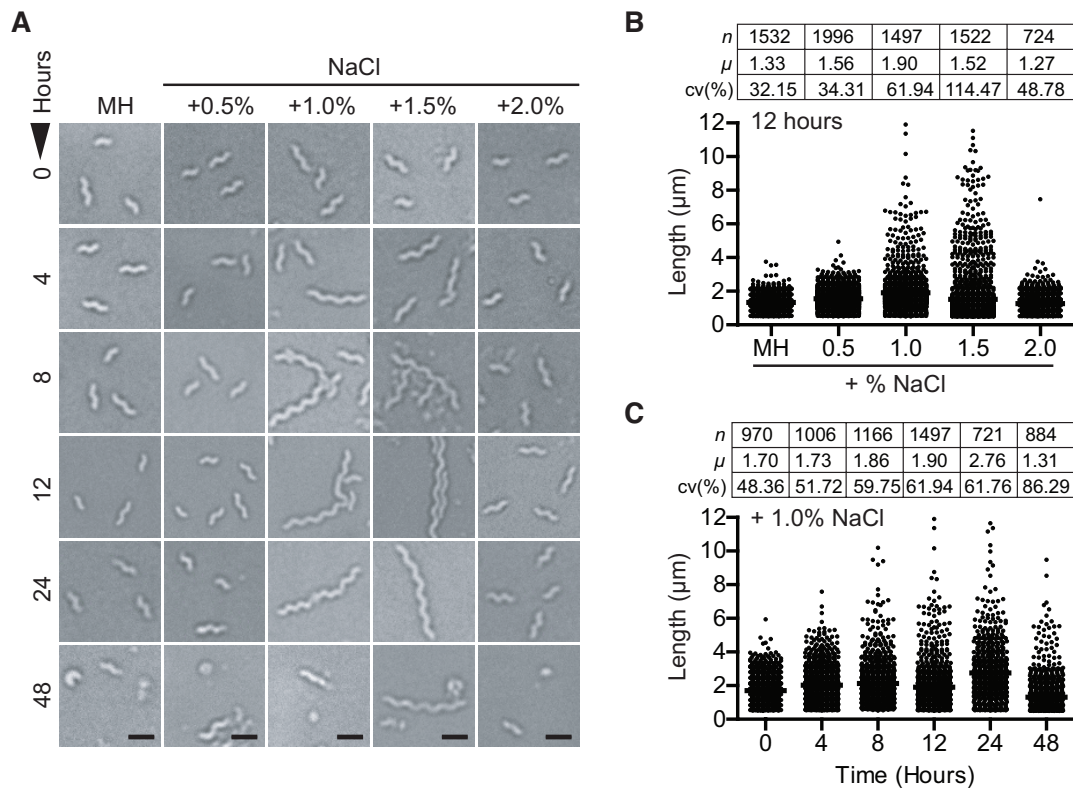
FIGURE 2.2 Hyperosmotic stress leads to *C. jejuni* cell length alteration.
(A) Brightfield microscopy of bacteria from NaCl-supplemented cultures sampled over a 48 hour period demonstrated that chaining occurs in a narrow hyperosmotic range. Increased progression

to the coccoid form was not observed, and not all cells are chained. Scale bars indicate 1 μm. (B) Measurement of chain length from NaCl-supplemented cultures demonstrated that the proportion of chains increased with osmolarity (12 hr time point shown) except under 2.0% NaCl conditions. (C) Chain length and abundance increased with time (1.0% NaCl condition shown). Data tables include number of bacteria analyzed (n), mean length (μ) in μm and coefficient of variation (cv%; standard deviation to mean ratio). All data are representative of at least 3 independent fields of view.

2.4.3 Growth inhibition and chaining are general responses to hyperosmotic stress

To determine if growth defects and chaining were a specific response to NaCl or a general response to hyperosmotic stress, the effect of other osmotic stressors was tested. Both ionic (KCl and MgCl$_2$) and non-ionic stressors (sucrose) were compared to differentiate between hyperosmotic or hyperionic responses. The salts KCl and MgCl$_2$ and the sugar sucrose were added to normal MH media at concentrations comparable to initial NaCl concentrations, and the osmolarity of the stressor solutions added to the media was calculated (see 2.3 METHODS AND MATERIALS). Representative growth curve OD$_{600}$ readings shown in FIGURE 2.3A indicated that growth was generally inhibited in an osmotic concentration-dependent manner. All osmotic stressors tested also resulted in chaining (representative examples shown in FIGURE 2.3B). The minimum inhibitory concentration (MIC$_{90}$) of each stressor was also determined, as was the minimum inhibitory osmotic concentration (TABLE 2.1). For these analyses, sucrose was replaced by glucose due to solubility limitations for MIC$_{90}$ determination. The minimum inhibitory osmotic concentration was equivalent for all osmotic stressors tested at + 0.313 osmol L^{-1}, or a total 0.620 osmol L^{-1} taking into account the basal osmolarity of MH medium. The ratio of MIC$_{90}$ to minimum inhibitory osmotic concentration for each stressor also correlated with the number of species into which that stressor dissociates. For instance, MgCl$_2$ dissociates into three species, NaCl into two species, and glucose is a single molecule. Correspondingly, the MIC$_{90}$ for added glucose was 3X that of added MgCl$_2$ and 2X that of added NaCl, with each stressor yielding an equivalent

25

minimum inhibitory osmotic concentration. These observations also held true for *C. jejuni* strains NCTC 11168 and 81116, with each strain exhibiting identical MIC_{90} and chaining characteristics as strain 81-176 (not shown). Based on the growth and chaining profiles shown in FIGURE 2.1 and FIGURE 2.2, and the fact that ionic and nonionic stressors yielded identical MIC_{90}, MH + 1.0% NaCl was used as a representative hyperosmotic stress condition for all further broth-based analyses. For plate-based assays, MH + 0.8% NaCl agar plates were used instead of + 1.0% plates, as general growth characteristics were more equivalent to MH + 1.0% NaCl broth due to moderate plate desiccation.
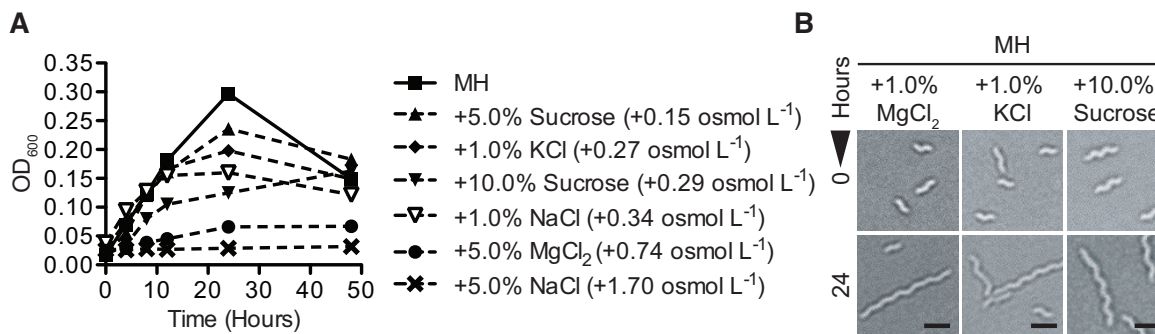
FIGURE 2.3 Growth inhibition and chaining occur under multiple types of hyperosmotic stress.

(A) OD_{600} readings of broth cultures of *C. jejuni* grown in MH media supplemented with various concentrations of ionic (NaCl, $MgCl_2$, KCl) and non-ionic (sucrose) osmotic stressors over 48h showed that growth inhibition generally correlated with osmotic concentration. Error bars are present but in most cases are too small to see. (B) Brightfield microscopy illustrated that chaining was an effect of both ionic ($MgCl_2$, KCl) and non-ionic (sucrose) osmotic stressors. Scale bars indicate 1 μm; data from microscopy is representative of at least 3 independent fields of view.

TABLE 2.1 Growth inhibition occurs at the same osmotic concentration in the presence of both ionic and non-ionic stressors.

Stressor	Number of species[a]	Minimum inhibitory concentration[b] (M)	Minimum inhibitory osmotic concentration[b] (osmol L^{-1})	Total inhibitory osmotic concentration[c] (osmol L^{-1})
NaCl	2	0.160	**0.313**	**0.620**
KCl	2	0.160	**0.313**	**0.620**
MgCl$_2$	3	0.109	**0.313**	**0.620**
Glucose	1	0.308	**0.313**	**0.620**

[a] Number of species in which the stressor molecule dissociates in solution.
[b] Minimum inhibitory concentration, or minimum inhibitory osmotic concentration, of added stressor required to inhibit the growth of ~90% of organisms (MIC$_{90}$).
[c] Total osmolarity calculated from the measurement of MH osmolarity (0.307 osmol L^{-1}) + the calculated osmolarity of added stressor.

2.4.4 Heterogeneity among cells and within chains in hyperosmotically stressed *C. jejuni*

We next wished to explore additional characteristics of the chains. DNA dyes traditionally used for live/dead enumeration were initially employed with the goal of exploring chain and population viability. Syto-9 (green) stains all bacteria, while propidium iodide (PI) is commonly used to identify dead bacteria because entry indicates membrane disruption indicative of cell death (185). Despite significant efforts to optimize staining procedures, we found that PI is not ideal for microscopic determination of live/dead *C. jejuni,* as nearly all living (motile) wild-type bacteria grown in standard conditions fluoresced when stained with PI (FIGURE 2.4A). In contrast, under hyperosmotic stress, a number of cells did not stain with PI. Furthermore, distinct regions of many chained cells excluded PI (FIGURE 2.4A, arrows) but were not anucleoid, as Syto-9 stained normally. As bacterial chaining occurs because of continued growth (elongation) in the absence of complete separation (division), this suggested that septa had formed, as PI entering a part of the chain would otherwise leach into neighboring cells that excluded PI. We further investigated septation in chained cells using a fluorescent vancomycin derivative (Vanco-FL), which has been used to highlight putative septa in *Helicobacter pylori* (4). Vanco-FL binds D-ala-D-

ala moieties of peptidoglycan and may represent the septa and/or sites of new peptidoglycan synthesis. By microscopy, most (>80%) *C. jejuni* growing in + 1.0% NaCl did not fluoresce with Vanco-FL at the concentration used, nor did most cells from conditions without added salt. However, chained cells that did fluoresce exhibited a highly symmetrical pattern of punctate dots, likely representing individual septa (FIGURE 2.4B, upper). Fluorescence distribution analysis of Vanco-FL and PI co-staining (FIGURE 2.4B, lower) suggested that PI and Vanco-FL did not co-localize. Collectively, these data indicate that individual cells within a hyperosmotically-stressed population, as well as within a chain, have the capacity for phenotypic heterogeneity.
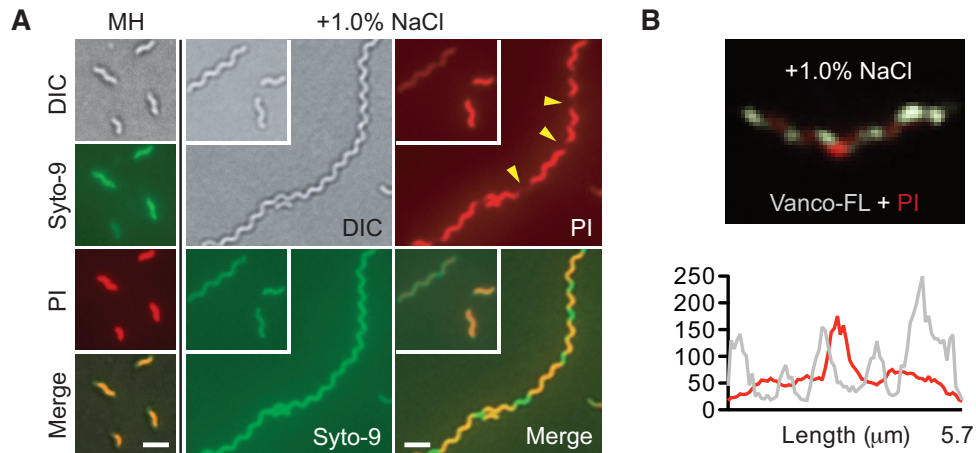
FIGURE 2.4 Heterogeneity within hyperosmotically stressed populations and chains and symmetrical staining with fluorescent vancomycin (Vanco-FL).
Bacteria were grown for 12h in unsupplemented MH broth or MH + 1.0% NaCl and prepared for microscopy. (A) *C. jejuni* stained with propidium iodide (PI, red) and Syto-9 (green) from the LIVE/DEAD BacLight kit. Wild-type under optimal conditions fluoresced with PI while some cells in hyperosmotic conditions excluded PI, as did many of the cells within chains (yellow arrows). (B) Chains stained with Vanco-FL (white-grey) and PI (red), and analysis by fluorescence distribution. Fluorescence units are arbitrary. Scale bars indicate 1 μm.

2.4.5 Salt-sensitive clones are identified within the wild-type population

Previous work in our laboratory identified several targeted and transposon mutants that were defective for growth on hyperosmotic media. Although salt sensitivity was linked to disruption of the targeted gene in a

number of instances (121, 151), in other cases salt sensitivity was not linked to the introduced mutation, with wild-type-levels of resistance restored when the mutation was re-introduced to a wild-type genetic background (unpublished observations). This suggested that salt-sensitive clones occur frequently within the wild-type population. To investigate this, and to establish the frequency with which this occurs, wild-type *C. jejuni* were streaked on MH media for single colonies, of which 200 were isolated and patched onto MH (control/passage) or MH + 0.8% NaCl (test) plates. Of the 200 clones, 21.6% ± 1.2% displayed either complete or partial growth inhibition ('sensitive') on hyperosmotic media based on a visual rating scheme comparing growth between isolates, whereas 13.3% ± 1.8% of the clones exhibited heavier growth than the original wild-type population ('enhanced') (FIGURE 2.5A-C). Phase variation of the capsular polysaccharide occurs at a comparable rate (27), and we have found that an acapsular mutant (Δ*kpsM*) is hypersensitive to osmotic stress (see below). However, CPS immunoblotting showed that 7 randomly selected salt-sensitive clones produced the CPS (not shown). As we also wished to explore the potential for reversibility of these phenotypes, 5 sensitive (F6, C10, E7, G8, G10), 5 wild-type-like (A14, B8, C19, D13, G21), and 5 enhanced (E20, F20, H9, B13, B22) clones were selected from the corresponding MH (control/passage) plate and passed daily on standard MH media for 2 days. 200 progeny from each of these 15 clones ('progeny of progeny') were assessed for salt sensitivity as above. Progeny from all 15 clonal populations exhibited heterogeneity in sensitivity and resistance to osmotic stress, with all populations again being composed of sensitive, wild-type-like or enhanced individuals (FIGURE 2.5D and E). However, sensitive clones yielded an increase in the number of sensitive 'progeny of progeny', up to 79.3% ± 1.5% of the population compared to 21.6% ± 1.2% observed for the starting wild-type population. The 5 sensitive clones (F6, C10, E7, G8, G10) were also quantitatively assessed for hyperosmotic stress survival in comparison to wild-type on MH, MH + 0.8% NaCl, and MH + 1.0% NaCl plates. Using CFU determinations, we found that F6, C10, E7, G8, G10

were 5.8-, 7.4-, 6.4-, 13.8- and 5.7-fold more sensitive on MH + 0.8% NaCl than wild-type, respectively, with 4 of these 5 clones exhibiting no growth on MH + 1.0% NaCl (FIGURE 2.5F). In summary, subpopulations of osmotic stress-sensitive bacteria were found within the population and selection of sensitive clones influenced the phenotype of progeny populations by altering the distribution of sensitive, wild-type-like and enhanced resistance subsets. These subset populations retained the capacity to generate progeny with the original phenotype restored.
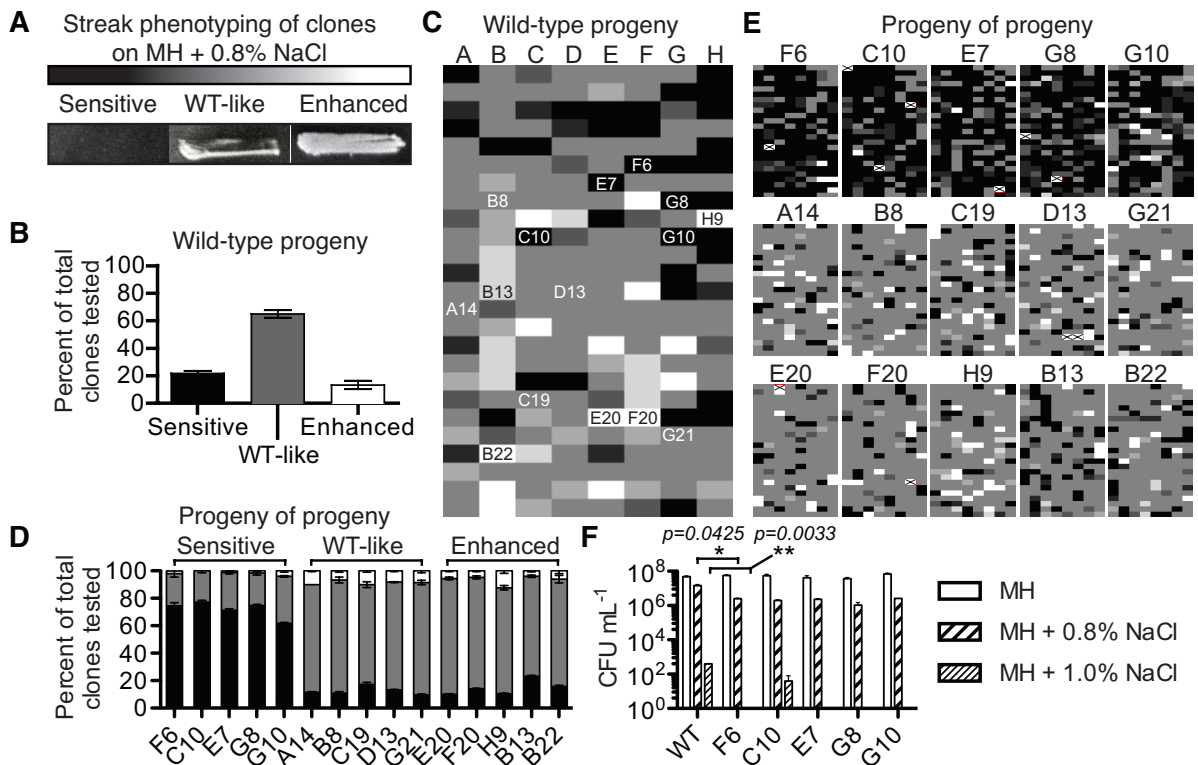
FIGURE 2.5 Salt-sensitive isolates within the wild-type population.
200 single colonies were isolated from MH plates and patched on MH (control/passage) or MH + 0.8% NaCl (test) plates. (A) Patches were assessed by microscopy and graded for growth by three categories; black represents minimal or no growth ('sensitive'), grey indicates characteristic ('WT-like') growth, and white represents heavy growth ('enhanced'). (B) Percent of 200 clones tested categorized as sensitive, WT-like or enhanced. Error bars represent the fact that streaks were graded 3X blind and that some streaks had intermediate phenotypes. (C) Visual heatmap representation of the sensitivity profiles of the 200 clones. Intermediate phenotypes are represented by lighter or darker shades of grey, and numbered clones indicate progeny that were then selected from the MH (control/passage) plates, passed 2X on MH, and then re-tested to examine the heritability of phenotypes. (D) Percent of 200 clones of 15 progeny (5 sensitive, 5 WT-like and 5 enhanced) falling into the same 3 categories. (E) Visual heatmap representation of

sensitivity profiles for 200 clones of the 15 progeny ('progeny of progeny'). For sensitive progeny, the majority of clones tested retained a sensitive phenotype, but WT-like or enhanced growth was also observed within those populations. Crossed-out boxes indicate tests where growth was not observed on the MH control plate. (D) CFU enumeration of sensitive clones F6, C10, E7, G8 and G10 in comparison to wild-type. 10-fold dilutions of an OD-standardized culture were plated on MH and MH + 0.8% or 1.0% NaCl plates and CFU enumerated, performed in triplicate. Most of the sensitive clones (F6, E7, G8, G10) exhibited no growth on MH + 1.0% NaCl (bars absent). All strains exhibited statistically significant $p \leq 0.05$) differences compared to wild type for growth on the two NaCl concentrations and insignificant differences on MH alone. Statistics are shown for wild-type vs. F6 only; *, $p \leq 0.05$; **, $p \leq 0.01$.

2.4.6 Single-cell analysis reveals bistable heterogeneity

In addition to the observation that pre-existing salt-sensitive clones occur in a wild-type population not previously subjected to salt stress (FIGURE 2.5), we also observed instances of phenotypic heterogeneity (i.e., differential growth and survival) that were induced by exposure of wild-type *C. jejuni* to hyperosmotic stress. One example of this was the appearance of 'large' and 'small' colony variants when wild-type *C. jejuni* was plated for single colonies on NaCl-supplemented agar. (FIGURE 2.6A). These variants were not observed on standard MH plates and were distinct from the salt-sensitive clones described above, as small variants were not defective for osmotic tolerance and gave rise to both large and small daughter colonies on NaCl plates at a similar frequency as the starting population (not shown). We further explored single-cell variability during hyperosmotic stress by transforming wild-type *C. jejuni* with a plasmid encoding the ATP synthase promoter fused to a stable green fluorescent protein gene (p*atpF'*-GFP) and examining expression in individuals across the entire population. The ATP synthase promoter was initially identified as a strong promoter (186) and is also upregulated under hyperosmotic conditions (see transcriptional profiling section below; TABLE 2.2). Since active growth requires ATP production and consumption, we hypothesized that increased expression of ATP synthase would occur in bacteria able to grow in +1.0% NaCl (187). Microscopy and flow cytometry revealed that plasmid-carrying *C. jejuni* exposed to MH + 1.0% NaCl for 12 hours bifurcated into GFP$_{low}$ and GFP$_{high}$

subpopulations, with the GFP$_{low}$ bacteria comprising 16.0% ± 2.3% of the total population (FIGURE 2.6B and C). In comparison, control bacteria grown in MH with no added NaCl (GFP$_0$) exhibited unimodal (typical bell curve) GFP expression. Fluorescence activated cell sorting (FACS) was used to sort 10^5 GFP$_0$, GFP$_{low}$, and GFP$_{high}$ bacteria that were then plated for CFU on both standard MH and NaCl-supplemented media. As with small colony variants, individuals from the GFP$_{low}$ population were not more salt-sensitive than the starting population after recovery (not shown); however, over 10-fold fewer total CFU were recovered for the GFP$_{low}$ population than for GFP$_{high}$ clones on both normal and NaCl-supplemented media (FIGURE 2.6D and not shown). The GFP$_{high}$ population comprised the majority of the total population and was nearly 100% culturable in normal and hyperosmotic conditions (FIGURE 2.6D and not shown). As with the colony size variants, colonies isolated from either the GFP$_{low}$ or GFP$_{high}$ populations that were grown overnight on standard medium then subjected to salt stress exhibited the same pattern of bifurcation by FACS as observed for the original population (not shown). The appearance of two distinguishable or bimodal phenotypes in a clonal population has been observed in other bacteria and is commonly referred to as bistability (173, 175).
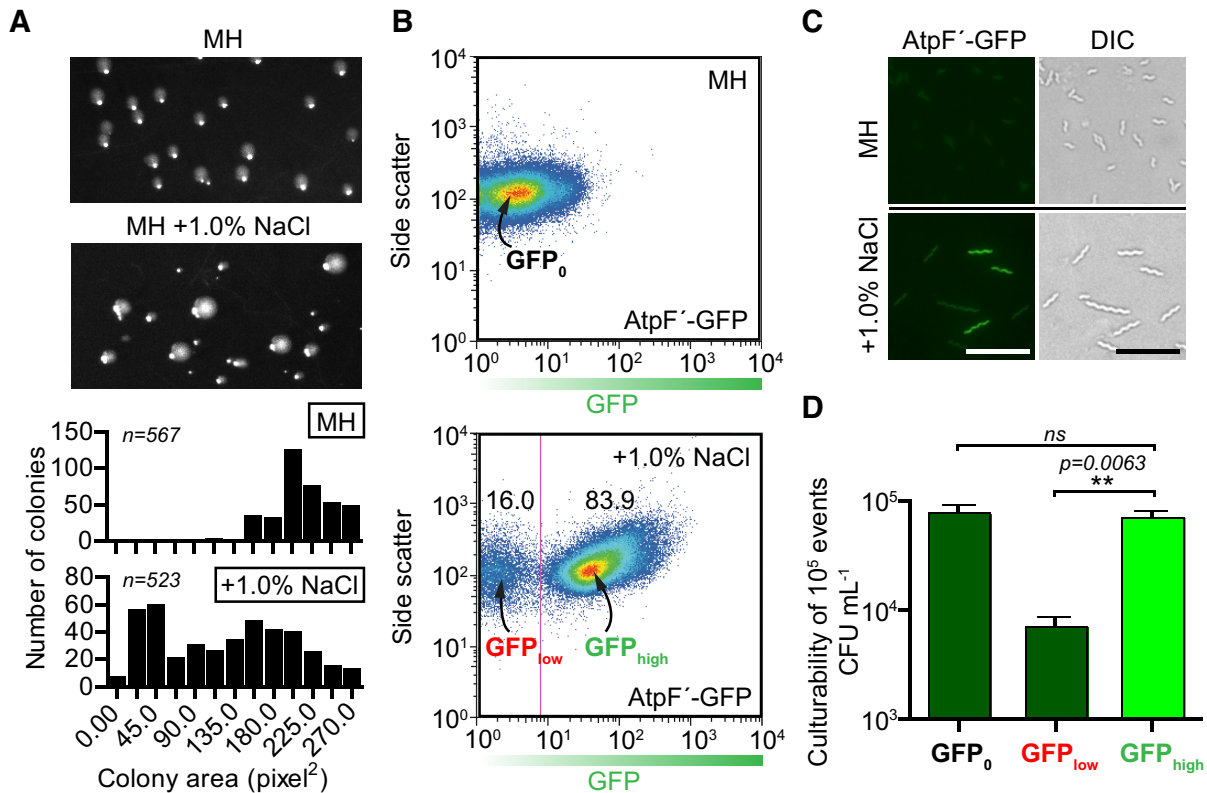
FIGURE 2.6 Bistability in colony size and expression of GFP from p*atpF'*.
(A) Heterogeneity in *C. jejuni* colony size when wild-type bacteria were plated on media supplemented with 0.8% NaCl and grown for 48 hours. (B) Bacteria harboring the p*atpF'*-GFP plasmid were analyzed by flow cytometry. Following 12hrs in MH + 1.0% NaCl, the population bifurcated into GFP_{low} and GFP_{high} populations (lower panel) while bacteria remaining in MH broth did not (upper panel). (C) Bifurcation was confirmed by fluorescence microscopy. Microscopy is representative of 3 independent fields of view. Scale bar = 3 μm. (D) FACS sorting of the GFP_0, GFP_{low}, and GFP_{high} populations and plating for CFU revealed that GFP_{high} bacteria were as culturable as GFP_0, and GFP_{low} bacteria had ~10X reduced culturability on MH medium (show n) and MH + 0.8% NaCl (not shown). Error bars are derived from 3 independent experiments. ** indicates p ≤ 0.01.

2.4.7 Temporal transcriptional profile of *C. jejuni* in response to hyperosmotic stress

In addition to the single-cell analyses described above, we also established the whole-genome transcriptional response of the overall population to hyperosmotic stress over a 12 hour timecourse corresponding to initial adaptation and post-adaptation log-phase growth (see the 1.0% NaCl condition in FIGURE 2.1C). Log-phase bacteria inoculated into either MH or MH + 1.0% NaCl were harvested after 15 minutes, 1.5 hours, 3 hours, 6 hours, and 12 hours

for RNA isolation and microarray analyses. Two biological replicates were assessed, each with consistent expression profiles; data shown represent the fold expression difference of genes in hyperosmotically shifted bacteria relative to those remaining in MH broth. TABLE 2.2 (genes upregulated in MH + 1.0% NaCl) and TABLE 2.3 (genes downregulated in MH + 1.0% NaCl) highlight genes that were the most highly dysregulated or genes associated with osmotic transcriptional responses in other bacteria. In general, there were three major expression profiles: (I) genes with early and transient expression changes; (II) genes with early and long-lasting changes and (III) genes with greater expression changes at later time points.

The early and transient hyperosmotic stress transcriptional profile included many genes with similar behavior in other bacteria. For example, general downregulation of ribosomal proteins (*rpl, rps*) was observed at 15 minutes post-exposure coinciding with a temporary growth arrest, while the same genes later returned to steady-state or greater expression levels with the resumption of growth. Genes with a potential role in osmoadaptation were also differentially expressed. These included *gltD* and *glnA*, encoding proteins for glutamate and glutamine synthesis, which were both highly upregulated at 15 minutes post-exposure but not at later time points, and *kdpB*, the ATPase subunit of the major potassium transporter. Additionally, rapid upregulation of heat shock protein genes occurred in salt-stressed *C. jejuni,* including *groEL*, *dnaK*, *grpE* and *clpB*. The degree of upregulation dropped sharply as growth resumed, but remained consistently higher than in unstressed bacteria.

Genes with early and long-lasting expression changes included upregulation of several amino acid biosynthesis enzymes, including *trpABFE* (tryptophan biosynthesis), *cysM* (cysteine biosynthesis) and *leuABCD* (leucine biosynthesis). In keeping with other bacteria, *C. jejuni* appeared to modestly upregulate oxidative stress genes such as catalase (*katA*) and superoxide

34

dismutase (*sodB*) at all time points. We also observed striking upregulation of *cj0561c* at all time points. This gene was previously identified as being controlled by the negative regulator CmeR and is also upregulated by bile salts and in the intestinal tract; however, a *cj0561c* mutant does not have increased sensitivity to bile (162, 176). Cj0561c is annotated as a putative periplasmic protein, although bioinformatic analysis suggests that it has a porin-like architecture. We constructed a targeted deletion of *cj0561c* but found that the mutant was not defective for growth or survival in hyperosmotic conditions (not shown). Several known and putative regulatory elements were also shown to have early and long-lasting expression changes. These included upregulation of the bipartite energy taxis response system *cetAB* and a putative helix-turn-helix domain containing protein, Cj1533c. Also upregulated continuously was *hrcA*, encoding a negative regulator of the *grpE, dnaK and groEL* heat shock proteins (128).

Genes with notable expression changes in response to NaCl at later time points include those involved in many metabolic and energy production pathways. For instance, there was downregulation of many genes encoding the TCA cycle (*gltA, acnB, icd, mdh, mqo, suc*) and genes for electron transport and other important metabolic functions (*nuo, oor, acs*). This was somewhat paradoxical given that this downregulation was accompanied by upregulation of genes encoding the primary ATP synthase. The *atpF"* gene is the first gene in the synthase operon, which was upregulated beginning at 6 hours post-NaCl exposure. Also of note was upregulation of *kpsM*, encoding the CPS export system inner membrane protein; however, there were no significant changes in any other genes of the capsular polysaccharide locus. Other upregulated genes included *pspA,* encoding a probable protease, and *pth*, encoding the peptidyl-tRNA hydrolase which is responsible for recycling excess peptidyl-tRNA, an essential requirement for continued protein synthesis (188). In this category were also two transcriptional regulators, *cbrR* and *hspR*. The CbrR '**c**ampylobacter **b**ile **r**esistance' response regulator is crucial for tolerance to

sodium deoxycholate and chicken colonization (158), while HspR is a negative regulator of the heat shock response (127). Downregulated genes included *sdaA* and *sdaC*, encoding the serine transporter and hydratase, *lctP* encoding lactate permease and *putP*, encoding a putative sodium/proline transporter. Expression trends of *dnaK*, *groEL, katA and kpsM* were confirmed by RTqPCR (not shown).

TABLE 2.2 Selected genes two-fold or greater upregulated under hyperosmotic stress.

Functional class	Name	Gene	Fold up-regulation				
			15 min	1.5 hours	3 hours	6 hours	12 hours
Regulation and signal transduction							
Campylobacter bile response regulator	*cbrR*	*cj0643*	-	-	2.2	2.9	2.9
Heat-inducible transcription repressor	*hrcA*	*cj0757*	6.7	2.0	2.2	2.6	2.9
Bipartate energy taxis response protein	*cetB*	*cj1189c*	2.2	3.5	3.3	2.1	-
Bipartate energy taxis response protein	*cetA*	*cj1190c*	2.0	3.6	2.4	2.1	-
Heat shock transcriptional regulator	*hspR*	*cj1230*	-	-	-	-	3.1
Putative helix-turn-helix containing protein		*cj1533c*	3.5	2.8	2.6	2.3	2.0
Detoxification and protection							
Superoxide dismutase	*sodB*	*cj0169*	2.0	2.5	2.4	-	-
Catalase	*katA*	*cj1385*	-	2.2	-	2.2	-
Chaperones, chaperonins, heat shock, proteases							
ATP-dependent Clp protease	*clpB*	*cj0509c*	2.3	-	-	-	-
Heat shock protein	*grpE*	*cj0758*	9.4	2.2	2.5	2.6	4.0
Heat shock protein	*dnaK*	*cj0759*	12.8	2.4	2.8	2.5	6.9
60 kD chaperonin	*groEL*	*cj1221*	6.9	3.0	5.0	2.6	-
Putative curved-DNA binding protein	*cbpA*	*cj1229*	-	-	-	-	2.7
Amino acid biosynthesis							
Glutamate synthase	*gltD*	*cj0009*	4.8	-	-	-	-
Putative anthranilate synthase component I	*trpE*	*cj0345*	2.1	-	-	3.1	13.9
N-(5'-phosphoribosyl)anthranilate isomerase	*trpF*	*cj0347*	3.4	2.9	4.4	2.9	3.5
Tryptophan synthase beta chain	*trpB*	*cj0348*	3.0	3.2	5.1	3.0	-
Tryptophan synthase alpha chain	*trpA*	*cj0349*	3.1	3.1	4.6	2.0	3.1
Glutamine synthetase	*glnA*	*cj0699c*	5.3	-	-	-	-
Cysteine synthase	*cysM*	*cj0912c*	2.2	3.8	3.8	2.4	-
Putative cystathionine beta-lyase		*cj1392*	2.4	4.1	3.8	2.9	3.9
3-isopropylmalate dehydratase small subunit	*leuD*	*cj1716c*	-	2.7	4.3	3.1	-
3-isopropylmalate dehydratase large subunit	*leuC*	*cj1717c*	2.4	3.4	6.5	3.4	-
3-isopropylmalate dehydrogenase	*leuB*	*cj1718c*	2.4	3.8	7.3	3.5	-
2-isopropylmalate synthase	*leuA*	*cj1719c*	2.2	3.1	6.1	3.3	-
ATP synthesis							
ATP synthase F0 sector, subunit B'	*atpF'*	*cj0102*	-	-	-	-	3.5
ATP synthase F0 sector subunit B	*atpF*	*cj0103*	-	-	-	-	4.9
ATP synthase F1 sector delta subunit	*atpH*	*cj0104*	-	-	-	2.1	4.3
ATP synthase F1 sector alpha subunit	*atpA*	*cj0105*	-	-	-	2.2	3.7
ATP synthase F1 sector gamma subunit	*atpG*	*cj0106*	-	-	-	2.1	3.6
ATP synthase F1 sector beta subunit	*atpD*	*cj0107*	-	-	-	-	3.4
ATP synthase F0 sector C subunit	*atpC*	*cj0936*	-	2.3	-	-	2.6
Transport/binding proteins							
Putative MATE family transport protein		*cj0560*	2.2	2.0	2.1	-	-
Degenerate K+-transporting ATPase, B subunit	*kdpB*	*cj0677*	2.1	-	-	-	-
Aspartate/glutamate-binding ABC transporter	*peb1B*	*cj0921c*	2.2	-	-	-	-
Putative glutamine permease	*glnP*	*cj0940c*	-	-	-	-	2.4
Surface, polysaccharides, antigens							
Putative periplasmic protein		*cj0561c*	5.4	5.0	11.2	9.2	11.8
Major antigenic peptide PEB2	*peb2*	*cj0778*	2.1	3.0	2.9	2.1	-
50 kDa outer membrane protein precursor	*omp50*	*cj1170c*	-	-	-	-	4.3
Capsule polysaccharide export system	*kpsM*	*cj1448c*	-	2.1	2.0	2.5	3.2
Miscellaneous							
Protease	*pspA*	*cj0068*	-	-	2.2	2.0	3.7
Peptidyl-tRNA hydrolase	*pth*	*cj0312*	2.2	2.9	3.1	3.6	3.8
Putative endoribonuclease L-PSP		*cj1388*	2.2	2.9	3.0	3.2	2.7

TABLE 2.3 Selected genes two-fold or greater downregulated under hyperosmotic stress.

Functional class	Name	Gene	Fold down-regulation				
			15 min	1.5 hours	3 hours	6 hours	12 hours
Surface, polysaccharides, antigens							
Major antigenic peptide PEB-cell binding factor	*peb4*	*cj0596*	2.1	-	2.0	2.4	6.2
50 kDa outer membrane protein precursor	*omp50*	*cj1170c*	2.6	2.9	-	-	-
Transport/binding proteins							
L-lactate permease	*lctP*	*cj0076c*	-	2.0	-	-	15.8
Degenerate K+-transporting ATPase A subunit	*kdpA*	*cj0676*	-	-	-	-	2.0
Degenerate K+-transporting ATPase, B subunit	*kdpB*	*cj0677*	-	-	-	-	2.2
Bifunctional adhesin/ABC transporter aspartate/glutamate-binding protein	*peb1A*	*cj0921c*	-	-	-	-	4.0
Putative MFS transport protein	*cjaB*	*cj0981c*	-	-	2.0	-	-
Putative amino-acid transporter periplasmic solute-binding protein	*cjaA*	*cj0982c*	2.3	3.2	3.7	2.8	3.9
Putative sodium/proline symporter	*putP*	*cj1502c*	-	-	2.5	4.6	8.7
Amino acid transporter (serine dehydratase)	*sdaC*	*cj1625c*	-	4.9	3.0	2.5	5.9
Chaperones, chaperonins, heat shock, proteases							
ATP-dependent protease peptidase subunit	*hslV*	*cj0663c*	-	-	-	-	3.0
Serine protease	*htrA*	*cj1228c*	-	-	-	-	3.6
Electron transport and TCA cycle							
Molybdopterin containing oxidoreductase		*cj0264c*	3.3	-	7.5	6.2	12.8
Putative cytochrome C-type haem-binding protein		*cj0265c*	4.1	2.6	6.9	8.4	10.2
Putative cytochrome C551 peroxidase		*cj0358*	-	3.1	3.1	2.3	-
Putative malate:quinone oxidoreductase	*mqo*	*cj0393c*	-	-	3.3	4.0	2.9
Putative oxidoreductase subunit		*cj0414*	-	-	-	4.4	9.1
Putative oxidoreductase subunit		*cj0415*	-	-	-	4.7	9.4
Isocitrate dehydrogenase	*icd*	*cj0531*	-	3.0	-	2.8	6.5
Malate dehydrogenase	*mdh*	*cj0532*	2.1	2.2	-	2.2	5.8
Succinyl-coA synthetase beta chain	*sucC*	*cj0533*	-	-	-	2.3	10.3
Succinyl-coA synthetase alpha chain	*sucD*	*cj0534*	-	-	-	-	7.5
2-oxoglutarate-acceptor oxidoreductase subunit	*oorD*	*cj0535*	-	-	-	2.2	6.8
2-oxoglutarate-acceptor oxidoreductase subunit	*oorA*	*cj0536*	-	2.1	-	2.5	7.7
2-oxoglutarate-acceptor oxidoreductase subunit	*oorB*	*cj0537*	-	2.4	-	2.8	8.5
2-oxoglutarate-acceptor oxidoreductase subunit	*oorC*	*cj0538*	-	-	-	2.4	6.7
Bifunctional aconitate hydratase 2	*acnB*	*cj0835c*	-	2.1	-	3.0	4.9
Malate oxidoreductase		*cj1287c*	2.2	2.0	2.5	2.3	-
NADH dehydrogenase I chain N	*nuoN*	*cj1566c*	-	-	2.4	3.0	4.4
NADH dehydrogenase I chain M	*nuoM*	*cj1567c*	-	-	2.3	3.2	4.3
NADH dehydrogenase subunit L	*nuoL*	*cj1568c*	-	-	2.3	2.8	4.6
NADH dehydrogenase I chain K	*nuoK*	*cj1569c*	-	-	2.1	2.7	4.0
NADH dehydrogenase subunit J	*nuoJ*	*cj1570c*	-	-	-	2.5	3.4
NADH dehydrogenase subunit I	*nuoI*	*cj1571c*	-	-	2.5	3.2	4.5
NADH dehydrogenase subunit G	*nuoG*	*cj1573c*	-	-	2.3	3.0	4.3
Citrate synthase	*gltA*	*cj1682c*	-	2.7	2.8	4.0	4.9
Other metabolism							
Putative phosphate acetyltransferase	*pta*	*cj0688*	-	-	-	3.0	6.9
Acetyl-CoA synthetase	*acs*	*cj1537c*	-	-	-	-	6.3
L-serine dehydratase	*sdaA*	*cj1624c*	-	4.1	3.8	3.2	6.8
Amino acid biosynthesis							
Glutamine synthetase	*glnA*	*cj0699c*	-	-	-	2.5	2.2
Aspartate aminotransferase	*aspB*	*cj0762c*	-	2.1	2.8	4.1	6.2
Isopropylmalate isomerase small subunit	*leuD*	*cj1716c*	-	-	-	-	3.0
Isopropylmalate isomerase large subunit	*leuC*	*cj1717c*	-	-	-	-	3.6
3-isopropylmalate dehydrogenase	*leuB*	*cj1718c*	-	-	-	-	4.9
2-isopropylmalate synthase	*leuA*	*cj1719c*	-	-	-	-	4.4

2.4.8 Cross-regulation of oxidative and temperature adaptation and a role for the capsule in *C. jejuni* hyperosmotic stress tolerance

Finally, we investigated whether the above gene expression changes from exposure to hyperosmotic stress might enhance or diminish survivability of *C. jejuni* to other biological stresses, and/or lead to the identification of new genes important for osmotic tolerance. It is known that exposure to one type of stress can condition bacteria against other stresses; for instance, hyperosmotic stress has been shown to increase the thermotolerance and oxidative stress resistance of other food-borne pathogens (132, 155, 163, 189). As the *C. jejuni* hyperosmotic transcriptome showed upregulation of oxidative stress genes (*katA, sodB*) and the majority of the heat shock genes (*groEL, dnaK, grpE, clpB, hrcA, hspR*), we explored whether exposure to hyperosmotic stress would cross-protect *C. jejuni* against oxidative or thermal stress. Logarithmic-phase bacteria were exposed to hyperosmotic stress (1.0% NaCl in MH) for 2 hours, washed, and then subjected to treatment with 5 mM H_2O_2 or heated to 45°C, after which survival was assessed by plating for CFU. Bacteria exposed to hyperosmotic stress were modestly, but significantly, protected against damage by oxidative stress (FIGURE 2.7A), with 2.6-fold more bacteria surviving a 40 minute exposure to 5 mM H_2O_2. In contrast, hyperosmotically stressed bacteria exposed to 45°C heat stress for 20, 40 or 80 minutes showed respective 13.9-, 135.2-, and 8.5-fold losses in culturability compared to *C. jejuni* not pre-treated with + 1.0% NaCl (FIGURE 2.7B). The transcriptome also revealed that *kpsM*, encoding the CPS export system inner membrane protein, was upregulated in hyperosmotic stress. A *kpsM* mutant (Δ*kpsM*) exhibited a 100-fold growth defect on solid hyperosmotic medium (FIGURE 2.7C), identifying the CPS or the capsule export apparatus as an important factor for *C. jejuni* hyperosmotic stress survival.
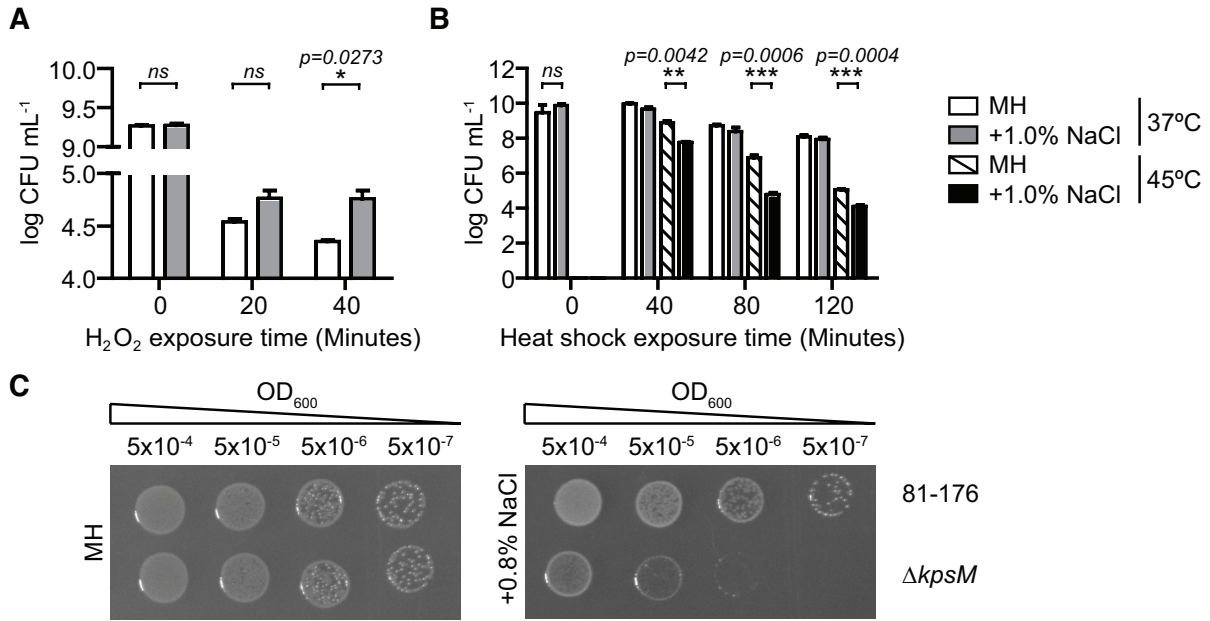
FIGURE 2.7 Hyperosmotic exposure cross-induces protective and detrimental effects on oxidative and heat shock stress responses respectively, and the capsular polysaccharide protects against salt stress.
Bacteria were incubated in 1.0% NaCl for 2 hours then exposed to (A) 5 mM H_2O_2 over 40 min or (B) 45°C conditions over 120 min. Cross-protection against oxidative stress but decreased tolerance to thermal stress occurred following hyperosmotic shock. Error bars represent three biological replicates. (C) Serial 10-fold dilutions of OD-standardized wild-type and $\Delta kpsM$ bacteria were spotted on MH agar +/- 0.8% NaCl. $\Delta kpsM$ exhibited increased sensitivity to hyperosmotic conditions; *, $p \leq 0.05$; **, $p \leq 0.01$; ***, $p \leq 0.001$.

2.5 DISCUSSION

The ability to adapt to a range of osmolarities is critical to the survival of bacteria under varied conditions and niches. In this study, we carried out the first comprehensive analysis of the *C. jejuni* response to hyperosmotic stress. Standard MH growth medium (0.307 osmol L^{-1}) was used as a baseline, with growth tested in osmolarities up to 0.99 osmol L^{-1} (+2.0% NaCl). Culturability similar to unsupplemented media was observed up to 0.48 osmol L^{-1} (+ 0.5% NaCl). At 0.64 osmol L^{-1} (+ 1.0% NaCl), a distinct pattern emerged whereby *C. jejuni* underwent an adaptive lag followed by normal logarithmic growth, then late stage culturability defects. Chaining also increased during late logarithmic

growth in +1.0% NaCl, peaking at 12 and 24 hours as CFUs declined. At 0.82 osmol L^{-1} (+ 1.5% NaCl), growth was significantly impaired, with complete growth arrest and loss of motility at or above 0.99 osmol L^{-1} (+ 2.0% NaCl), which we speculate is indicative of lethality. Examination of multiple ionic and nonionic stressors established that the minimum inhibitory osmotic concentration was identical for all compounds (0.620 total osmol L^{-1}), as were phenotypic outcomes such as chaining. Based on these similarities and the growth profile data, we selected MH + 1.0% NaCl broth or MH + 0.8% NaCl plates as representative conditions to explore the nature of hyperosmotic-induced chains, investigate global gene expression changes, assess cross-regulation with other stress responses, test the effect of loss of specific gene products on surviving hyperosmotic stress, and uncover aspects of population heterogeneity that were revealed or induced by hyperosmotic stress conditions.

C. jejuni formed long, helical chains in hyperosmotic stress. This 'defective' cell division is commonly observed for numerous bacterial species under stress conditions (164, 190); for instance, during hyperosmotic stress for the *C. jejuni*-related ε-proteobacteria *H. pylori* and the δ-proteobacteria *Desulfovibrio vulgaris* (153, 187). Other biological stresses such as heat and oxidative shock, certain antibiotics, DNA damage, exposure to grazing by single-celled eukaryotes, and mutation or alteration of the stoichiometry of cell division components also give rise to filamentous morphologies (191). It remains unclear as to the molecular mechanisms that inhibited complete *C. jejuni* cell separation, although we speculate potential involvement of the heat shock chaperones, which have roles in ensuring proper division (192-194). Filamentous bacteria have traditionally been viewed as abnormal, sick members of the population (191, 195, 196), but more recent evidence indicates an importance in bacterial survival and pathogenesis (169). For example, filamentous uropathogenic *E. coli* can evade phagocytosis by neutrophils due to their large size (197), and the helical filamentous forms of *Caulobacter crescentus* have increased resistance to

heat, oxidative stress and changes in pH (198). In our study, increased chaining correlated with decreased CFU counts. Since chains are composed of numerous daughter cells but likely only give rise to one macroscopic colony on a Petri plate, chains may affect the accuracy of viable counts in our analyses and in food safety assessments. Furthermore, our observations indicated that the *C. jejuni* chains were motile and therefore likely as viable as non-chained bacteria.

The temporal transcriptional response to added 1.0% NaCl revealed a number of interesting gene expression profiles. Striking changes occurred in the acute phase of adaptation, with upregulation of genes for the endogenous synthesis of potential osmoprotectants glutamate and glutamine (*gltD, glnA*) and genes encoding chaperones and regulators in various heat shock operons (*hrcA, grpE, dnaK, groEL*). The cytoplasmic glutamate pool increases in most microorganisms after exposure to high osmolarity media to counter charge imbalances imposed by K^+ accumulation (152), and increased transcription of genes encoding enzymes involved in glutamate/glutamine production suggests the conservation of this role in *C. jejuni*. It is possible that osmotic adaptation in *C. jejuni* may also be due to increased expression of the heat shock proteins as *C. jejuni* preferentially uses glutamate as a carbon source (29), and while high *gltD* and *glnA* expression was transient, the heat shock proteins were expressed at high levels continuously. Despite evidence of increased thermotolerance in other enteric pathogens such as *E. coli* and *Salmonella* spp. following osmotic challenge and upregulation of heat shock proteins, we observed decreased survival for *C. jejuni* under 45°C heat shock following exposure to hyperosmotic conditions. Upregulation of heat shock genes may account for this decreased ability to respond to heat upshock, as increased heat sensitivity was also observed for a *C. jejuni* mutant in the heat shock gene repressor HspR (127). Expression of heat shock genes is not a typical response to osmotic stress in *E. coli* (189), but has been observed for *H. pylori* (153, 199) and *Lactococcus lactis* (134), suggesting that heat shock proteins are deployed by a wide variety of

bacteria to counter hyperosmotic stress-induced protein misfolding and other damage (115, 127, 128, 199, 200).

The *C. jejuni* hyperosmotic stress transcriptome shares key expression changes with the transcriptome of *C. jejuni* in a rabbit ileal loop (intra-intestinal) model (162). This includes upregulation of heat shock and oxidative stress genes and downregulation of the NADH dehydrogenase *nuo* and several TCA cycle genes. Both conditions also resulted in upregulation of transcripts for the CbrR bile response regulator and the KpsM capsule export protein. This suggests that the hyperosmotic stress response may play an important role in vivo. When we compared our expression results to hyperosmotic transcriptional profiling studies in *E. coli* (189) and *Pseudomonas aeruginosa* (165), very few similarities were observed, reinforcing our observation that the long-term *C. jejuni* osmotic response is atypical. To the best of our knowledge, the only similarity between these studies was upregulation of anti-oxidative catalases (*katE* in *E. coli* and *P. aeruginosa* and *katA* in *C. jejuni*). In contrast, *C. jejuni* shares several expression changes with the more closely related *D. vulgaris* (187). Like *C. jejuni, D. vulgaris* salt stress microarray profiling and proteomics showed upregulation of oxidative stress pathways, the ATP synthase, and the tryptophan biosynthesis operon (*trp*). However, despite this commonality, and like *E. coli* and *P. aeruginosa, D. vulgaris* possesses proline and glycine betaine transporters/synthesis machinery (absent from *C. jejuni*) and K$^+$ uptake and signalling systems, and mounts a more typical response to hyperosmotic challenge. In *E. coli* and most bacteria, a two-component signal transduction system and high affinity K$^+$ transporter are encoded by the osmoresponsive *kdp* operon (115, 171, 172). Members of the *kdp* operon are truncated or missing in *C. jejuni*, and only *kdpB* (ATPase catalytic subunit) appears to encode a functional protein. We noted that *kdpB* was transiently upregulated following osmotic upshock. The gene for *kdpB* also contains a hypervariable sequence, so expression of this gene may phase-off/on (19). It is possible that KdpB interacts

with other translocation channels, but further study is required to ascertain if *kdpB* participates in *C. jejuni* osmotolerance.

We also observed upregulation of *kpsM* under hyperosmotic stress and demonstrated that the acapsular Δ*kpsM* mutant was sensitive to hyperosmotic stress. The capsular polysaccharide of strain 81-176 is phase variable and important for serum resistance, invasion of epithelial cells, and virulence in a ferret diarrheal disease model (27, 201). Other bacteria, including *E. coli* and *Vibrio cholerae*, actively increase or utilize modified capsular polysaccharides to tolerate osmotic changes, protecting the bacterium from additional stresses, such as desiccation and antibiotics (202, 203). We have now established a role for the *C. jejuni* capsule in resisting hyperosmotic stress and hypothesize that this may in part contribute to colonization defects in capsule-minus mutants.

An unexpected outcome of this study was the identification of significant intercellular heterogeneity within an apparently isogenic population. The genetic factors or processes that govern heterogeneity remain to be determined. Nonetheless, as shown by three different single cell analyses, variation in osmotic sensitivity in the population was apparently unimodal under standard conditions (FIGURE 2.5B-C; FIGURE 2.6A-B, top), but became notably bistable/bimodal after either selection of single colonies on standard MH agar (FIGURE 2.5D-E) or by growth in salt stress conditions as indicated by colony morphology and p*atpF'*-GFP expression (FIGURE 2.6A-B, bottom) (this will be discussed further below). Surprisingly, variation was also observed between cells constituting single chains. At present it is difficult to determine if heterogeneous 'variants' within chains are biologically important, but it is of note that similar observations were reported for chains of *Lactobacillus plantarum* under acid stress (204). PI entry or extrusion from chains could be associated with membrane alterations, increased efflux pump activity, or even DNA supercoiling. As with other types of population heterogeneity, it can be

envisaged that chains with heterogeneous member cells may be better prepared for diverse new challenges than a completely homogeneous chain. For example, one cell in the chain with the necessary fitness characteristics could quickly take advantage of a suddenly available nutrient and survive or out-compete other bacteria. Other cells of the chain may in turn be better suited to re-adapt to non-stressed conditions. Collectively, those heterogeneous single cells could allow survival of the chain under numerous different circumstances.

We also observed that clonal isolates from a wild-type *C. jejuni* population propagated under standard growth conditions exhibited salt sensitivity (FIGURE 2.5). Because 79% of the progeny from sensitive clones retained sensitivity compared to 22% of the progeny from the original population, populations derived from sensitive clones were quantitatively more sensitive to hyperosmotic stress and mimicked a 'stable' phenotype. However, in all instances sensitive isolates also exhibited the ability to re-generate progeny with original wild-type sensitivity levels. The presence of these stress-fit progeny indicates a population subset optimized for growth in hyperosmotic and other potential stress conditions. Given that the *kpsM* mutant was salt-sensitive, and the relative rate with which these sensitive isolates occurred, we initially suspected the involvement of capsule phase variation (3); however, sensitive isolates retained their capsule. We hypothesize that additive point mutations and/or phase variation of contingency loci likely contribute to this phenomenon. Why *C. jejuni* would generate sensitive (defective) subpopulations is unclear, but these heterogeneous clones may have increased fitness at lower osmolarities or attributes important for other times in the *C. jejuni* lifestyle. It is also of note that our sensitivity experiments were carried out following continuous growth on laboratory media, whereas in nature, frequent nutrient limitation and simultaneous action of other stresses are more typical. *C. jejuni* variation will almost certainly be more abundant or useful under such circumstances. Even within the laboratory, it is important to recognize that heterogeneity between

single colonies may result in pleiotropic effects that can influence the outcome of experiments. Observations of heterogeneity are also a reminder that transcriptomic gene expression profiles, while highly useful, can only provide information on the average behavior of bacteria in a population.

We also observed bimodal heterogeneity in the colony size of wild-type *C. jejuni* plated on MH plates + 0.8% NaCl (FIGURE 2.6A). Cells differentially expressing GFP from the *atpF'* promoter following growth in MH broth +1.0% NaCl likewise exhibited bistable survival characteristics (FIGURE 2.6B). Bistability is a biological phenomenon that typically arises randomly from expression fluctuations in a master regulatory gene (173, 175). This suggests that osmotic stress may influence the expression of a *C. jejuni* regulator controlling metabolic process(es), as both colony size and ATP synthase expression suggest a correlation with growth rate. The more phenotypically stable salt sensitive clones described above may also contribute to the bistability observed for colony size and ATP synthase expression. A model for this is *E. coli hip* (**h**igh **i**ncidence of **p**ersister) mutants that exhibit an increased abundance of cells in the persister state (dormant cells that can survive exposure to antibiotics and other stresses) versus actively growing cells (173, 205). We envision that '*hip*-like' mutations in *C. jejuni* may increase the abundance of certain subpopulations. For example, a 'salt-sensitive' mutation could increase the abundance of the non-culturable GFP$_{low}$ subpopulation, which would be perceived as sensitivity on hyperosmotic media. However, there are also likely to be mutations arising in true osmotolerance genes. Overall, the most plausible explanation for multiple mechanisms of population heterogeneity is that it is a defensive 'bet-hedging' strategy – i.e., a cautious investment in diverse phenotypes that weighs the loss of growth efficiency under a certain condition against the chance of lethality if conditions change abruptly (175). Ongoing and future work is aimed at uncovering genes and molecular mechanisms driving

these potentially complex layers of heterogeneity within a clonal *C. jejuni* population.

Finally, it is of note that the human intestine has been reported to have a lower osmolarity [0.27 – 0.29 osmol L^{-1} (161)] than the chicken cecum [0.70 osmol L^{-1} (168)], which in turn has a lower osmolarity than the chicken duodenum [0.90 osmol L^{-1} (168)]. As FIGURE 2.1A illustrates, these conditions span the osmolarities assessed in our study, with MH medium more closely approximating human intestinal conditions and the +1.0% NaCl condition somewhat approximating the chicken cecum. While numerous other factors influencing *C. jejuni* growth, survival, and behavior are obviously present in vivo than in vitro (i.e., other bacteria, metabolites, mucus, host cells, additional stressors, potential buffers and as-yet-unidentified compatible solutes, osmolarity changes during digestion and water reabsorption, etc.), this study may at least partially reflect differential conditions *C. jejuni* encounters as it traverses *in vivo* niches. Future work characterizing additional genes dysregulated under hyperosmotic stress and exploring molecular strategies modulating population heterogeneity should lend insight into the fundamental processes that allow *C. jejuni* to survive stress conditions and prevail as a major food-borne pathogen.

CHAPTER THREE: High frequency genetic variation of purine biosynthesis genes is a mechanism of success in *Campylobacter jejuni*

3.1 SYNOPSIS

Phenotypic variation is prevalent among progeny of the zoonotic pathogen *Campylobacter jejuni.* Heterogeneity bestows increased survival to bacterial populations because variable phenotypes ensure that some cells will be protected against hostile stress conditions. Exposure to hyperosmotic stress revealed prevalent resistant/sensitive growth differences between *C. jejuni* strain 81-176 colonies. These isolated colonies continued to produce cells with differential phenotypes. Whole-genome sequencing discovered allelic variants of two purine biosynthesis genes, *purF* and *apt*, which encode phosphoribosyltransferases that utilize a shared substrate. Genetic analysis determined that only *purF* was an essential gene, but *apt* was critical for fitness. Further population analysis confirmed extensive genetic variation of *purF/apt* that resulted in viable alleles from in-frame insertion duplications, deletions, or missense polymorphisms. Exposure of *purF/apt*-genotyped colonial variants to a variety of niche-relevant stresses determined that alleles were associated with differential stress survival, thus contributing to the total population phenotype distribution. Alleles also contributed to differential intracellular survival in an epithelial cell model of infection. Via high-depth amplicon sequencing, the intracellular *purF/apt* mutant distribution was tracked during infection, and intracellular survival was found to select for stress-fit *purF/apt* alleles, as did exposure to oxygen and hyperosmotic stress. Potential protein binding sites were identified in *purF/apt*, and a preliminary DNA-protein affinity screen captured a potential exonuclease that promoted the global spontaneous mutation rate. Taken together, the current study illustrated adaptive properties of novel high frequency genetic variation of two required housekeeping genes, and thus identified a mechanism of pathogen success.

3.2 INTRODUCTION

The helical bacterium *Campylobacter jejuni* is notable for extensive intrapopulation genetic variation. As revealed by the first genome sequence of *C. jejuni* NCTC11168 (19), much of this genetic variation is dubbed "phase variation", and results from lengthening/shortening of simple sequence repeat homopolymeric nucleotide tracts, influencing the expression or functionality of surface-structure genes primarily involved in flagellar motility (80, 206, 207), lipooligosaccharide structure (90), and capsular polysaccharide biosynthesis (208). Variation of these "contingency loci" is accepted as an important lifecycle strategy of *C. jejuni* and other important pathogens, promoting niche/host adaption, virulence, and/or antigenic diversity for immune system evasion (209). Thus, genetic variation is thought to enable the global success of *C. jejuni* as the leading cause of bacterial food-borne diarrheal disease and the most frequent antecedent to Guillain-Barré syndrome demyelinating polyneuropathy (210).

Phase variation in homopolymeric tracts is thought to occur via slip-strand mispairing (SSM) during DNA synthesis. Since *C. jejuni* does not possess homologues of DNA mismatch repair (MMR) systems (*mutS, mutL, mutH*) (19, 211), the failure to detect and repair SSM is thought to facilitate the high frequency of phase variation, which is experimentally determined to be between 10^{-3} to 10^{-5} mutations/cell division (207). In this current study, we describe novel high frequency genetic mutations associated with colony phenotypic variation that is unusual for several reasons: (I) the affected genes were not involved in the biosynthesis of surface-exposed structures; (II) the genetic variation was not mediated by homopolymeric tracts; and (III), unlike homopolymeric tract changes, the DNA sequence changes described below did not result in frameshift truncations, but are predicted to result in relatively modest amino acid sequence changes. Therefore, the variation did not result in the "ON-OFF" phenotypic behavior of phase variation, but enabled a spectrum of phenotypic outcomes

between individual bacteria. As we demonstrate, this genetic diversity occurred in two purine biosynthesis genes, and drove adaptive "bet-hedging-like" phenotypic behavior, and thus enabled niche exploitation through multistress resistance/sensitivity to promote the success of *C. jejuni*.

3.3 METHODS AND MATERIALS

3.3.1 Bacterial strains, colony isolation and growth conditions

Studies were performed with *C. jejuni* human isolate strain 81-176 (33), unless otherwise stated (see TABLE A.1.2 for a full list of bacterial strains and plasmids). Strain 81-176, as used in our laboratory, was purified as a single colony then passaged 1X on MH agar from a stock of 81-176 received from Patricia Guerry (NRMC), which is the lineage of the TIGR-sequenced 81-176 (212). *C. jejuni* was grown on MH agar or broth (Oxoid), supplemented with vancomycin (10 µg ml^{-1}) and trimethoprim (5 µg ml^{-1}), in microaerobic/increased-CO_2 atmosphere (6% O_2, 12% CO_2) in a Sanyo tri-gas incubator (solid media), or generated via CampyGen (Oxoid) system (shaken broth cultures). For colony variant identification, strains were plated to give ~150 colonies/per plate on MH agar, and grown for 48 h. Individual colonies were selected and inoculated into 200 µl of MH broth in each well of a 96-well plate, and grown for 24 h prior to preservation/phenotypic testing.

3.3.2 Deletions, allelic complementation, and fluorescence microscopy

All PCR was performed with high-fidelity iProof polymerase (Bio-Rad). For replacement deletion, the *purF* and *apt* genes were PCR-amplified from 81-176 genomic DNA with oligonucleotides 6409/6410 and 6413/6414 respectively, and ligated to pGEM-T vector (see TABLE A.2.2 for oligonucleotides). Inverse

PCR-amplification of the resulting plasmids with oligonucleotides 6411/6412 and 6415/6416, introduced *Kpn*I/*Xba*I and *Kpn*I/*Bam*HI restriction sites. Similarly-digested apramycin resistance cassettes from pAC1A (2) were ligated to the inverse PCR products. Resulting plasmids were introduced into *C. jejuni* 81-176, and homologous recombinants were selected for on MH agar containing 60 µg ml^{-1} apramycin. Transformants were only recovered for Δ*apt::apr*^{R}. Deletion of *cj1132c* was carried out via similar methodology. Allelic complementations/gene-introductions were performed via introduction of *purF/apt* allele variant operons or other constructs into the appropriate strain with the genome-insertional gene-delivery plasmids pRRH or pRRA (2). For fluorescent microscopy, 1 µl bacterial culture was incubated with 30 µM propidium iodide and 1 µl Alexa Fluor® 350 annexin V conjugate (Life Technologies) for 10 minutes prior to mounting on a 1.0% agarose pad for visualization. Cells were imaged at 100x with a Nikon TE 2000-U microscope equipped with an argon-ion laser (EXFO X-Cite), and a CCD-camera (Hamamatsu).

3.3.3 Phenotypic stress assessments, ATP determination and cell infection

To ascertain mutant phenotypes, single colony cultures in 96-well plates were diluted with MH broth to an OD_{600} of 0.05, and 5 µl was spotted on test condition plates. Test conditions included MH agar + 0.8% NaCl, +1.0% NaCl, growth at 42°C/45°C, and 72 h aging or exposure to atmosphere for 48 h prior to resumption of growth in standard conditions. Growth/non-growth of spots were quantified from scanned plates by ImageJ densitometry tools, and converted to heatmap visualizations via Matrix2png (178). NaCl-sensitivity/resistance phenotypes were analyzed by plating serial dilutions of OD_{600} 0.1 of representative strains on MH or MH + 1.0% NaCl agar and enumerating CFU. Luciferase-based ATP determination was carried out on dilutions of OD_{600} 0.2 of *C. jejuni* exposed to 1.0% NaCl for 30 s, and quantified by Varioskan

luminometer (Thermo Scientific) as per manufacturer's instructions (ATP determination kit, Life Technologies). Cell infection gentamicin protection assays were performed with INT 407 intestinal epithelial cells, as previously described (213). <u>A</u>ry<u>s</u>ulfa<u>t</u>ase (AstA) assays were performed as previously described (214). All T-test statistical analyses were performed in Prism (GraphPad) unless otherwise stated.

3.3.4 Conventional, whole-genome and amplicon sequencing

Genomic DNA for all experiments was harvested via Wizard genomic DNA purification (Promega). Conventional dideoxy Sanger sequencing was performed at GENEWIZ on high-fidelity PCR-amplified DNA using the listed oligonucleotides (TABLE A.2.2), and manually assembled and verified. Whole-genome sequencing of five isolates to a depth of ~16x was performed on the 454 GS FLX Titanium (Roche 454) sequencing platform. Shotgun library preparation, read mapping, and variant analysis were performed according to established procedures (215). Amplicon sequencing of *purF/apt/prsA* was performed on the Illumina MiSeq system. To avoid PCR bias, optimized semi-universal oligonucleotides were designed for minimized 25-cycle PCR reactions, and resulting amplicons were used in the preparation of Nextera XT libraries, as per manufacturer's preparation guide (Illumina). Variant discovery was performed using GATK (Broad Institute) software (variant information not shown).

3.3.5 SILAC-based DNA-protein interaction screen

Affinity capture of DNA-binding proteins from <u>s</u>table <u>i</u>sotope <u>l</u>abeled <u>a</u>mino a<u>c</u>id (SILAC) extracts was performed as previously described (216), with modification. Briefly, *C. jejuni* (Δ*argH::cat* arginine auxotroph, unpublished) was metabolically labeled with 400 μM either light $^{13}C_6$-arginine or heavy $^{14}N_4{}^{13}C_6$-

arginine (Cambridge Isotope Laboratories) as the SILAC amino acid in modified DMEM medium (Sigma, supplemented with 20 mM glutamine, 10 μM iron ascorbate) and lysed via sonication in 50 mM Tris pH 8.0, 150 mM NaCl, 0.1% Triton X-100. Affinity purifications were performed with biotinylated Biotin-TEG-dsDNA *purF* "bait" (or *prsA* control DNA) immobilized on streptavidin beads (Invitrogen). Protein–DNA complexes were pooled, eluted by PstI (NEB) restriction enzyme cleavage, digested with ArgC, and purified peptides were analyzed by reverse phase LC-MS. MaxQuant (217) was used for identification and quantification for data from two independent experiments (data not shown) were statistically assessed with a Benjamini-Hochberg false discovery rate of 0.05 (Perseus).

3.4 RESULTS

3.4.1 Whole-genome sequencing identification of *purF* and *apt* mutations in colonial variants

Previous work identified prevalent phenotypic heterogeneity among single colonies of *C. jejuni* strain 81-176, observed in their relative survival fitness after transfer to Mueller-Hinton (MH) agar supplemented with 1.0% NaCl (hyperosmotic stress)(1). Briefly, colonies grown on MH agar were selected and then spotted on NaCl-containing medium and assessed for growth or non-growth (cartoon schematic, FIGURE 3.1A). Hyperosmotic stress sensitivity/resistance differences were observed between individual colonies. To assess the heritability of these phenotypes, progeny from five sensitive colonies (maintained on MH without added NaCl) were tested for sensitivity/resistance to hyperosmotic stress as before. The majority of the progeny colonies retained the sensitive parental phenotype, but frequent phenotypic reversion was evident (FIGURE 3.1B). To quantify the phenotypic difference between the 5 sensitive isolates and

the heterogeneous wild-type, OD-standardized cultures were plated on MH or MH + 1.0% NaCl, and colony counts were taken. Approximately 30% of the heterogeneous population survived hyperosmotic challenge, but only 3-7% of the populations derived from the sensitive isolates survived (FIGURE 3.1C). To determine if these growth defects were due to a genetic cause, whole-genome sequencing of the five sensitive strains and the parental wild-type was carried out via 454 pyrosequencing to depth of ~16x. Variant analysis detected a single non-synonymous mutation with 100% variation frequency in each of the five sensitive strains, occurring in either of two ORFs; *CJJ81176_0227* (encoding the glutamate amidophosphoribosyltransferase PurF), and *CJJ81176_0934* (encoding the adenine phosphoribosyltransferase Apt). Of the five mutations, 3/5 were distinct changes in *purF* (FIGURE 3.1D); colony variant two was a G-C transversion resulting in an A304G mutation, colony three was a C-T transition resulting in a G292S mutation, and colony five was a 3bp insertion resulting in the deletion/insertion G95delinsGV. The *apt* mutation was identical in the remaining 2/5 colonies, thus colonies one and four harbored a T-C transition resulting in an I61T change in Apt. The operons of *purF* and *apt* encode genes of unrelated or unknown function, and are not found nearby each other on the chromosome (FIGURE 3.1E). PurF and Apt share domain homology (FIGURE 3.1F), and both *purF* and *apt* are purine biosynthesis pathway genes encoding phosphoribosyltransferases that use 5-phospho-α-D-ribose-1-diphosphate (PRPP) in their respective reactions (FIGURE 3.1G).
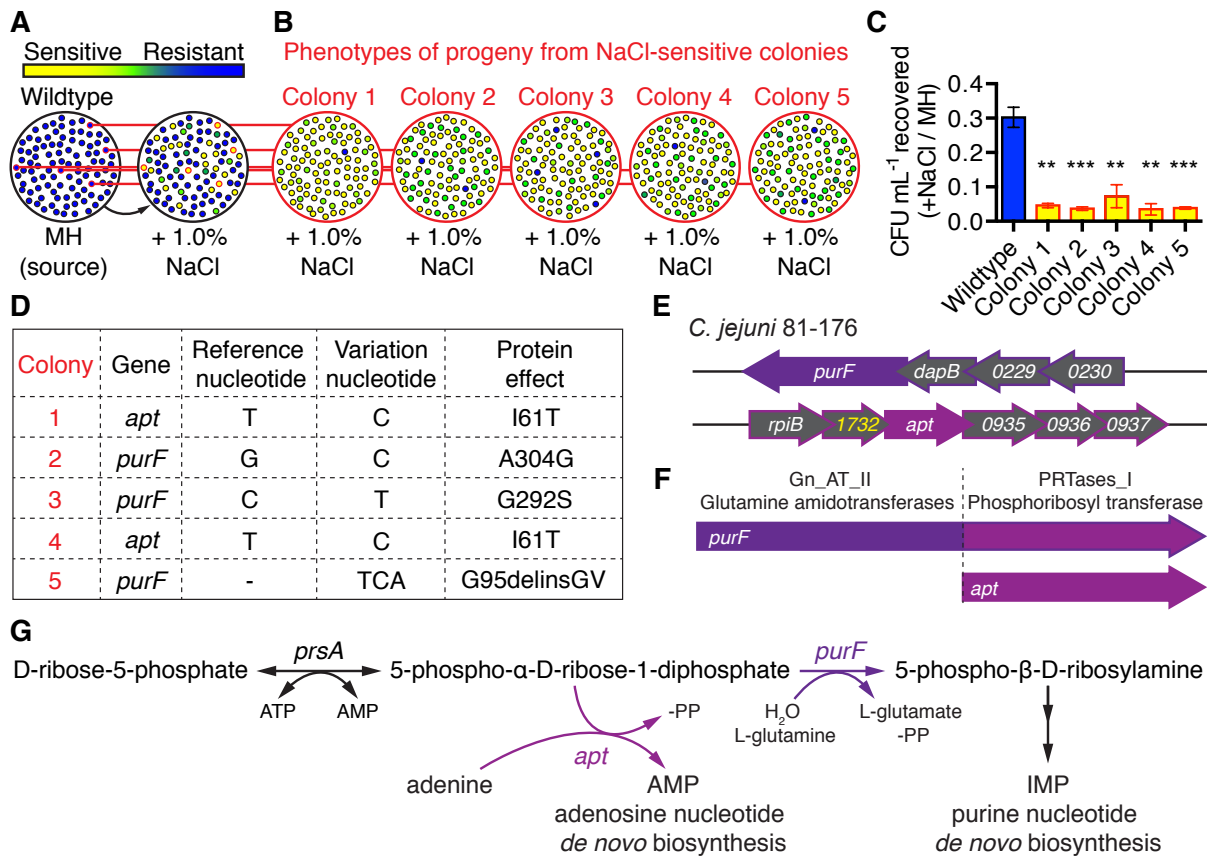
FIGURE 3.1 Heritable colony stress phenotype variation linked with *purF* and *apt* mutations.

(A) Schematic illustration depicting 100 single colonies (blue), with defective growth/sensitivity (yellow) revealed after transfer to Mueller-Hinton (MH) agar + 1.0% NaCl (hyperosmotic stress). (B) Heritability assessment of phenotypes of 100 progeny each derived from five sensitive strains. The five strains were maintained on MH (red outline) prior to phenotypic testing of their progeny on MH + 1.0% NaCl. (C) Relative NaCl-stress sensitivity of colony isolates compared to parental wild-type. Mean with SEM from three independent experiments, presented as ratio of CFU recovered on MH + 1.0% NaCl vs. CFU recovered on MH only; **, P ≤ 0.01; ***, P ≤ 0.001. (D) Whole-genome sequencing identification of a single mutation with 100% variant frequency in either *purF* or *apt* in each sensitive strain, with anticipated protein effect. (E) Genomic loci of *purF* and *apt*. (F) Conserved domains of *purF* and *apt*. (G) Purine biosynthesis pathway schematic with purine substrates involved in *purF* and *apt* reactions.

3.4.2 Deletion of *apt* results in growth defects, and a *purF* deletion mutant cannot be generated

To determine if the detected mutations in *purF*/*apt* were equivalent to loss-of-function deletion mutants, deletion of *purF*/*apt* was attempted via antibiotic marker replacement. Deletion of *purF* was not possible in the absence

of a second gene copy (not shown). Thus, *purF* was an essential gene. Deletion of *apt* was possible, but the $\Delta apt::apr^R$ strain (Δapt) was severely growth-compromised, which was assessed by plating OD-standardized equivalents from wild-type and Δapt cultures for CFU quantification. In comparison to wild-type, the Δapt strain produced 10^7-fold fewer CFU (FIGURE 3.2A), and was recalcitrant to further genetic modification (not shown). Microscopy of 6-hr (log-phase) cultures revealed aberrant Δapt morphologies, which was explored with phosphotidylserine-binding fluorescent annexin V, and DNA-binding ethidium bromide, which respectively revealed widespread permeabilization and lysis of Δapt bacteria, and the presence of extracellular DNA (FIGURE 3.2B). Since Δapt was highly defective, it was not useful for comparative studies. Overall, these data showed that the sequenced *apt* mutants were unlike the *apt* deletion strain. Furthermore, *purF* deletion was impossible; thus, the sequenced mutations resulted in *purF/apt* alleles that did not confer complete loss-of-function.
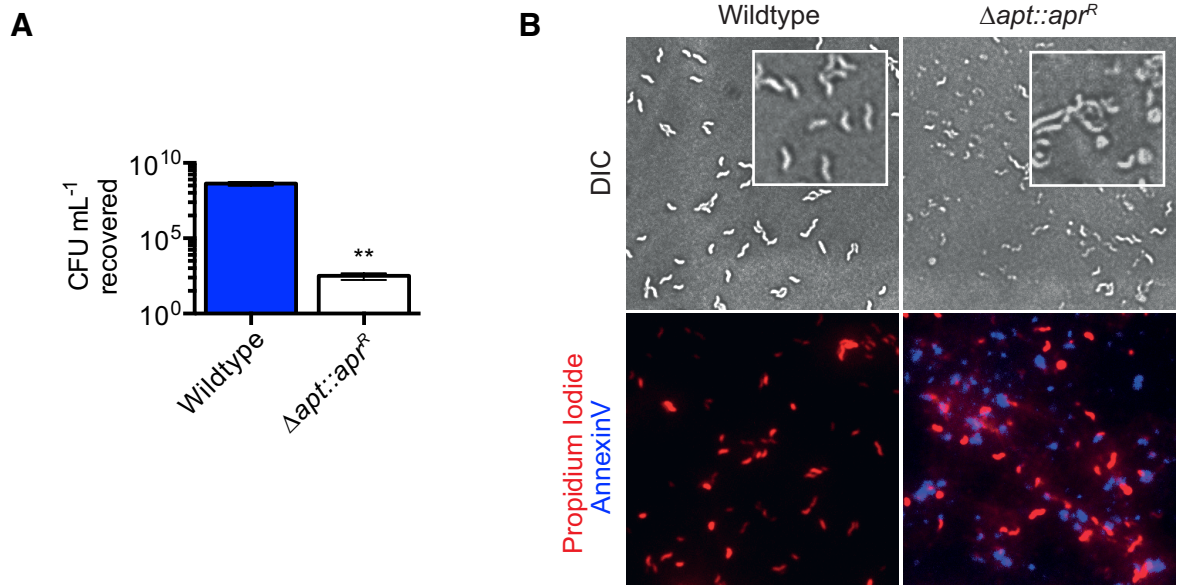
FIGURE 3.2 Effect of *apt* deletion.
(A) Relative CFU recovered on MH from OD-equivalent cultures of the parental wild-type and $\Delta apt::apr^R$ strains. Mean with SEM from six independent experiments; **, P $\leq$ 0.01. (B) Brightfield and fluorescence microscopy examining morphology and integrity of wild-type and $\Delta apt::apr^R$ strains. Fluorescence microscopy samples were co-stained with propidium iodide for DNA (red) and annexin V conjugate for permeabilization/phosphotidylserine (blue). Representative field-of-view of two independent experiments.

3.4.3 Allelic complementation restores resistant phenotypes to sensitive isolates

To show that *purF/apt* alleles were responsible for the observed sensitive/resistant phenotypes, allelic complementation was performed via chromosomal integration of *purF/apt* variants in operon context (FIGURE 3.3A). Insertion of the sensitive *purF*A304G or *apt*I61T allele into wild-type did not result in hyperosmotic sensitivity (FIGURE 3.3B). Insertion of the reference *apt* copy into the *apt*I61T strain, and insertion of another *purF* allele into the *purF*A204G mutant rescued the hyperosmotic defects of both strains (FIGURE 3.3C). A new mutation was identified in the *purF* genetic construct used for the allelic complementation, thus complementation was not via the known reference *purF* sequence, but with a *purF*T91del allele.
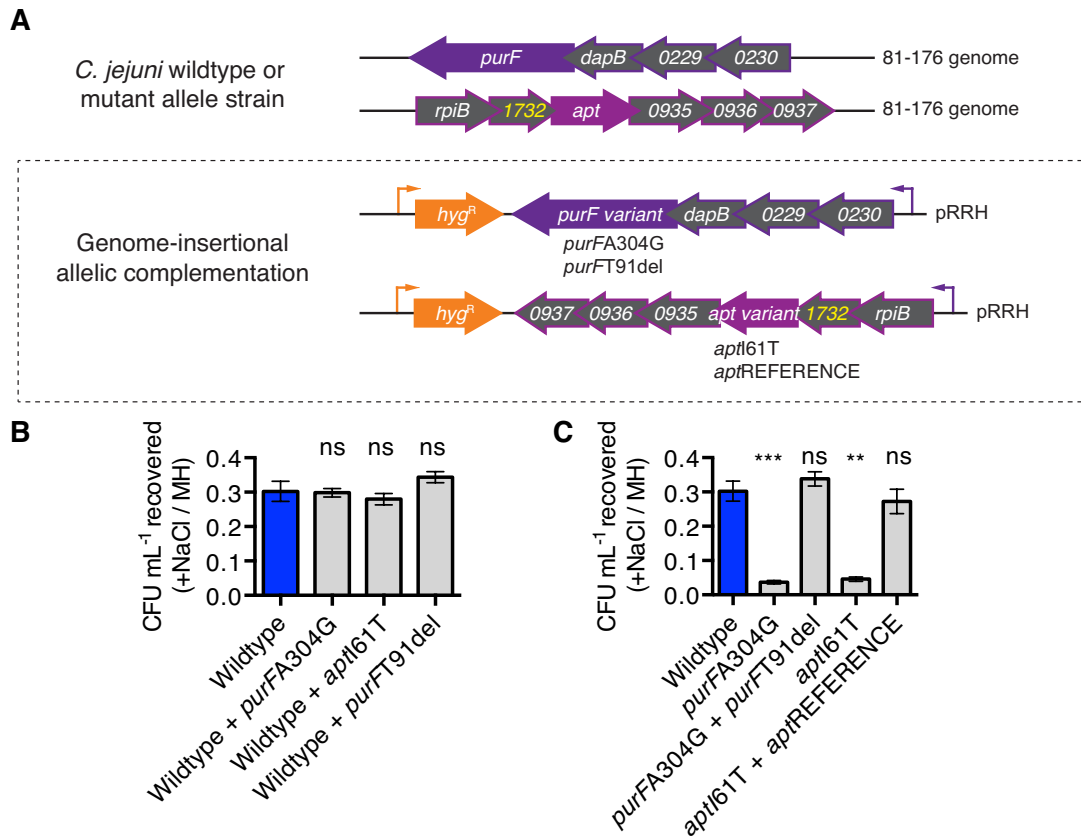
FIGURE 3.3 Effect of allelic complementation with *purF* and *apt* sequence variants.
(A) Schematic of wild-type gene loci and plasmid-borne construct for allelic complementation. Non-native gene-dosage/differential expression of *purF/apt* confounded initial allelic complementation experiments; thus, allelic complementation was performed with *purF/apt* variants in native operon context, inserted into the genome via gene-delivery plasmid pRRH. (B) Relative NaCl resistance/sensitivity of parental wild-type after introduction of variant alleles. CFU enumerated from OD-standardized cultures plated on MH or MH + 0.8% NaCl agar. Mean with SEM from three independent experiments, presented as ratio of CFU recovered on MH + 1.0% NaCl vs. CFU recovered on MH only; ns, not significantly different compared to wild-type. (C) Relative NaCl resistance/sensitivity of single colony isolates after introduction of reference/variant alleles. CFU enumerated from OD-standardized cultures plated on MH or MH + 0.8% NaCl agar. Mean with SEM from three independent experiments, presented as ratio of CFU recovered on MH + 1.0% NaCl vs. CFU recovered on MH only; ns, not significantly different compared to wild-type; **, $P \leq 0.01$; ***, $P \leq 0.001$.

3.4.4 Differential phenotypes of single colony isolates are associated with high-frequency variation of *purF* and *apt*

A comprehensive analysis of the allelic variation in the heterogeneous population was carried out to associate *purF/apt* genotypes to stress-related

phenotypes. From the parental heterogeneous population, 96 colonies were chosen randomly for growth in MH broth for preservation and genomic extraction. Via traditional Sanger dideoxy methodology, the *purF*, *apt* and *prsA* genes from each of the 96 single colonies were PCR-amplified and sequenced. The *prsA* sequencing control was chosen because the gene product acts upstream of *purF*/*apt* in purine biosynthesis (FIGURE 3.1G). PrsA is the ribose-phosphate pyrophosphokinase encoded by *CJJ81176_0925*. The 96 colonies were simultaneously tested under a variety of stress conditions using OD-standardized equivalent cell numbers spotted onto MH agar, which either contained the stressor (NaCl) or was subjected to a stress/combination stress (atmospheric O_2 exposure, 42°C/45°C). The effects of aging/stationary phase were examined by growing the 96 single colony isolates for 72 hours prior to testing. The resulting growth/non-growth phenotypes of each of the 96 strains/spots was digitized into a heat map and arranged by *purF*/*apt* genotype (FIGURE 3.4A).

Certain sibling alleles of *purF*/*apt* were highly associated with corresponding phenotypes. Colonies with sensitive phenotypes were most obvious, and comprised 20% - 30% of the total colonies tested, verifying previous estimations (1). Multistress sensitivity was associated with specific alleles (e.g. *purF*G95V, *purF*G292S, *apt*E154A), as were resistant phenotypes to other mutations (e.g. *purF*V336F). In contrast, a number of sibling families continued to display phenotypic variation between isolated colonies bearing the same mutation (e.g. *purF*V93_D96del). Overall, the different stresses were closely related in terms of phenotypic outcome, as such a NaCl-sensitive colony was typically sensitive to all stressors tested. Interestingly, aging of cultures improved the phenotypic outcome for NaCl-sensitive strains.

FIGURE 3.4 Identification of extensive *purF/apt* mutant alleles and association to stress phenotype distribution.

(A) Heatmap of stress phenotypes of 96 colonies clustered vertically by sequenced *purF/apt* genotype (predicted protein effect listed for clarity), with stress conditions arranged horizontally. Each heatmap box represents the average of spot-growth densitometry measurements from three independent experiments performed with OD-standardized cultures, with the average densitometry value presented relative to the average value for all colony isolates grown on MH agar alone (control). Comparative/enhanced growth is shown as blue (resistant) and defective growth is yellow (sensitive). Color bars identify allele families from which representative mutant allele strains are derived. (B) Circle graph of relative abundance of representative alleles among 96 colonies, with non-listed alleles shown in grays. Reference refers to colonies with both *purF* and *apt* identical to known *C. jeju*ni 81-176 genome sequence. (C) Sequence identity plots of 96 aligned sequences of *purF/apt/prsA*. Arrows/white area indicates mutations/loss of identity, and white gaps in *apt* indicate the presence of 48bp/51bp duplication insertions. Not to scale. (D) Quantification of hyperosmotic stress resistance/sensitivity of representative mutant allele strains. CFU enumerated from OD-standardized cultures plated on MH or MH + 0.8% NaCl agar. Mean with SEM of three independent experiments. (E) ATP determination of OD-standardized representative allele strains and wild-type exposed to MH broth + 1.0% NaCl for 30 s, and compared to Δapt without NaCl-exposure. Luminometric values are relative to average luminometric value of parental wild-type. Mean with SEM of six independent experiments; * P ≤ 0.05 **, P ≤ 0.01; ****, P ≤ 0.0001.

3.4.5 Multifarious *purF* and *apt* mutations are prevalent in the *C. jejuni* population

The 96-colony *purF/apt/prsA* sequence analysis revealed that the reference allele was not most prevalent, and comprised only 11.5% [11/96] of the population (FIGURE 3.4B). Certain alleles were rare (e.g. *purF*S256R [1/96]), and other alleles were abundant (e.g. *purF*T91del [14/96]). All of the mutations were missense only, with no apparent transition/transversion bias. Mutations were more common in *purF* [71/96] than in *apt* [17/96], multiple same-gene mutations were uncommon/potential artifacts [4/96], and no colonies with mutations in both *purF* and *apt* were detected. The most common mutations in *purF* were single SNPs [34/71], followed by deletion/insertion of single codons [18/71]. The most abundant mutations in *apt* were large insertions of 48bp [7/17] or 51bp [1/17]. These insertions were duplications of sequence flanking the insertion. SNPs were also detected in *apt*, and were typically found in the coding region between the sites of the larger insertions (FIGURE 3.4C). Mutations in *purF* were concentrated in a hypervariable region in the glutamate binding domain; however, mutations were also found elsewhere in *purF* (not shown).

61

3.4.6 Mutant alleles contribute to distribution of phenotypes in the population

Mutations were also associated with multistress resistance, but the initial growth/non-growth phenotypic assay could not quantify enhanced or relative growth defects. To quantify increases/decreases in hyperosmotic stress survival, a more sensitive CFU-based NaCl stress test was carried out on strains derived from single colony isolates harboring representative resistant/sensitive alleles. The representative strains had no relative growth defects when grown on MH agar alone. In contrast, the *purF*V336F allele strain [12/96] showed ~15-fold increased CFU recovery on NaCl-supplemented MH agar in comparison to the heterogeneous wild-type (FIGURE 3.4D). The *purF*T91del allele also showed ~1.6-fold higher CFU recovery. All other representative alleles strains tested were sensitive to NaCl, the most sensitive of which (*purF*G292S) recovered ~10^5-fewer colonies. Thus, the alleles in the heterogeneous population contributed a wide spectrum of specific stress phenotypes to the overall wild-type phenotype.

Given that *purF/apt* are purine biosynthesis genes, mutations may affect the global purine pool and cell energetics. An ATP determination assay was carried out as a proxy for the purine pool, and to assess respiration and ATP production. Log-phase cultures of the representative allele strains were standardized by total cell number, exposed to 1.0% NaCl for 30 s, and lysed for ATP determination by luciferase assay. Allele mutants associated with stress sensitivity had less total ATP compared to the heterogeneous wild-type or the *purF*V336F allele (FIGURE 3.4E, FIGURE 3.5D). Without NaCl treatment, no differences in total ATP were observed (not shown). Consistent with all data thus far, the phenotypic effects of *purF/apt* mutations were only revealed post-stress exposure.

3.4.7 Underproduction of Apt correlates with stress-sensitivity

Colony 15 was found to have a unique mutation in the Shine-Dalgarno **r**ibosome **b**inding **s**ite (RBS) of *apt*, effecting a change from CGA**G**GCA to CGA**A**GCA. Since colony 15 was also stress-sensitive (FIGURE 3.5A), we reasoned that modulation of *apt* translation might have analogous phenotypic outcomes to certain primary sequence mutations. To test translation, the reporter gene *astA* was fused to the reference or mutant RBS under promoter-equivalent expression, and inserted separately into the 81-176Δ*astA* genetic background (FIGURE 3.5B). Reporter measurement demonstrated that the mutant RBS reduced translation (FIGURE 3.5C). Therefore, reduced enzyme production had the equivalent effect of mutations in *apt* that confer sensitivity; thus, those mutations negatively affected enzyme activity.
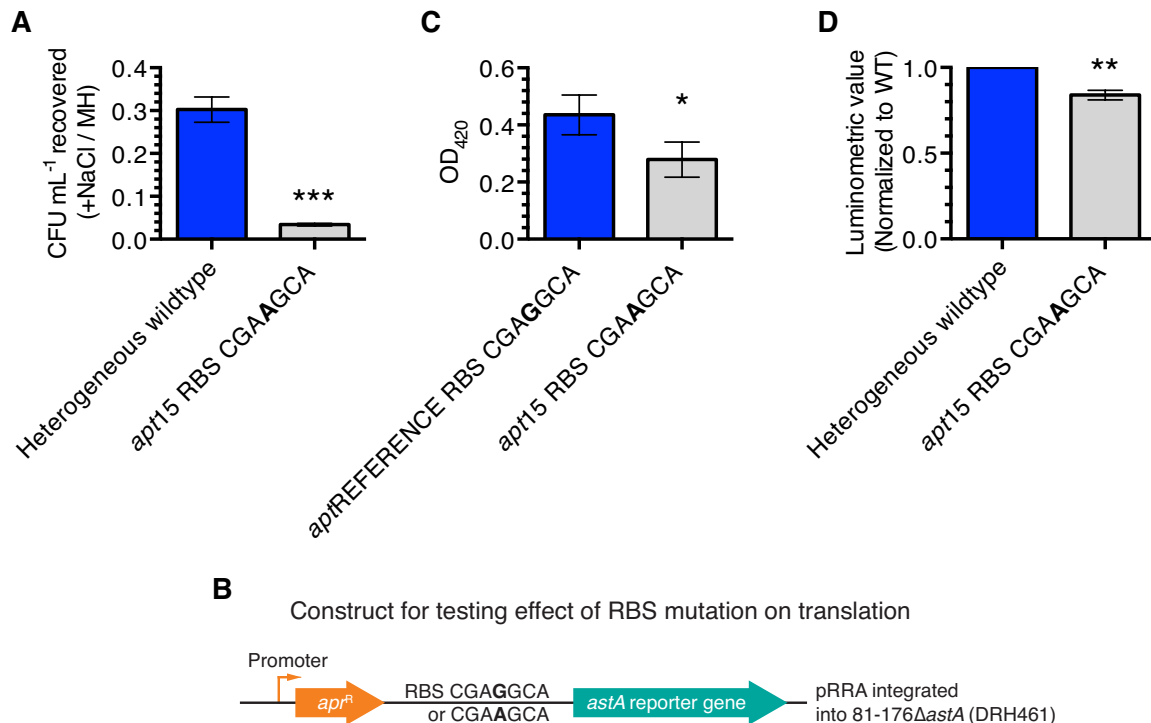
FIGURE 3.5 Effect of differential translation of *apt* on NaCl-stress phenotypes.
(A) Relative NaCl resistance/sensitivity of Colony 15/96 (*apt*15). CFU enumerated from OD-standardized cultures plated on MH or MH + 0.8% NaCl agar. Mean with SEM from three independent experiments, presented as ratio of CFU recovered on MH + 1.0% NaCl vs. CFU recovered on MH only; ***, P ≤ 0.001. (B) Schematic of promoter-RBS-reporter fusion constructs.

The reference (CGA**G**GCA) or variant RBS (CGA**A**GCA) was placed in context to the arylsulfatase reporter gene *astA* and cloned into pRRA genome-insertional plasmid for delivery into 81-176Δ*astA* strain. Expression in both constructs is polycistronic via the promoter of the apramycin antibiotic resistance marker. (C) Spectrophotometric measurement of *astA* gene product production, via colorimetric arylsulfatase assay. Mean with SEM from four independent experiments; * P ≤ 0.05. (D) ATP determination of OD-standardized representative *apt*15 and wild-type strains exposed to MH broth + 1.0% NaCl for 30 s. Luminometric values are relative to average luminometric value of parental wild-type. Mean with SEM of three independent experiments; **, P ≤ 0.01.

3.4.8 High-depth amplicon sequencing reveals *purF/apt* genetic heterogeneity in single colony isolate progeny

The high rate of phenotypic reversion in the progeny of single colony isolates, and prevalence of *purF/apt* mutations, suggested that phenotypic reversion might be due to further mutation of *purF/apt,* or back mutation to the reference sequence. To assess this, genomic extractions from the representative allele isolates were used for PCR-amplification and high-depth (~5,000-fold) Illumina MiSeq-based amplicon sequencing of *purF/apt/prsA*. Hyperosmotic stress testing was also carried out on 96 single colony progeny from each of the representative allele strains (FIGURE 3.6A). This overall phenotype of the representative strain was related to abundance of that same phenotype in the colony's progeny. Phenotypic revertants were not observed for some mutants, and amplicon sequencing revealed that those mutants either did not mutate further or did so beyond the limit of detection (e.g. *apt*E154A, contains 100% variation sequence), or had low frequency reversion (e.g. *purF*G95V, contains 99% variation sequence). This analysis also revealed that certain mutant isolate populations (e.g. *purF*V336F, *purF*V93_V96del) contained both reference back mutations, and new mutations at high frequencies. For simplicity, amplicon variants were mapped to the reference 81-176 sequence; thus, the prevalent large duplication insertions in *apt* are poorly represented in this analysis. To control for sequencing artifacts, *prsA* was included in every analysis. No *prsA* mutations were observed, thus highlighting the peculiarity of random *purF/apt* mutant frequencies.

3.4.9 Purine allele heterogeneity in other *C. jejuni* type strains

To determine if *purF/apt* variation was also found in other type strains of *C. jejuni*, phenotypic testing under NaCl stress, and amplicon sequencing of *purF/apt/prsA* was carried out on strains 81-116, the genome sequenced (GS) and original (O) versions of NCTC11168, and the initial heterogeneous 81-176 for comparison (FIGURE 3.6B). Results of these analyses demonstrated that 81-176 is the most heterogeneous strain; however, all strains exhibited heterogeneity either phenotypically, or in the frequency and type of variation in *purF/apt*. The two versions of NCTC11168—known for a variety of phenotypic differences (218)—also differed in their overall sensitivity to hyperosmotic stress, the frequency of phenotypic variation, and in *purF/apt* alleles. For example, *apt*C99Y comprised 22% of the 11168-O population, yet was absent in the 11168-GS strain. Phenotypic and sequencing results for strain 81-116 revealed that sequence variation in *purF* did not produce phenotypic variation in this instance, perhaps because the mutation identified (*purF*S113L) was phenotypically silent. Overall, these data confirmed that high rates of variation in *purF/apt* are present in *C. jejuni spp*.

A

Sensitive Resistant

Colony Sanger sequence

purF G95V   *apt* A133T   *purF* G292S   *apt* E154A   *purF* V336F   *apt* G135_136GinsGTA...   *purF* T91del   *purF* V93_D96del   *apt* P93_F94insFET...

Colony progeny phenotypes

purF	*apt*	*purF*	*apt*	*purF*	*apt*	*purF*	*purF*	*apt*
0.99 G95V	0.98 A133T	1.00 G292S	1.00 E154A	0.82 V336F	0.10 I139K	0.89 T91del	0.98 V93_D96del	0.11 V110L
				0.13 D96G	0.10 I139I S		0.03 A98G	0.10 V110V S
							0.16 I97N	0.05 L112I
							0.39 D96E	0.03 L112P
							0.58 D96A	
							0.42 D96Q	
							0.21 G95G-1FRAMESHIFT	
							0.99 G95V	
							0.16 G95C	
							0.21 L94F	
							0.27 L94S	
							0.37 L94V	
							0.35 V93_L94insA	

Amplicon sequencing

B *C. jejuni* wildtypes   81116   11168-GS   11168-O   81-176

Colony phenotypes

Amplicon sequencing

purF	*purF*	*purF*	*purF*
0.45 S113L	0.17 A136K	0.27 G95C	0.19 I97N
		apt	0.19 I97V
		0.22 C99Y	0.19 D96G
			0.18 A98T
			0.17 A98V
			0.16 T91S
			0.14 T91T S
			0.12 S92A
			0.09 S256R
			0.08 I99V

C Oxidative and osmotic stress exposure

Grown in: MH → MH

48 hr ←
O₂ exposure

NaCl → MH

NaCl

Test media: MH   MH   NaCl   NaCl   NaCl   NaCl   NaCl

Colony phenotypes

Amplicon sequencing

purF	*purF*	*purF*	*purF*
0.27 T91del	0.19 I97N	**0.19 V336F**	**0.22 V336F**
0.17 S92A	0.19 I97V	0.17 D96G	0.18 S256R
0.19 G95V	0.19 D96G	0.11 S256R	0.16 D96G
0.07 V336F	0.18 A98T	0.09 I97N	0.12 T91S
	0.17 A98V	0.09 I97V	0.09 S92A
	0.16 T91S	0.09 T91S	*apt*
	0.14 T91T S	0.08 A98V	**0.24 L92F**
	0.12 S92A	0.08 A98T	
	0.09 S256R	*apt*	
	0.08 I99V	**0.16 L92F**	

FIGURE 3.6 Identification of genetic heterogeneity within single colonies and other *C. jejuni* type strains, and effect of stress selection on mutant populations.

Each figure panel presents a list of alleles detected and their relative abundance (max = 1.0) and the blue/yellow resistant/sensitive stress phenotypes of 96 progeny derived from the described strains or conditions. Each heatmap circle represents the average of spot-growth densitometry measurements from three independent experiments performed with OD-standardized cultures, with the average densitometry value presented relative to the average value for all colony isolates grown on MH agar alone in standard conditions. (A) Stress phenotype variation and heterogeneity of *purF/apt* alleles within single colony-derived representative isolates. Original Sanger sequence genotype of colony listed in comparison to sequence variants detected by Illumina MiSeq-based amplicon sequencing. (B) Stress phenotype analysis of 96 colonies derived from each parental *C. jejuni* type strain, and heterogeneity of *purF/apt* alleles of each strain. Sequence variant analysis performed using the known reference sequence specific to each type strain. (C) Effect of exposure to atmospheric O₂ or repeated treatment with MH + 1.0% NaCl broth on progeny phenotypes and *purF/apt* genotypes. For O₂ exposure, the parental 81-176 strain was exposed to atmosphere for 48 hours, then plated for single colonies on MH agar, from which 96 progeny were derived. The resistant/sensitive phenotype of the 96 progeny was tested by re-exposure to atmospheric O₂ for 48 hours prior to resumption of growth in standard conditions. Genomic DNA was obtained for amplicon sequencing from pooled viable colonies after initial O₂ exposure. For NaCl exposure, strain 81-176 was grown in MH or MH + 1.0% NaCl

66

broth for 24 hours, then NaCl treated cells were used for repeated treatment. At each treatment endpoint, cultures were plated for viable single colonies on MH agar. Stress phenotypes were obtained for 96 random colonies from MH agar by subsequent testing on MH + 1.0% NaCl agar. Genotypes of *purF/apt* were assessed by amplicon sequencing genomic DNA from pooled viable colonies from MH agar.

3.4.10 Stress exposure selects fitter *purF/apt* alleles

Assigning phenotypic causation to a single mutation is difficult given the potential for high rates of phase variation, secondary mutations, and other confounding behavior. We hypothesized that if *purF/apt* mutations affected cellular responses to oxidative/osmotic stress, then oxidative/osmotic stress should select for stress-resistant *purF/apt* alleles. Cultures of heterogeneous wild-type were thus exposed to atmosphere (O_2 stress), or subjected to repeated and increased NaCl treatment. At each endpoint, genomic DNA was harvested for amplicon sequencing, and the NaCl-stress phenotypes of 96 colonies grown from the culture were assessed. Exposure to atmospheric oxidative stress selected for the multistress-resistant *purF*T91del and O_2-resistant *purF*G95V alleles, which both increased, from undetected, to 27% and 19%, respectively, of the post-O_2 exposure population (FIGURE 3.6C). For hyperosmotic stress effects, the heterogeneous wild-type was exposed to MH broth containing 0.8% NaCl for 24 h, followed by re-inoculation of fresh broth and another 24 h exposure to 1.0% NaCl. The allele most differentially represented was *purF*V336F, which increased from undetected in the unstressed heterogeneous wild-type, to 19% and 22% at each successive exposure end-point. The *apt*L92F allele also increased from undetected to 16% and 24% at each end-point. Phenotypic analyses showed that stress-sensitive progeny decreased in abundance after exposure to both O_2 and NaCl. Most of the alleles detected via amplicon sequencing were not previously identified in the screen of 96 colonies.

3.4.11 Intracellular survival in epithelial cells is affected by genetic heterogeneity in *purF/apt*

Successful host cell invasion and intracellular survival of *C. jejuni* is correlated with oxidative stress resistance (131). Since *purF/apt* alleles affected O_2 and hyperosmotic stress tolerance, the representative allele strains were used to infect INT407 host epithelial cells, and assessed for intracellular survival by gentamicin protection assay. The stress resistant allele strains *purF*V336F and *purF*T91del survived intracellularly at higher levels, determined by lysing the epithelial cells and recovering intracellular bacteria for CFU enumeration (FIGURE 3.7A). These strains recovered 12.1- and 6.8-fold more bacteria than the sensitive allele strain *apt*E154A. All strains were determined to invade the INT407 epithelial cells equally well, but the heterogeneous wild-type had the greatest CFU recovery at all time points assessed. A high degree of error between biological replicates representative strain infections was observed; even more evident was the unpredictable intracellular behavior of the 96 single colony isolates, despite invading equally well (FIGURE 3.7B, upper and lower panels). Generally, hyperosmotic stress sensitivity/resistance for allele siblings was similar to intracellular trends, such as defects for siblings of *apt*E154A, and improved survival for siblings harboring *purF*V336F.

A typical INT407 *C. jejuni* infection proceeds with high numbers of viable bacteria, followed by a bottlenecking event in which only a fraction of the total population invades, and then intracellular survival until bacteria are killed/quiesced (FIGURE 3.7C). We hypothesized that the cell infection/survival process would select for alleles conferring fitness in epithelial cells. INT407 cells were infected with the heterogeneous wild-type, and the *purF/apt/prsA* alleles were assessed by amplicon sequencing prior to infection, and at 5 h, 8 h, and 12 h post-infection (FIGURE 3.7D). Sequencing was carried out on pooled colonies obtained from plating harvested epithelial cell lysates. The most-selected allele

in the population was *purF*V336F, which increased in abundance from 14% of the pre-infection population, to 22%, 31% and 77% at 5, 8 and 12 h post-infection. Since replication of *C. jejuni* within host cells is minimal (103), this represented increased survival rather than growth. The pre-infection control, grown in MH broth, also served as a comparator for bacteria grown on MH agar plates in FIGURE 3.6B. Differences between the two growth methods were relatively modest, and the major difference was the detection of the *purF*V336F allele in the broth-grown sample.
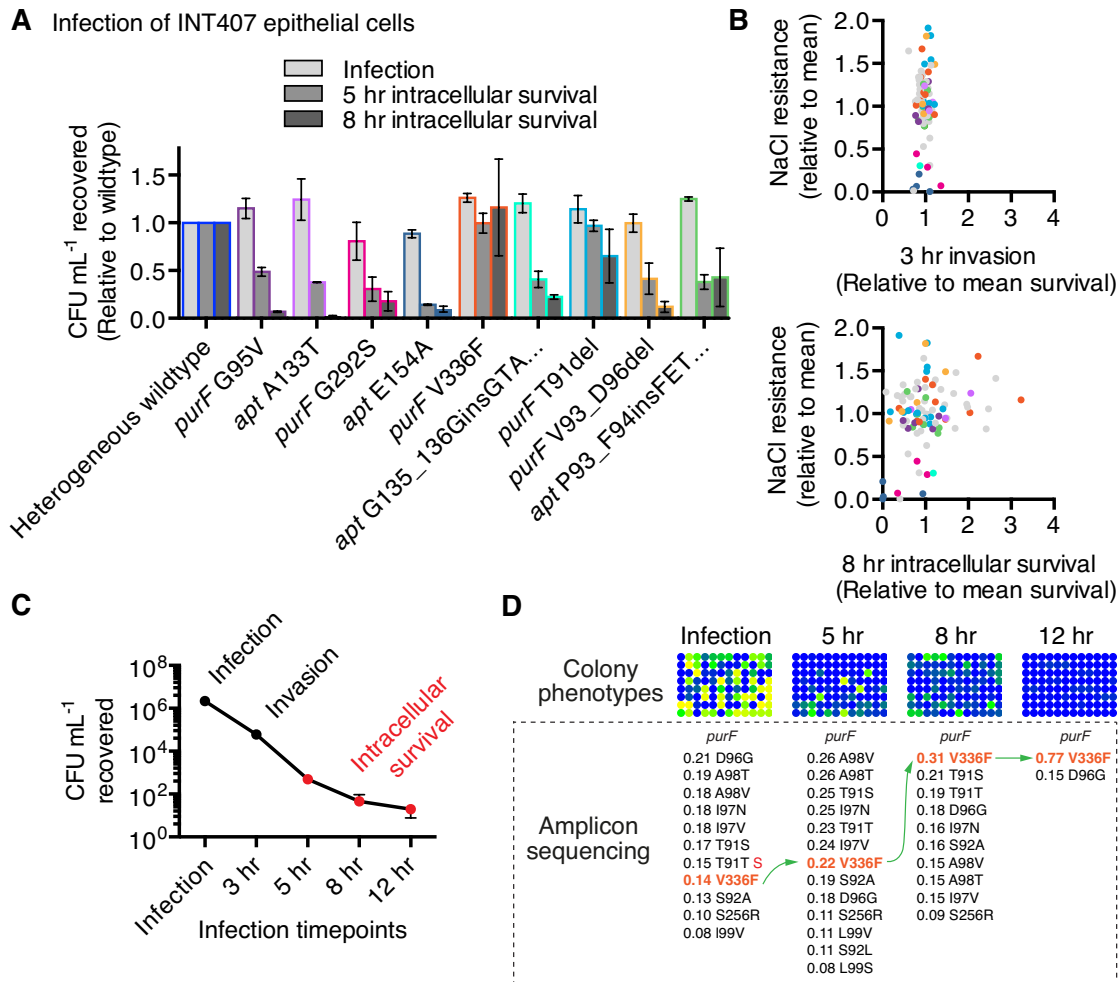
FIGURE 3.7 Fitness selection and effect of *purF/apt* mutations in invasion and intracellular survival in epithelial cell model of infection.
(A) Invasiveness and intracellular survival of representative allele strains in confluent INT 407 intestinal epithelial cells assessed by gentamicin protection assay. Recovered bacterial CFU from host cell lysis is presented relative to CFU recovered for parental wild-type at each assay timepoint. Mean with SEM of three independent experiments. (B) Early invasion (3 hours, upper

panel) and later intracellular survival (8 hours, lower panel) of 96 *purF/apt*-genotyped single colony isolates. Each dot represents an isolate (out of 96); x-axis, the average CFU recovered from host cells for an individual isolate relative to average CFU recovered for entire population; y-axis, growth on NaCl relative to population average (data from FIGURE 3.4). Colored dots are families of representative alleles. CFU data from three independent experiments; CFU recovered at 3 hours includes bacteria adhered and intracellular, CFU recovered at 8 hours from gentamicin-treated host cells are from intracellular bacteria only. (C) CFU recovered for typical INT 407 infection with parental *C. jejuni* 81-176 at invasion and intracellular timepoints. Infection CFU is total number of bacteria used to infect host cells, MOI = 100. (D) Allele fitness selection by intracellular survival, and examination of NaCl-stress resistance/sensitivity phenotypes in 96 colonies after liberation from host cells. Amplicon sequencing variant analysis was performed on genomic DNA from pooled colonies recovered on MH plates at each intracellular timepoint. Each pool was the equivalent of three independent experiments with 24 technical replicates (total 72 infections at each intracellular timepoint to maximize CFU/allele recovery).

3.4.12 The putative DNA-binding PolB-like exonuclease Cj1132c promotes spontaneous mutation

Considering that mutations affecting purine biosynthesis might affect mutational frequencies (219), the representative allele strains were tested for differences in the spontaneous mutation rate. Mutation frequency was assessed by enumerating spontaneous resistance to the fluoroquinolone ciprofloxacin, which is conferred by DNA gyrase (*gyrA*) point mutations. No significant differences in the spontaneous mutation rate of *gyrA* was detected for the representative allele strains and the heterogeneous wild-type (not shown), consistent with *prsA* sequencing data. Although the observed mutations in *purF* were not limited to the hypervariable region, a direct repeat [**AATCGCTAT**AGGGCATA**ATCGCTAT**] was found in *purF* directly upstream from the hypervariable region, potentially a DNA binding site. Likewise, a similar, yet imperfect sequence [**AAT**AG**CAA**CTGG_ins_CGG**AA**CA**GCTAT**] was found at the boundaries of an *apt* duplication-insertion. Thus, we reasoned that a specific DNA-binding factor promoted hypervariation. A protein pull-down using a 5'-biotinylated truncated *purF* "bait" sequence, containing the direct repeat and hypervariable region, was performed via **s**table **i**sotope **l**abeling of **a**mino a**c**ids (SILAC)-based proteomics (216). Two putative DNA binding

70

proteins were similarly pulled down in two independent experiments: Cj1132c (*CJJ81176_1149*, gene annotated as *wlaX*), and SSB (*CJJ81176_1089*, single stranded DNA binding protein) (FIGURE 3.8A). Pulled-down proteins with non-specific interactions with the *purF* DNA probe, such as PorA (FIGURE 3.8B, upper panel), have an equal ratio of $^{13}C_6$-arginine-labelled and $^{14}N_4{}^{13}C_6$-arginine-labelled peptides, whereas potentially specific interactions are identified by primarily $^{13}C_6$-arginine-labelled peptides (FIGURE 3.8B, lower panel). Since SSB is a ubiquitous protein, Cj1132c was chosen for further assessment, and is predicted to belong to an uncharacterized bacterial group of DEDDy 3'-5' exonucleases, which have homology with the proof-reading DNA replication/repair exonuclease domains of family-B DNA polymerases (Pfam DNA_pol_B_exo2). To assess roles for Cj1132c specifically in *purF* mutation, *cj1132c* was deleted (Δ*cj1132c*) in the *purF*T91del allele background, because the rate of mutation/phenotypic switching was known/amenable to testing in this strain, and because T91del is located in the hypervariable region of *purF*. However, in the *purF*T91del background, Δ*cj1132c* did not seem to affect the rate of NaCl-stress phenotypic variation (not shown). However, Δ*cj1132c* influenced the spontaneous mutation rate, and Δ*cj1132c* produced fewer ciprofloxacin resistant colonies than the comparator strain or Δ*cj1132c* genetic complement (FIGURE 3.8C). Thus, Cj1132c did not actively promote hypermutation of *purF* in these limited analyses, but may have a role in DNA maintenance.

A

Pull-down of *purF* DNA interacting proteins

B

PorA
Non-specific interaction
+ purF DNA   DNA Absent
Light isotopologue   Heavy isotopologue

Cj1132c
Specific interaction
+ purF DNA   DNA Absent
Light isotopologue   Heavy isotopologue

C
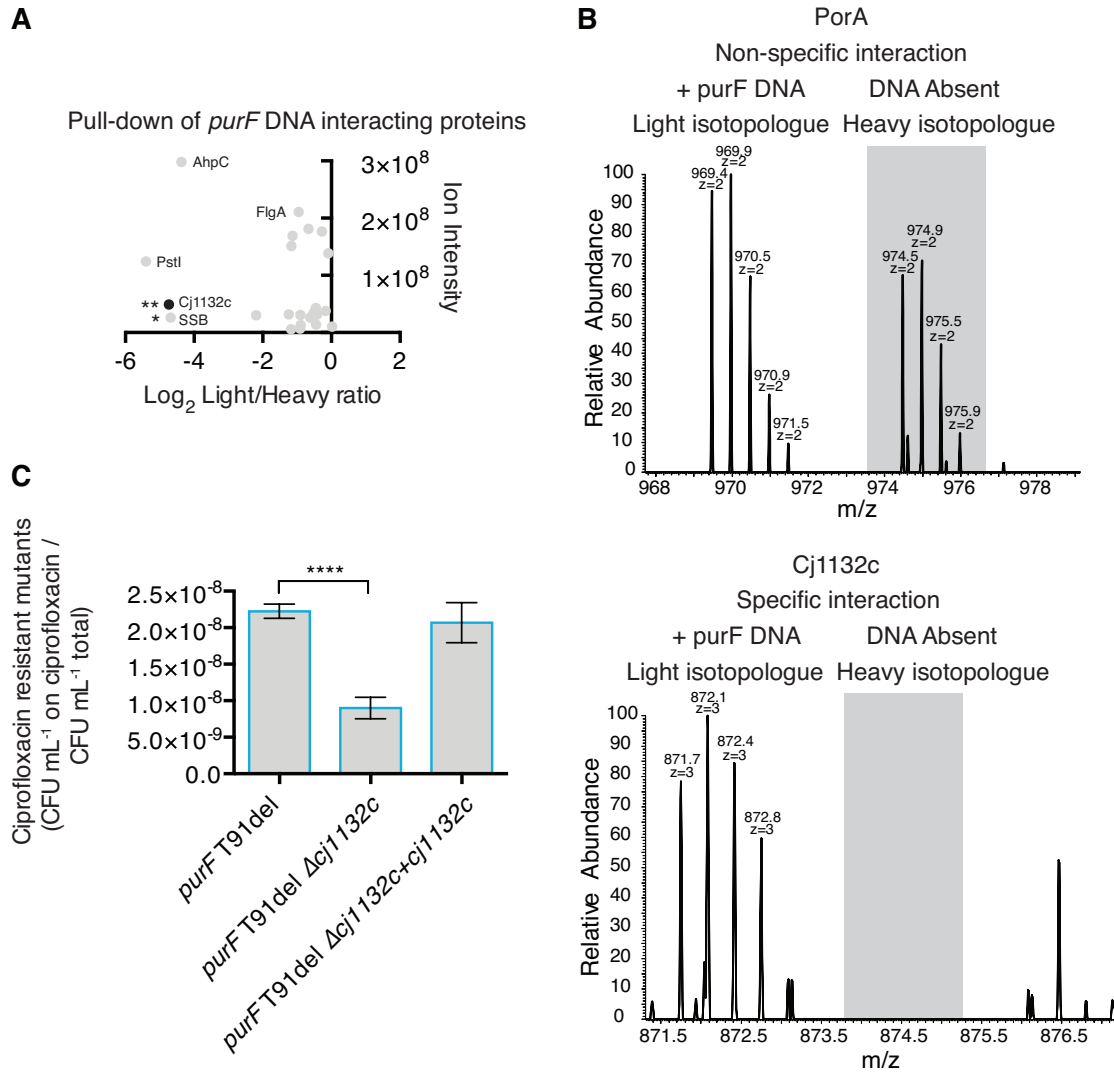
FIGURE 3.8 SILAC-based affinity capture of Cj1132c with *purF* DNA bait and effect of *cj1132c* deletion on spontaneous mutation rate.

(A) Screen for DNA-binding proteins captured with *purF* DNA bait. Differentially labeled light ($^{13}C_6$-arginine) and heavy ($^{14}N_4$$^{13}C_6$-arginine) *C. jejuni* total protein lysate was incubated with biotinylated *purF* DNA or *prsA* DNA respectively. A 1:1 light:heavy mixture of DNA:protein complexes was captured on streptavidin beads. Proteins were eluted from beads by digestion with PstI restriction enzyme, and trypsinized proteins were analyzed by GeLC-MS. Each dot represents an identified peptide. SILAC analysis discriminates specificity of interaction; peptides with low heavy:light ratio indicate higher affinity capture. Data is representative of two independent experiments statistically assessed by Benjamini-Hochberg False Discovery Rate. FDR Q significance value; *, Q = 0.024; **, Q = 0.014. (B) Representative mass spectra for SILAC-labeled captured peptides. Top panel: equal mass:charge of light and heavy forms of PorA peptide indicating non-specific interaction. Bottom panel: the light form of Cj1132c is present in a ratio > 16.8 higher than the heavy form, indicating high probability of interaction with *purF*. (C) Frequency of emergence of spontaneous ciprofloxacin resistance (spontaneous mutation rate) of Δ*cj1132c* mutant and complement, in *purF*T91del genetic background. Number of spontaneous ciprofloxacin resistant mutants presented relative to total CFU per OD_{600} equivalent. Mean with SEM from six independent experiments each with two technical replicates; ****, P ≤ 0.0001.

3.5 DISCUSSION

Purines are evolutionarily ancient molecules, and the biosynthesis or uptake of purines is essential to life. Purines are involved in the synthesis of DNA and RNA (adenosine/guanosine), cell energetics (ATP/GTP), cell signaling alarmones and stress responses (cyclic AMP, cyclic di-GMP and (p)ppGpp), and are central to metabolism (NADH/coenzyme A) (220). The purine precursor, PRPP, is also important for amino acid biosynthesis (histidine/tryptophan) (221, 222), and for pyrimidine synthesis and salvage (220, 223). PRPP is used by PurF for *de novo* IMP nucleoside biosynthesis (and thus AMP/GMP production), and by Apt for the recycling/salvage of adenine nucleotide back to the nucleoside form. Except for *apt*, the purine salvage pathway of *C. jejuni* is absent, and the bacteria encodes neither nucleotide/nucleoside transporters, nor the array of phosphoribosyltransferases, deaminases or phosphorylases for guanine, thymidine, hypoxanthine and xanthosine salvage (19). Thus, *C. jejuni* appears to be incapable of extracellular purine salvage. In agreement with this, we found that Δ*purF* mutants could not be generated on media supplemented with adenine, adenosine, guanine, and/or guanosine, and exogenous supply of adenosine did not rescue the growth defect of the Δ*apt* mutant (not shown). Thus, our data suggest that *de novo* purine biosynthesis is essential for *C. jejuni,* and salvage is absent/dispensable. In contrast, the related *Helicobacter pylori* does not encode the *de novo* purine biosynthesis pathway, and relies solely on purine salvage, utilizing an outer membrane nuclease not present in *C. jejuni* to digest extracellular DNA (224). As *C. jejuni* is a naturally competent organism, whole DNA uptake is a potential source of nucleobases for Apt salvage, although this remains to be tested.

Mutations in the purine biosynthetic pathway ultimately lead to changes in the availability of purines and intermediates—with complex consequences given the central role of purine metabolites, and the integration of stress

responses with cellular metabolic pathways. Purine limitation effects are described for many bacterial species. Purine auxotrophs ($\Delta purF$ mutants) of *Mycobacterium smegmatis* have reduced viability in O_2-depleted stationary phase (225). In *Bacillus subtilis*, purine deprivation promotes sporulation, resulting from a reduction in the synthesis of AMP/GMP (226). Purine auxotrophic mutants of *Listeria, Mycobacterium, Francisella* and *Brucella* are severely attenuated for virulence/colonization in animal models (227-231), and *Shigella flexneri* purine biosynthesis mutants have been evaluated as vaccines because of the attenuation of those strains (232).

How might changes in the purine pool affect *Campylobacter's* response to osmotic and oxidative stress? In *E. coli,* hyperosmotic stress (233), and $\Delta purF$ deletion (234), activates expression of the polyphosphate kinase *ppk*, which results in the accumulation of polyphosphate, a high energy phosphate storage polymer (122, 123). In *C. jejuni*, polyphosphate is required for hyperosmotic stress survival, for survival during carbon starvation, for intracellular survival in epithelial cells, and is accumulated in stationary growth phase (213). Furthermore, the guanosine-based alarmones ppGpp and pppGpp are known to enhance polyphosphate accumulation, which may be absent in ppGpp^0 mutants (119, 233). Additional mechanisms lead to polyphosphate accumulation, and include ppGpp-mediated inhibition of the exopolyphosphatase *ppx* (233). Thus, altered polyphosphate reservoirs may account for the phenotypic effects of the mutations in *purF* and *apt*.

In *Lactococcus lactis*, mutations in *guaA* (*de novo* purine biosynthesis) and *hpt* (purine salvage) confer multistress (acid, oxidative and heat stress) resistance, as do mutations in the ppGpp synthetase *relA* (235). This suggests that flux in the purine biosynthesis pathway, and/or ppGpp fluctuations, are stress signals that lead to stress resistance. For *C. jejuni*, our data supports this, but also reveals that specific mutations have the opposite consequence,

contributing to multistress sensitivity. Other modified purines, such as the second messengers cAMP and c-di-GMP, may also be affected by mutations in *purF/apt*. In *C. jejuni*, c-di-GMP is implicated in deoxycholate stress resistance (236), and in other bacteria, has roles in biofilm formation (237). In addition, *C. jejuni* uses nucleotide-activated sugars such as the GDP precursor of the *O*-linked glycans of the flagellin (83, 238). Thus, because purine biosynthesis mutations may influence numerous signaling cascades, metabolic regulation and specific stress response systems, *purF/apt* mutations in *C. jejuni* are likely to have pleotropic consequences for stress resistance and sensitivity mechanisms.

Why are the mutant *purF/apt* phenotypes only expressed under stress? The different *purF/apt* mutant allele strains—except for Δ*apt*—all grow equally well under the replete, non-stressed conditions of standard MH media (not shown). This justifies the prevalence of allelic mutants in the MH-grown population because there is minimal selective pressure acting against those mutant alleles. In rich MH media, the growth rate of *C. jejuni* is many times faster than in many transmission and colonization environments (44, 239-242); thus, accelerated growth rates may contribute to the generation of mutants. High DNA replication rates are known to outpace and saturate post-replicative DNA MMR mechanisms (243, 244), and since known MMR mechanisms are absent in *C. jejuni*, accelerated growth rates may contribute to the mutational frequency (211). Since the Δ*apt* null mutant could not grow properly in MH, and Δ*purF* could not grow at all, selective pressure is maintained for overall functional alleles of both *purF/apt* in MH media. The effect of additional selective pressure on the mutant allele population was demonstrated via exposure to NaCl, O_2 and the intracellular environs of INT407 epithelial cells (FIGURE 3.6C and 3.7D). In each experiment, a stress-fit allele was selected for, and the allele was prominently represented in the post-stress population. Since genome-wide association of phenotypes to particular mutations is not evidence of linkage, these experiments provide additional support for the specific role of

purF/apt mutations in stress fitness.

Highly expressed genes are known to undergo higher mutational frequencies (245), but both *purF* and *apt* were expressed at similar levels as the non-hypermutable *prsA* (not shown). Furthermore, transcription of *purF/apt* was not significantly affected by exposure to osmotic stress (not shown), signifying that the observed phenotypic effects are post-transcriptional or post-translational. The mutation in the *apt15* RBS demonstrated that reduced translation of Apt had synonymous effects to *purF/apt* mutations that conferred stress sensitivity. Thus, changes in translation efficiency do have a role in this process; however, given that the majority of observed mutations altered the primary sequence of *purF/apt*, phenotypes primarily arise from differential enzyme kinetics, and/or insensitivity/hypersensitivity to allosteric feedback (246). As PurF is responsible for purine commitment in the biosynthesis pathway, the enzyme receives feedback from GMP/AMP, and from other adenine and guanine nucleotides (247-249). Apt activity is competitively inhibited by various 5' nucleotides and diphosphate, in cooperation with PRPP, and is subject to end product inhibition by AMP (250-252).

Conserved domain analysis of the *purF/apt* allele mutations suggest that the mutations do not occur in conserved active site residues. No conclusions can thus far be made about the specific enzymatic effects of altered residues based solely on the different phenotypic outcomes. Although phenotypes of mutants with low ATP levels correlated with the phenotype of a strain underproducing Apt, ATP levels are a measure of cell energy/respiration and do not necessarily provide insight into the effect of primary sequence mutations in *purF/apt* on their respective reactions. In this current study, ATP determination was used to exemplify major phenotypic differences between single colony isolates under stress. Addressing the specific effect of mutations on the *purF/apt* reactions requires in-depth analysis of substrate/product ratios. This is an interesting

question for future experiments, but high rates of *purF/apt* reversion/mutation in most single colony isolates resulted in mixed populations that will complicate comparative metabolomic approaches. The caveat of measurements performed on mixed populations is that they reflect the average population behavior (253), which may not be consistent with the specific effect of the original founder mutation.

The hypermutation of *purF/apt* represents a novel phenomenon. A recent study by Mohawk *et al* (212) found similar patterned—but deleterious— mutations in the *motA* flagellar motor protein gene in *C. jejuni* 81-176; taken together, our studies confirm that *C. jejuni* strain 81-176 demonstrates high variability, exceeding known phase variation and mutator frequencies of other bacteria (211). Mutator phenotypes in model bacteria typically result from "mutator alleles"—often mutant MMR genes—with corresponding genome-wide 100-1000-fold increases in transitions, frameshifts and chromosomal rearrangements (254). Given the absence of MMR genes in *Campylobacter*, this implies that this is a genus of "constitutive mutators". The spontaneous mutation rate of the heterogeneous *C. jejuni* 81-176 parent strain was determined to be ~ 10^{-8}, equivalent to previously established rates determined by equivalent spontaneous ciprofloxacin resistance-based methodologies (255, 256). Since flaws in purine biosynthesis have been shown to have genome-wide mutational consequences in other organisms (219), purine biosynthesis mutants could be potential "mutator alleles". However, despite differences in *purF/apt* variant frequencies between isolates, the global spontaneous mutation rate was unaffected in each representative isolate, and other gene mutations were not detected, evident from no differences in *gyrA* or *prsA* respectively (not shown). Thus, *purF/apt* mutations are not classic "mutator alleles". Given that contingency loci phase variation occurs at ~10^{-3} (19, 90, 206, 257), and since 85/96 random colonies had a mutation in *purF/apt*, spontaneous mutation rate assessments via ciprofloxacin resistance do not assess the true scale of mutation

frequency in the *C. jejuni* population. Ignoring recombination and horizontal gene transfer, we speculate that (I) the basal mutation frequency, (II) homopolymeric tract-based contingency loci phase variation, and (III) non-homopolymeric high frequency variation of *purF/apt* and other specific genes each make lesser-or-greater contributions to the total variation in the population. An important caveat of this study is that it is difficult to measure mutation rates of specific genes, like *purF/apt*, because the DNA sequences and phenotypes are examined many generations after the mutation occurred, during which time selective pressure—and unknown factors—have acted to confound determination of gene-specific mutation rates; thus we make no claims to this here. Instead, since each process likely relies on basal polymerase error during DNA replication, the difference in the observed mutant frequencies must have alternate explanations.

Why then, are mutations in *purF* and *apt* so prevalent if the same variation is not observed for all genes? Why does the observed selective pressure not ensure sequence fidelity in *purF/apt*? Current evolutionary opinion is that mutations occur randomly (258), unless a specific mechanism exists to increase the rate of mutation. In the absence of a conventional homopolymeric tract-based phase variation mechanism, we assessed if a specific DNA binding factor was responsible for *purF* hypermutation, reasoning that a sequence-specific protein might affect DNA replication fidelity. The putative exonuclease Cj1132c was identified as a candidate *purF* binding protein. Although Cj1132c deletion decreased emergence of spontaneous ciprofloxacin resistant mutants, the gene did not appear to promote *purF* hypermutation within the limitations of the study performed here. Since the PCR-generated *purF* probe "bait" would contain mismatched/ssDNA sequence, the pull-down experiment and subsequent mutation frequency analyses may have identified Cj1132c as a potential repair/DNA maintenance mediator. In *C. jejuni*, the transcription-repair coupling factor, Mfd (mutation frequency decline), promotes spontaneous

fluoroquinolone resistance, and Δ*cj1132c*, like Δ*mfd*, decreased the spontaneous mutation rate (259). Despite no clear role in *purF/apt* hypervariation, our experiments with Cj1132c are included in this study because the SILAC-based affinity screen exemplified new experimental proteomics approaches available for *C. jejuni* researchers. This data was also included because it demonstrated challenges posed by heterogeneous populations on reductionist genetics-based methodologies, which are further discussed below.

Natural populations of bacteria are assumed to be genetically heterogeneous, but laboratory isolates, which are often derived from a single colony isolate, are assumed to be reasonably homogenous. Our data is evidence that this is a false assumption for *C. jejuni* laboratory strains and their progeny. The creation of a deletion mutant necessitates the selection of a single colony, and comparative analyses (often a deletion mutant compared to the original wild-type) requires otherwise isogenic backgrounds to assure that phenotypes are not due to secondary mutations. The multiple mutative properties of *C. jejuni* therefore complicate such analyses. Homopolymeric tract-mediated phase variation has previously been seen as driving the majority of *C. jejuni* genetic/phenotypic variation, but despite being a stochastic process, we speculate that effects of phase variation are partly mitigated by the high rates of both ON *and* OFF switching in homopolymeric tracts, resulting in a "predictable" ON-to-OFF equilibrium (257). In contrast, *purF/apt* high frequency mutation appears to be purely random. Since there is no homopolymeric tract or obvious mechanism to revert back to the original sequence, the effects of *purF/apt* hypermutation are considerable for bottlenecked populations derived from a single mutation-bearing bacterium. Furthermore, phase variation results only in ON or OFF phenotypic states, whereas *purF/apt* hypermutation has the potential for multiple phenotypic states.

A population of variable genomes enhances the probability of survival of a bacterial species. In this current study, conclusive evidence was provided for genetic variation in *purF/apt*, and was identified as a mechanism promoting extensive phenotypic heterogeneity in a mixed *C. jejuni* population. We provided further evidence for the role of this genetic diversity in relevant niche exploitation, and thus conclude that *purF/apt* mutation is a novel success strategy, akin to phenotypic bet-hedging (260-262), yet reliant on mutation of specific genes. How non-deleterious hypermutation of *purF/apt* occurs remains unexplained, and will be the focus of future investigations, as will analyses of the specific cellular effects of various *purF/apt* mutants. Furthermore, the current findings have major pathogenesis implications, and future work will be carried out to assess if *purF/apt* mutations affect disease outcome. Also of interest is whether any other *C. jejuni* genes (in addition to *purF*, *apt* and *motA*) undergo similar hypermutation. Even though this study examined only *purF/apt*, the genetic heterogeneity in the parental population was so enormous that mutant allele prevalence exceeded that of the wild-type allele, which begs the question of what exactly is the wild-type? Others have speculated that *Campylobacters* are a type of quasispecies (19, 263, 264); i.e., a population of genotypes, often organized around more prevalent genotypes of higher fitness (265), with a defined wild-type sequence that is the average of all present genotypes (266). Our data supported this definition, and demonstrated the effect of selection on the mutant distribution. In conclusion, our current findings presented information contrary to a number of paradigms, including high frequency genetic variability that was not due to homopolymeric tract-based phase variation, and which occurred in essential/fitness-requisite housekeeping genes not associated with any surface structure. The current study illustrated novel adaptive properties of high frequency *purF/apt* variation that are important for the lifestyle of *C. jejuni*, and which may have serious consequences for the investigation and containment of this widespread pathogen.

CHAPTER FOUR: Genetic heterogeneity enhances *Campylobacter jejuni* biofilm formation

4.1 SYNOPSIS

The aggregation of *Campylobacter jejuni* into complex matrix-bound multicellular communities, or biofilms, is increasingly viewed as a survival strategy, enabling success of the pathogen in otherwise hostile natural environments and in commensal host animals. We previously identified high frequency genetic variation of two purine biosynthesis genes that resulted in differential stress survival between colonial *C. jejuni* isolates. In the current study, the role of purine genetic variants in biofilm formation was examined, and population genetic variation was found to be critical for enhanced biofilm formation. Via high-throughput sequencing, individual variants were tracked during biofilm formation, and were found to preferentially exist in biofilms or as free-swimming cells in planktonic niches. Biofilms contained more diverse allelic variants, but biofilm variants were more sensitive to aerobic stress than planktonic variants. In contrast, enhanced horizontal gene transfer occurred primarily between biofilm variants. A model explaining the role of genetic variation in enhanced biofilm formation was proposed, and we provided preliminary evidence that interactions between genetic variants in early biofilm microcolonies promotes differential phenotypic behavior. This was characterized by chaining of one of the interacting variants, and we speculated that this may lead to cell death, contributing DNA and other cellular polymers to enhance the biofilm matrix. These findings improve our understanding of the adaptive repertoire of *C. jejuni.*

4.2 INTRODUCTION

In the laboratory, *C. jejuni* is a considerably fastidious pathogen that requires oxygen, yet is sensitive to the level of oxygen found in the atmosphere (135). *C. jejuni* is also relatively sensitive to a variety of niche-relevant stressors (1, 114, 139, 267). Despite this, successful oral transmission to humans commonly occurs via colonized poultry, unpasteurized milk, or contaminated water (33). The biofilm forming capabilities of *C. jejuni* are thought to maintain the bacterium in such environments (268, 269), and thus biofilms promote survival both outside and within hosts (270). Consequently, biofilms are a reservoir of contamination for *Campylobacter,* and many other pathogenic bacteria (271).

Biofilms are adherent sessile cellular communities that are enclosed in a stress-protective polymeric extracellular matrix barrier (268, 272-275). Biofilms emerge in distinct phases, beginning with adherence mediated by species-specific mechanisms including flagellar, fimbrial or pili structures, and/or via secreted adhesins and carbohydrates (276-279). Biofilm formation advances with microcolony formation, matrix release, and eventual planktonic cell dispersal (269-271, 280-282). In *C. jejuni*, flagella-mediated adhesion and extracellular DNA release contribute to biofilm formation and stress tolerance (73, 283). Extracellular DNA is increasingly viewed as an important matrix polymer, contributing structure and integrity (284), and in biofilms, community proximity to the DNA-containing matrix enhances gene transfer from bacteria-to-bacteria, promoting recombination and antibiotic resistance (73, 285). In certain bacteria, programmed autolytic release of DNA stimulates biofilm formation and/or dispersal (286, 287).

In CHAPTER THREE, we discovered widespread colonial phenotypic variation that was due to high frequency multifarious genetic mutations in two

C. jejuni purine biosynthesis housekeeping genes—*purF* and *apt*. Characterization of these allelic variants revealed that certain mutations were associated with differential stress survival outcomes, thus illustrating novel adaptive properties of *C. jejuni*. In this current study, we examined the role of this genetic heterogeneity in biofilm and planktonic lifestyles, and found that diversity was an important factor in robust biofilm formation. We confirmed that certain allelic variants exhibit biofilm/planktonic microniche preferences, and associated planktonic survival with enhanced aerobic tolerance. We also demonstrated that biofilm-preferring variants had higher rates of recombination than planktonic-associated variants. Furthermore, to explain the enhanced biofilm formation of heterogeneous populations, we propose a mechanism in which antagonistic interactions between niche-competing variants in early biofilm microcolonies results in possible loser-cell death—contributing DNA to the biofilm matrix, and enhancing overall biofilm formation.

4.3 METHODS AND MATERIALS

4.3.1 Bacterial strains and growth conditions

Studies were performed with *C. jejuni* human isolate strain 81-176 (33), unless otherwise stated (see TABLE A.1.3 for a full list of bacterial strains and plasmids). *C. jejuni* was grown on Mueller-Hinton (MH) agar or broth (Oxoid), supplemented with vancomycin (10 µg ml^{-1}) and trimethoprim (5 µg ml^{-1}), in microaerobic/increased-CO_2 atmosphere (6% O_2, 12% CO_2) in a Sanyo tri-gas incubator (solid media), or generated via CampyGen (Oxoid) system (shaken broth cultures), or exposed to atmospheric conditions at 38°C. *E. coli* strains were maintained on standard LB medium.

4.3.2 Biofilm growth conditions

Biofilm formation was assessed as previously described (283, 288), with modifications. Briefly, *C. jejuni* cultures were diluted to OD_{600} 0.005 in MH broth, and 1 mL was added to a 10 cm borosilicate glass tube. Standing biofilm tubes were incubated at 38°C microaerobically for 24, 48 or 72 hours. For biofilm visualization and quantification, biofilm growth was stained with 250 µL of a solution of 1% crystal violet in 100% ethanol for 20 minutes, then rinsed with water. Following imaging of tubes, the adhered crystal violet was quantified in a Varioskan spectrometer (Thermo Scientific) at OD_{570} by the addition of 1 mL of 30% methanol, 10% glacial acetic acid solution.

For biofilm/planktonic CFU determination and other experiments, 200 µL of the 1 mL "planktonic" broth was carefully removed (avoiding biofilm/settled bacteria) for CFU enumeration or downstream experiments. The remaining 800 µL was discarded by aspiration, and a sterile swab was used to scrape the biofilm from the liquid-air interface, for re-suspension in 1 mL of fresh MH broth for CFU enumeration or downstream experiments.

4.3.3 Sequence variant analysis from planktonic/biofilm cells by amplicon sequencing

Biofilm/planktonic bacteria were isolated from 10 independent biofilm formation tubes for DNA extraction by Wizard genomic DNA purification (Promega) or for CFU isolation by plating on MH agar plates. Biofilm/planktonic-derived colonies formed ($\sim 10^5$) were separately pooled for DNA extraction. Amplicon sequencing of *purF/apt/prsA* was performed on the Illumina MiSeq system via established procedures (215), using amplicons PCR-generated by the listed oligonucleotides (TABLE A.2.3). To avoid PCR bias, optimized oligonucleotides were designed for minimized 25-cycle PCR reactions,

and resulting amplicons were used in the preparation of Nextera XT libraries, as per manufacturer's preparation guide (Illumina). Variant discovery was performed using GATK (Broad Institute) software (variant information not shown).

4.3.4 Competition assays

For assessment of relative fitness and genetic recombination, antibiotic resistance markers were genome-integrated into variant isolates using the pRRK (Brendan Wren) or pRRH/pRRA (2) genome-insertion gene delivery vectors. Each of the three variants (*purF*V336F, *purF*D96G and *purF*T91del) was previously isolated (CHAPTER THREE), and genotyped by traditional sequencing methodologies using oligonucleotides 6417 and 6418 (TABLE A.2.3). Each of the three antibiotic resistance markers was integrated into each of the three variants for a total of nine strains. For competitions, equal cell numbers (OD$_{600}$ 0.005) of each strain with a different antibiotic marker were inoculated in the test condition, and biological replicates were performed using a different marker combination each time. For example, the first competition replicate included *purF*V336F-kanamycin[R], *purF*D96G-hygromycin[R] and *purF*T91del-apramycin[R], and the second replicate used *purF*V336F-apramycin[R], and *purF*D96G-kanamycin[R] etc. CFU was enumerated at each timepoint by plating 10-fold dilutions on media containing no antibiotic (MH alone), or 250 μg mL^{-1} hygromycin B, 60 μg mL^{-1} apramycin, or 50 μg mL^{-1} kanamycin, (for tracking fitness of each variant) or combinations of hygromycin B/apramycin, apramycin/kanamycin, hygromycin B/kanamycin or all three antibiotics (for recombination determination). All T-test statistical analyses were performed in Prism (GraphPad) unless otherwise stated.

4.3.5 Construction of RFP-expressing plasmid

For variant microscopy, a RFP expression construct was cloned for use in *C. jejuni* 81-176, using a strong *C. jejuni* gene promoter (*dps, cj1534c*) in context with a native ribosome binding site. The promoter-RBS was amplified from genomic DNA using oligonucleotides 3112 and 3213, digested with KpnI and XhoI, and introduced into the similarly-digested conjugative multi-copy plasmid pRY112 (289), creating pRY112-P*dps*. The RFP gene (monomeric RFP) was amplified from pBca1020-R0040 with oligonucleotides 3214 and 3215, digested with SmaI and SpeI and introduced into similarly-digested pRY112-P*dps*, creating pRY112-P*dps*-mRFP. This plasmid was conjugated into streptomycin[R] *C. jejuni* strain DRH461 by tri-parental mating with *E. coli* harboring the transfer helper pRK600, and selection on MH agar containing 200 μg mL^{-1} streptomycin. Plasmid was extracted, and transferred to the appropriate *purF* variant strain by natural transformation.

4.3.6 Fluorescent microscopy

For fluorescent microscopy, biofilms were grown on glass cover slides immersed in 1 mL of biofilm inoculum. The cover slide was removed at each timepoint, gently washed with fresh MH, or MH containing DAPI (4',6-diamino-2-phenylindol; Invitrogen) and the biofilm side was implanted onto a 1.0% agarose pad. For visualization/enumeration of planktonic bacteria or biofilms disassembled by vigorous pipetting, 1 μl bacterial culture was mounted on a 1.0% agarose pad for visualization. Cells were imaged at 1000x with a Nikon TE 2000-U microscope equipped with an argon-ion laser (EXFO X-Cite), appropriate emission/excitation filters, and a CCD-camera (Hamamatsu). ImageJ (179) was used for minimal image processing, multi-channel merging, and particle analysis to count bacteria where appropriate.

4.4 RESULTS

4.4.1 Differential variant populations are identified in biofilm and planktonic growth phases

We have established that high frequency genetic variation of the purine biosynthesis genes *purF* and *apt* is a mechanism of success in *C. jejuni*, enabling adaptation to a variety of bacterial lifestyle-relevant niches (CHAPTER THREE). Since biofilms are an important part of the *C. jejuni* lifecycle, we assessed if there was a role for purine genetic variants in biofilm formation. The heterogeneous *C. jejuni* 81-176 wild-type was used to inoculate a broth-based biofilm tube assay, and grown under standard microaerobic conditions for 72 hours. The biofilm that formed at the liquid-air interface was scraped off the glass tube for extraction of DNA, followed by *purF/apt/prsA* amplicon sequencing via Illumina MiSeq (schematic, FIGURE 4.1A). Since the "planktonic" broth phase initially contained the entire population at the time of inoculation, the population composition of broth removed from the biofilm tube was also examined at 72 hours via the same methodology. Additionally, since mature biofilms contain large quantities of non-culturable cells, cells from either the planktonic or biofilm phases were also plated for colonies (culturable), which were pooled for DNA extraction and variant analysis. Sequence analysis did not detect any *prsA* or *apt* variants in any planktonic/biofilm samples, but a variety of *purF* variants were present in both planktonic/biofilm samples. The most frequent variant in the planktonic growth phase was *purF*T91del (22% - 29%). In biofilms, the *purF*V336F (19% - 20%) and *purF*D96G (26% - 27%) variants were more frequent than in the planktonic media. Overall, the biofilm contained more different variants than the planktonic phase. Few variant frequency differences were observed between DNA obtained via colony plates or directly from the biofilm tube; thus, the impact of differential culturability on population diversity assessment via either methodology was minimal. Since the population

composition of the wild-type inoculum was previously established (CHAPTER THREE), the greater population diversity of the biofilm was due mostly to migration from the planktonic phase into the biofilm; thus the planktonic population diversity decreased as the biofilm was established.

4.4.2 Single variant isolates have diminished biofilm formation

Phenotypic testing previously revealed differential phenotypes between single colonies containing specific *purF* variants (CHAPTER THREE). We hypothesized that the variants over-represented in either the biofilm or planktonic media would either produce more biofilm or less biofilm, respectively. To test this, three *purF* variants were obtained from a genotyped collection of single colony isolates. The *purF*T91del variant was selected because it was over-represented in planktonic growth, and the *purF*V336F and *purF*D96G alleles were chosen because of their prominence in biofilms. The *purF*S256R allele was not selected because of possible culturability differences on MH agar plates (data not shown), and other variants did not exist in the genotyped isolate collection. Contrary to expectations, biofilm formation assessments of the three variant strains showed that all three variants formed less biofilm (FIGURE 4.1B and C). Additional single colony variants were tested and all produced less biofilm than the heterogeneous wild-type (not shown).
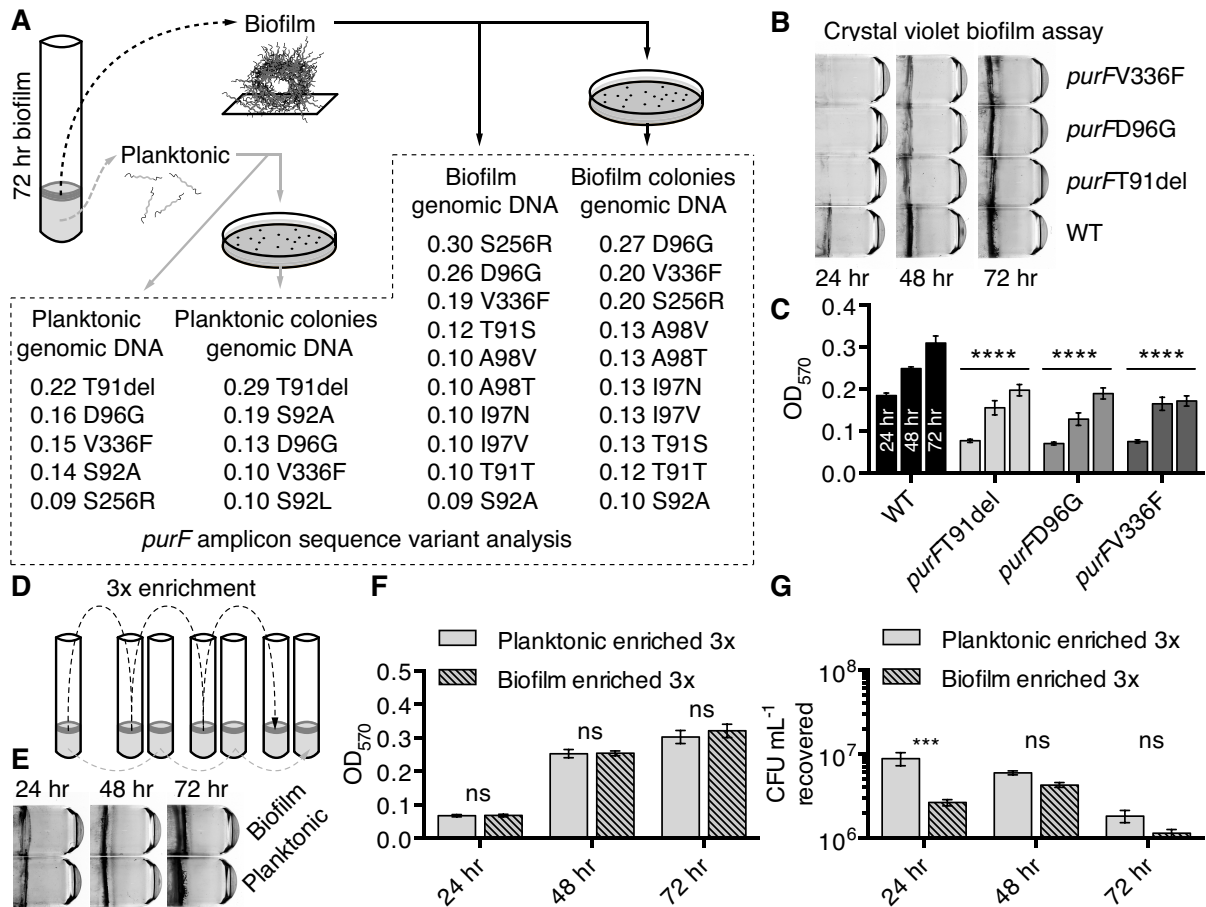
FIGURE 4.1 Differential sequence variant composition of planktonic/biofilm bacteria.
(A) Sequence variant analysis of the purine biosynthesis gene *purF*, amplified either directly from harvested planktonic/biofilm growth, or from pooled colonies obtained after plating planktonic/biofilm growth. Genetic variant frequency (max = 1.0) and predicted protein effect listed. (B) Diminished biofilm formation of three prominent genotyped single colony isolate variants. Representative images of crystal violet-stained biofilms at 24, 48 and 72 hours. (C) Biofilms quantified by dissolving adhered crystal violet and spectrophotometric measurement. Mean with SEM of three independent experiments; ****, $P \leq 0.0001$ (compared to WT at each timepoint). (D) Schematic of enrichment procedure to determine effect of selective pressure on variant population for planktonic survival and biofilm formation. (E) Equivalent biofilm formation by cells enriched from either planktonic or biofilm growth. Representative images of crystal violet-stained biofilms at 24, 48 and 72 hours. (F) Biofilms quantified by spectrophotometric measurement. Mean with SEM of three independent experiments; ns, not significant. (G) Reduced planktonic survival of cells derived from biofilm growth at early timepoint. Samples were taken from the planktonic media and assessed for CFU formation. Mean with SEM of three independent experiments; ***, $P \leq 0.001$.

4.4.3 Enriched biofilm variant populations have decreased planktonic culturability during early biofilm formation

Because single variants alone did not produce the mature biofilms of the heterogeneous wild-type, we speculated that robust biofilm formation might require a combination of both diversity and specific *purF* genotypes—i.e. the genotypes over-represented in the biofilm. Thus, biofilm formation and planktonic culturability of enriched variant populations was examined, with the expectation that enrichment of biofilm-associated variants would enhance biofilm formation, and enrichment for planktonic bacteria would decrease biofilm formation. Both biofilm and planktonic variant bacteria were enriched by growing biofilms for 72 hours before isolation of the biofilm cells from the planktonic cells, and vice-versa, for re-inoculation into new biofilm tubes (schematic, FIGURE 4.1D). After the third enrichment, both the planktonic- and biofilm-enriched cells were assessed for planktonic culturability and biofilm formation. Biofilm- and planktonic-derived cells were equally capable of producing biofilm (FIGURE 4.1E and F), but fewer biofilm-derived cells were cultured from the planktonic media at 24 hours (FIGURE 4.1G). Since there was no concomitant enhanced biofilm formation at 24 hours (i.e. no enhanced movement of planktonic cells to biofilms) this suggests that the enriched biofilm cells were sensitive to a stress imposed by planktonic growth. All data thus far suggests variant populations migrate into specific niches in which they have greatest fitness, but overall are capable of either biofilm or planktonic survival, potentially influenced by the presence/absence of competition from other variant populations.

4.4.5 Different variants have preferred planktonic/biofilm niches

To confirm that different variants had niche preferences, the three variant strains were directly competed against each other to test for relative abundance

in planktonic media or the biofilm during biofilm formation. This necessitated introduction of different antibiotic resistance markers into each of the three variant strains tested—*purF*T91del, *purF*V336F and *purF*D96G—such that the performance of each variant could be tracked by colony counts of resistant bacteria on agar containing the appropriate antibiotic (FIGURE 4.2A). Equivalent cell numbers of the three variants were mixed together for biofilm tube inoculation (FIGURE 4.2B), and the relative fitness of each variant in the planktonic media and biofilm was assessed over the course of biofilm formation at 24, 48 and 72 hours. Mirroring the amplicon sequencing data, the *purF*T91del allele variant had the highest relative fitness among planktonic bacteria, followed by the *purF*D96G variant (FIGURE 4.2C, upper panel). The variant with the highest relative fitness in the biofilm was *purF*V336F (FIGURE 4.2C, lower panel). Although this variant was not predicted by amplicon sequencing to outcompete *purF*D96G in the biofilm, both the *purF*V336F and *purF*D96G variants did outcompete *purF*T91del. Since this data approximates initial observations, any differences may stem from the fact that the competition biofilm assay was performed with only three variants—genetically modified—whereas the wild-type biofilm is many times more diverse.

To visually explore the location of the three variants in the context of the wild-type biofilm, plasmids harboring red and green fluorescent proteins were introduced into each variant strain for fluorescent microscopy. Equivalent cell numbers of variant + GFP, variant + RFP, and the heterogeneous wild-type were combined and used to inoculate a biofilm tube. Microscopy of biofilm formation was carried out, as was microscopy of the planktonic cells, to determine the localization and relative abundance of each variant. Again, the *purF*V336F variant was more prevalent in the biofilm than *purF*T91del or *purF*D96G, and the *purF*D96G variant was more prevalent than *purF*T91del (FIGURE 4.3A). Variants were evenly distributed throughout the DNA-containing (DAPI-stained) biofilm mass at 72 hours; thus, there was no specific variant

localization/structure in the biofilm. However, microscopy indicated that parts of the biofilm could contain greater numbers of any variant (not shown). Since biofilm formation is an emergent process, this may identify the allele of the cell that initially founded that biofilm. Given the subjectivity of choosing representative biofilm images, fluorescent planktonic bacteria and fluorescent bacteria from a disassembled biofilm were enumerated from images (FIGURE 4.3B). The *purF*V336F variant was again more prevalent in the biofilm than *purF*T91del or *purF*D96G, and the *purF*D96G variant was more prevalent than *purF*T91del. Among planktonic bacteria, *purF*T91del was over-represented in all tests, and *purF*D96G was more prevalent than *purF*V336F. Thus, data consistently show that *purF*T91del has a planktonic preference, and *purF*D96G and *purF*V336F prefer the biofilm, although all are capable of overlapping planktonic/biofilm lifestyles.
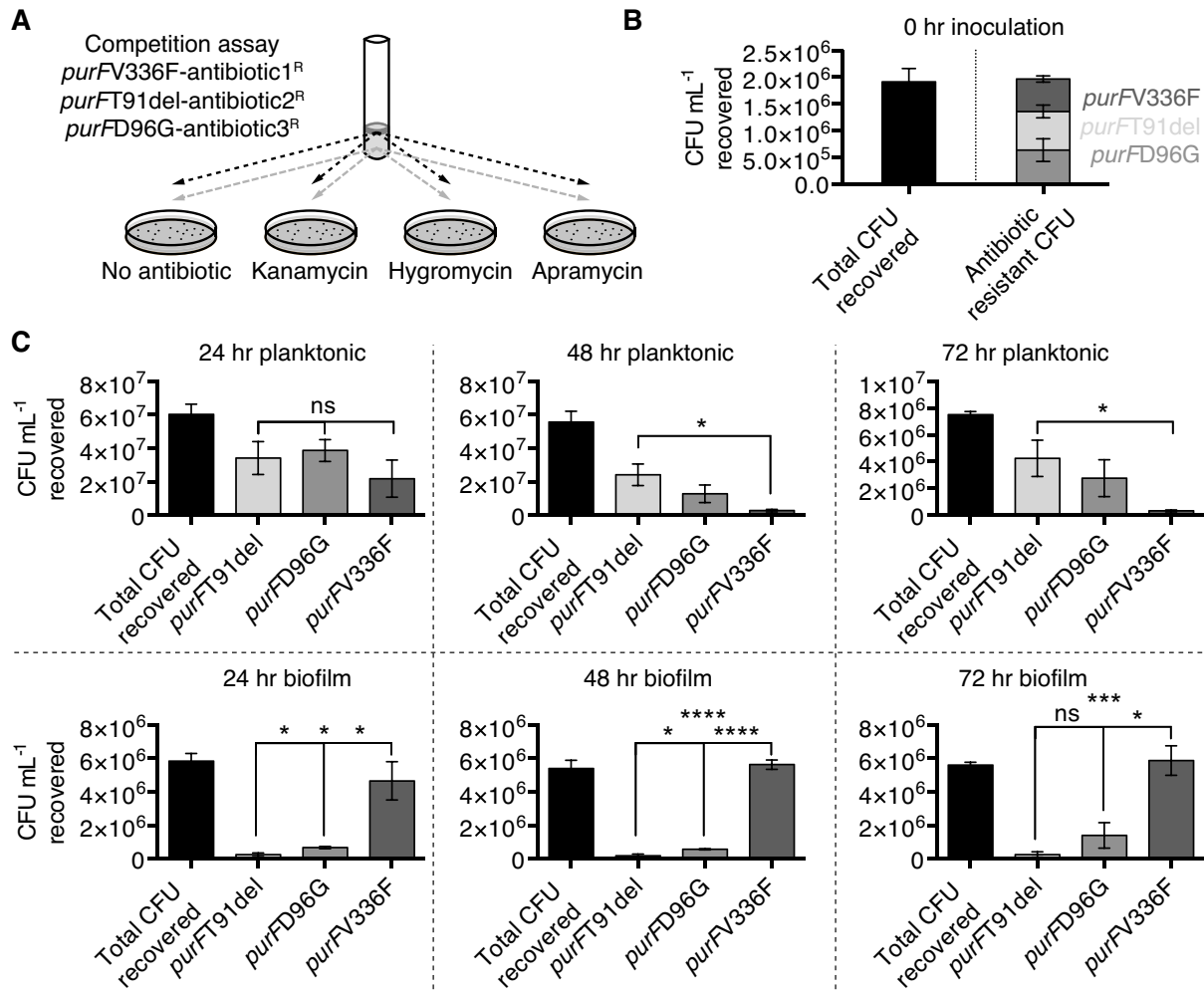
FIGURE 4.2 Niche competition between genetic variants for planktonic or biofilm lifestyles.

(A) Schematic of competition assay. Three different antibiotic resistance markers were integrated into the genomes of *purF*V336F, *purF*T91del and *purF*D96G variants. Equivalent cell numbers of each were used for biofilm assay inoculation. At each timepoint, the planktonic media or re-suspended biofilm was plated for CFU on media containing either hygromycin B, apramycin, kanamycin or no antibiotic (total CFU). (B) Equivalent CFU (stacked bar graph) recovered for each strain in competition at time of inoculation. (C) Increased planktonic fitness of the *purF*T91del variant, and over-representation in biofilms of the *purF*D96G and *purF*V336F variants. Competition CFU recovered at 24, 48 and 72 hours from both the planktonic (upper) and biofilm (lower) growth. Data from three independent competitions, showing mean with SEM; *, $P \leq 0.05$; ***, $P \leq 0.001$; ****, $P \leq 0.0001$.
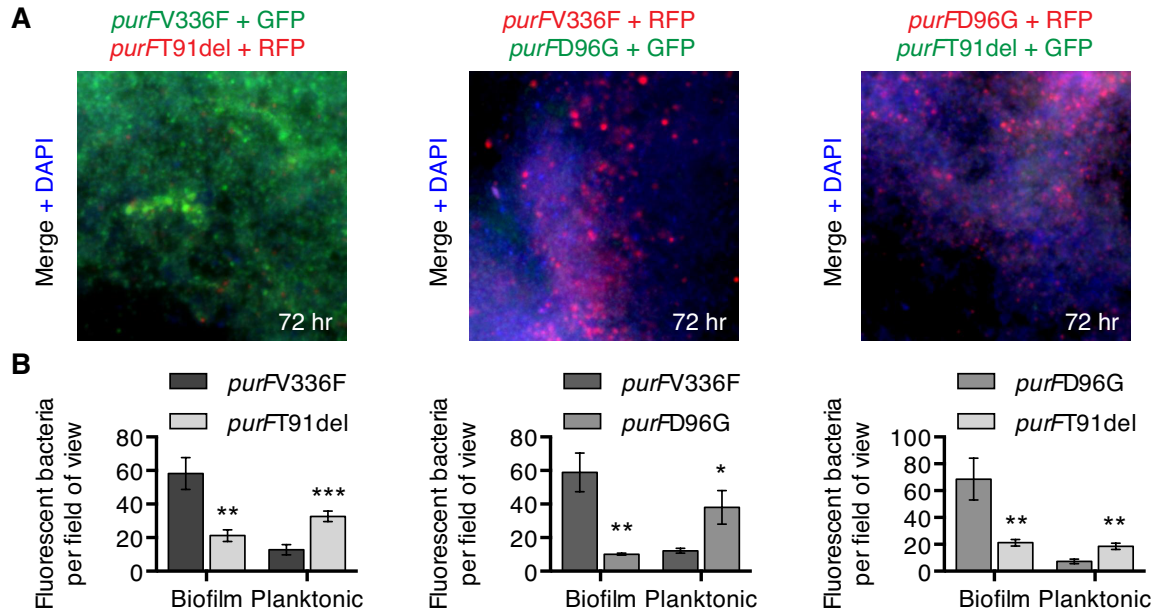
FIGURE 4.3 Microscopic visualization of competition between GFP/RFP-marked genetic variant strains in the context of a WT biofilm.

Plasmids expressing GFP or RFP were introduced into *purF*V336F, *purF*T91del or *purF*D96G. Biofilms were inoculated with equivalent cell numbers of the heterogeneous WT and any two GFP/RFP variants. Intact biofilms or re-suspended biofilms and planktonic cells were imaged at 1000X magnification. (A) The *purF*V336F and *purF*D96G variants dominate late-stage biofilms. Representative images of 72 hour biofilms merged with DAPI (Blue, DNA) to show non-RFP/GFP cells and extracellular DNA. (B) The *purF*T91del variant dominates the planktonic population. Fluorescent cells were enumerated from 10 fields-of-view. Data from six independent competitions, showing mean with SEM; *, $P \leq 0.05$; **, $P \leq 0.01$; ***, $P \leq 0.001$.

4.4.6 Enhanced genetic recombination between biofilm-preferring variants

C. jejuni is a naturally competent bacterium that can readily uptake and integrate extracellular DNA (73, 238, 290, 291). Mature biofilms contain large quantities of DNA that contribute to the biofilm matrix in *Campylobacter* and other bacterial species (73, 275, 283). Considering that certain variants are overrepresented in biofilms, we hypothesized that variants with greater niche overlap should have higher rates of recombination. In contrast, variants with less niche overlap should have less opportunity for DNA transfer and recombination. To test this, the same antibiotic-marker based competition assay was carried out as previously, except that the harvested biofilm and planktonic

94

bacteria were plated on double combinations of the relevant antibiotics. Thus, a bacterium that was resistant to two different antibiotics would have received a copy of the resistance gene from another variant. As expected, the greatest exchange was in biofilms, between the *purF*V336F and *purF*D96D biofilm-preferring variants (FIGURE 4.4). Exchange was not detected between *purF*T91del and *purF*V336F in biofilms, and no recombination between any planktonic bacteria was detected within the limits of the assay (not shown). Thus, variants that prefer the biofilm lifestyle have greater opportunity for genetic recombination.
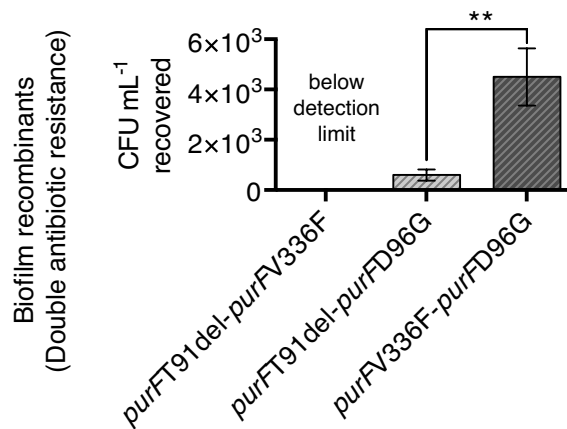
FIGURE 4.4 Enhanced genetic exchange and recombination between biofilm-associated variants.
The transfer of a second antibiotic resistance marker to any of the three marked variant strains in the competition assay (FIGURE 4.2) was measured by enumerating CFU on plates containing double-combinations of hygromycin, apramycin and kanamycin. Data shown is from cells harvested from 24 hour biofilm only. Limit of detection is 10^2 CFU. Data from three independent competitions, showing mean with SEM; **, $P \le 0.01$.

4.4.6 Atmospheric oxygen selects for a planktonic niche variant

The potential for genetic recombination in biofilms is a powerful advantage for those variants, but what is the advantage for planktonic cells? Motile planktonic cells can move to new nutrient-rich niches via chemotactic cues (70), but in doing so they are potentially exposed to a wider variety of environmental stresses than biofilm cells. When forcibly returned to the

planktonic media, biofilm cells decreased in CFU relative to planktonic cells (FIGURE 4.1G); thus, we hypothesized that planktonic bacteria experience an additional stress that biofilm bacteria do not. We also previously showed that exposure to atmospheric oxygen selects for certain *purF* allelic variants—notably *purF*T91del, the variant most over-represented among planktonic bacteria (*in* CHAPTER THREE). Therefore, we speculated that *purF*T91del has enhanced oxygen survival properties. To test this, a similar antibiotic-marker based competition assay was carried out using *purF*T91del, *purF*V336F and *purF*D96G, and equivalent cell numbers were used to inoculate shaking cultures, which were then incubated microaerobically or aerobically for colony counts. Under microaerobic conditions, all three strains competed equally (FIGURE 4.5, left panel), and this experiment also showed that competition bias was not introduced into previous experiments by use of any particular antibiotic resistance marker. In clear contrast, under aerobic conditions, the *purF*T91del variant outperformed both *purF*V336F and *purF*T91del (FIGURE 4.5, right panel). Thus, the *purF*T91del variant has enhanced aerobic survival properties; correspondingly, planktonic bacteria may be exposed to greater concentrations of oxygen than biofilm bacteria.
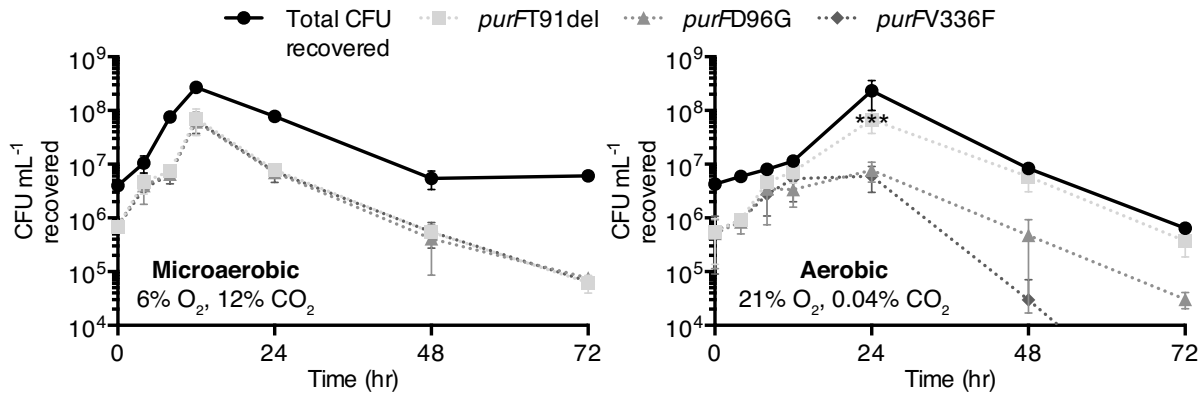
FIGURE 4.5 Fitness selection of *purF*T91del in aerobic stress conditions.
Relative fitness of antibiotic resistance-marked *purF*V336F, *purF*T91del or *purF*D96G was assessed by growth competition in standard atmospheric conditions (microaerobic), and in oxygen stress (aerobic). Growth was assessed from shaking cultures at 38°C by plating for CFU on media containing the appropriate antibiotic. Mean with SEM of three independent experiments; ***, $P \leq 0.001$ (compared to next fittest variant *purF*D96G).

4.4.7 Enhanced biofilm formation can be restored by re-constitution of the heterogeneous population

Since single variant isolates did not produce the enhanced biofilms of the heterogeneous wild-type, we hypothesized that population diversity was the factor responsible for improved biofilm formation. To test this, we speculated that mixing ("de-isolating") single colony isolates would restore the enhanced biofilm. Mixing the three variants *purF*T91del, *purF*V336F and *purF*D96G did not restore the enhanced biofilm (not shown), neither did pooling ten different *purF* variants nor even 100 single colony isolates (FIGURE 4.6A and B). Enhanced biofilms were only restored when ~1,000 colonies or greater were used. To ensure equivalency, all colonies were isolated on MH agar plates before pooling, and all biofilms were set up with equivalent cell numbers at time of inoculation. Taken together, data thus far suggests that population diversity is key for enhanced biofilm formation, which may rely on both specific variants and their relative abundance.
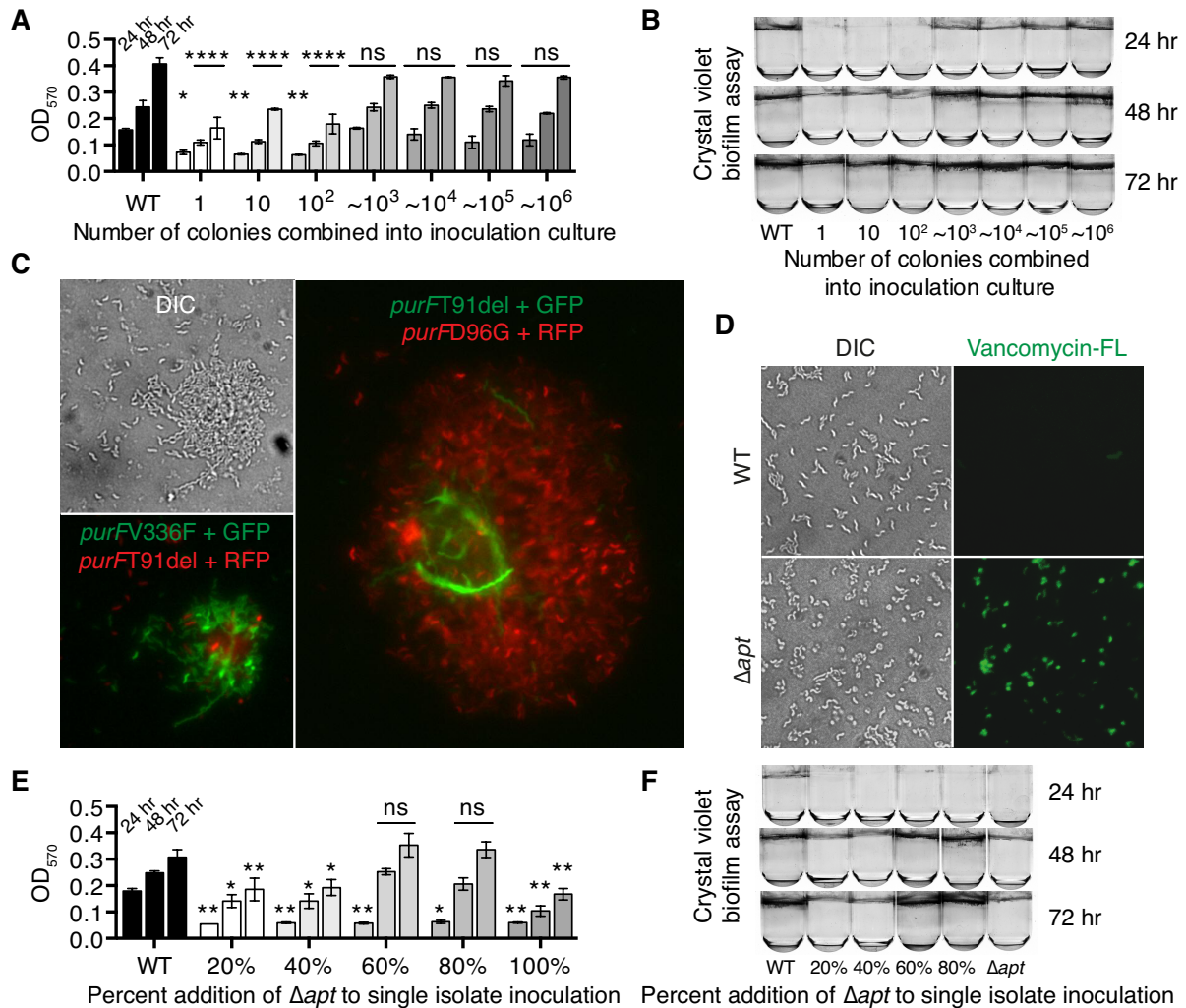
FIGURE 4.6 Increased genetic heterogeneity enhances biofilm formation.
(A) All single colony variants tested produced less biofilms than the heterogeneous WT (FIGURE 4.1). To reconstitute the original variant composition of the population, pools of colonies increasing 10-fold in colony numbers from 10 to ~10^6 were tested for full biofilm restoration. Enhanced biofilm formation was observed for pools of ~10^3 colonies or greater. Mean with SEM of three independent experiments; ns, not significant (compared to WT at each timepoint). (B) Representative images of crystal violet-stained biofilms of colony pools at 24, 48 and 72 hours. (C) Heterogeneity-mediated microcolony interactions occurring during initial biofilm formation. Aberrant morphology/differential behavior of co-localized GFP/RFP-tagged variants in microcolonies imaged at 24 hours. (D) Deletion of the fitness-required purine biosynthesis gene *apt* causes late-stage cell lysis and aberrant morphologies. (E) Restoration of enhanced biofilm formation by increasing addition of Δ*apt* to the inoculum of a single colony variant biofilm assay. Mean with SEM of three independent experiments; ns, not significant (compared to WT at each timepoint). (F) Representative images of Δ*apt*-added crystal violet-stained biofilms from at 24, 48 and 72 hours.

4.4.8 Heterogeneity-mediated variant interactions at early biofilm founding may promote enhanced biofilm formation

Biofilms are thought to arise from a founding cell that propagates into a microcolony that eventually matures into a complex DNA-containing matrix of cells (269). How does heterogeneity in the *C. jejuni* population enhance biofilm formation in this model? Microscopy of GFP/RFP-tagged variants in the context of the heterogeneous wild-type showed unusual phenotypic behavior occurring in microcolonies at early biofilm formation (FIGURE 4.6C). An early (24 hr) microcolony was observed (FIGURE 4.6C, upper left panel, differential interference contrast) and predominantly contained the *purF*V336F variant (FIGURE 4.6C, lower left panel). Unusually, a number of those microcolony cells exhibited chaining, whereas bacteria not associated with the microcolony did not. Differential behavior was observed in a number of microcolonies; interestingly, one was observed in which the planktonic-associated *purF*T91del was "trapped" within a microcolony primarily composed of *purF*D96G (FIGURE 4.6C, right panel). In that example, the *purF*T91del cells were discreetly localized within the growing microcolony, and exhibited extensive chaining. Although it is unclear what prompted that phenotypic behavior in microcolonies, *C. jejuni* chains under a number of stress conditions, some of which may lead to cell death (1, 126). Thus, we hypothesize that the increased occurrence of spontaneous encounters between variants in the heterogeneous population promoted those interactions. Given that variants have differential stress resistance/sensitivity, entrapment/association with a competing variant may result in context-dependent lysis (i.e. a variant in "the wrong place at the wrong time"). The addition of DNA is known to promote enhanced *C. jejuni* biofilm formation (73). To test if lysis of a population of cells could promote enhanced biofilm formation, the purine biosynthesis mutant Δ*apt* was added to a single colony isolate biofilm. Although mutation of *apt* is possible, the mutant is fragile, morphologically aberrant, and undergoes frequent lysis, as indicated by

99

permeabilization and entry of fluorescent vancomycin (FIGURE 4.6D). Thus, Δ*apt* was added to a single colony isolate (*purF*D96G) biofilm tube assay in increasing concentrations, but the overall cell number was held constant such that the total number of cells in the biofilm inoculum was equivalent to OD_{600} 0.005. Addition of Δ*apt* was found to enhance biofilm formation when Δ*apt* comprised >60% of the population, but the Δ*apt* strain alone was a poor biofilm-former (FIGURE 4.6E and F). Taken together, this data suggests that if lysis of "unfortunate" variants in microcolonies occurs, the release of DNA may promote enhanced biofilm formation.

4.5 DISCUSSION

C. jejuni is a significant public health concern because the prevalence of the bacterium leads to frequent foodborne contamination, and the post-infectious afflictions are major personal and economic burdens. Understanding the successful transmission of the bacterium is key to limiting such costs, and the biofilm lifestyle represents a key mode of survival in adverse environments. Mechanisms for *C. jejuni* biofilm/aggregate formation are not fully understood, but formation is stimulated by a number of stress conditions, including aerobic exposure (268, 269). Cells are protected within biofilms, and resist otherwise lethal osmotic concentrations, oxidative stress, pH, UV-exposure, antimicrobials, host immune responses, predation, and inter-species competition (114, 271-275, 281, 282, 292-294). Thus, the rapid formation of mature, robust biofilms is a potential success strategy in the *C. jejuni* pathogenesis cycle.

With these experiments, we showed that population genetic heterogeneity of the essential *C. jejuni* purine biosynthesis gene *purF* contributed to enhanced biofilm formation. The precise cellular effects of these purine biosynthesis mutations are presently under scrutiny in our laboratory, but their association

with differential stress survival outcomes implies they are a novel adaptive strategy. Because *purF* is an essential housekeeping gene, the high frequency of mutation and reversion in this gene—and others (212)—is astounding, and currently unexplained. *C. jejuni* is already well known as a phase variable bacterium (19), wherein mispairing during DNA replication promotes rapid phenotypic switching of surface-exposed structures, such as flagella, capsule, and lipooligosaccharide, thus providing community phenotypic variation (62, 208, 295). In natural bacterial populations, both planktonic and biofilm, intra-population genetic heterogeneity is normal (296, 297), in contrast to artificially isolated homogenous laboratory recreations.

DNA is required for the maturation of *C. jejuni* biofilms (73), and is integral to biofilms of many species (275, 282, 284). Cell lysis is implicated in *C. jejuni* biofilms, but the exact DNA-contributing mechanism is not understood (283). In the current study, we observed differential behavior of variants in proximal sessile association, and proposed that local antagonistic interactions between variants at the initial stage of biofilm formation could result in death/lysis of the less-fit or loser variant. We speculated that these intra-species interactions contributed DNA to the biofilm matrix, and enhanced the rate of formation of biofilm. Although this model requires that a cell die—a regrettable event for the individual cell—such behavior within the microbial community may be altruistic—i.e. for "the greater good", promoting the global success of the group. As we demonstrated, high rates of recombination occurred between biofilm-preferring variants; thus, the genetic individuality of the loser cell may persist after death via horizontal gene transfer, lessening the sacrifice. Despite this, selfless conduct is acknowledged as "multicellular behavior" (281, 298-300). Similar multicellular biofilm-forming behaviors in bacteria often rely on specific mechanisms such as toxin-antitoxin systems and autolysins (301, 302).

Microcolony interactions between variants were characterized by chaining of one of the variants, which formed a discrete cluster of chains. Interestingly, chains are a transient morphology of *Bacillus subtilis* and ovococci during their early biofilm formation, and in the established biofilm, the chains disband and form an aggregate of cells (298, 303, 304). Enhanced biofilm formation in heterogeneous *C. jejuni* populations may result from the increased potential for variant encounters that promote chaining. Although we speculate that chains, or parts of chains, may lyse, the specific fate of chained variants in the biofilm is unclear. However, chain clusters seen in microcolonies were not observed in mature *C. jejuni* biofilms, where the primary morphology was coccoid (FIGURE 4.3). *C. jejuni* chains under stress conditions; previously, we showed that chaining occurred in hyperosmotic stress, and cells within the same chain exhibited differential phenotypic behavior (1). Different *purF* variants also chained more-or-less under hyperosmotic stress (unpublished observations). Although there are benefits to chaining, such growth is not sustainable in the long-term because impaired motility and increased cell density limit nutrient availability (126, 298). Since chains are physically connected, they are literally "multicellular" entities, a characteristic shared with biofilms.

The over-representation of the aerotolerant *purF*T91del allelic variant in planktonic bacteria suggested that the planktonic milieu had increased concentrations of oxygen. Selection for advantageous genotypes within and outside of biofilms may occur in part because chemical gradients create microniches; vice-versa, chemical gradients may be established by spatially structured cells in communities. For example, *Pseudomonas aeruginosa* biofilms deplete oxygen, creating anoxic microniches because of cellular respiration, and because oxygen only permeates the biofilm to a depth of 90 μm (305, 306). *C. jejuni* forms increased quantities of biofilm under aerobic conditions (268), and deletion mutants lacking the oxidative stress defense alkyl hydroperoxidase (*ahpC*) display increased biofilm formation (141). As a highly motile bacterium,

C. jejuni is both aerotactic (chemotaxis with air/oxygen as the repellent/attractant) and chemotactic, and swims to preferentially occupy a point in the O_2 gradient in which the energy obtained from the oxidation of different electron donors/substrates outweighs the cost of the negative effects of oxidative stress (70, 135, 139, 242). Thus, the benefit of the planktonic lifestyle for the *purF*T91del variant may be efficient oxidative phosphorylation that providing more energy for flagella motivation. This "adventurer" variant may gain access to more nutrients, and new colonization sites, at the risk of greater stress exposure. As we demonstrated, variants with planktonic niche preferences are precluded from biofilm genetic recombination opportunities.

Overall, our data pointed to an important role for the adaptive properties of *purF* genetic variation in enhanced biofilm formation, and thus illustrated the functional importance of variation within natural populations. Thus, the current study also provided additional evidence that deliberate non-clonality via non-phase variable mechanisms has importance for *C. jejuni* fitness. To the best of our knowledge, our data provide the first example of intraspecies/intraspecific microniche preference, and the first observation of differential phenotypic behavior caused by cell-cell interactions in *Campylobacter*. In conclusion, new insight revealed the complexity of biofilm formation, with implications for infectious transmission and pathogenesis of *C. jejuni*.

CHAPTER FIVE: Elucidating the role of *cj1533c* in hyperosmotic and oxidative stress survival of *Campylobacter jejuni*

5.1 SYNOPSIS

Transcriptional modulation of the hyperosmotic stress response in multiple bacterial species commonly utilizes widely conserved regulatory mechanisms, such as the EnvZ/OmpR osmoregulation system. Despite this, *Campylobacter jejuni* does not encode known osmotic stress regulators, which is remarkable for a small 1.5 Mbp genome that contains relatively few transcription factors. Transcriptional profiling by DNA microarray of *C. jejuni* in NaCl-stress identified a putative transcription factor upregulated in hyperosmotic conditions that was encoded by *cj1533c*, a previously uncharacterized gene. In the current study, *cj1533c* was found to be critical for hyperosmotic and oxidative stress survival, as a deletion mutant was sensitive to both NaCl and H_2O_2 exposure. Under hyperosmotic stress, the *cj1533c* deletion mutant also exhibited extensive chaining. Despite a clear role in adaptation, a DNA microarray transcriptome of the *cj1533c* mutant did not reveal any stress-protective transcriptional modulation, but suggested that *cj1533c* was co-transcribed with an upstream gene encoding the oxidative stress-activated iron-sequestering bacterioferritin Dps. Northern blotting determined that *dps* and *cj1533c* could be co-transcribed on a polycistron regulated by the iron and oxidative stress regulators Fur, PerR and CosR. Structural homology analysis of Cj1533c determined that protein had been misannotated as a DNA-binding regulator, and instead indicated that the protein was an ATPase. Site-directed mutagenesis of critical ATPase residues deleted Cj1533c function. A directed evolution screen for *cj1533c* mutations that enhanced hyperosmotic tolerance identified a putative sRNA encoded within the *cj1533c* sequence. SILAC-based proteomics revealed reduced expression of iron-sulfur containing central

metabolic proteins in the proteome of the *cj1533c* deletion strain. In the deletion strain harboring the putative sRNA, proteins involved in sulfur homeostasis/cysteine metabolism were found to have enhanced expression. A SILAC-based protein-protein affinity interaction screen identified putative interaction partners for Cj1533c, which included the ATP sulfurylase, and Ppx1/GppA, a protein with roles in hydrolysis of stress-relevant polyphosphate, and the stringent response alarmone guanosine pentaphosphate, or pppGpp. Thus, this investigation potentially identified a novel protein/sRNA system as a determinant of hyperosmotic/oxidative stress tolerance, and provided initial evidence for functions in the coordination of multiple *C. jejuni* homeostatic processes.

5.2 INTRODUCTION

As an emerging zoonotic water- and food-borne human pathogen (26), *Campylobacter jejuni* inhabits many animal species harmlessly (43, 307), but is also frequently isolated from external water sources and other environments (44, 183, 240, 308). During this transmission, the bacterium encounters a variety of stresses, including osmotic and oxidative stress, and nutrient limitation, which *C. jejuni* successfully surpasses despite stringent microaerophilic, temperature, and nutrient requirements (64, 135, 143, 200). Thus, the bacterium must sense and adapt to stress stimuli, altering gene expression and other behavior appropriately for survival. The *C. jejuni* transcriptome is likewise altered during animal colonization and host cell interaction (117, 143, 162). The genomes of multiple *C. jejuni* isolates encode comparatively few transcription factors/regulatory proteins, and many classic bacterial regulatory systems are absent (19, 24, 309-311). Furthermore, *C. jejuni* encodes only three σ factors—σ^{70} (housekeeping gene expression), and σ^{28} and σ^{54}, which are primarily involved in *C. jejuni* flagellar gene control (19). A large portion of the transcription factor-based regulatory arsenal is devoted to expression modulation of heat shock

(128), iron homeostasis (149, 150), and aerobic/oxidative stress response systems (140, 142), which are increasingly well-characterized in *C. jejuni* (115, 139, 145), and which often cross-protect against associated stresses (1, 126, 127, 141, 176).

Transcriptional profiling of the hyperosmotic stress response of *C. jejuni* identified *cj1533c* (*CJJ81176_1518*) as a NaCl-upregulated gene encoding a putative transcription factor (1). Cj1533c is annotated as containing a putative helix-turn-helix, a structural DNA-binding motif found in certain transcriptional repressors (94, 312). Thus, we initially hypothesized that *cj1553c* encoded an uncharacterized transcription factor involved in the *C. jejuni* hyperosmotic stress response. In the current study, *cj1533c* was found to be critical for hyperosmotic and oxidative stress survival, but despite this, deletion of *cj1533c* did not significantly alter the transcriptome in whole-genome DNA microarray transcriptional analyses. Contrary to the gene annotation, structural homology analysis suggested that Cj1533c is an AAA+ family protein (**A**TPases **A**ssociated with various cellular **A**ctivities). These proteins universally contain a structurally conserved ATP binding/ATPase domain, which contains Walker A and Walker B motifs (313). The Walker A P-loop (**p**hosphate **loop**) coordinates the β and γ phosphates of ATP during nucleotide hydrolysis. The Walker A motif is recognized by a critical lysine in the consensus sequence $G_{XXXX}GK[T/S]$ (where $_X$ is any amino acid), and the consensus sequence of the Walker B motif is $_{hhhh}DE$ (where h is any hydrophobic amino acid) (314). In Cj1533c, the predicted Walker A motif sequence is $G_{PRFC}GKKT$ (residues 33-41) and the predicted Walker B motif is $_{ILFL}DL$ (residues 55-60). In many cases, AAA+ proteins assemble into oligomeric structures, which change conformation during ATP binding and/or hydrolysis cycles (314-318). These conformational changes may in turn mediate conformational changes/activities in interacting or substrate proteins (314).

In this preliminary investigation, screening for protein-protein interactions via quantitative proteomics suggested that Cj1533c interacted with

106

ATP sulfurylase and Ppx1/GppA, proteins responsible for sulfur activation (319), and hydrolysis of polyphosphate and the stringent response alarmone pppGpp (120). In *C. jejuni*, the stringent response facilitates aerobic stress survival (117). Proteome comparisons between *C. jejuni* wild-type and a *cj1533c* deletion mutant also suggested that Cj1533c promotes the biogenesis of central metabolic (TCA cycle) and amino acid biosynthetic protein complexes. These complexes are notable for subunits containing iron-sulfur (Fe-S) clusters (66, 144), which have demonstrable oxygen-lability (148). Reactive oxygen species (ROS) inactivate Fe-S proteins, which liberates iron and sulfur and further promotes oxidative damage by metal-catalyzed free radical production via the Fenton reaction (135, 139, 148). Here, we also demonstrated that *cj1533c* was co-transcribed with the oxidative stress-activated iron-sequestering bacterioferritin Dps (145, 146), and further demonstrated that both genes were transcriptionally regulated by the Fur, PerR, and CosR iron/oxidative stress regulators (140, 144, 149, 150). Lastly, a possible sRNA (bacterial **s**mall regulatory **RNA**) encoded within *cj1533c* was putatively identified, and was found to modulate the expression of sulfur homeostasis proteins. Taken together, the current investigation provides initial evidence for a major role for the *cj1533c* locus in the coordination of key cellular processes via the regulation of sulfur homeostasis and the stringent response.

5.3 METHODS AND MATERIALS

5.3.1 Bacterial strains and growth conditions

Studies were performed using the *C. jejuni* wild-type strain 81-176 (see TABLE A.1.4 for a list of strains and plasmids) (33). All *C. jejuni* strains were maintained at 38°C on Mueller-Hinton (MH) agar or broth (Oxoid) supplemented with vancomycin (10 µg ml^{-1}) and trimethoprim (5 µg mL^{-1}) under microaerobic and increased CO_2 conditions (6% O_2, 12% CO_2) in a Sanyo tri-gas incubator

107

(solid media) or generated using the Oxoid CampyGen system (shaken broth cultures). MH was supplemented with chloramphenicol (15 µg mL^{-1}), kanamycin (50 µg mL^{-1}), hygromycin B (250 µg mL^{-1}) or apramycin (60 µg mL^{-1}) where appropriate. *E. coli* strains were maintained on LB agar, supplemented with ampicillin (200 µg mL^{-1}) or other antibiotics when appropriate.

5.3.2 Gene deletion and complementation

All gene deletions and transformation were carried out via antibiotic marker replacement and using standard *C. jejuni* cloning/genetic techniques (214). For mutagenesis of *cj1533c*, the *cj1533c* gene was PCR-amplified from wild-type 81-176 genomic DNA with oligonucleotides 5712 and 5713 using iProof DNA polymerase (see TABLE A.2.4 for oligonucleotides used in this study). The PCR product was purified, A-tailed and ligated to pGEM-T to make pGEM-T+*cj1533c*, which was transformed into *E. coli* DH5α and selected for with ampicillin. Inverse PCR was performed on the resulting plasmid with oligonucleotides 5714 and 5715 which deleted residues 39 - 316 of the 346 aa *cj1533c,* and introduced *Kpn*I and *Xba*I sites. The inverse PCR product was digested with *Kpn*I and *Xba*I, and ligated to a similarly-digested *aphA-2* non-polar kanamycin resistance marker (289). The resulting construct, pGEM-T+*cj1533c::aphA-2* was purified, sequence-verified, and then transformed into *C. jejuni* 81-176 to create Δ*cj1533c::aphA-2* (Δ*cj1533c*, kanamycin^R). Replacement mutations in *fur, perR,* and *dps* were similarly constructed, with hygromycin, apramycin, and apramycin resistance markers respectively (oligonucleotides in TABLE A.2.4) (2). Overexpression of *cosR* (*atpF'-cosR* or *cosR^{OE}*) was carried out by fusion to the strong *atpF'* promoter in pRY112 (289). Overexpression was confirmed by Western blotting with α-CosR antibody gifted from Stuart A. Thompson, Medical College of Georgia (73).

For complementation of *cj1533c*, iProof PCR was used to amplify *cj1533c* (and derivatives) with 75 bp of the preceding intergenic promoter via oligonucleotides 8610 and 8613, which introduced *Xba*I and *Mfe*I restriction sites. The PCR products, and pRRC, were digested with *Xba*I and *Mfe*I, and the plasmid was dephosphorylated with Antarctic Phosphatase (NEB). The *cj1533*c gene was ligated to the plasmid and transformed into *E. coli* DH5α. The resulting plasmid was introduced into the Δ*cj1533c* mutant. The site-directed mutant *cj1533c*KK40,41GG was introduced into Δ*cj1533c* via pRRC in the same manner, and was created via standard *Dpn*I-mediated site-directed mutagenesis (320). For the directed evolution of *cj1533c*, the same promoter-*cj1533c* sequence as used in Δ*cj1533c* complementation was amplified via Taq polymerase in the presence of increasing concentrations of $MnCl_2$, as per established protocol (321). The resulting erroneous PCR products were digested with *Kpn*I and *Xba*I, and cloned into similarly digested pRY112 (chloramphenicol[R]) (322). The resulting library (~100,000 colonies) was conjugated into Δ*cj1533c* via triparental mating with the helper strain pRK600 (79, 323), and selection on MH agar containing kanamycin and chloramphenicol. The resulting *C. jejuni* library was pooled, and used to inoculate 10 mL MH +1.0% NaCl broth. Enrichment for resistant clones was carried out by growing the cells for 24 hours, and then sub-culturing ($1/10^5$) in fresh broth for further growth, repeated three times. Clones with hyperosmotic stress resistance were identified, sequenced, and the resulting *cj1533c* modification was transferred into pRRC for genome-insertion into the original Δ*cj1533c* background. Hyperosmotic stress testing confirmed the genome-inserted copy of the erroneous *cj1533c* sequence (the putative sRNA) was equivalent to the plasmid-borne copy in phenotype.

5.3.3 Examination of growth and stress tolerance

C. jejuni strains were grown in MH broth overnight to mid-log phase then diluted to an OD_{600} of 0.005 in the appropriate pre-warmed media. Cultures

109

were incubated under standard *C. jejuni* growth conditions at 38°C with shaking at 200 rpm. Growth and culturability were assessed by plating serial 10-fold dilutions for CFU on MH agar. For percent survival sensitivity comparisons between strains, a spot CFU count method was used. Strains were standardized to an OD_{600} of 0.1, and 10 µl of serial 10-fold dilutions was spotted on MH or MH + 1.0% agar for CFU enumeration. For oxidative stress tolerance studies, OD_{600} 0.1 of each strain tested was washed in PBS and then re-suspended in either PBS or PBS + 1 mM H_2O_2 (Sigma). After 15 minutes, serial 10-fold dilutions were plated on standard MH medium, and CFU were enumerated. Oxidative stress studies were carried out in room atmosphere. Microscopy of bacterial cells was carried out as previously described (1, 126). All T-test statistical analyses were performed in Prism (GraphPad) unless otherwise stated.

5.3.4 RNA extraction and Northern blotting

Bacteria from log phase overnight cultures were diluted to OD_{600} 2.0 in MH and inoculated into an equal volume of MH or MH + 2.0% NaCl (final starting OD_{600} of 1.0, and final NaCl concentration of 1.0%). At indicated time points, bacteria were removed into a 1/10 volume of 10X Stop solution (5% buffer-saturated phenol in 95% ethanol), collected by centrifugation at 10,000 x *g* for 5 min at room temperature, flash frozen in a dry ice/ethanol bath, and stored at -80°C. Total RNA was extracted from growth curve time points based on methods described (174). RNA concentration was quantified using a ND-1000 spectrophotometer (NanoDrop), and RNA quality was assessed by electrophoresis on 1.0% agarose TAE gels. For RT-PCR, cDNA was synthesized via SuperScript III first strand synthesis reverse transcriptase, as per the manufacturer's instruction (Invitrogen). RT-PCR confirmation of the *dps-cj1533c* polycistron was carried out with oligonucleotides 2435 and 2436. For Northern blotting, a **di**oxy**g**enin (DIG)-labeled probe was PCR-generated with oligonucleotides 5714 and 2432 as per the manufacturer's instruction (Roche,

DNA labeling and detection kit). Northern blotting was carried out using 7 μg total RNA separated on a 1% agarose, 1X MOPS, 6.3% formaldehyde gel, and transferred to nylon membranes for chemiluminescent detection as described (324).

5.3.5 SILAC-based proteomic expression profiling

Total proteome expression profiling SILAC-based mass spectrometry was carried out via standard methodologies (217, 325-328). Briefly, the *C. jejuni* arginine auxotroph Δ*argH::cat* (Δ*argH,* chloramphenicol^R) was used as the wild-type strain, and all *cj1533c* genetic modifications were introduced into this strain, necessitating modification of complementation and putative sRNA plasmid constructs. Thus, the *+cj1533c* complement and putative sRNA were each shuttled from pRRC (chloramphenicol^R) to pRRA (apramycin^R) for integration into Δ*argH*Δ*cj1533c* (chloramphenicol^R and kanamycin^R). The resulting cell lines were metabolically labeled with 400 μM either "light" L-arginine (Δ*argH*Δ*cj1533c*), "medium" $^{13}C_6$-L-arginine (Δ*argH*Δ*cj1533c+cj1533c* or Δ*argH*Δ*cj1533c*+putative sRNA), or "heavy" $^{14}N_4{}^{13}C_6$-L-arginine (Δ*argH*) (Cambridge Isotope Laboratories) as the SILAC amino acid in modified SILAC DMEM medium (Sigma, DMEM (Lys/Arg -/-) containing 4500 mg/L glucose, 4 mM L-glutamine, supplemented with 20 mM glutamine, 10 μM iron ascorbate). Cells were grown in 10 mL of the SILAC media overnight (shaking, 38°C), then sub-cultured at OD$_{600}$ 0.3 and grown for 4 hours to achieve complete labeling/log-phase growth. To assess the effect of hyperosmotic shock, an equivalent volume of the appropriate DMEM alone or containing 1.0% NaCl was added to OD$_{600}$ 4.0 of cells. The cells were re-suspended and exposed for 15 minutes. At the end-point, equivalent 1:1:1 ratios of three different strains ("light", "medium" and "heavy") were combined prior to lysis by boiling in Lysis Buffer (4% SDS, 100 mM Tris/HCl pH 7.6, 0.1 M DTT) for 10 minutes, and pre-clearing via centrifugation at 12,000 x g for 20 minutes. Proteins were precipitated, digested

with ArgC, and purified peptides were analyzed by reversed phase LC-MS as per standard techniques (additional techniques described in Appendix A3 Additional Methods and Materials). MaxQuant (v1.3.0.5)(217) was used for identification and quantification of the resulting experiments. Database searching was carried out against the NCBI *C. jejuni* 81-176 database (Accession: PRJNA58503, downloaded 27/08/2013) (total 1758 protein sequences). ANOVA statistical analysis was carried out across all samples to identify peptides expressed at significantly different levels between samples. Hierarchical cluster analysis was performed/visualized in TM4 MeV Multiexperiment viewer (329).

5.3.6 Affinity purification of Cj1533c

Purification of recombinant Cj1533c was carried out with gravity flow chromatography as per the procedures detailed in the Ni-NTA-agarose Qiagen Protein Purification Handbook (Qiagen). Briefly, *cj1533c* was cloned into pET28a(+) utilizing *Nco*I and *Xho*I restriction sites to fuse the *cj1533c* sequence to a C-terminal 6XHIS tag. The resulting plasmid was transferred into BL21(DE3) competent *E. coli* (New England Biolabs) for protein expression. Expression was achieved in 500 mL LB cultures (+ 50 μg mL^{-1} kanamycin) inoculated 1/1000, and grown to log-phase (OD$_{600}$ 0.5) shaking at 37°C. Prior to *lac* promoter induction with 1 mM IPTG (Sigma), cultures were cooled to RT, and induced overnight shaking at RT. Cells were pelleted and frozen, then lysed by sonication in 3 mL Lysis Buffer (50 mM NaH$_2$PO$_4$, 300 mM NaCl, 10 mM imidazole, pH 8.0). Lysates were centrifuged for 30 minutes at 12,000 x g at 4°C, and then 1 mL of Ni-NTA-agarose resin was added to the pre-cleared lysate for 1 hour. Immobilized protein was either washed and eluted for downstream experiments, or used in the SILAC-based Cj1533c-protein interaction screen, in which the purification, washing and elution buffers/procedures are identical. Standard SDS-PAGE/Coomassie Blue was used to visualize purified recombinant protein.

5.3.7 SILAC-based Cj1533c-protein interaction screen

Affinity capture of binding proteins from SILAC extracts was performed as previously described (330-332), with modification. Briefly, *C. jejuni* (Δ*argH*) was metabolically labeled with 400 μM of either "light" L-arginine or "heavy" $^{14}N_4^{13}C_6$-arginine (Cambridge Isotope Laboratories) as the SILAC amino acid in the modified DMEM medium, and lysed via gentle sonication in 50 mM Tris pH 8.0, 150 mM NaCl, 0.1% Triton X-100. Affinity purifications were performed with purified Cj1533c-6XHIS immobilized on 0.25 mL 50% Ni-NTA-agarose resin (Qiagen). The "light" lysate was incubated with Ni-NTA-agarose alone, and the "heavy" lysate was incubated with Cj1533c-6XHIS-Ni-NTA-agarose in two separate Ni-NTA resin columns. Columns were washed 8X with 4 mL of Wash Buffer (50 mM NaH_2PO_4, 300 mM NaCl, 30 mM imidazole, pH 8.0). Protein–protein complexes were eluted with 2 mL Elution Buffer (50 mM NaH_2PO_4, 300 mM NaCl, 250 mM imidazole, pH 8.0). The eluted proteins from each column were mixed (1:1), and the imidazole and Triton X-100 was removed and the proteins were concentrated with a 10 kDa spin filter (Millipore), and washed 3X with 3 mL of 300 mM $(NH_4)_2CO_3$ buffer (trypsin compatible). Proteins were precipitated with ethanol, digested with trypsin, and purified peptides were analyzed by Q-TOF LC-MS. MaxQuant (217) was used for identification and quantification for data from two independent experiments.

5.4 RESULTS

5.4.1 The Δ*cj1533c* mutant is sensitive to hyperosmotic and oxidative stress

Transcriptional profiling by DNA microarray identified *cj1533c* as upregulated under hyperosmotic stress (1). Initially annotated as a helix-turn-

helix containing protein (DNA binding protein), we hypothesized that *cj1533c* encoded a novel transcriptional regulator of the hyperosmotic stress response. The *cj1533c* gene was deleted in *C. jejuni* strain 81-176 via antibiotic marker replacement, and the resulting mutant strain (Δ*cj1533c*) was assessed for growth differences in standard MH broth and MH broth containing 1.0% NaCl (hyperosmotic stress). In MH broth, no significant growth differences by viable CFU count were observed between Δ*cj1533c* and the wild-type (FIGURE 5.1A, left). In contrast, growth of Δ*cj1533c* was inhibited in hyperosmotic MH broth (FIGURE 5.1A, right). Exposure to hyperosmotic stress was also lethal for Δ*cj1533c*, and viable CFU counts decreased in a time-dependent manner until no CFU were recovered at 72 hours post-stress exposure. Given that the hyperosmotic/general stress response is cross-regulated with the oxidative stress response in *C. jejuni* (1), Δ*cj1533c* was also tested for survival phenotypes after exposure to the reactive oxygen species H_2O_2. Consistent with the hyperosmotic survival trends, Δ*cj1533c* was ~100-fold more sensitive to oxidative stress than wild-type when exposed to H_2O_2 for 15 minutes (FIGURE 5.1B). A genome-integrated genetic complement strain (Δ*cj1533c+cj1533c*) was constructed, in which *cj1533c* was expressed from its native promoter, and this restored the wild-type phenotype in the deletion strain. Plasmid-borne overexpression of *cj1533c* did not enhance hyperosmotic survival or produce other phenotypic effects (not shown). Since *C. jejuni* 81-176 exhibits extensive colonial genetic/phenotypic variation (1), multiple different colonial isolates of the mutant were tested to ensure the veracity of the NaCl/H_2O_2-sensitive phenotype. The mutant was not defective in other phenotypic tests, which included heat shock and anaerobic stress testing, chick colonization, and invasion/intracellular survival in INT407 or Caco-2 cell lines (not shown).
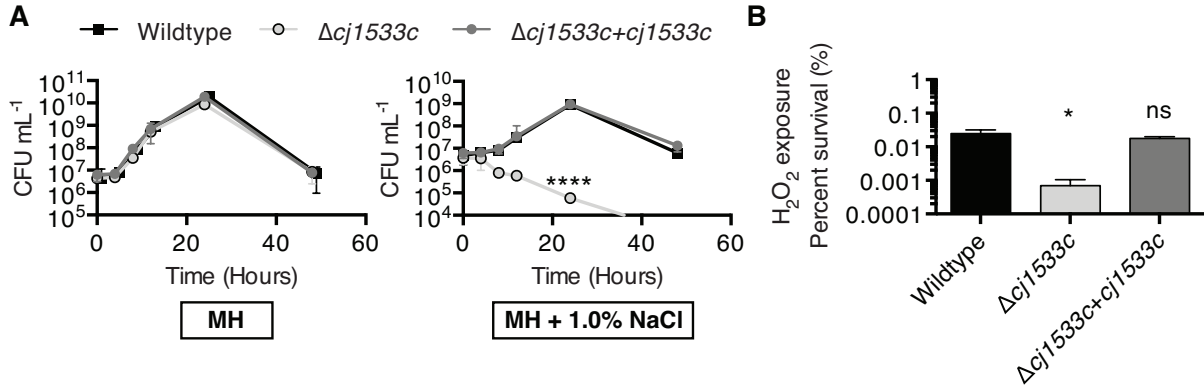
FIGURE 5.1 The Δ*cj1533c* mutant is sensitive to hyperosmotic and oxidative stress.
(A) Viable count growth profile of wild-type, Δ*cj1533c*, and Δ*cj1533c-cj1533c* complement strains growth in Mueller-Hinton (MH) broth (left) or MH broth supplemented with 1.0% NaCl (hyperosmotic stress). Growth was assessed from shaking cultures at 38°C by plating for CFU at the timepoints shown. Mean with SEM of three independent experiments; ****, P ≤ 0.0001 (versus wild-type). (B) Percent survival of wild-type, Δ*cj1533c*, and Δ*cj1533c-cj1533c* complement strains after 15 minute exposure to 1 mM H_2O_2 in PBS. Percentage calculated from CFU recovered after treatment and CFU recovered from PBS alone. Mean with SEM of three independent experiments; *, P ≤ 0.05 (versus wild-type).

5.4.2 Extensive chaining of the Δ*cj1533c* mutant occurs in hyperosmotic stress

A fraction of the *C. jejuni* population undergoes incomplete cell division under hyperosmotic and other stress conditions (1, 126). This results in the formation of long bacterial chains, the importance of which is as-yet unclear, but which may have roles in the biofilm lifestyle of *C. jejuni* (see Chapter 4). Despite growth inhibition leading ultimately to death in hyperosmotic stress, microscopy of Δ*cj1533c* cells exposed to 1.0% NaCl revealed that surviving cells continue to divide without separation (FIGURE 5.2A). Thus, nearly all cells of Δ*cj1533c* were hyper-chained compared to the wild-type. This was quantified by single-cell measurement of cell length for both wild-type and the mutant grown in both MH and MH + 1.0% NaCl for 24 hours. For the wild-type, cell length heterogeneity was observed in hyperosmotic stress, but the majority of the population was

composed of shorter single-cell bacteria (FIGURE 5.2B). In contrast, the Δ*cj1533c* population was primarily composed of excessively long multi-cell chains (FIGURE 5.2C). Taken together, all data thus far confirms the sensitivity of Δ*cj1533c* to hyperosmotic stress, and demonstrates the importance of *cj1533c* in hyperosmotic stress adaptation.
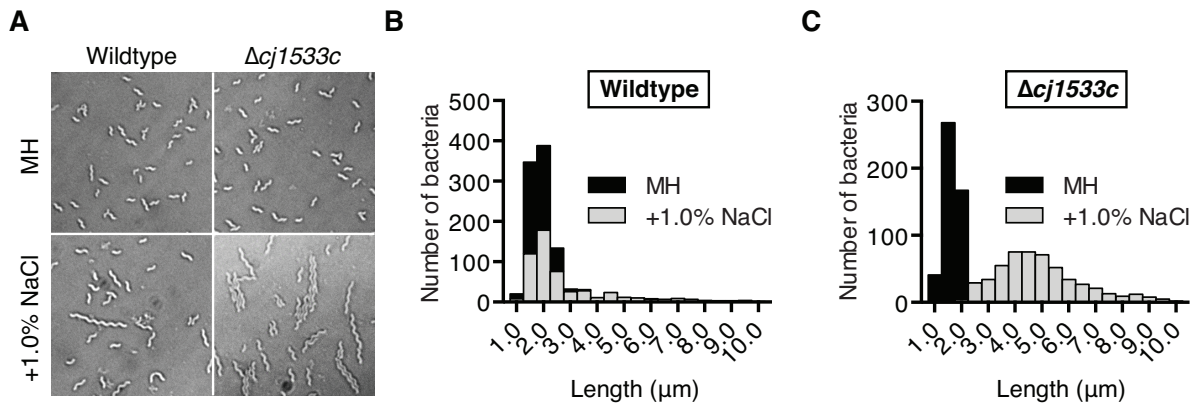
FIGURE 5.2 The Δ*cj1533c* mutant exhibits increased chaining under hyperosmotic stress.
(A) 1000X Magnification brightfield microscopy of wild-type and Δc*j1533c* grown in MH or MH + 1.0% NaCl. Images are representative of ten fields of view. (B) Cell length distribution of wild-type grown for 24 hours in MH (number of bacteria analyzed, n = 517) and MH + 1.0% NaCl (n = 545). (C) Cell length distribution of Δ*cj1533c* grown for 24 hours in MH (n = 514) and MH + 1.0% NaCl (n = 533). Data was obtained from ten fields of view.

5.4.3 Expression of *cj1533c* is transiently enhanced after hyperosmotic stress exposure, but can also be modulated by Fur-, PerR- and CosR-mediated regulation of a rare bicistron encoding the iron-sequestering ferritin Dps

DNA microarray profiling of Δ*cj1533c* compared to wild-type at 3, 6, and 9 hours grown in MH broth revealed only one significantly differentially expressed gene in all time points: *dps* (*cj1534c*), which encodes the iron-sequestering bacterioferritin Dps, and which is the gene immediately preceding *cj1533c* in the 81-176 genome (FIGURE 5.3A). Given that previous microarray profiling suggested that *dps* and *cj1533c* had similar expression profiles in hyperosmotic

stress (1), we explored the possibility that both genes were co-transcribed on a single transcript (a polycistron). To ascertain this, RT-PCR of cDNA was carried out using oligonucleotides spanning both *dps* and *cj1533c*. This detected a *dps-cj1533c* polycistron (FIGURE 5.3B), and thus confirmed that both genes could be co-transcribed, offering a possible explanation for dysregulation of *dps* in the artificial Δ*cj1533*c mutant background. Quantitative RT-PCR to determine the relative expression of *cj1533c* via the *dps-cj1533c* polycistron versus the *cj1533c*-specific promoter was attempted, but was unable to resolve potential expression differences because (I) *dps* was highly expressed, (II) *cj1533c* was not highly expressed, and (III) the gene arrangement and location of the *dps* transcriptional terminator stem-loop impeded polycistron-specific PCR (not shown). Instead, Northern blotting using a probe designed to detect all possible transcripts (*dps*, *cj1533c*, *dps-cj1533c*) was carried out with RNA obtained from wild-type cells grown in MH or exposed to MH + 1.0% NaCl for 15, 90 and 180 minutes. Via Northern blot, both *cj1533c* and *dps* were shown to be independently upregulated in hyperosmotic stress (FIGURE 5.3C). Northern blotting also confirmed that a *dps-cj1533c* polycistron was made, thus enhancing expression of *cj1533c* during hyperosmotic shock. Interestingly, *cj1533c* was only highly expressed transiently and immediately following hyperosmotic shock (15 minutes), and was minimally expressed at later timepoints. In contrast, *dps* was highly expressed at all timepoints, even in standard MH broth. Thus, this data implies that *cj1533c* is important in the initial stages of hyperosmotic stress adaptation.

Given that the *dps-cj1533c* polycistron may have biological importance, the effect of modulation of known regulators (Fur, PerR, and CosR) of the *dps* promoter was examined (140, 142, 144-147, 149, 150). To assess this, deletion mutants in *fur* and *perR* (Δ*fur*, Δ*perR*) were constructed and the essential CosR was overexpressed with a strong promoter on a multi-copy plasmid (140, 289). Overexpression of CosR (*cosR^{OE}*) was confirmed via Western blotting (FIGURE

5.3D). Northern blotting using the same *dps-cj1533c* probe was carried out using RNA harvested from wild-type, Δ*fur*, Δ*perR*, and *cosR^{OE}* grown in MH or exposed to MH +1.0% NaCl for 15 minutes (FIGURE 5.3E). Expression of *dps* was increased in Δ*fur* and Δ*perR* in MH, consistent with known negative regulatory actions. Overexpression of *cosR* decreased expression of *dps*, also consistent with negative regulation of *dps* by CosR. Interestingly, under hyperosmotic stress, CosR-repression of *dps* was de-repressed. Neither Fur, PerR or CosR directly affected the *cj1533c* promoter. However, expression of *cj1533c* was modulated by Fur and PerR via the *dps-cj1533c* polycistron, which was confirmed by densitometry measurement (FIGURE 5.3F). CosR modulation of *dps-cj1533c* expression was not shown within the limits of these experiments. Despite this, this data shows that *cj1533c* expression can be regulated by Fur, PerR and CosR.

Given the possibility that *dps* dysregulation might account for the hyperosmotic/oxidative stress sensitivity of the Δ*cj1533c* mutant, a Δ*dps* mutant and a Δ*dps*Δ*cj1533c* double mutant were constructed for phenotypic assessment. The hyperosmotic stress sensitivity of each strain was compared by enumerating CFU recovered from OD-equivalent cell dilution series plated on MH agar or MH agar supplemented with 1.0% NaCl. By percent survival, Δ*dps* was 10-fold more defective for hyperosmotic stress tolerance than wild-type (FIGURE 5.3G). However, the Δ*cj1533c* mutant was $> 10^3$-fold more sensitive to 1.0% NaCl than Δ*dps*, but not significantly different to Δ*dps*Δ*cj1533c*. Thus, Dps is an important hyperosmotic stress factor—consistent with known iron homeostasis/oxidative stress resistance roles (145, 146)—but Δ*cj1533c* sensitivity phenotypes are not due to the presence/absence/dysregulation of *dps*. Given the global regulatory importance of Fur, PerR and CosR in the cellular regulation of iron homeostasis/oxidative stress response, Δ*fur*, Δ*perR* and *cosR^{OE}* were also assessed for hyperosmotic stress survival via the same methodology. The 10^4-fold stress defect of Δ*cj1533c* was statistically greater than the phenotypic defects

caused by Δ*fur* and Δ*perR,* but statistically equivalent to the hyperosmotic defect caused by *cosR* overexpression. Thus, this data confirmed the importance of *cj1533c* in hyperosmotic stress survival and affirms the relative importance of *cj1533c* compared to known global transcriptional regulators.
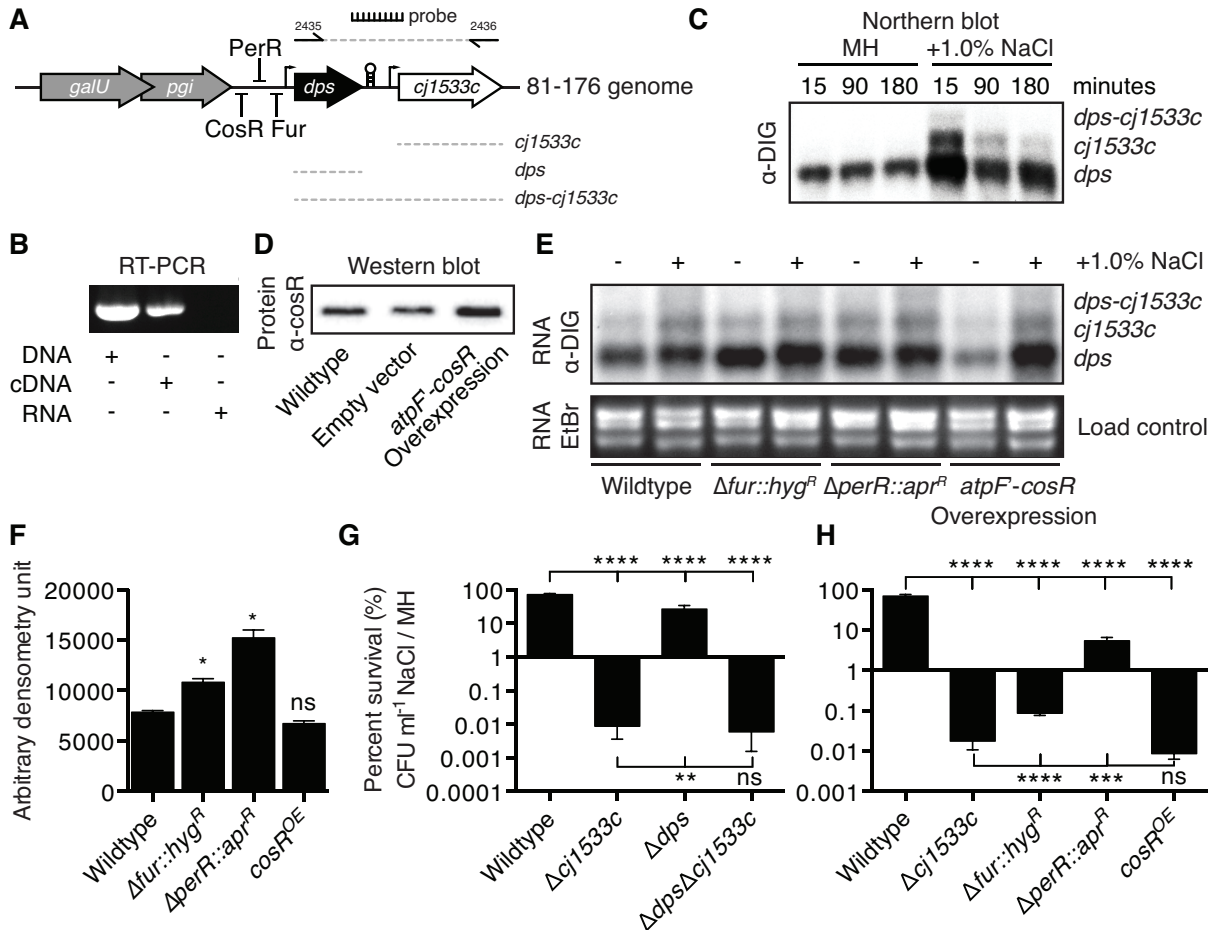
FIGURE 5.3 Expression of *cj1533c* is upregulated transiently after hyperosmotic stress exposure, but can also be modulated by Fur-, PerR- and CosR-mediated regulation of a rare bicistron encoding the ferritin Dps.
(A) Schematic of the *cj1533c* loci. An inverted repeat or stem-loop after *dps* is within the putative *cj1533c* promoter sequence. CosR, Fur and PerR are negative regulators of *dps.* Probe and 2435/2436 oligonucleotide binding sites are for Northern blotting and RT-PCR respectively. Dashed lines represent mRNA transcripts. (B) RT-PCR of cDNA shows that *cj1533c* may be expressed via a *dps* polycistron. (C) Transient induction of *cj1533c* expression in hyperosmotic stress at 15, 90 and 180 minutes detected by Northen blot. Both *cj1533c* and *dps* were independently upregulated in hyperosmotic stress, but expression of *cj1533c* was enhanced by increased *dps-cj1533c* polycistronic expression. The DIG-labeled probe detected three transcripts *dps, cj1533c, dps-cj1533c* (in order of increasing size) (D) Plasmid-borne overexpression of CosR was confirmed by Western blotting. (E) Fur-, PerR- and CosR-modulated expression of the *dps-cj1533c* polycistron. Northern blot of wild-type and regulator mutants in MH or MH + 1.0% NaCl

representative of three independent experiments. (F) Densitometry quantification of polycistron expression modulation by Fur, PerR, and CosR (15 minutes, MH). Densitometry performed on three independent Northern blots; *, P ≤ 0.05; ns, not significant (versus wild-type). (G) Percent survival of wild-type, Δ*cj1533c*, Δ*dps*, and Δ*dps*Δ*cj1533c* in hyperosmotic stress. Percentage calculated from CFU recovered on MH + 1.0% NaCl agar and CFU recovered MH agar alone. Mean with SEM of three independent experiments; **, P ≤ 0.01; ****, P ≤ 0.0001. (H) Percent survival of wild-type, Δ*cj1533c*, Δ*fur*, and Δ*perR* and the *cosR* overexpressing strain in hyperosmotic stress. Percentage calculated from CFU recovered on MH + 1.0% NaCl agar and CFU recovered MH agar alone. Mean with SEM of three independent experiments; ***, P ≤ 0.001; ****, P ≤ 0.0001; ns, not significant (versus wild-type).

5.4.4 Error-prone PCR directed evolution of *cj1533c* reveals a putative sRNA in *cj1533c*, and site-directed mutagenesis reveals the importance of Walker A motif residues in *cj1533c* gene product function

Given that deletion of *cj1533c* did not significantly affect transcription in the DNA microarray profile (not shown), further bioinformatic analysis was carried out on *cj1533c*. Despite annotation as a putative transcription factor, improved structural homology/conserved domain searches indicated that *cj1533c* was misannotated (333). Instead, Cj1533c is a predicted ATPase (ATP binding protein) in the AAA+ superfamily. The gene encodes a protein with a predicted AAA_14 domain, which contains a P-loop motif (314, 334, 335). Cj1533c is also predicted to harbor a domain-of-unknown function (DUF4143), which are almost always found C-terminal to an ATPase domain (336).

Initially under the impression that *cj1533c* was a transcription factor, we hypothesized that it might be possible to identify mutations in *cj1533c* that conferred active conformation or constitutive/"locked" transcriptional action, equivalent to active-trapped or de-sensitized response regulator mutants (337-339)—with the idea of using such a strain in future transcriptional profiling. Thus, error-prone PCR directed evolution was carried out by random mutagenesis of the *cj1533c* gene, via PCR amplification in the presence of polymerase fidelity-altering $MnCl_2$ (FIGURE 5.4A). The erroneous *cj1533c* copies were introduced into plasmids, and the resulting plasmid library was

transferred into the Δ*cj1533c C. jejuni* mutant. The resulting clone library was pooled, and enriched for bacteria with enhanced hyperosmotic stress survival by repeated growth in MH + 1.0% NaCl broth. Six clones with enhanced NaCl tolerance were selected, and their plasmid insert was sequenced. The same erroneous *cj1533c* sequence was found in all six clones. The erroneous copy of *cj1553c* was found to be a truncation of the protein that conserved important Walker A motif residues, but the sequence immediately after the motif was scrambled in such a way that the resulting peptide does not contain the entire AAA_14 domain. Interestingly, a recent RNA-seq transcriptome identified a strain-specific and putative antisense RNA transcription start site (TSS) in the conserved *cj1533c* sequence (340). Thus, we hypothesized that the erroneous copy of *cj1533c* encoded a putative asRNA/sRNA and promoter, as well as the *cj1533c* promoter.

Given the conservation of the Walker A motif (canonical: G$_{xxxx}$GK(T/S), *cj1533c*: G$_{XXXX}$GKKT), site-directed mutagenesis of the two di-lysine residues was carried out, resulting in the modification *cj1533c*KK40,41GG. Both *cj1533c*KK40,41GG and the putative sRNA were separately integrated into the Δ*cj1533c* strain via the same gene-delivery plasmid. This resulted in the strains Δ*cj1533c*+*cj1533c*KK40,41GG and Δ*cj1533c*+*putative sRNA* (FIGURE 5.4B). Hyperosmotic phenotypic testing of these strains showed that replacement of the Walker A motif KK residues conferred sensitivity equivalent to Δ*cj1533c* (FIGURE 5.4C). The addition of the putative sRNA to the Δ*cj1533c* mutant enhanced hyperosmotic tolerance. The Δ*cj1533c*+*putative sRNA* strain was shown to have stationary phase growth defects when grown in MH broth. In MH + 1.0% NaCl broth, the strain had slower growth rates, but enhanced viability at stationary-phase timepoints (FIGURE 5.4D). Taken together, these results confirm the importance of the Walker A motif, and suggest that the *cj1533c* locus is extremely complex, with multiple levels of regulation. Interestingly, the putative sRNA (FIGURE 5.4E) is predicted to bind the mRNA of a number of

121

relevant genes (FIGURE 5.4F). The sRNA has been detected by strand-specific RT-PCR (not shown), but this methodology is low confidence (341), and gold-standard Northern blotting via DIG-labeled or ^{32}P- labeled α-sRNA probes did not detect the sRNA (not shown).

A

MnCl$_2$-error prone PCR of *cj1533c* → Cloned into plasmids

3x enrichment/selection in 1.0% NaCl for resistant clones ← Library conjugated into Δ*cj1533c*

B

dps → *cj1533c* → 81-176 genome

Δ*cj1533c* + *cj1533c* → +*cj1533c*

Δ*cj1533c* + *cj1533c* → +*cj1533c*KK40,41GG

Δ*cj1533c* + *q* → +*putative sRNA*

C

Percent survival (%)

ns | *

**** | ****

Wildtype, Δ*cj1533c*, Δ+*cj1533c*, Δ+*putative sRNA*, Δ+*cj1533c*KK40,41GG

- ■ Wildtype
- ○ Δ*cj1533c*
- ● Δ*cj1533c*+*cj1533c*
- ▽ Δ*cj1533c*+*putative sRNA*
- □ Δ*cj1533c*+*cj1533c*KK40,41GG

D

MH

CFU mL^{-1} vs Time (Hours)

MH + 1.0% NaCl

**** | ****

CFU mL^{-1} vs Time (Hours)

E

```
TTTTGAAATTTGATTTTTTCTTTCATAACT
TACTTCAAATTTAGGGTGGTTTTCATAAAA
AAAATTAAGTACTTTCAATTTTATCCTTTA
AAAAAGGA...
```

F

Putative sRNA mRNA targets

cj81176_1518 Cj1533c
cj81176_0919 Sco1/SenC family
cj81176_0977 DnaJ-containing protein
cj81176_0265 Cysteine desulfurylase
cj81176_0356 AhpC
cj81176_0624 Peb4
cj81176_0173 Hypothetical protein
cj81176_0671 CbrR GGDDEF
cj81176_0696 RNAP σ54
cj81176_1019 RNAP σ70

FIGURE 5.4 Error-prone PCR directed evolution of *cj1533c* reveals a putative sRNA in *cj1533c*, and site-directed mutagenesis reveals the importance of Walker A motif residues in *cj1533c* gene product function.
(A) Schematic of directed evolution of *cj1533c* to identify mutations that confer increased hyperosmotic stress survival. PCR error was introduced by increasing MnCl$_2$ concentrations. Error fragments were cloned into pRY112 and the resulting library was introduced in Δ*cj1533c* via conjugation/natural transformation. The library was enriched 3x in MH +1.0% NaCl, and strains with enhanced hyperosmotic stress survival were sequenced. (B) Illustration of genetic differences between depicted strains. All gene-insertions were performed in the Δ*cj1553c* mutant with the genome-insertional gene-delivery plasmid, pRRC. (C) (H) Percent survival of wild-type, Δ*cj1533c*+*cj1533c*, Δ*cj1533c*+*putative sRNA* (directed evolution mutant), and Δ*cj1533c*+*cj1533c*KK40,41GG (site-directed mutant) in hyperosmotic stress. Percentage calculated from CFU recovered on MH + 1.0% NaCl agar and CFU recovered MH agar alone. Mean with SEM of three independent experiments; *, P ≤ 0.05; ****, P ≤ 0.0001; ns, not significant (versus wild-type). (D) Viable count growth profile of directed evolution and site-

directed mutant strains growth in MH broth (top) or MH broth + 1.0% NaCl (bottom). Growth was assessed from shaking cultures at 38°C by plating for CFU at the timepoints shown. Mean with SEM of three independent experiments; ****, $P \leq 0.0001$ (versus wild-type). (E) Preliminary sequence and folded structure of the putative *cj1533c* sRNA (mFold). (F) List of ten highest-predicted mRNA targets of the putative *cj1533c* sRNA (RNApredator).

5.4.5 The proteome of Δ*cj1533c* differs significantly in the reduced expression of iron-sulfur containing central metabolic proteins

Given the possibility for post-transcriptional regulation in the mechanism of *cj1533c* stress tolerance, quantitative proteomics via triple-label SILAC was carried out. Since this required metabolic labeling of the proteome with "light", "medium", or "heavy" arginine, the Δ*cj1533c* mutant was transferred into the *C. jejuni* arginine auxotroph strain (Δ*argH*), and the complementation and putative sRNA constructs were transferred into antibiotic-compatible plasmids for gene-insertion into the resulting Δ*argH*Δ*cj1533c* strain. Thus, proteomic comparisons were made between Δ*argH* as the wild-type, Δ*argH*Δ*cj1533c* (Δ*cj1533c*), and either Δ*arg*HΔ*cj1533c+cj1533c* (+*cj1533c* complement) or Δ*arg*HΔ*cj1533c+putative sRNA* (putative sRNA strain) (FIGURE 5.5A). OD-equivalent labeled cells were either grown in the appropriate SILAC broth, or in SILAC broth containing 1.0% NaCl for 15 minutes (hyperosmotic shock), after which proteins from the resulting cells were extracted for LC-MS and peptide quantitation. Quantitative data was obtained for ~665 proteins, and of those, ANOVA analysis determined statistically relevant expression (*sensu stricto*, mass ratio) differences in ~200 proteins.

In contrast to the DNA microarray transcriptome, significant expression differences were detected between Δ*cj1533c* and the wild-type in the absence of NaCl-induction of *cj1533c* expression, consistent with post-transcriptional regulation at work in the *cj1533c* system. Expression differences between wild-type/Δ*cj1533c* with or without the addition of NaCl were similar (FIGURE 5.5B).

The most significant differences were observed for TCA cycle-related proteins (TABLE 5.1). The succinate dehydrogenase complex (SdhABC, Fe-S subunit) was the most upregulated protein complex in wild-type, and the leucine biosynthesis pathway (LeuABC, Fe-S subunit), and the heat-shock chaperone/co-chaperones (GroEL/GroES) were also upregulated. Interestingly, iron-sulfur containing proteins were over-represented among the most highly dysregulated peptides. In addition, many of the expression differences occurred in genes known to be transcriptionally upregulated in hyperosmotic stress survival (1). Thus, this data confirms a central role for the *cj1533c* locus in *C. jejuni* osmotic homeostasis.
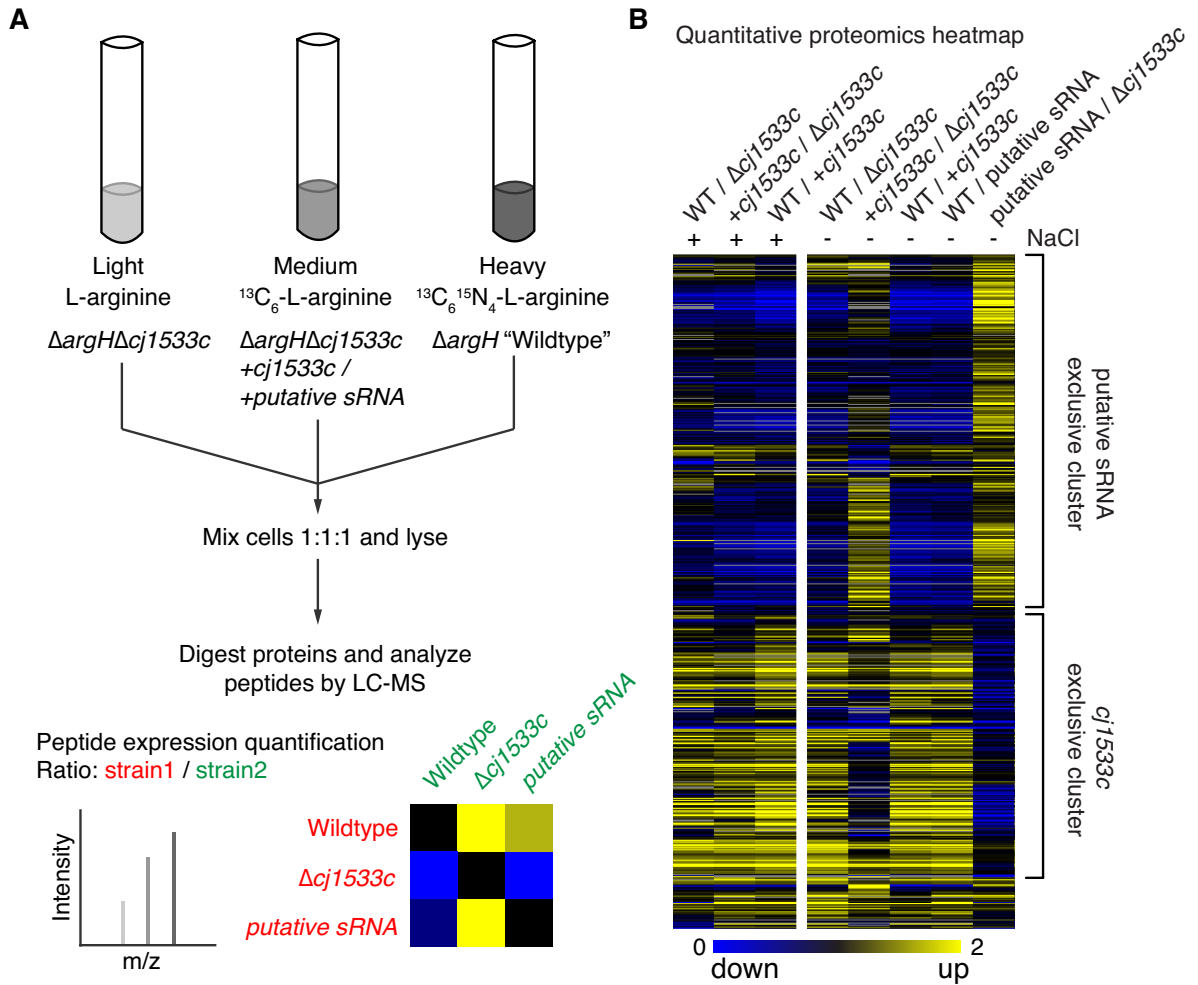
FIGURE 5.5 Global protein expression differences of the Δ*cj1533c* mutant revealed by SILAC-based quantitative proteomics.

(A) Schematic of triple SILAC-based metabolic labeling and quantitation protocol. The Δ*argH* derivatives of *C. jejuni* wild-type, Δ*cj1533c*, Δ*cj1533c+cj1533c* (complement) and Δ*cj1533c+putative sRNA* were grown in modified DMEM broth for metabolic protein labeling, and exposed for 15 minutes to DMEM + 1.0% NaCl or DMEM alone. The wild-type proteome was labeled with "heavy" $^{13}C_6^{15}N_4$-L-arginine, and Δ*cj1533c* was labeled with "light" L-arginine. The complement and putative sRNA strains were labeled with "medium" $^{13}C_6$-L-arginine. Comparisons were made between three OD-equivalent strains (wild-type, mutant and complement or wild-type, mutant, and putative sRNA) combined in a 1:1:1 ratio. Mixed bacterial protein lysates were precipitated, digested with trypsin, and the peptides were analyzed by LC-MS. Peptide peak intensity was used to quantitate relative peptide abundance, and the heavy/medium, medium/light and heavy/light ratios identified the sample origin and expression differences between two comparator strains. For example, upregulated proteins in wild-type versus Δ*cj1533c* are distinguishable by increased intensity of $^{13}C_6^{15}N_4$-L-arginine-labeled peptides. Equal peptide ratios indicate no expression difference. (B) Heat map array of proteomic differences between Δ*cj1533c* and comparator strains, with upregulated proteins shown in yellow versus blue for downregulated proteins. Hierarchical clustering analysis of detected peptide ratios shows that expression differences cluster primarily into two categories: differences that are due to presence of *cj1533c* (and the putative sRNA), and differences that are due to the

putative sRNA alone. Average expression ratios are calculated from four (wild-type and Δ*cj1533c*) or two (complement and putative sRNA) independent experiments.

TABLE 5.1 Selected peptides with highest SILAC ratios in wild-type versus Δ*cj1533c*.

Locus	Protein	Description	Ratio	ANOVA	Predicted sRNA target
CJJ81176_0463	SdhA	succinate dehydrogenase, flavoprotein subunit	2.90	*	-
CJJ81176_0464	SdhB	succinate dehydrogenase, iron-sulfur protein	2.80	*	-
CJJ81176_0017	LeuA	2-isopropylmalate synthase	2.18	*	-
CJJ81176_0015	LeuC	isopropylmalate isomerase, iron-sulfur protein	1.91	*	-
CJJ81176_0016	LeuB	3-isopropylmalate dehydrogenase	1.90	*	-
CJJ81176_0122	AspA	aspartase, fumarate from/to aspartate	1.86	*	-
CJJ81176_0869	HemL	glutamate-1-semialdehyde aminotransferase	1.85	*	-
CJJ81176_0056	AnsA	L-asparaginase	1.82	*	-
CJJ81176_1233	GroES	co-chaperonin	1.77	*	-
CJJ81176_0112	-	hypothetical protein	1.73	*	-
CJJ81176_1234	GroEL	chaperonin	1.72	*	-
CJJ81176_0792	-	NLPA family lipoprotein	1.61	*	-
CJJ81176_0111	-	iron-sulfur cluster binding protein	1.59	*	-
CJJ81176_0023	MetX	homoserine O-acetyltransferase	1.55	*	-
CJJ81176_0434	FrdB	fumarate reductase, iron-sulfur protein	1.55	*	-
CJJ81176_1500	FdhD	formate dehydrogenase, accessory protein	1.52	*	-
CJJ81176_0127	-	hypothetical protein	1.50	*	-
CJJ81176_0110	-	hypothetical protein	1.50	*	-
CJJ81176_0433	FrdA	fumarate reductase, flavoprotein subunit	1.50	*	-
CJJ81176_1418	-	putative methyltransferase	1.50	*	-
CJJ81176_1488	-	hypothetical protein	1.45	*	-
CJJ81176_0882	AstA	arylsulfate sulfotransferase	1.45	*	-
CJJ81176_0850	-	short chain dehydrogenase/reductase family oxidoreductase	1.44	*	-
CJJ81176_0928	PebA	adhesin/ABC aspartate/glutamate-binding protein	1.42	*	-
CJJ81176_0107	-	hypothetical protein	1.42	*	-
CJJ81176_0126	-	putative lipoprotein	1.37	*	-
CJJ81176_1410	-	cytochrome P450 family protein	1.30	*	-
CJJ81176_1161	-	CMP-Neu5Ac synthetase	1.27	*	-
CJJ81176_1615	SdaA	L-serine ammonia-lyase	1.25	*	-
CJJ81176_0738	-	transthyretin-like protein	1.25	*	-

[a] Statistical significance of ratio difference between all comparisons assessed by ANOVA (*, significant).
[b] Prediction of sRNA targets via RNApredator and IntaRNA.

5.4.6 The proteome of a strain expressing the putative *cj1533c* sRNA differs in the enhanced expression of phosphonucleotide and sulfur relay proteins

In addition to major proteome differences between wild-type and Δ*cj1533c*, significant differences were also observed for the putative sRNA strain compared to Δ*cj1533c* (FIGURE 5.5B). These included the upregulation of sulfur-relay related proteins (TABLE 5.2), which included a putative cysteine desulfurylase, (CJJ81176_0265); LuxS, S-ribosylhomocysteinase (a cysteine-methionine transulfuration enzyme in the related bacterium *Helicobacter pylori* (342)); CysK, cysteine synthase (O-acetylserine sulfhydrolase); BioB, biotin synthase (S-adenosylmethionine-dependent Fe-S protein, which transfers sulfur to biotin (343, 344)); and CJJ81176_0584, (pyridine nucleotide-disulfide reductase). Several phosphorelay proteins were also prominently differentially expressed, including CJJ81176_1483 (DNA-binding response regulator); Ndk, nucleoside diphosphate kinase (transfers phosphate to nucleoside-diphosphates(345)); and ThrC, threonine synthase (dephosphorylation of O-phospho-homoserine to make L-threonine (346)). Interestingly, the putative sRNA was predicted to interact with the mRNA of several of these differentially regulated proteins (predicted via RNApredator / IntaRNA (347, 348)). When the putative RNA strain was compared to wild-type, these expression differences were not observed (FIGURE 5.5B). This is expected since the wild-type strain encodes both the putative sRNA and *cj1533c*, whereas the putative sRNA strain does not encode a functional copy of *cj1533c*. Taken together, this proteomic data suggests roles for the *cj1533c* locus in sulfur/phosphate homeostasis, and thus, roles for sulfur/phosphate homeostasis in hyperosmotic/oxidative stress survival.

TABLE 5.2 Selected peptides with highest SILAC ratios in Δ*cj1533c* + *putative sRNA* versus Δ*cj1533c*.

Locus	Protein	Description	Ratio	ANOVA[a]	Predicted sRNA target[b]
CJJ81176_0004	-	metallo-beta-lactamase family protein	2.00	*	-
CJJ81176_1276	DnaJ	chaperone protein	1.81	*	YES
CJJ81176_0315	PEB3	major antigenic peptide	1.72	*	-
CJJ81176_1011	-	hypothetical protein	1.61	*	-
CJJ81176_1678	TopA	DNA topoisomerase I	1.59	*	YES
CJJ81176_1213	LuxS	S-ribosylhomocysteinase	1.53	*	-
CJJ81176_0265	-	cysteine desulfurase	1.51	*	YES
CJJ81176_0584	-	pyridine nucleotide-disulphide oxidoreductase	1.48	*	-
CJJ81176_1190	ArgS	arginyl-tRNA synthetase	1.47	*	-
CJJ81176_1084	-	nitroreductase family protein	1.46	*	-
CJJ81176_0904	AroA	3-phosphoshikimate 1-carboxyvinyltransferase	1.44	*	-
CJJ81176_1083	-	nitroreductase family protein	1.43	*	-
CJJ81176_1304	-	NADP-dependent malic enzyme	1.41	*	-
CJJ81176_0920	CysK	cysteine synthase A	1.41	*	-
CJJ81176_1677	BioB	biotin synthase, iron-sulfur protein	1.40	*	-
CJJ81176_1483	-	DNA-binding response regulator	1.39	*	-
CJJ81176_0354	Ndk	nucleoside diphosphate kinase	1.39	*	-
CJJ81176_1599	PrfA	peptide chain release factor 1	1.39	*	-
CJJ81176_1019	RpoD	RNA polymerase sigma factor RpoD	1.37	*	YES
CJJ81176_0462	-	hypothetical protein CJJ81176_0462	1.37	*	-
CJJ81176_0485	NusA	transcription elongation factor	1.36	*	-
CJJ81176_1592	-	N-succinyltransferase	1.35	*	-
CJJ81176_0652	HypB	hydrogenase accessory protein	1.33	*	-
CJJ81176_0987	-	hypothetical protein	1.33	*	-
CJJ81176_1600	-	hypothetical protein	1.33	*	-
CJJ81176_1294	TrmB/YggH	tRNA (guanine-N(7)-)-methyltransferase	1.32	*	-
CJJ81176_1289	TpoZ	DNA-directed RNA polymerase subunit omega	1.32	*	-
CJJ81176_0833	ThrC	threonine synthase	1.32	*	-
CJJ81176_0587	DnaB	replicative DNA helicase	1.32	*	-
CJJ81176_1187	-	hypothetical protein	1.31	*	-

[a] Statistical significance of ratio difference between all comparisons assessed by ANOVA (*, significant).

[b] Prediction of sRNA targets via RNApredator and IntaRNA.

5.4.7 A SILAC-based Cj1533c-protein interaction screen identifies putative interactions with ribosomal proteins, an exopolyphosphatase and a sulfate adenylyltransferase (ATP sulfurylase)

All data thus far pointed to Cj1533c regulating a cellular process directly, and not via transcription. Given the putative ATPase function of Cj1533c, we hypothesized that Cj1533c must interact with other key proteins. To assess this, a SILAC-based screen for protein-protein interactions was carried out. This required the expression and purification of 6XHIS-C-terminal-tagged recombinant Cj1533c via immobilized nickel ion affinity chromatography (FIGURE 5.6A). To screen for potential interactions, SILAC-based quantitative mass spectrometry provided the sensitivity required to detect the transient protein-protein interactions of an AAA+ ATPase (349). SILAC was also advantageous because the isotope ratio can distinguish specific interactions from contaminating proteins (325, 349, 350). For this protein-protein interaction screen, the recombinant Cj1533c-6XHIS was immobilized on a Ni-NTA-agarose column. The Δ*argH* strain was metabolically labeled in SILAC broth containing either "light" or "heavy" L-arginine (FIGURE 5.6B), and total protein was extracted. Briefly, the "light" protein extract was incubated with Ni-NTA-agarose alone, and the "heavy" protein extract was incubated with the Cj1533c-6XHIS-Ni-NTA-agarose. The bound proteins were eluted, and mixed in a 1:1 ratio for downstream peptide quantitation by LC-MS.

Peptides identified in the interaction screen included those corresponding to many different ribosomal proteins (FIGURE 5.6C). Ribosomal proteins are frequent contaminants/artifacts due to their abundance, but they may have biological significance here. Interestingly, three non-ribosomal proteins with isotope ratios > 2.0 were identified in the screen: Cj0353c (CJJ81176_0377), Cj1609 (CJJ81176_1596) and oorD (CJJ81176_0560). Interestingly, Cj0353c is a

putative exopolyphosphatase, harboring the Ppx/GppA domain. Thus, this protein may cleave phosphate from polyphosphate or guanosine pentaphosphate (pppGpp). In *C. jejuni*, polyphosphate has known importance in hyperosmotic stress survival (121), and (p)ppGpp mediates the stringent response (117). Intriguingly, Cj1609 encodes a putative sulfate adenylyltransferase, or ATP sulfurylase. This enzyme acts in sulfate assimilation, reversibly transferring intracellular sulfate onto ATP, forming adenosine 5'-phosphosulfate (APS), and liberating diphosphate (351, 352). The 2-oxoglutarate:acceptor oxidoreductase OorD, is a subunit of the OorABCD α-ketoglutarate respiration complex in the TCA cycle (111, 353, 354), and is another iron-sulfur containing protein. Combined with the proteome data showing differential expression of phosphate/sulfur relay proteins, the results of this protein-protein interaction screen suggest that Cj1533c may interact with, and bridge, key phosphate/sulfur pathways/central metabolism in *C. jejuni*. However, these putative interactions will require further validation to ascertain their biological relevance. Despite this, our data suggests a key regulatory role for Cj1533c, and the putative sRNA, in the hyperosmotic/oxidative stress response that is connected to altered phosphate/sulfur homeostasis.
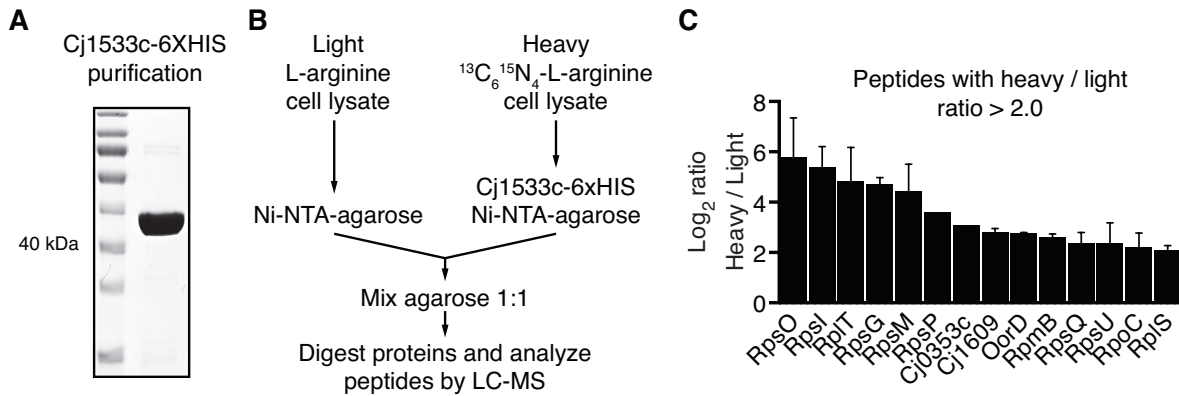
FIGURE 5.6 SILAC-based screen for Cj1533c protein-protein interactions identifies potential binding partners.
(A) Affinity chromatography purification of Cj1533c fused to a C-terminal 6-HIS tag. Cj1533c is a ~47 kDa protein. (B) Schematic of SILAC-based metabolic labeling and Cj1533c-protein interaction screen. The $\Delta argH$ derivative of *C. jejuni* wild-type was grown in modified DMEM broth for metabolic proteome labeling with either with "heavy" $^{13}C_6{}^{15}N_4$-L-arginine or "light" L-arginine. Total protein lysates were then incubated on-column with Ni-NTA-agarose beads (for "light" lysates) or Cj1533c-6XHIS-Ni-NTA-agarose beads (for "heavy" lysates). The bound protein (and potential interacting partners) was eluted from each Ni-NTA-agarose column, and the eluted proteins were mixed 1:1. Proteins were precipitated, digested with trypsin, and the peptides were analyzed by LC-MS. Relative peptide abundance was determined from peptide peak intensity, and the heavy/light ratios were used to assess the interaction specificity. For example, specific interactions are distinguishable by increased intensity of $^{13}C_6{}^{15}N_4$-L-arginine-labeled peptides. Non-specific interactions are indicated by equal (or < 1) heavy/light peptide ratios. (C) Potential Cj1533c-protein interactions determined via SILAC-based affinity chromatography. Only proteins with a heavy/light SILAC ratio > 2.0 are shown. Data shown are from two independent interaction screens.

5.5 DISCUSSION

Cj1533c has clear stress-survival importance for *C. jejuni*, but elucidation of the mechanism of action has been challenging—in part because of multiple levels of regulation at the *cj1533c* locus. The current study points to a role for Cj1533c as a regulator, not of genes, but of proteins important in sulfur relay and homeostasis, and in the stringent response. Thus, we hypothesize that Cj1533c is a key player at the intersection of sulfur and phosphonucleotide homeostasis, which enables coordination of the stringent response with central metabolism, and integrates feedback from iron and oxidative stress gene regulators. Further enhancing the importance of Cj1533c, the putative sRNA

was shown to control expression of proteins with known reversible roles in the biosynthesis of sulfur-containing metabolites, particularly cysteine amino acid.

How does Cj1533c enable hyperosmotic/oxidative stress resistance? How are the two stresses related? Transcriptional profiling of *C. jejuni* grown in hyperosmotic media (Chapter 2) showed that the bacterium increased expression of genes for the dehydrogenase and ATP synthase of the electron transport chain, and also genes for the majority of the TCA cycle (1). Furthermore, NaCl-exposure highly upregulated heat-shock chaperones and proteases (e.g. *dnaK*, *groEL*, *clpB*), and also upregulated superoxide dismutase (*sodB*) and catalase (*katA*) oxidative stress response genes (1). We speculate that enhanced expression of central metabolism genes facilitates replacement of the damaged proteins, and provides energy for the enhanced synthesis of heat shock chaperones for re-folding of other damaged proteins, and proper folding of newly translated proteins during continued stress exposure (355). Damage to *C. jejuni* Fe-S cluster proteins is thought to release iron that that can participate in the Fe^{2+}-catalyzed free radical Fenton chain reaction (136, 144, 148, 356). The TCA cycle of *C. jejuni* may be particularly vulnerable to ROS because it utilizes certain Fe-S proteins—a primary target of ROS (357)—normally found in obligate anaerobes (144, 148). Aerobic respiration also inadvertently produces H_2O_2, which can further oxidize Fe^{2+} to produce the ROS hydroxide (OH^-) and hydroxyl radical ($OH\cdot$) (136, 356). This provokes further cellular damage, oxidizing nucleic acids, lipids and proteins—in which lysine, arginine, proline and threonine residues are carbonylated/oxidized (358). Thus, generalities in the effects of hyperosmotic and oxidative stress require similar/overlapping stress responses.

Sulfur is required in the cell as a component of Fe-S clusters, but also in cysteine and methionine sulfur-containing amino acids, and in the cofactors biotin, co-enzyme A, and thiamine (359, 360). High levels of cysteine alone have

been shown to promote oxidative DNA damage via the Fenton reaction (137). *C. jejuni* cannot assimilate sulfate (SO_4^{2-}) or grow solely on methionine for cysteine biosynthesis, but it can synthesize cysteine *de novo* from reduced sulfurs such as sulfide (S^{2-}) and thiosulfate ($S_2O_3^{2-}$) (319). *C. jejuni* can oxidize toxic sulfite (SO_3^{2-}) to sulfate in the periplasm via the SorAB cytochrome *c* oxidoreductase (65). To participate in cellular metabolism, unreactive sulfate must be activated (360). A potential interaction partner for Cj1533c was the ATP sulfurylase (Cj1609 / CJJ81176_1596), which, in other bacteria, generates nucleotide-activated sulfate (APS, **a**denosine 5'-**p**hospho**s**ulfate) for cysteine metabolism, and releases diphosphate. Despite this, *C. jejuni* cannot assimilate sulfate in this manner because it does not encode downstream reductases that would enable cysteine biosynthesis (19, 319). However, *C. jejuni* does encode APS kinase (CysC, Cj1415c/CJJ81176_1414), which phosphorylates APS to PAPS (3'-**p**hospho**a**denosine-5'-**p**hospho**s**ulfate). Transfer of the sulfuryl group of PAPS via sulfotransferases to various metabolites is common in bacteria and eukarya (361, 362), but at present has not been studied in *C. jejuni*. Thus, the cellular role of the ATP sulfurylase or APS/PAPS is unclear at present.

Another putative interaction partner of Cj1533c was Ppx1/GppA, which has recently been characterized in *C. jejuni* (120). Ppx1/GppA (Cj0353c / CJJ81176_0377) is a dual function exopolyphosphatase/guanosine pentaphosphate phosphohydrolase protein that cleaves polyphosphate, and also increases ppGpp levels by cleaving pppGpp. *C. jejuni* encodes one other non-redundant Ppx/GppA homolog (19, 120). Polyphosphate accumulation has known importance in *C. jejuni* hyperosmotic stress tolerance (121). The high-energy phosphoanhydride bonds of polyphosphate provide energy for biosynthesis in many different metabolic pathways (109). Furthermore, polyphosphate is a determinant of bacterial survival in numerous stresses, and is often important for virulence in pathogenic species (109). Amino acid starvation initiates RelA-mediated synthesis of pppGpp, which is converted to ppGpp by Ppx1/GppA (120),

but is also affected by activation of SpoT, which coordinates both pppGpp hydrolysis and ppGpp synthesis in *C. jejuni* (117). The primary effector of the stringent response is ppGpp, which binds to RNA polymerase and alters promoter specificity for stress-survival transcriptional modulation (117). Next, ppGpp is hydrolyzed to GDP, which is eventually converted back to GTP by nucleoside diphosphate kinase or Ndk. Interestingly, Ndk was upregulated in the putative sRNA strain. Taken together, a possible role for Cj1533c is to enhance the rate of ppGpp formation via Ppx1/GppA-mediated phosphohydrolase activity. Additional studies will be required to confirm the Cj1533c-Ppx1/GppA interaction. And whether or not the interaction promotes or inhibits Ppx1/GppA activity is yet to be determined.

The putative sRNA strain—which does not encode a functional copy of Cj1533c—was remarkable for enhanced expression of cysteine synthase, S-ribosylhomocysteinase, cysteine desulfurase, and pyridine nucleotide-disulfide oxidoreductase. These expression changes were not significant in a strain (wild-type) that encoded both Cj1533c and the putative sRNA. Thus, it may follow that expression modulation by components of the *cj1533c* locus is differentially mediated via Cj1533c, or via the putative sRNA, but not simultaneously. Although both Cj1533c and the putative sRNA may behave synergistically, the putative sRNA may be conditionally expressed, and its effects may only be noticeable during times of extreme stress, when the action of Cj1533c has been insufficient for restoring normal cell function. Bacterial small RNAs have diverse roles and mechanisms in stress responses and virulence (363-366), but sRNA have only recently been identified in *C. jejuni* (340), and none have been phenotypically characterized thus far. Further experiments will be required to confirm the existence of the putative *cj1533c* sRNA, but the current study points to a role for the putative sRNA in the post-transcriptional regulation of cysteine/sulfur metabolism.

The biological relevance of the *cj1533c* locus in hyperosmotic/oxidative stress tolerance is clear, demonstrating the importance of this novel system in *C. jejuni*. With proteomic data indicating roles in sulfur and phosphonucleotide homeostasis, and with the initial identification of relevant Cj1533c-interaction partners, a mechanistic elucidation of Cj1533c-mediated hyperosmotic/oxidative stress resistance is more feasible than ever. The investigation of this challenging system has required unique approaches, utilizing high-throughput proteomic techniques to characterize protein expression modulation. The identification of the as-yet unproven sRNA via directed evolution was unexpected, but the directed evolution technique proved to be a powerful method of selection for relevant mutations, and may prove useful in other investigations. Furthermore, the complex genetic modifications to *C. jejuni* that were required in this investigation were facilitated by the development of new hygromycin B and apramycin antibiotic resistance markers, which are described in CHAPTER SIX (2). Taken together, our study identified a new determinant of hyperosmotic and oxidative stress resistance and provided evidence for a novel role in coordination of multiple vital cellular pathways.

CHAPTER SIX: Hygromycin B and apramycin antibiotic resistance cassettes for use in *Campylobacter jejuni* genetics

6.1 SYNOPSIS

Campylobacter jejuni genetic manipulation is restricted by the limited number of antibiotic resistance cassettes available for use in this diarrheal pathogen. In this study, two antibiotic resistance cassettes were developed, encoding for hygromycin B and apramycin resistance, for use in mutagenesis or for selection of gene expression and complementation constructs in *C. jejuni*. First, the marker genes were successfully modified to allow for insertional mutagenesis or deletion of a gene-of-interest, and were bracketed with restriction sites for the facilitation of site-specific cloning. These hygromycin B and apramycin markers are encoded by plasmids pAC1H and pAC1A, respectively. We also modified an insertional gene-delivery vector to create pRRH and pRRA, containing the hygromycin B and apramycin resistance genes, and 3 unique restriction sites for the directional introduction of genes into the conserved multi-copy rRNA gene clusters of the *C. jejuni* chromosome. We determined the effective antibiotic concentrations required for selection, and established that no harmful effects or fitness costs were associated with carrying hygromycin B or apramycin resistance under standard *C. jejuni* laboratory conditions. Using these markers, the arylsulfatase reporter gene *astA* was deleted, and the ability to genetically complement the *astA* deletion using pRRH and pRRA for *astA* gene insertion was demonstrated. Furthermore, the relative levels of expression from the endogenous *astA* promoter were compared to that of polycistronic mRNA expression from the constitutive promoter upstream of the resistance gene. The development of additional antibiotic resistance cassettes for use in *Campylobacter* will enable multiple gene deletion and expression

combinations as well as more in-depth study of multi-gene systems important for the survival and pathogenesis of this important bacterium.

6.2 INTRODUCTION

The relative paucity of genetic techniques available for the manipulation of *Campylobacter jejuni* has historically been a limiting factor in the study and molecular biology of the leading cause of bacterial gastroenteritis in the developed world (238). Many laboratories are actively studying the bacterium to understand the genetic determinants and physiological features that contribute to *C. jejuni's* virulence and prevalence as a food-borne enteric pathogen. Today, research in the area continues to benefit from and depends on a small arsenal of molecular tools, such as gene deletion strategies and plasmids for genetic complementation. Since the 1980's, only selection for kanamycin and chloramphenicol resistance has been widely adopted for the genetic manipulation of *Campylobacter*.

The development of the first genetic tools for *C. jejuni* was precipitated after the demonstration of gene transfer from *Escherichia coli* to *C. jejuni* via plasmids carrying kanamycin resistance in 1987 (367). This led to the development, in 1988, of a kanamycin resistance cassette for use in gene disruption experiments (368). Cloning and expression of a chloramphenicol resistance gene from *Campylobacter coli* in 1990 (369) was followed by development of replicative cloning vectors and mutational constructs marked with chloramphenicol resistance in 1993 (289). Approximately a decade later, three groups successfully mutagenized *C. jejuni* with transposons carrying kanamycin or chloramphenicol resistance genes (370-372). The finite number of resistance markers has limited genetic analyses to single-gene or single-operon studies, and has prevented complementation of double-deletion strains. As our

understanding of *C. jejuni* grows, so does the need for new markers to rapidly delete and restore complex multi-gene systems, and/or to simultaneously express a reporter such as green fluorescent protein (GFP), arylsulfatase, or luciferase in mutant and/or complemented strains. To address this need, we adapted current *C. jejuni* genetic technologies to harbor resistance genes against the antibiotics hygromycin B and apramycin.

Hygromycin B is an aminoglycoside antibiotic produced by *Streptomyces hygroscopicus* that inhibits protein synthesis in both prokaryotes and eukaryotes (373). Apramycin is another aminoglycoside, an aminocyclitol synthesized by *Streptomyces tenebrarius* (374). Like other aminoglycosides, such as kanamycin, both hygromycin B and apramycin prevent ribosome translocation during translation elongation by binding the 30s rRNA proximal to the ribosomal E, P and A sites (375). Hygromycin B is not used clinically, but is sometimes a component of poultry feed where it has antihelminthic activity against nematode parasites of chickens (376). Apramycin is also used as a veterinary antibiotic (376, 377). The hygromycin B (*Hyg^R*) resistance marker used in this study confers resistance by the activity of a specific **a**minoglycoside **ph**osphotransferase encoded by the 999 bp *aph*(7") gene, encoding hygromycin B 7"-O-kinase or simply hygromycin phosphotransferase (378). The specific modification of hygromycin B is a phosphorylation at the 7"-OH of the destomic acid ring (379). Resistance to apramycin (*Apr^R*) is conferred by the 777 bp *aac*(3)IV **a**minoglycoside 3-*N*-**ac**etyltransferase gene (377). Specifically, the enzyme acetylates the 3-amino group of apramycin's deoxystreptamine ring (380). Neither *aph*(7") nor *aac*(3)IV confers resistance to the other's respective antibiotic, nor do they confer resistance to kanamycin. Vice versa, the *C. jejuni* kanamycin resistance gene *aph*A-3 does not bestow resistance to either hygromycin B or apramycin (data not shown).

In this study, we modified existing *C. jejuni* gene deletion/mutagenesis and insertion strategies and plasmids to encode either *Hyg^R* or *Apr^R*. We based our construction of a non-polar mutagenesis construct on the approach devised by Ménard, Sansonetti and Parsot (381), in which the resistance gene is promoterless, does not harbor a terminator, and transcription is driven from the promoter of the operon into which the gene is introduced. We also modified Karlyshev and Wren's pRRC *C. jejuni* genome-insertional gene delivery and expression system (382), replacing the *cat* **c**hloramphenicol **a**cteyl**t**ransferase cassette with either *aph*(7'') or *aac*(3)IV. The expression of *aph*(7'') and *aac*(3)IV was not detrimental to *C. jejuni* under common laboratory conditions. Furthermore, to demonstrate the potential of these new markers and plasmids, we deleted and then complemented the *C. jejuni* **a**rylsulfate **s**ulfo**t**ransferase *astA,* since the product of *astA* cleaves a chromogenic substance that can be used to report transcriptional activity (79, 322). With the addition of hygromycin B and apramycin resistance markers, we have provided several new, but relatively familiar, well defined and easy-to-use tools to aid other *Campylobacter* researchers in a variety of genetic approaches.

6.3 METHODS AND MATERIALS

6.3.1 Bacterial strains and growth conditions

Bacterial strains and plasmids used in this study are listed in TABLE A.1.5. *E. coli* strains used for plasmid construction were grown at 37°C in Luria-Bertani (LB, Sigma) broth or on 1.7% (w/v) agar plates supplemented with ampicillin (100 µg mL, Ap), chloramphenicol (15 µg mL^{-1}, Cm), kanamycin (50 µg mL^{-1}, Kan), hygromycin B (100 µg mL^{-1}) or apramycin (50 µg mL^{-1}), as necessary. *C. jejuni* strains were grown at 37°C or 42°C in Mueller-Hinton (MH, Oxoid) broth or agar supplemented with vancomycin (10 µg mL^{-1}) and trimethoprim (5

µg mL^{-1}). *C. jejuni* were grown under standard growth conditions (6% O_2, 12% CO_2) using the Oxoid CampyGen system for shaking broth cultures, or in a Sanyo tri-gas incubator for plates. MH was supplemented with chloramphenicol (15 µg mL^{-1}), kanamycin (50 µg mL^{-1}), hygromycin B (250 µg mL^{-1}) or apramycin (60 µg mL^{-1}) where appropriate.

6.3.2 Construction of plasmids pAC1H and pAC1A, pRRH and pRRA

Oligonucleotide primers used in this study are listed in TABLE A.2.5 and were synthesized by Integrated DNA Technologies. The design of pAC1H and pAC1A plasmids containing the non-polar *aph*(7'') or *aac*(3)IV markers is described in Results. The *aph*(7'') or *aac*(3)IV sequence was amplified from pMV261.hyg or p261comp.apra with ultramer set 5631 and 5632, or 5633 and 5634, respectively. The polymerase chain reaction (PCR) was carried out with iProof high-fidelity DNA polymerase (Bio-Rad). A-ends were incorporated on the purified products by incubation with Taq DNA polymerase (Invitrogen) and dATP. The purified products were then introduced to linearized pGEM-T Easy (Novagen), ligated overnight with T4 DNA ligase (NEB), and transformed into *E. coli* DH5α (Invitrogen). Transformants were selected for on LB media supplemented with ampicillin and either hygromycin B or apramycin.

Sequencing verified that the fragment containing *aac*(3)IV was correctly inserted into pGEM-T and this plasmid was then designated pAC1A. Sequencing of pGEM-T containing *aph*(7'') indicated that the restriction sites flanking *aph*(7'') and *aph*(7'') sequence itself were incorrect. The initial *aph*(7'') PCR product was instead digested with *Mfe*I and *Sph*I (NEB), purified, and ligated to low-copy pBAD24 digested with *Eco*RI and *Sph*I. The ligation was transformed into *E. coli* DH5α and sequencing of the transformants indicated the correct *aph*(7'') sequence was incorporated. The resulting plasmid with the *aph*(7'') non-polar marker inserted in pBAD24 was designated pAC1H.

The design of the pRRH and pRRA gene delivery and expression plasmids is also described in the text. Inverse PCR amplification of pRRC was carried out using iProof with primers 5705 and 5706. The resulting PCR product was purified and digested with *Kpn*I and *Xba*I, and ligated to gel-purified *aph*(7'') or *aac*(3)IV markers from similarly-digested pAC1H and pAC1A. Transformants were selected on LB supplemented with hygromycin B or apramycin, and the resulting plasmids were named pRRH or pRRA respectively. *C. jejuni* were transformed with 15 µg of plasmid DNA from pRRH, pRRA, pRRK and pRRC as per established procedure (383) to create antibiotic resistant strains, and verified by PCR against the corresponding resistance gene.

6.3.3 Growth analyses and competition assays

For standard growth curve analyses, 10 mL overnight broth cultures of *C. jejuni* 81-176 integrated with pRRH (Hyg^R), pRRA (Apr^R), pRRK (Kan^R), and pRRC (Cm^R) were inoculated from growth on agar plates containing the appropriate antibiotic. The next day, at the zero time point, strains were standardized to OD_{600} 0.005 in 10 mL of pre-warmed MH (no antibiotics) and grown for 48 hours shaking at 200 rpm at either 37°C or 42°C. Colony forming units (CFU) were assessed over time by plating 10-fold dilutions of aliquots on MH agar plates. Plates were incubated for 48 hours and colonies counted. To assess relative fitness of each antibiotic resistant strain, a co-culture competition was set up. Cultures were inoculated as above, but at the zero time point, 2.5 mL from each of the 10 mL OD_{600} 0.005 cultures were mixed to create a 10 mL culture containing the 4 marked strains. These were grown at 37°C alongside a wild-type control, and CFU were assessed by plating 10-fold dilutions on MH only, or MH containing one of the four antibiotics. Colonies were counted after 48 hours incubation. Three biological replicates, each with 2 technical replicates, were carried out for each assay.

6.3.4 Deletion and complementation of *astA* and assay for enzymatic activity

For mutagenesis, the *astA* gene was PCR-amplified from wild-type 81-176 genomic DNA with primers 5707 and 5708 using iProof DNA polymerase. The PCR product was purified, A-tailed and ligated to pGEM-T to make pGEM-T+*ast*A, which was transformed into *E. coli* DH5α and selected for with ampicillin. Inverse PCR was performed on the resulting plasmid with primers 5709 and 5710 which deleted all 1,863 bp of *astA* and introduced *Kpn*I and *Xba*I sites. The inverse PCR product was digested with *Kpn*I and *Xba*I, ligated to similarly-digested *aph*(7″) or *aac*(3)IV non-polar markers from pAC1H or pAC1A, and transformed into *E. coli* DH5α. The resulting constructs, pGEM-T+*astA::hyg^R* and pGEM-T+*astA::apr^R*, were purified, verified and then transformed into *C. jejuni* 81-176 to create Δ*astA::hyg^R* and Δ*astA::apr^R*. For complementation, iProof PCR was used to amplify *astA* with primer sets 0688 and 0689 (promoterless *astA*), 0690 and 0691 (promoterless *astA* in reverse), and 0691 and 0692 (promoter and *astA* in reverse). This introduced *Xba*I and *Mfe*I restriction sites to each of the 3 products. The PCR products, and pRRH and pRRA, were digested with *Xba*I and *Mfe*I, and the plasmids were dephosphorylated with Antarctic Phosphatase (NEB). Following clean-up, each *astA* gene was ligated to each plasmid and transformed into DH5α. Colonies were screened by PCR for inserts, sequenced, and the resulting plasmids were introduced into a Δ*astA* strain, DRH461 (79). To assess arylsulfatase activity, overnight cultures of bacteria were standardized to OD_{600} 0.05 and 10 μL of bacterial culture was spotted on MH agar supplemented with 100 μg mL^{-1} of 5-bromo-4-chloro-3-indolyl sulfate potassium salt (XS, Sigma). For quantification, the liquid arylsulfatase assay was carried out as described (79, 383), with the exception that strains were incubated in AB3 buffer for 2 h instead of 1 h. Two biological replicates, each with two technical replicates, were carried out.

6.4 RESULTS

6.4.1 Creation of hygromycin and apramycin resistance markers for *C. jejuni* gene replacement/deletion

To construct Hyg^R and Apr^R cassettes that could be used for mutagenesis, we synthesized PCR ultramers to *aph*(7″) or *aac*(3)IV, which included the restriction enzyme cut sites and features depicted in FIGURE 6.1A based on the non-polar Kan^R cassette described by Ménard, Sansonetti and Parsot (381). This construct contains neither a promoter nor a transcription terminator, with the resistance genes preceded at the 5'-end by translational stop codons in all reading frames and also including a Shine-Dalgarno sequence or ribosome binding site (RBS). The 3'-end is followed by another RBS, multiple restriction sites for cloning, and a start codon upstream of and in-frame with the *Sma*I and *Bam*HI cut sites. This start codon is designed to overcome translational coupling of genes in polycistrons if the *Sma*I or *Bam*HI cut sites are employed. The **Apr**^{R} construct was subsequently introduced into high-copy pGEM for clonal amplification (pAC1**A**, FIGURE 6.1B). However, unwanted recombination and loss of restriction cut sites flanking the **Hyg**^{R} gene necessitated introducing the Hyg^R construct into the low-copy pBAD24 vector instead (pAC1**H**, FIGURE 6.1D). Via restriction analyses, we confirmed that all introduced restriction sites can be effectively used to excise the resistance cassettes (FIGURE 6.1C and E). When harbored by *E. coli*, expression of the resistance markers is driven by *lac* or *ara* inducible promoters in pGEM and pBAD respectively; however, induction was not required for *E. coli* growth in the presence of the corresponding antibiotic. Each antibiotic resistance cassette, lacking a transcriptional terminator, is thus now in an *E. coli* cloning vector convenient for non-polar insertional mutagenesis and constructing additional clones for *C. jejuni* manipulation.
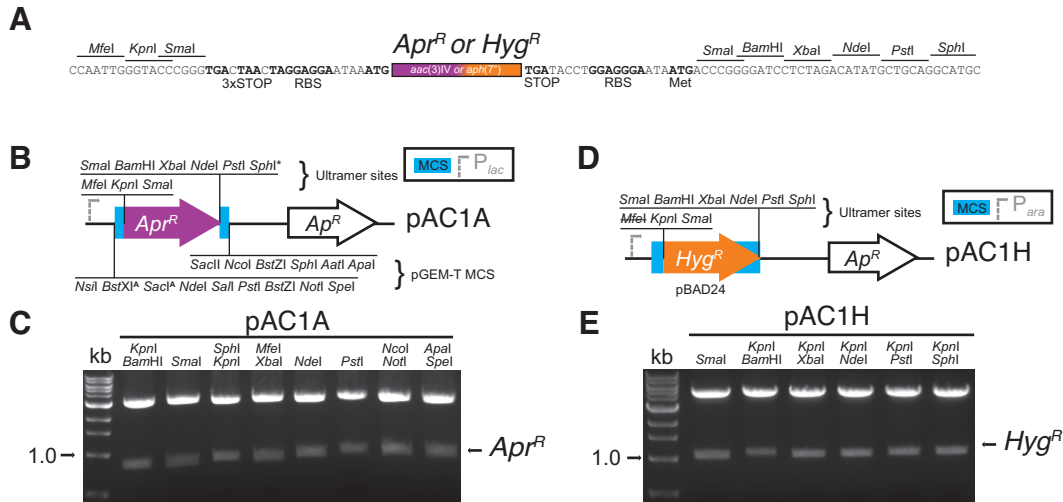
FIGURE 6.1 Synthesis of plasmids containing *aph*(7ʺ) or *aac*(3)IV as non-polar hygromycin B and apramycin resistance markers.
(A) Schematic of ultramers designed to amplify *aph*(7ʺ) or *aac*(3)IV. The 5' ultramers 5631 and 5633, for *aph*(7ʺ) or *aac*(3)IV respectively, include *Mfe*I, *Kpn*I and *Sma*I restriction sites, stop codons in all three reading frames, and a ribosome binding site. The 3' ultramers 5632 and 5634 include a ribosome binding site, a start codon in-frame with restriction sites for *Sma*I and *Bam*HI, and restriction sites for *Xba*I, *Nde*I, *Pst*I and *Sph*I. (B) The amplified *aac*(3)IV was introduced by TA cloning into linearized pGEM-T, conserving the restriction sites in the pGEM-T multiple cloning site (MCS). The resulting plasmid is pAC1A. The pGEM sites may also be used for the sub-cloning of the apramycin resistance marker (*Apr^R*). MCS sites that cut *aac*(3)IV are indicated with a superscript 'A'. (C) All introduced sites in pAC1A were tested by restriction digest. (D) The *Mfe*I- and *Sph*I-digested *aph*(7ʺ) amplification product was cloned into pBAD24 digested with *Eco*RI (*Mfe*I-compatible) and *Sph*I. The *Mfe*I site was lost in the resulting plasmid, pAC1H. (E) All restriction sites introduced to pAC1H were tested by digest.

6.4.2 Modification of the pRRC genome-insertional gene delivery vector to carry *aph*(7ʺ) or *aac*(3)IV

The chloramphenicol resistance marker (*cat*, *Cm^R*) encoded on vector pRRC (FIGURE 6.2A) (382) was exchanged with *Hyg^R* or *Apr^R*. The endogenous *aph*(7ʺ) or *aac*(3)IV promoters were non-functional in *C. jejuni* (data not shown), so the pRRC *cat* promoter was retained to ensure expression. Exchange of *cat* was achieved using an inverse PCR methodology, in which a *Kpn*I site was introduced to the 5'-end of the antisense primer (FIGURE 6.2B). The antisense primer was targeted to the DNA immediately upstream of *cat*, allowing conservation of the *cat* promoter. The inverse PCR product was next digested

144

with *Kpn*I and *Xba*I and ligated to the marker from a similarly-digested pAC1H or pAC1A. For the insertion of genes, the resulting plasmids, pRR**H** and pRR**A** (FIGURE 6.2C), for **H**yg*R* or **A**pr*R* respectively, now include an additional *Bam*HI site in addition to the *Xba*I and *Mfe*I sites present in pRRC. Both pRRA and pRRH also contain *Sma*I sites that flank the resistance cassette; as such, these *Sma*I sites cannot be used for gene insertion for complementation or heterologous gene expression purposes. Functionality of all sites was confirmed by restriction enzyme mapping (FIGURE 6.2D).
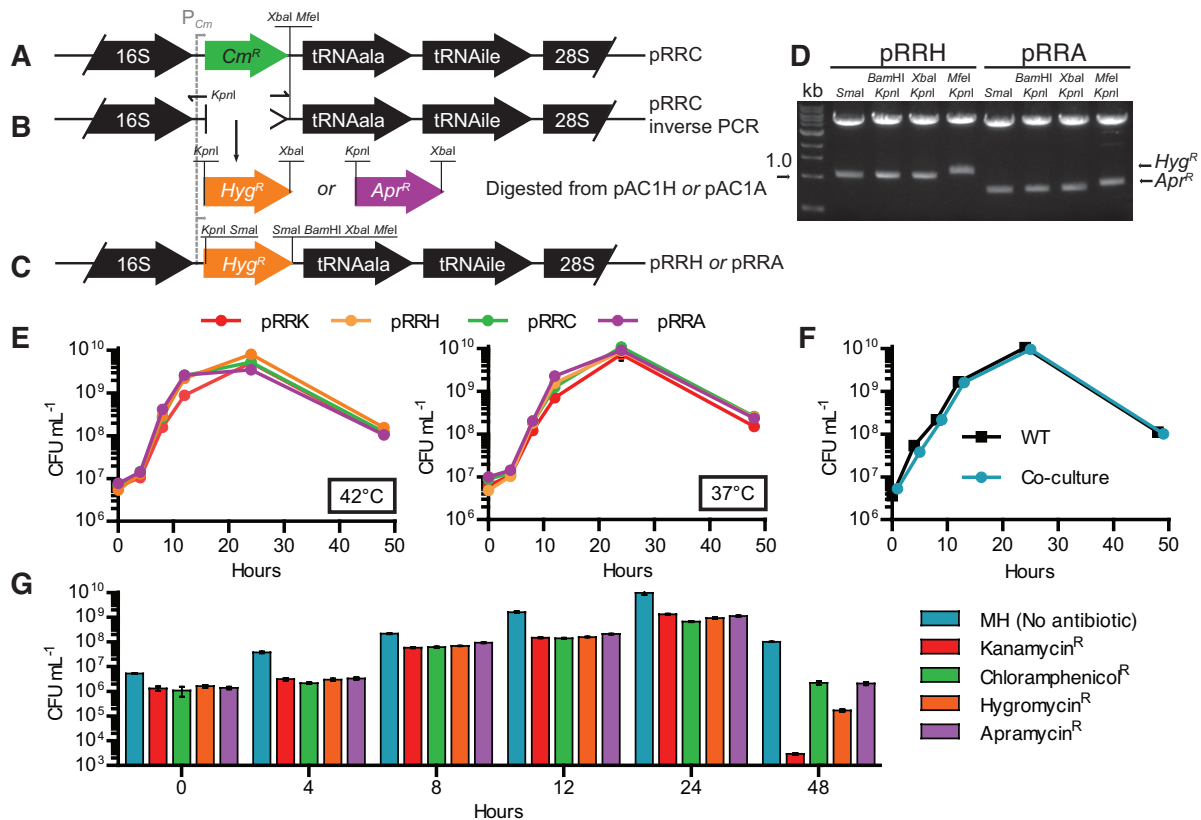
FIGURE 6.2 Adaptation of the pRRC gene delivery and expression system to harbor hygromycin B or apramycin resistance, and testing of genome-integrated markers for detrimental effects of resistance genes.
(A) Schematic of pRRC, which inserts into any of 3 rRNA clusters in the genome by homologous recombination. (B) Inverse PCR amplification of pRRC with primers 5705 (*Kpn*I) and 5706 deleted the chloramphenicol resistance gene but conserved the *Campylobacter*-optimized *cat* promoter. (C) The inverse PCR product was digested with *Kpn*I and *Xba*I, and ligated to similarly digested *aph*(7″) or *aac*(3)IV from pAC1H or pAC1A to create pRRH and pRRA respectively (only pRRH is shown). (D) Restriction digest analysis confirmed the function of all introduced sites. (E) The resistance markers from pRRK, pRRC, pRRH and pRRA were inserted

into the *C. jejuni* 81-176 genome, and each resulting strain was analyzed for microaerobic growth and survival in shaken Mueller-Hinton (MH) broth by counting CFU over 48 hours at both 42°C (left panel) and 37°C (right panel). (F) To determine if the introduction of either marker contributed any fitness cost that could affect competitiveness against wild-type or the other marked strains, a competition assay was performed. Equal numbers of wild-type marked with hygromycin, apramycin, chloramphenicol and kanamycin resistance markers were co-cultured with unmarked wild-type in shaking MH broth at 37°C under microaerobic conditions. CFU were assessed by plating a dilution series on MH agar. (G) CFU were further assessed from the co-culture by plating on MH only (the total CFU, same data as in F) or MH supplemented with each antibiotic, representing the number of bacteria resistant to each antibiotic.

6.4.3 The presence of *aph*(7″) or *aac*(3)IV in *C. jejuni* is not detrimental to growth

To test if the hygromycin B or apramycin resistance genes affected *C. jejuni* growth and survival, pRRH and pRRA were integrated into the genome of *C. jejuni* 81-176 to create *Hyg^R* or *Apr^R* wild-type strains. In the absence of their respective antibiotics, we assessed the time-course growth profile of these strains and compared CFU recovered to those of wild-type and wild-type marked with *aph*A-3 from pRRK and *cat* from pRRC. Neither the *Hyg^R* or *Apr^R* strains were defective for growth in MH broth under microaerobic conditions in at 37°C or 42°C, the optimal temperature range of the bacterium (FIGURE 6.2E). However, because differences in fitness cost of the antibiotic markers may not have been detected in the first experiment, we also carried out a competitive index-style assay. Broth cultures were inoculated with equal numbers of each of the 4 resistant strains, and the mixed cultures were grown at 37°C alongside a wild-type only control (FIGURE 6.2F). At each time point, CFU were assessed by plating dilutions on MH or MH containing hygromycin B, apramycin, kanamycin or chloramphenicol. The total CFU were represented on the MH-only plate, while the number of resistant bacteria were determined on each antibiotic-containing plate. No fitness cost was observed for either *Hyg^R* or *Apr^R* strains between 0 − 24 hours (FIGURE 6.2G). At 48 hours there was a modest decrease in CFU recovered for *Hyg^R* strains; however, this was less pronounced than the defect observed for strains carrying the well-established *Kan^R* marker. It should

be noted that at the 48 hour timepoint, each culture exhibited an overall decrease in the relative CFU recovered under antibiotic selection, suggesting that older cultures are generally more sensitive to antibiotic pressure.

6.4.4 Deletion and complementation of arylsulfatase *astA* with *Hyg^R* or *Apr^R* constructs

In *C. jejuni*, expression of arylsulfatase (*astA*) can be monitored via colorimetric plate and broth assays (79, 383). To further test the usability of pAC1H, pAC1A, pRRH and pRRA, we mutagenized *astA* with the non-polar *Hyg^R* or *Apr^R* markers from pAC1H and pAC1A and also restored a copy of *astA* to the genome of a Δ*astA* strain using pRRH or pRRA. First, *astA* (FIGURE 6.3A) was completely deleted and replaced with the non-polar *Hyg^R* or *Apr^R* markers from pAC1H and pAC1A, respectively (FIGURE 6.3B). Next, a promoterless *astA* was cloned into pRRH or pRRA in the transcriptional direction of, and thus expressed by, the *cat* promoter (FIGURE 6.3C), and these constructs were integrated into DRH461, an unmarked Δ*astA* strain (79). The *astA* gene was also cloned without (FIGURE 6.3D) and with (FIGURE 6.3E) its native promoter into pRRH or pRRA in the reverse orientation to the *cat* promoter. These latter constructs test expression only from the endogenous *astA* promoter and were likewise integrated into DRH461. Each strain was spotted onto MH solid media containing the chromogenic substrate XS, which is cleaved by arylsulfatase (322), and grown for 72 hours. No arylsulfatase activity was observed in any deletion strain. Partial complementation was observed for *astA* expressed from the *cat* promoter, full complementation was observed for *astA* expressed from its native promoter, and no complementation was observed for the promoterless *astA* cloned in the reverse orientation to the *cat* promoter (FIGURE 6.3F). A quantitative liquid spectrophotometric assay confirmed the plate readouts (FIGURE 6.3G).

147
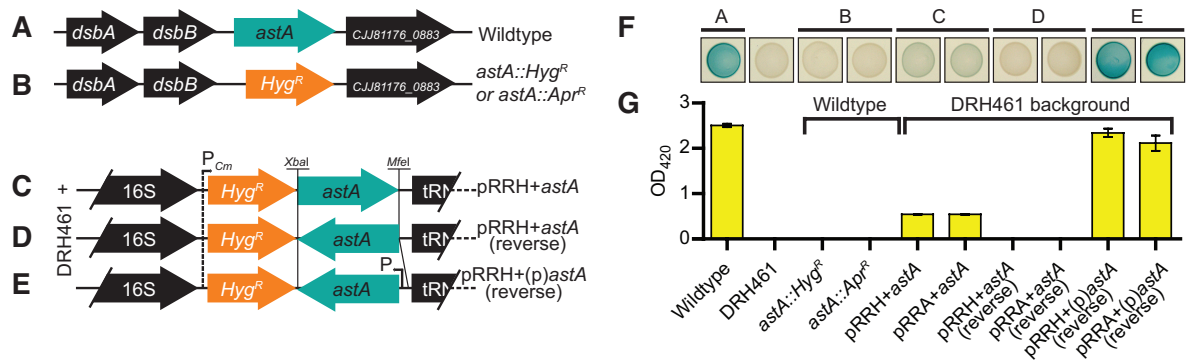
FIGURE 6.3 Mutagenesis of the arylsulfatase gene *astA* with *aph*(7") or *aac*(3)IV non-polar markers and complementation of Δ*astA* via genomic insertion with pRRH or pRRA.
(A) Loci arrangement of *astA* single-gene operon in *C. jejuni* 81-176. (B) Deletion of *astA* with either *aph*(7") or *aac*(3)IV from pAC1H or pAC1H. (C) Introduction of promoterless *astA* into pRRH or pRRA in the same orientation as the *cat* promoter created pRRH+*astA* or pRRA+*astA* and resulted in polycistronic expression of *astA* with *aph*(7") or *aac*(3)IV. (D) Promoterless *astA* inserted in the opposite orientation to the *cat* promoter (designated pRRH+*astA* (reverse) or pRRA+*astA* (reverse) (E) Insertion of the endogenous *astA* promoter and *astA* in the opposite orientation to the *cat* promoter in pRRH and pRRA created pRRH+(p)*astA* (reverse) and pRRA+(p)*astA* (reverse). Only *Hyg^R* plasmids/strains are depicted in B-E, but both *Hyg^R* and *Apr^R* plasmids represented with *Hyg^R* in C, D and E were integrated into the genome of the Δ*astA* strain, DRH461. (F) Arylsulfatase activity of the deletion and complementation strains was assessed by spotting 10 µL of OD-standardized cultures onto MH agar plates supplemented with the chromogen XS cleaved by arylsulfatase. A blue-green color indicates activity, and the spots correspond to labels on the bar graph below. (G) Quantification of arylsulfatase activity from broth cultures to assess transcription of *astA*.

6.5 DISCUSSION

With the introduction of hygromycin B and apramycin resistance markers, we have provided researchers in the *C. jejuni* field with additional genetic tools, essentially doubling the number of broadly usable markers for this organism. We envision that these markers will be especially useful for deletion of multiple genes, complementation, and/or the addition of various promoter-reporter constructs. Although it is possible to construct a potentially unlimited number of unmarked deletion mutants in *C. jejuni* (371), a disadvantage of unmarked mutations is that they cannot be easily transferred from one genetic background to another. This is especially critical for an organism like *C. jejuni* with high rates of phenotypic variation associated with phase variable, highly mutable

148

contingency loci (1, 218, 238). This variation is often unpredictable and may result in phenotypes unlinked to the intended mutation, and it is often pertinent to test several mutant clones or re-introduce a marked mutation to a wild-type background to ensure the veracity of any phenotype.

The non-polar markers harbored by gene disruption cassettes in pAC1H and pAC1A have both advantages and disadvantages when compared to markers that also introduce a promoter, such as the *C. jejuni cat* cassette in pRY109 (289). Primarily, the main advantage of a promoterless disruption construct is that the introduction of a non-endogenous promoter affects transcription of any co-transcribed gene at the 3'-end of the deleted gene in an operon. Vice versa, one disadvantage of the promoterless marker is that it is reliant on transcription from the promoter of the gene into which it has inserted. Therefore, if the target gene is not highly expressed, then the same will be true for the resistance gene, and antibiotic resistance will not be conferred to the bacterium. Our laboratory has experienced this problem, and if a mutant cannot be made with a non-polar marker, then it can be attempted using the *cat* cassette from pRY109. Another advantageous feature of the non-polar markers in pAC1H and pAC1A is the start codon at the 3'-end of the resistance gene; specifically, use of the 3' *Sma*I or *Bam*HI restriction sites allows placement of the start codon in the reading frame of the stop codon of the mutated gene. This configuration allows for translation of a remainder of the gene into which the marker is inserted, preventing polar effects on the downstream gene due to translational coupling. Translational coupling is the interdependence of translation efficiency of co-transcribed genes on a polycistronic mRNA (381, 384). We do not routinely design our deletion/replacement strategies to take translational coupling into account for the initial study of a gene; however, translational coupling was recently observed for the *C. jejuni dsb* genes (385), so remains an important consideration.

149

Many of the features of the pRRC vector were conserved in the new pRRA and pRRH gene delivery vectors. In particular, the *cat* promoter is common to all three plasmids, which is advantageous because it allows for constitutive expression of an introduced gene as part of the polycistronic mRNA coding the resistance marker. This is helpful for the expression of genes with no directly adjacent promoters, such as those found within operons. However, as we demonstrated in FIGURE 6.3F-G, the level of polycistronic expression can be out of context with that of the endogenous system. For *astA*, expression from the *cat* promoter is considerably lower than from the *astA* promoter. Likewise, for a gene that is not highly expressed, or expressed only under certain conditions, expression from the *cat* promoter can be higher than normal or expressed at inappropriate times. Nonetheless, under some circumstances the *cat* promoter can provide full complementation, as we and others have shown (91, 382, 386). A new advantage of pRRA and pRRH is the addition of the *Bam*HI site in addition to the pre-existing *Xba*I and *Mfe*I sites, which permits greater choice in the directional cloning of insertions for complementation and heterologous expression.

The fitness cost of harboring *aph*(7″) or *aac*(3)IV was minimal or comparable to either kanamycin or chloramphenicol resistance markers (FIGURE 6.2G). In addition, the length of time required for transformants to grow on media containing either hygromycin B or apramycin was comparable to that of kanamycin-supplemented MH. Transformants also appeared 3-4 days earlier than with chloramphenicol, reducing the time needed to delete or introduce a gene. For cloning in *E. coli*, 50-100 μg mL^{-1} of apramycin or 100-250 μg mL^{-1} hygromycin B was generally sufficient. In *C. jejuni*, we found that 60 μg mL^{-1} of apramycin was the optimal concentration for selection. The minimum inhibitory concentration of hygromycin B for *C. jejuni* was determined to be >32 μg mL^{-1} (not shown), but this value was not useful in determining a working concentration, possibly because the high culture densities typically used in *C.*

jejuni transformation protocols easily overcame the antibiotic. By trial-and-error, we found that 250 μg mL^{-1} hygromycin B was necessary to ensure selection. Apramycin and hygromycin B are also attractive reagents because they are relatively inexpensive drugs, although the high concentrations of hygromycin B increase the cost of using *aph*(7″) as a marker. One potential drawback of *aac*(3)IV is that it is reported to confer resistance to gentamicin (380), an antibiotic used to kill bacteria during assessments of host cell invasion. However, our *Apr^R* (*aac*(3)IV) strains behaved identically to other marked strains in gentamicin-protection assays, indicating that invasion and intracellular survival can be accurately assessed with mutants harboring this marker (data not shown).

In summary, we have adapted a set of well-established plasmids to encode hygromycin B and apramycin resistance for gene deletion, replacement, and expression in *C. jejuni*. We also established the optimal concentrations of both hygromycin B and apramycin for the purposes of selection. In addition, we determined that introduction of *aph*(7″) or *aac*(3)IV was not detrimental and that there was no appreciable fitness cost to *C. jejuni* when compared to chloramphenicol or kanamycin resistance markers. These constructs were validated using the *astA* reporter, and are currently being utilized in our laboratory for exploratory studies of uncharacterized genes. These new molecular tools will provide a broader range of possible experiments, will assist in the mechanistic study of *C. jejuni*, and contribute to a better understanding of the microorganism's lifecycle and pathogenicity.

CHAPTER SEVEN: Conclusion

The tremendous success of *C. jejuni* as the leading cause of bacterial gastroenteritis is poorly understood, but it is clear that differential global physiological changes underlie stress adaptation, host colonization, and disease in humans. What is remarkable about these physiological changes is that they are mediated by a relatively small cadre of cross-protective stress proteins, and limited transcriptional regulatory mechanisms. In contrast, the greatest physiological adaptations stem from the metabolic potential of *C. jejuni,* which is far greater than many host-adapted bacterial species (387). Often in evolution, selective pressure compels the production of niche-fit strains, which is typically accompanied by genome reduction (and therefore loss of redundant genes for survival in alternate environments) (387). At first glance, it would appear that genome reduction in *C. jejuni* has occurred; yet the pathogen remains ubiquitous, and clearly capable of multiple lifestyles. Thus, *C. jejuni* represents a unique opportunity for elucidating the minimal/essential requirements for enteric disease-causing bacteria, environmental survival, and success as a commensal bacterium in a wide-range of animals.

In CHAPTER TWO, comprehensive transcriptional profiling was carried out on *C. jejuni* to identify genes dysregulated in hyperosmotic conditions—provided by exposure to NaCl. From these DNA microarray analyses, a detailed temporal gene expression profile was constructed, and which shed new light on an unstudied aspect of *C. jejuni* physiology. The most highly dysregulated genes encoded prototypical heat shock proteins. Furthermore, the most highly dysregulated transcription factors were regulators of the heat shock stimulon. This finding is observed in several other bacterial species (152, 189), but is not typical in species which encode "classic" osmotic stress response systems. This begs the question of which is more classic from an evolutionary standpoint—a generalized heat shock protein-enabled response, or a response that requires

multiple different osmoadaptive systems? Despite this, we did identify one hallmark of osmoadaptation that we speculate is a core function. The upregulation of glutamine/glutamate synthases in *C. jejuni* potentially results in a greater intracellular pool of glutamate, which would be similar to the known accumulation of glutamate in other bacteria (152). We also hoped to identify possible compatible solutes in *C. jejuni*, but did not characterize this further during these studies. For future experiments, an initial hypothesis would indicate a role for L-proline as a compatible solute, because the PutP transporter for this amino acid was highly dysregulated in hyperosmotic stress. Furthermore, L-proline is a common compatible solute in many species (169, 171), and *C. jejuni* does not preferentially utilize L-proline for glycogenic processes (66). However, L-tryptophan and L-leucine also may have greater physiological roles, and genes in both biosynthesis loci have been found to be dysregulated in host animals, and in other stress conditions (125, 143). In this study, we also confirmed a role for the capsular polysaccharide in osmotic stress defense, which is a common attribute for bacterial capsules (202). Since the structures of capsules of different *C. jejuni* strains are known to be highly divergent and phase variable (27, 58, 89, 102), an interesting possibility is that differential capsular modifications provide differential osmotic stress survival capabilities. Thus, a future direction would be a comparison of different capsule types and their ability to protect against hyperosmotic stress.

An unanticipated finding was the enormous phenotypic heterogeneity within the *C. jejuni* population—some of which we later attributed to high frequency mutations occurring in *purF/apt*. However, different cells in hyperosmotic stress exhibited an unusual characteristic, which was observed by bimodal gene expression from the ATP synthase promoter. Currently, it is unknown if bimodal expression is related to high frequency mutations in *purF/apt*, but it is likely to be a completely different phenomenon. Bimodal gene expression is typically the result of mutually-repressing repressors (173, 175,

153

253), but the likelihood of this is also low considering that *C. jejuni* has so few regulators, none of which are known to regulate the σ^{70} ATP synthase promoter. Flow cytometry of a variety of promoter-GFP fusions indicated promoter-specific unimodal/bimodal expression within populations (unpublished observations). Future studies might uncover the mechanism behind this phenomenon by individually screening clones of a promoter-GFP library, recording the modality of the GFP expression, and searching for native gene commonalities between promoters of interest. Multiple observations of heterogeneity in the population have major implications for analyses, which typically rely on the average behavior in the population. Our data clearly showed that gene expression profiles via DNA microarray might not capture important changes occurring only in a small percentage of the population. This has physiological importance, and may help to explain why *C. jejuni* is so ubiquitous. Such individuality may also be important for disease in humans. To give a human analogy, only a small fraction of a rioting crowd is responsible for looting and property destruction. It is already known that *C. jejuni* exhibits different tissue tropism based on differential strain metabolic capabilities (29). Thus, future investigations might wish to investigate the roles of bacterial individuality in infection/colonization. Although this would be extremely challenging, with growing RNA-seq capabilities, and improved GFP-tagging/flow cytometry, future studies might be able to assess genotype/physiology at the single-cell level from bacteria in different host micro-niches.

In CHAPTER THREE, we continued to examine the cause of differential colonial stress survival phenotypes. We initially assumed that if a genetic cause were responsible for the different colonial stress survival outcomes, then it would be identified in phase variable homopolymeric tracts of the culprit gene. To our astonishment, the genetic variation was in the housekeeping purine biosynthesis genes *purF* and *apt*, which could not have been predicted. Thus, we established that a certain percentage of phenotypic variation in the population

was due to those mutations, and not phase variation. We also contrasted the frequency with known phase variation frequencies. What was clear is that the high frequency mutations in *purF/apt* do not have the same ability as phase variation to seamlessly switch "ON-OFF". This contributed to the differential phenotypes, and also differential rates of reversion among progeny bacteria. Another stark contrast was that phase variation results only in "ON-OFF" expression of a particular trait (209), whereas the multifarious mutations in *purF/apt* resulted in different behavior specific to the particular allele. What was also evident was that mutations were occurring in *purF/apt* but were not occurring in the *prsA* gene. We speculated that the *prsA* gene mutability rate is representative of most *C. jejuni* genes, and that there was a specific mechanism that promoted hypervariation in *purF/apt*. Although we utilized a novel SILAC-based approach to determine if any DNA-binding proteins were responsible for this phenomenon (216), and identified a putative candidate protein, results of mutant-based analyses were inconclusive. Furthermore, those experiments illustrate an important concept in scientific research, in which reductionist approaches cannot be used to meaningfully assess a complex system (388). The challenge of identifying a mechanistic determinant of *purF/apt* hypermutation stemmed from the fact that the original diversity within the parental population was not observed in single colony-derived populations. Although we also showed that other *C. jejuni* type strains exhibited mutations in *purF/apt*, those strains exhibited phenotypic traits that were not necessarily related to different *purF/apt* alleles, and overall, other type strains exhibited less heterogeneity that strain 81-176. Thus, a future investigation might assess 81-176-specific genes for roles in phenotypic variation (22). Incidentally, the 81-176 strain-specific hypothetical gene *CJJ81176_1732* is encoded directly upstream from *apt* in the *apt* operon, and has domains potentially related to YabA (COG4467), a DNA replication initiation-suppressing control protein (389). Although we wanted to use a non-biased approach to identify mechanisms of *purF/apt* hypervariation, a targeted approach directed toward this putative YabA may be

interesting for future experiments. However, such experiments will be subject to similar pitfalls already encountered. In this study, the specific cellular effects of different *purF/apt* mutants were not assessed. Thus, future experiments—already underway—include additional physiological characterizations of different *purF/apt* mutants. These experiments include measurement of pppGpp and ppGpp levels, and SILAC-based proteomic comparisons between different mutant strains. Considering that mutations in *purF/apt* are likely to modulate intracellular purine levels, these analyses may also identify the purine stimulon of *C. jejuni*, which has not been characterized—in part because *C. jejuni* does not encode known purine gene regulators (19). Thus, the different *purF/apt* mutants may represent a unique opportunity to assess purine regulation, which, in the absence of transcription factors, may rely on purine riboswitches in mRNA (390). Thus, a whole new area of *C. jejuni* biology remains to be explored.

In CHAPTER FOUR, we expanded on our initial studies with the *purF/apt* mutants, and described a role for these variants in biofilm formation, and survival in the planktonic state. Via high-throughput Illumina-based amplicon sequencing, we identified variants that preferred either planktonic- or biofilm-based micro-niches, and showed that variants in mixed populations preferentially migrated into those preferred niches. Since it is known that *C. jejuni* biofilms promote horizontal gene transfer (73), we also demonstrated that variants with biofilm preferences were more likely to acquire new genes, which has importance for further speciation/genetic adaptation in the already-widely divergent *C. jejuni* genus. In this study, we also introduced a new RFP tag to the *C. jejuni* field, which enabled us to visualize differential phenotypic behavior occurring in mixed-variant biofilm formation. These interactions were unexpected, and we proposed that the differential phenotypic behavior, identified by variant chaining, resulted in enhanced biofilm formation. In that study, the importance of variation within the population was reinforced with observations that biofilm formation enhancement only occurred when a

sufficient level of variation was reached (FIGURE 4.6). It is not clear how relevant this is to a natural mixed-species biofilm. Furthermore, planktonic bacteria, or bacteria dispersed from an already-formed biofilm, are thought to promote the establishment of new biofilms alone. Thus, the model of enhanced biofilm formation from genetic variant interactions would seem to be incompatible with this. However, we also showed that all variants tested were equally capable of forming biofilms. Variant-mediated enhanced biofilm formation might be important within hosts, where the total bacterial population is confined to a relatively small volume, increasing the likelihood of variant-variant interactions.

Another common theme in these studies has been the formation of chains, a hitherto unappreciated aspect of *C. jejuni* biology. In CHAPTER TWO, a percentage of the NaCl-stressed *C. jejuni* population was found to chain extensively. Given that CFU counts are used to assess viability, and depend on a colony growing from a single cell deposited on nutrient agar, this observation indicated that CFU estimates for chained bacteria under-represented the number of viable cells. Another striking observation was that individual cells within the multi-cell chain exhibited different phenotypic properties—evident from microscopy with PI and Syto-9 (FIGURE 2.4). Differential chaining was also observed for different *purF/apt* mutants, and NaCl-sensitive variants were found to chain most extensively (unpublished observation). Given that chaining was also observed during heterogeneity-mediated biofilm formation, it appears that *C. jejuni* chaining has physiological importance and has been overlooked.

In CHAPTER FIVE, a preliminary analysis of the *cj1533c* locus was carried out because that gene had been identified as a putative regulator upregulated in hyperosmotic stress. The Δ*cj1553c* mutant was defective in hyperosmotic and oxidative stress survival; thus, an important stress tolerance role was confirmed. However, DNA microarray profiling indicated that Cj1533c

was not significantly modulating transcription. Comprehensive analyses of expression at the *cj1533c* locus determined that expression of *cj1553c* was only observed immediately following stress exposure. Furthermore, *cj1533c* was sometimes co-transcribed on a bicistron with *dps*, and *dps-cj1533c* expression was regulated via the iron and oxidative stress regulators Fur, PerR and CosR. Structural homology analyses later indicated that Cj1533c was not a transcription factor, but more likely a Walker A-containing ATPase. Substitution of a critical Walker A motif residue eliminated protein functionality. Attempts to identify mutations in *cj1533c* that conferred activation/enhanced NaCl-tolerance instead identified a putative sRNA. And further experiments were stalled until the new antibiotic resistance markers described in CHAPTER SIX were developed (2). Thus, the hygromycin B and apramycin antibiotic resistance markers enabled more complex SILAC-based experiments to be performed in the elucidation of Cj1533c function.

With proteomics, differential protein expression was observed in the Δ*cj1533c* mutant. Furthermore, the same SILAC-based approach identified proteins dysregulated by the putative sRNA in the absence of Cj1533c. Screening for Cj1533c-protein interactions identified putative interaction partners with possible related roles. Taken together, these data have provided new avenues for further confirmation and exploration of Cj1533c function. Future experiments include confirmation of Cj1533c-protein interactions, which is currently under investigation utilizing another relatively new proteomics technique called proximity-dependent **bio**tin **id**entification (bioID) (391). In these experiments, the BirA biotin ligase is fused to the protein of interest, and interacting proteins are thus biotinylated, and can be recovered with streptavidin for LC-MS. Considering that Cj1533c may interact with the polyphosphatase/pppGpp-hydrolyzing Ppx1/GppA (120), both polyphosphate quantitation and analysis of pppGpp/ppGpp levels will be carried out with Δ*cj1533c* mutant strains. Although we have not been successful at detecting the putative sRNA, it may be

conditionally expressed only when Cj1533c is absent. Thus, future Northern blotting will be performed with RNA isolated from the Δ*cj1533c+putative sRNA* strain. Although the sRNA is only putative at this juncture, our proteomics data would provide the only known sRNA-mediated physiology in *C. jejuni* at present. This has been enabled by the introduction of additional genetics capabilities represented by the hygromycin B and apramycin markers, and by arginine auxotroph (Δ*argH*) SILAC-based proteomics.

Taken together, the experiments described in this thesis reveal unconventional adaptive properties of *C. jejuni*. In particular, novel high frequency genetic variation was shown to be important for multiple aspects of *C. jejuni* biology, and the *cj1533c* locus was shown to be important for hyperosmotic and oxidative stress tolerance. In conclusion, a number of *C. jejuni* success mechanisms were identified via their importance for hyperosmotic stress tolerance.

REFERENCES

1. **Cameron A, Frirdich E, Huynh S, Parker CT, Gaynor EC.** 2012. Hyperosmotic stress response of *Campylobacter jejuni*. J Bacteriol **194:**6116-6130.

2. **Cameron A, Gaynor EC.** 2014. Hygromycin B and apramycin antibiotic resistance cassettes for use in *Campylobacter jejuni*. PloS one **9:**e95084.

3. **Silva J, Leite D, Fernandes M, Mena C, Gibbs PA, Teixeira P.** 2011. *Campylobacter spp.* as a Foodborne Pathogen: A Review. Frontiers in microbiology **2:**200.

4. **Altekruse SF, Stern NJ, Fields PI, Swerdlow DL.** 1999. *Campylobacter jejuni*--an emerging foodborne pathogen. Emerging infectious diseases **5:**28-35.

5. **Kusters JG, van Vliet AH, Kuipers EJ.** 2006. Pathogenesis of *Helicobacter pylori* infection. Clinical microbiology reviews **19:**449-490.

6. **Pereira L, Sampaio S, Tavares I, Bustorff M, Pestana M.** 2014. Bacteremia due to *Campylobacter* in renal transplantation: a case report and review of literature. Transplant infectious disease : an official journal of the Transplantation Society.

7. **Liu P.** 2012. Campylobacteremia in stage IV gliosarcoma with bevacizumab treatment. Journal of community hospital internal medicine perspectives **2**.

8. **Hopkins S, Abuzakouk M, Brannigan E, Bergin C, Feighery C.** 2011. *Campylobacter jejuni* cellulitis in a patient with pan-hypogammaglobulinaemia. BMJ case reports **2011**.

9. **van den Bruele T, Mourad-Baars PE, Claas EC, van der Plas RN, Kuijper EJ, Bredius RG.** 2010. *Campylobacter jejuni* bacteremia and *Helicobacter pylori* in a patient with X-linked agammaglobulinemia. European journal of clinical microbiology & infectious diseases : official publication of the European Society of Clinical Microbiology **29:**1315-1319.

10. **Monselise A, Blickstein D, Ostfeld I, Segal R, Weinberger M.** 2004. A case of cellulitis complicating *Campylobacter jejuni* subspecies jejuni bacteremia and review of the literature. European journal of clinical microbiology & infectious diseases : official publication of the European Society of Clinical Microbiology **23:**718-721.

11. **Nielsen H, Hansen KK, Gradel KO, Kristensen B, Ejlertsen T, Ostergaard C, Schonheyder HC.** 2010. Bacteraemia as a result of *Campylobacter* species: a population-based study of epidemiology and clinical risk factors. Clinical microbiology and infection : the official publication of the European Society of Clinical Microbiology and Infectious Diseases **16:**57-61.

12. **Skirrow MB.** 1990. *Campylobacter*. Lancet **336:**921-923.

13. **Skirrow MB.** 1991. Epidemiology of *Campylobacter* enteritis. Int J Food Microbiol **12:**9-16.

14. **Nelson MR, Shanson DC, Hawkins DA, Gazzard BG.** 1992. *Salmonella, Campylobacter* and *Shigella* in HIV-seropositive patients. Aids **6:**1495-1498.

15. **Kist M.** 1986. Who discovered *Campylobacter jejuni/coli*? A review of hitherto disregarded literature. Zentralblatt fur Bakteriologie, Mikrobiologie, und Hygiene. Series A, Medical microbiology, infectious diseases, virology, parasitology **261:**177-186.

16. **Dekeyser P, Gossuin-Detrain M, Butzler JP, Sternon J.** 1972. Acute enteritis due to related vibrio: first positive stool cultures. J Infect Dis **125:**390-392.

17. **Svachko AG, Formaziuk VE, Sergienko VI.** 1990. Decrease of singlet oxygen chemiluminescence by the presence of carnosine. Biulleten' eksperimental'noi biologii i meditsiny **110:**155-157.

18. **Merrell DS, Stintzi A.** 2012. Research advances in the study of *Campylobacter*, *Helicobacter*, and related organisms. Frontiers in cellular and infection microbiology **2:**159.

19. **Parkhill J, Wren BW, Mungall K, Ketley JM, Churcher C, Basham D, Chillingworth T, Davies RM, Feltwell T, Holroyd S, Jagels K, Karlyshev AV, Moule S, Pallen MJ, Penn CW, Quail MA, Rajandream MA, Rutherford KM, van Vliet AH, Whitehead S, Barrell BG.** 2000. The genome sequence of the food-borne pathogen *Campylobacter jejuni* reveals hypervariable sequences. Nature **403:**665-668.

20. **Pearson BM, Gaskin DJ, Segers RP, Wells JM, Nuijten PJ, van Vliet AH.** 2007. The complete genome sequence of *Campylobacter jejuni* strain 81116 (NCTC11828). J Bacteriol **189:**8402-8403.

21. **Johnson JG, Carpentier S, Spurbeck RR, Sandhu SK, Dirita VJ.** 2014. Genome Sequences of *Campylobacter jejuni* 81-176 Variants with Enhanced Fitness Relative to the Parental Strain in the Chicken Gastrointestinal Tract. Genome announcements **2**.

22. **Hofreuter D, Tsai J, Watson RO, Novik V, Altman B, Benitez M, Clark C, Perbost C, Jarvie T, Du L, Galan JE.** 2006. Unique features of a highly pathogenic *Campylobacter jejuni* strain. Infect Immun **74:**4694-4707.

23. **Zhou Y, Bu L, Guo M, Zhou C, Wang Y, Chen L, Liu J.** 2013. Comprehensive genomic characterization of *Campylobacter* genus reveals some underlying mechanisms for its genomic diversification. PloS one **8:**e70241.

24. **Meric G, Yahara K, Mageiros L, Pascoe B, Maiden MC, Jolley KA, Sheppard SK.** 2014. A reference pan-genome approach to comparative bacterial genomics: identification of novel epidemiological markers in pathogenic *Campylobacter*. PloS one **9:**e92798.

25. **Gaynor EC, Szymanski CM.** 2012. The 30th anniversary of *Campylobacter, Helicobacter,* and Related Organisms workshops-what have we learned in three decades? Frontiers in cellular and infection microbiology **2:**20.

26. **Young KT, Davis LM, DiRita VJ.** 2007. *Campylobacter jejuni*: molecular biology and pathogenesis. Nat Rev Microbiol **5:**665-679.

27. **Bacon DJ, Szymanski CM, Burr DH, Silver RP, Alm RA, Guerry P.** 2001. A phase-variable capsule is involved in virulence of *Campylobacter jejuni* 81-176. Mol Microbiol **40:**769-777.

28. **Hendrixson DR.** 2006. A phase-variable mechanism controlling the *Campylobacter jejuni* FlgR response regulator influences commensalism. Mol Microbiol **61:**1646-1659.

29. **Hofreuter D, Novik V, Galan JE.** 2008. Metabolic Diversity in *Campylobacter jejuni* Enhances Specific Tissue Colonization. Cell Host Microbe **4:**425-433.

30. **Andersen-Nissen E, Smith KD, Strobe KL, Barrett SL, Cookson BT, Logan SM, Aderem A.** 2005. Evasion of Toll-like receptor 5 by flagellated bacteria. Proc Natl Acad Sci U S A **102:**9247-9252.

31. **O'Hara JR, Feener TD, Fischer CD, Buret AG.** 2012. *Campylobacter jejuni* disrupts protective Toll-like receptor 9 signaling in colonic epithelial

cells and increases the severity of dextran sulfate sodium-induced colitis in mice. Infect Immun **80:**1563-1571.

32. **de Zoete MR, Keestra AM, Roszczenko P, van Putten JP.** 2010. Activation of human and chicken toll-like receptors by *Campylobacter spp*. Infect Immun **78:**1229-1238.

33. **Korlath JA, Osterholm MT, Judy LA, Forfang JC, Robinson RA.** 1985. A point-source outbreak of campylobacteriosis associated with consumption of raw milk. J Infect Dis **152:**592-596.

34. **Hu L, Kopecko DJ.** 1999. *Campylobacter jejuni* 81-176 associates with microtubules and dynein during invasion of human intestinal cells. Infect Immun **67:**4171-4182.

35. **Everest PH, Goossens H, Butzler JP, Lloyd D, Knutton S, Ketley JM, Williams PH.** 1992. Differentiated Caco-2 cells as a model for enteric invasion by *Campylobacter jejuni* and *C. coli*. Journal of medical microbiology **37:**319-325.

36. **Russell RG, Blaser MJ, Sarmiento JI, Fox J.** 1989. Experimental *Campylobacter jejuni* infection in Macaca nemestrina. Infect Immun **57:**1438-1444.

37. **Black RE, Levine MM, Clements ML, Hughes TP, Blaser MJ.** 1988. Experimental *Campylobacter jejuni* infection in humans. J Infect Dis **157:**472-479.

38. **Blaser MJ.** 1997. Epidemiologic and clinical features of *Campylobacter jejuni* infections. J Infect Dis **176:**S103-S105.

39. **Girard MP, Steele D, Chaignat CL, Kieny MP.** 2006. A review of vaccine research and development: human enteric infections. Vaccine **24:**2732-2750.

40. **Tauxe RV.** 1992. Epidemiology of *Campylobacter jejuni* Infections in the United-States and Other Industrialized Nations. Camplylobacter Jejuni**:**9-19
300.

41. **Allos BM.** 2001. *Campylobacter jejuni* infections: update on emerging issues and trends. Clinical infectious diseases : an official publication of the Infectious Diseases Society of America **32:**1201-1206.

42. **Hrudey SE, Payment P, Huck PM, Gillham RW, Hrudey EJ.** 2003. A fatal waterborne disease epidemic in Walkerton, Ontario: comparison with

other waterborne outbreaks in the developed world. Water Sci Technol **47:**7-14.

43.   **Humphrey S, Chaloner G, Kemmett K, Davidson N, Williams N, Kipar A, Humphrey T, Wigley P.** 2014. *Campylobacter jejuni* is not merely a commensal in commercial broiler chickens and affects bird welfare. mBio **5:**e01364-01314.

44.   **Buswell CM, Herlihy YM, Lawrence LM, McGuiggan JT, Marsh PD, Keevil CW, Leach SA.** 1998. Extended survival and persistence of *Campylobacter spp.* in water and aquatic biofilms and their detection by immunofluorescent-antibody and -rRNA staining. Appl Environ Microbiol **64:**733-741.

45.   **Doyle MP, Roman DJ.** 1982. Prevalence and survival of *Campylobacter jejuni* in unpasteurized milk. Appl Environ Microbiol **44:**1154-1158.

46.   **Longenberger AH, Palumbo AJ, Chu AK, Moll ME, Weltman A, Ostroff SM.** 2013. *Campylobacter jejuni* infections associated with unpasteurized milk--multiple States, 2012. Clinical infectious diseases : an official publication of the Infectious Diseases Society of America **57:**263-266.

47.   **Newell DG, Fearnley C.** 2003. Sources of *Campylobacter* colonization in broiler chickens. Appl Environ Microbiol **69:**4343-4351.

48.   **Kramer JM, Frost JA, Bolton FJ, Wareing DR.** 2000. *Campylobacter* contamination of raw meat and poultry at retail sale: identification of multiple types and comparison with isolates from human infection. Journal of food protection **63:**1654-1659.

49.   **Nichols GL, Richardson JF, Sheppard SK, Lane C, Sarran C.** 2012. *Campylobacter* epidemiology: a descriptive study reviewing 1 million cases in England and Wales between 1989 and 2011. BMJ open **2**.

50.   **Nachamkin I, Allos BM, Ho T.** 1998. *Campylobacter* species and Guillain-Barre syndrome. Clinical microbiology reviews **11:**555-567.

51.   **McCarthy N, Giesecke J.** 2001. Incidence of Guillain-Barre syndrome following infection with *Campylobacter jejuni*. American journal of epidemiology **153:**610-614.

52.   **Salloway S, Mermel LA, Seamans M, Aspinall GO, Nam Shin JE, Kurjanczyk LA, Penner JL.** 1996. Miller-Fisher syndrome associated with *Campylobacter jejuni* bearing lipopolysaccharide molecules that mimic human ganglioside GD3. Infect Immun **64:**2945-2949.

53. **Ang CW, De Klerk MA, Endtz HP, Jacobs BC, Laman JD, van der Meche FG, van Doorn PA.** 2001. Guillain-Barre syndrome- and Miller Fisher syndrome-associated *Campylobacter jejuni* lipopolysaccharides induce anti-GM1 and anti-GQ1b Antibodies in rabbits. Infect Immun **69:**2462-2469.

54. **Mishu B, Blaser MJ.** 1993. Role of infection due to *Campylobacter jejuni* in the initiation of Guillain-Barre syndrome. Clinical infectious diseases : an official publication of the Infectious Diseases Society of America **17:**104-108.

55. **Griggs DJ, Johnson MM, Frost JA, Humphrey T, Jorgensen F, Piddock LJ.** 2005. Incidence and mechanism of ciprofloxacin resistance in *Campylobacter spp.* isolated from commercial poultry flocks in the United Kingdom before, during, and after fluoroquinolone treatment. Antimicrob Agents Chemother **49:**699-707.

56. **Luangtongkum T, Jeon B, Han J, Plummer P, Logue CM, Zhang Q.** 2009. Antibiotic resistance in *Campylobacter:* emergence, transmission and persistence. Future microbiology **4:**189-200.

57. **Monteiro MA, Baqar S, Hall ER, Chen YH, Porter CK, Bentzel DE, Applebee L, Guerry P.** 2009. Capsule polysaccharide conjugate vaccine against diarrheal disease caused by *Campylobacter jejuni*. Infect Immun **77:**1128-1136.

58. **Guerry P, Poly F, Riddle M, Maue AC, Chen YH, Monteiro MA.** 2012. Campylobacter polysaccharide capsules: virulence and vaccines. Frontiers in cellular and infection microbiology **2:**7.

59. **Cawthraw SA, Feldman RA, Sayers AR, Newell DG.** 2002. Long-term antibody responses following human infection with *Campylobacter jejuni*. Clinical and experimental immunology **130:**101-106.

60. **Havelaar AH, van Pelt W, Ang CW, Wagenaar JA, van Putten JP, Gross U, Newell DG.** 2009. Immunity to *Campylobacter*: its role in risk assessment and epidemiology. Critical reviews in microbiology **35:**1-22.

61. **Jacobs BC, Endtz HP, van der Meche FG, Hazenberg MP, de Klerk MA, van Doorn PA.** 1997. Humoral immune response against *Campylobacter jejuni* lipopolysaccharides in Guillain-Barre and Miller Fisher syndrome. Journal of neuroimmunology **79:**62-68.

62. **Linton D, Gilbert M, Hitchen PG, Dell A, Morris HR, Wakarchuk WW, Gregson NA, Wren BW.** 2000. Phase variation of a beta-1,3

galactosyltransferase involved in generation of the ganglioside GM1-like lipo-oligosaccharide of *Campylobacter jejuni*. Mol Microbiol **37:**501-514.

63.   **Mendz GL, Smith MA, Finel M, Korolik V.** 2000. Characteristics of the aerobic respiratory chains of the microaerophiles *Campylobacter jejuni* and *Helicobacter pylori*. Arch Microbiol **174:**1-10.

64.   **Hofreuter D.** 2014. Defining the metabolic requirements for the growth and colonization capacity of *Campylobacter jejuni*. Frontiers in cellular and infection microbiology **4:**137.

65.   **Myers JD, Kelly DJ.** 2005. A sulphite respiration system in the chemoheterotrophic human pathogen *Campylobacter jejuni*. Microbiology **151:**233-242.

66.   **Stahl M, Butcher J, Stintzi A.** 2012. Nutrient acquisition and metabolism by *Campylobacter jejuni*. Frontiers in cellular and infection microbiology **2:**5.

67.   **Barnes IH, Bagnall MC, Browning DD, Thompson SA, Manning G, Newell DG.** 2007. Gamma-glutamyl transpeptidase has a role in the persistent colonization of the avian gut by *Campylobacter jejuni*. Microb Pathog **43:**198-207.

68.   **Lin AE, Krastel K, Hobb RI, Thompson SA, Cvitkovitch DG, Gaynor EC.** 2009. Atypical Roles for *Campylobacter jejuni* Amino Acid ATP Binding Cassette Transporter Components PaqP and PaqQ in Bacterial Stress Tolerance and Pathogen-Host Cell Dynamics. Infect Immun **77:**4912-4924.

69.   **Hartley-Tassell LE, Shewell LK, Day CJ, Wilson JC, Sandhu R, Ketley JM, Korolik V.** 2010. Identification and characterization of the aspartate chemosensory receptor of *Campylobacter jejuni*. Mol Microbiol **75:**710-730.

70.   **Lertsethtakarn P, Ottemann KM, Hendrixson DR.** 2011. Motility and chemotaxis in *Campylobacter* and *Helicobacter*. Annu Rev Microbiol **65:**389-410.

71.   **Rahman H, King RM, Shewell LK, Semchenko EA, Hartley-Tassell LE, Wilson JC, Day CJ, Korolik V.** 2014. Characterisation of a multi-ligand binding chemoreceptor CcmL (Tlp3) of *Campylobacter jejuni*. PLoS Pathog **10:**e1003822.

72.   **Guerry P.** 2007. *Campylobacter* flagella: not just for motility. Trends in microbiology **15:**456-461.

73. **Svensson SL, Pryjma M, Gaynor EC.** 2014. Flagella-mediated adhesion and extracellular DNA release contribute to biofilm formation and stress tolerance of *Campylobacter jejuni*. PloS one **9:**e106063.

74. **Samuelson DR, Eucker TP, Bell JA, Dybas L, Mansfield LS, Konkel ME.** 2013. The *Campylobacter jejuni* CiaD effector protein activates MAP kinase signaling pathways and is required for the development of disease. Cell communication and signaling : CCS **11:**79.

75. **Joslin SN, Hendrixson DR.** 2009. Activation of the *Campylobacter jejuni* FlgSR two-component system is linked to the flagellar export apparatus. J Bacteriol **191:**2656-2667.

76. **Wassenaar TM, Bleumink-Pluym NM, Newell DG, Nuijten PJ, van der Zeijst BA.** 1994. Differential flagellin expression in a flaA flaB+ mutant of *Campylobacter jejuni*. Infect Immun **62:**3901-3906.

77. **Reuter M, van Vliet AH.** 2013. Signal balancing by the CetABC and CetZ chemoreceptors controls energy taxis in *Campylobacter jejuni*. PloS one **8:**e54390.

78. **Elliott KT, Dirita VJ.** 2008. Characterization of CetA and CetB, a bipartite energy taxis system in *Campylobacter jejuni*. Mol Microbiol **69:**1091-1103.

79. **Hendrixson DR, DiRita VJ.** 2003. Transcription of σ54-dependent but not σ28-dependent flagellar genes in *Campylobacter jejuni* is associated with formation of the flagellar secretory apparatus. Mol Microbiol **50:**687-702.

80. **Park SF, Purdy D, Leach S.** 2000. Localized reversible frameshift mutation in the flhA gene confers phase variability to flagellin gene expression in *Campylobacter coli*. J Bacteriol **182:**207-210.

81. **Vijayakumar S, Merkx-Jacques A, Ratnayake DB, Gryski I, Obhi RK, Houle S, Dozois CM, Creuzenet C.** 2006. Cj1121c, a novel UDP-4-keto-6-deoxy-GlcNAc C-4 aminotransferase essential for protein glycosylation and virulence in *Campylobacter jejuni*. J Biol Chem **281:**27733-27743.

82. **Guerry P, Ewing CP, Schirm M, Lorenzo M, Kelly J, Pattarini D, Majam G, Thibault P, Logan S.** 2006. Changes in flagellin glycosylation affect *Campylobacter* autoagglutination and virulence. Mol Microbiol **60:**299-311.

83. **McNally DJ, Hui JP, Aubry AJ, Mui KK, Guerry P, Brisson JR, Logan SM, Soo EC.** 2006. Functional characterization of the flagellar glycosylation locus in *Campylobacter jejuni* 81-176 using a focused metabolomics approach. J Biol Chem **281:**18489-18498.

84. **Karlyshev AV, Everest P, Linton D, Cawthraw S, Newell DG, Wren BW.** 2004. The *Campylobacter jejuni* general glycosylation system is important for attachment to human epithelial cells and in the colonization of chicks. Microbiology **150:**1957-1964.

85. **Szymanski CM, St Michael F, Jarrell HC, Li JJ, Gilbert M, Larocque S, Vinogradov E, Brisson JR.** 2003. Detection of conserved N-linked glycans and phase-variable lipooligosaccharides and capsules from *Campylobacter* cells by mass spectrometry and high resolution magic angle spinning NMR spectroscopy. J Biol Chem **278:**24509-24520.

86. **Szymanski CM, Burr DH, Guerry P.** 2002. *Campylobacter* protein glycosylation affects host cell interactions. Infect Immun **70:**2242-2244.

87. **Keo T, Collins J, Kunwar P, Blaser MJ, Iovine NM.** 2011. *Campylobacter* capsule and lipooligosaccharide confer resistance to serum and cationic antimicrobials. Virulence **2:**30-40.

88. **St Michael F, Szymanski CM, Li JJ, Chan KH, Khieu NH, Larocque S, Wakarchuk WW, Brisson JR, Monteiro MA.** 2002. The structures of the lipooligosaccharide and capsule polysaccharide of *Campylobacter jejuni* genome sequenced strain NCTC 11168. Eur J Biochem **269:**5119-5136.

89. **Karlyshev AV, Champion OL, Churcher C, Brisson JR, Jarrell HC, Gilbert M, Brochu D, St Michael F, Li J, Wakarchuk WW, Goodhead I, Sanders M, Stevens K, White B, Parkhill J, Wren BW, Szymanski CM.** 2005. Analysis of *Campylobacter jejuni* capsular loci reveals multiple mechanisms for the generation of structural diversity and the ability to form complex heptoses. Mol Microbiol **55:**90-103.

90. **Guerry P, Szymanski CM, Prendergast MM, Hickey TE, Ewing CP, Pattarini DL, Moran AP.** 2002. Phase variation of *Campylobacter jejuni* 81-176 lipooligosaccharide affects ganglioside mimicry and invasiveness in vitro. Infect Immun **70:**787-793.

91. **Naito M, Frirdich E, Fields JA, Pryjma M, Li J, Cameron A, Gilbert M, Thompson SA, Gaynor EC.** 2010. Effects of sequential *Campylobacter jejuni* 81-176 lipooligosaccharide core truncations on biofilm formation, stress survival, and pathogenesis. J Bacteriol **192:**2182-2192.

92. **Papp-Szabo E, Kanipes MI, Guerry P, Monteiro MA.** 2005. Cell-surface alpha-glucan in *Campylobacter jejuni* 81-176. Carbohyd Res **340:**2218-2221.

93. **Jones MA, Marston KL, Woodall CA, Maskell DJ, Linton D, Karlyshev AV, Dorrell N, Wren BW, Barrow PA.** 2004. Adaptation of *Campylobacter jejuni* NCTC11168 to high-level colonization of the avian gastrointestinal tract. Infect Immun **72:**3769-3776.

94. **Woodall CA, Jones MA, Barrow PA, Hinds J, Marsden GL, Kelly DJ, Dorrell N, Wren BW, Maskell DJ.** 2005. Campylobacter jejuni gene expression in the chick cecum: evidence for adaptation to a low-oxygen environment. Infect Immun **73:**5278-5285.

95. **Stahl M, Ries J, Vermeulen J, Yang H, Sham HP, Crowley SM, Badayeva Y, Turvey SE, Gaynor EC, Li X, Vallance BA.** 2014. A novel mouse model of *Campylobacter jejuni* gastroenteritis reveals key pro-inflammatory and tissue protective roles for Toll-like receptor signaling during infection. PLoS Pathog **10:**e1004264.

96. **Smith CK, Kaiser P, Rothwell L, Humphrey T, Barrow PA, Jones MA.** 2005. *Campylobacter jejuni* - Induced cytokine responses in avian cells. Infect Immun **73:**2094-2100.

97. **Konkel ME, Christensen JE, Keech AM, Monteville MR, Klena JD, Garvis SG.** 2005. Identification of a fibronectin-binding domain within the *Campylobacter jejuni* CadF protein. Mol Microbiol **57:**1022-1035.

98. **Tu QV, McGuckin MA, Mendz GL.** 2008. *Campylobacter jejuni* response to human mucin MUC2: modulation of colonization and pathogenicity determinants. Journal of medical microbiology **57:**795-802.

99. **Jin S, Song YC, Emili A, Sherman PM, Chan VL.** 2003. JlpA of *Campylobacter jejuni* interacts with surface-exposed heat shock protein 90alpha and triggers signalling pathways leading to the activation of NF-kappaB and p38 MAP kinase in epithelial cells. Cellular microbiology **5:**165-174.

100. **Jin S, Joe A, Lynett J, Hani EK, Sherman P, Chan VL.** 2001. JlpA, a novel surface-exposed lipoprotein specific to *Campylobacter jejuni,* mediates adherence to host epithelial cells. Mol Microbiol **39:**1225-1236.

101. **Gaynor EC, Naito M, Frirdich E, Fields JA, Pryjma M, Li JJ, Cameron A, Gilbert M, Thompson SA.** 2010. Effects of Sequential *Campylobacter jejuni* 81-176 Lipooligosaccharide Core Truncations on

Biofilm Formation, Stress Survival, and Pathogenesis. J Bacteriol **192:**2182-2192.

102. **Maue AC, Mohawk KL, Giles DK, Poly F, Ewing CP, Jiao Y, Lee G, Ma Z, Monteiro MA, Hill CL, Ferderber JS, Porter CK, Trent MS, Guerry P.** 2013. The polysaccharide capsule of *Campylobacter jejuni* modulates the host immune response. Infect Immun **81:**665-672.

103. **Watson RO, Galan JE.** 2008. *Campylobacter jejuni* survives within epithelial cells by avoiding delivery to lysosomes. PLoS Pathog **4:**e14.

104. **Bouwman LI, de Zoete MR, Bleumink-Pluym NM, Flavell RA, van Putten JP.** 2014. Inflammasome activation by *Campylobacter jejuni*. Journal of immunology **193:**4548-4557.

105. **Krutkiewicz A, Klimuszko D.** 2012. The viability of the genetically diverse *C. jejuni* and *C. coli* strains in the macrophage J774 cell line. Polish journal of veterinary sciences **15:**155-157.

106. **Fimlaid KA, Lindow JC, Tribble DR, Bunn JY, Maue AC, Kirkpatrick BD.** 2014. Peripheral CD4+ T Cell Cytokine Responses Following Human Challenge and Re-Challenge with *Campylobacter jejuni*. PloS one **9:**e112513.

107. **Malik A, Sharma D, St Charles J, Dybas LA, Mansfield LS.** 2014. Contrasting immune responses mediate *Campylobacter jejuni*-induced colitis and autoimmunity. Mucosal immunology **7:**802-817.

108. **van Alphen LB, Bleumink-Pluym NM, Rochat KD, van Balkom BW, Wosten MM, van Putten JP.** 2008. Active migration into the subcellular space precedes *Campylobacter jejuni* invasion of epithelial cells. Cellular microbiology **10:**53-66.

109. **Moreno SN, Docampo R.** 2013. Polyphosphate and its diverse functions in host cells and pathogens. PLoS Pathog **9:**e1003230.

110. **Gangaiah D, Liu Z, Arcos J, Kassem, II, Sanad Y, Torrelles JB, Rajashekara G.** 2010. Polyphosphate kinase 2: a novel determinant of stress responses and pathogenesis in *Campylobacter jejuni*. PloS one **5:**e12142.

111. **Weerakoon DR, Borden NJ, Goodson CM, Grimes J, Olson JW.** 2009. The role of respiratory donor enzymes in *Campylobacter jejuni* host colonization and physiology. Microb Pathogenesis **47:**8-15.

112. **Heimesaat MM, Alutis M, Grundmann U, Fischer A, Tegtmeyer N, Bohm M, Kuhl AA, Gobel UB, Backert S, Bereswill S.** 2014. The role of serine protease HtrA in acute ulcerative enterocolitis and extra-intestinal immune responses during *Campylobacter jejuni* infection of gnotobiotic IL-10 deficient mice. Frontiers in cellular and infection microbiology **4:**77.

113. **Alter T, Scherer K.** 2006. Stress response of *Campylobacter spp.* and its role in food processing. J Vet Med B **53:**351-357.

114. **Murphy C, Carroll C, Jordan KN.** 2006. Environmental survival mechanisms of the foodborne pathogen *Campylobacter jejuni*. J Appl Microbiol **100:**623-632.

115. **Park S.** 2005. *Campylobacter jejuni* stress responses during survival in the food chain and colonisation. *In* J.M. Ketley and M.E. Konkel (ed.), *Campylobacter jejuni:* Molecular and cellular biology. Horizon Scientific Press, New York, USA.**:**pp. 311-330.

116. **Park SF.** 2002. The physiology of *Campylobacter* species and its relevance to their role as foodborne pathogens. Int J Food Microbiol **74:**177-188.

117. **Gaynor EC, Wells DH, MacKichan JK, Falkow S.** 2005. The *Campylobacter jejuni* stringent response controls specific stress survival and virulence-associated phenotypes. Mol Microbiol **56:**8-27.

118. **Potrykus K, Cashel M.** 2008. (p)ppGpp: still magical? Annu Rev Microbiol **62:**35-51.

119. **Kuroda A, Murphy H, Cashel M, Kornberg A.** 1997. Guanosine tetra- and pentaphosphate promote accumulation of inorganic polyphosphate in *Escherichia coli*. J Biol Chem **272:**21240-21243.

120. **Malde A, Gangaiah D, Chandrashekhar K, Pina-Mimbela R, Torrelles JB, Rajashekara G.** 2014. Functional characterization of exopolyphosphatase/guanosine pentaphosphate phosphohydrolase (PPX/GPPA) of *Campylobacter jejuni*. Virulence **5:**521-533.

121. **Candon HL, Allan BJ, Fraley CD, Gaynor EC.** 2007. Polyphosphate kinase 1 is a pathogenesis determinant in *Campylobacter jejuni*. J Bacteriol **189:**8099-8108.

122. **Kornberg A, Rao NN, Ault-Riche D.** 1999. Inorganic polyphosphate: a molecule of many functions. Annual review of biochemistry **68:**89-125.

123. **Rao NN, Gomez-Garcia MR, Kornberg A.** 2009. Inorganic polyphosphate: essential for growth and survival. Annual review of biochemistry **78:**605-647.

124. **Gangaiah D, Kassem, II, Liu Z, Rajashekara G.** 2009. Importance of polyphosphate kinase 1 for *Campylobacter jejuni* viable-but-nonculturable cell formation, natural transformation, and antimicrobial resistance. Appl Environ Microbiol **75:**7838-7849.

125. **Taveirne ME, Theriot CM, Livny J, DiRita VJ.** 2013. The complete *Campylobacter jejuni* transcriptome during colonization of a natural host determined by RNAseq. PloS one **8:**e73586.

126. **Apel D, Ellermeier J, Pryjma M, Dirita VJ, Gaynor EC.** 2012. Characterization of *Campylobacter jejuni* RacRS reveals roles in the heat shock response, motility, and maintenance of cell length homogeneity. J Bacteriol **194:**2342-2354.

127. **Andersen MT, Brondsted L, Pearson BM, Mulholland F, Parker M, Pin C, Wells JM, Ingmer H.** 2005. Diverse roles for HspR in *Campylobacter jejuni* revealed by the proteome, transcriptome and phenotypic characterization of an *hspR* mutant. Microbiol-Sgm **151:**905-915.

128. **Holmes CW, Penn CW, Lund PA.** 2010. The *hrcA* and *hspR* regulons of *Campylobacter jejuni*. Microbiol-Sgm **156:**158-166.

129. **Brondsted L, Andersen MT, Parker M, Jorgensen K, Ingmer H.** 2005. The HtrA protease of *Campylobacter jejuni* is required for heat and oxygen tolerance and for optimal interaction with human epithelial cells. Appl Environ Microbiol **71:**3205-3212.

130. **Doyle MP, Roman DJ.** 1982. Response of *Campylobacter jejuni* to Sodium-Chloride. Appl Environ Microb **43:**561-565.

131. **Fields JA, Thompson SA.** 2008. *Campylobacter jejuni* CsrA mediates oxidative stress responses, biofilm formation, and host cell invasion. J Bacteriol **190:**3411-3416.

132. **Fletcher SA, Csonka LN.** 1998. Characterization of the induction of increased thermotolerance by high osmolarity in *Salmonella*. Food Microbiol **15:**307-317.

133. **Fox EM, Raftery M, Goodchild A, Mendz GL.** 2007. *Campylobacter jejuni* response to ox-bile stress. Fems Immunol Med Mic **49:**165-172.

134. **Kilstrup M, Jacobsen S, Hammer K, Vogensen FK.** 1997. Induction of heat shock proteins DnaK, GroEL, and GroES by salt stress in *Lactococcus lactis*. Appl Environ Microb **63:**1826-1837.

135. **Kaakoush NO, Miller WG, De Reuse H, Mendz GL.** 2007. Oxygen requirement and tolerance of *Campylobacter jejuni*. Res Microbiol **158:**644-650.

136. **Imlay JA, Chin SM, Linn S.** 1988. Toxic DNA damage by hydrogen peroxide through the Fenton reaction in vivo and in vitro. Science **240:**640-642.

137. **Park S, Imlay JA.** 2003. High levels of intracellular cysteine promote oxidative DNA damage by driving the fenton reaction. J Bacteriol **185:**1942-1950.

138. **Clark RA.** 1999. Activation of the neutrophil respiratory burst oxidase. J Infect Dis **179 Suppl 2:**S309-317.

139. **Atack JM, Kelly DJ.** 2009. Oxidative stress in *Campylobacter jejuni*: responses, resistance and regulation. Future microbiology **4:**677-690.

140. **Hwang S, Kim M, Ryu S, Jeon B.** 2011. Regulation of oxidative stress response by CosR, an essential response regulator in *Campylobacter jejuni*. PloS one **6:**e22300.

141. **Oh E, Jeon B.** 2014. Role of alkyl hydroperoxide reductase (AhpC) in the biofilm formation of *Campylobacter jejuni*. PloS one **9:**e87312.

142. **Palyada K, Sun YQ, Flint A, Butcher J, Naikare H, Stintzi A.** 2009. Characterization of the oxidative stress stimulon and PerR regulon of *Campylobacter jejuni*. BMC genomics **10:**481.

143. **Woodall CA, Jones MA, Barrow PA, Hinds J, Marsden GL, Kelly DJ, Dorrell N, Wren BW, Maskell DJ.** 2005. *Campylobacter jejuni* gene expression in the chick cecum: Evidence for adaptation to a low-oxygen environment. Infect Immun **73:**5278-5285.

144. **van Vliet AH, Ketley JM, Park SF, Penn CW.** 2002. The role of iron in Campylobacter gene regulation, metabolism and oxidative stress defense. Fems Microbiol Rev **26:**173-186.

145. **Huergo LF, Rahman H, Ibrahimovic A, Day CJ, Korolik V.** 2013. *Campylobacter jejuni* Dps protein binds DNA in the presence of iron or hydrogen peroxide. J Bacteriol **195:**1970-1978.

146. **Ishikawa T, Mizunoe Y, Kawabata S, Takade A, Harada M, Wai SN, Yoshida S.** 2003. The iron-binding protein Dps confers hydrogen peroxide stress resistance to *Campylobacter jejuni*. J Bacteriol **185:**1010-1017.

147. **Holmes K, Mulholland F, Pearson BM, Pin C, McNicholl-Kennedy J, Ketley JM, Wells JM.** 2005. *Campylobacter jejuni* gene expression in response to iron limitation and the role of Fur. Microbiology **151:**243-257.

148. **Kendall JJ, Barrero-Tobon AM, Hendrixson DR, Kelly DJ.** 2014. Hemerythrins in the microaerophilic bacterium *Campylobacter jejuni* help protect key iron-sulphur cluster enzymes from oxidative damage. Environmental microbiology **16:**1105-1121.

149. **van Vliet AH, Baillon ML, Penn CW, Ketley JM.** 1999. *Campylobacter jejuni* contains two fur homologs: characterization of iron-responsive regulation of peroxide stress defense genes by the PerR repressor. J Bacteriol **181:**6371-6376.

150. **van Vliet AH, Wooldridge KG, Ketley JM.** 1998. Iron-responsive gene regulation in a *Campylobacter jejuni fur* mutant. J Bacteriol **180:**5291-5298.

151. **Svensson SL, Davis LM, MacKichan JK, Allan BJ, Pajaniappan M, Thompson SA, Gaynor EC.** 2009. The CprS sensor kinase of the zoonotic pathogen *Campylobacter jejuni* influences biofilm formation and is required for optimal chick colonization. Mol Microbiol **71:**253-272.

152. **Csonka LN.** 1989. Physiological and Genetic Responses of Bacteria to Osmotic-Stress. Microbiol Rev **53:**121-147.

153. **Gancz H, Jones KR, Merrell DS.** 2008. Sodium chloride affects *Helicobacter pylori* growth and gene expression. J Bacteriol **190:**4100-4105.

154. **Loh JT, Torres VJ, Cover TL.** 2007. Regulation of *Helicobacter pylori* cagA expression in response to salt. Cancer Res **67:**4709-4715.

155. **Tesone S, Hughes A, Hurst A.** 1981. Salt Extends the Upper Temperature Limit for Growth of Food-Poisoning Bacteria. Can J Microbiol **27:**970-972.

156. **Faherty CS, Redman JC, Rasko DA, Barry EM, Nataro JP.** 2012. Shigella flexneri effectors OspE1 and OspE2 mediate induced adherence to the colonic epithelium following bile salts exposure. Mol Microbiol **85:**107-121.

157. **Mizusaki H, Takaya A, Yamamoto T, Aizawa S.** 2008. Signal pathway in salt-activated expression of the *Salmonella* pathogenicity island 1 type III secretion system in *Salmonella enterica serovar Typhimurium*. J Bacteriol **190:**4624-4631.

158. **Raphael BH, Pereira S, Flom GA, Zhang QJ, Ketley JM, Konkel ME.** 2005. The *Campylobacter jejuni* response regulator, CbrR, modulates sodium deoxycholate resistance and chicken colonization. J Bacteriol **187:**3662-3670.

159. **Reezal A, McNeil B, Anderson JG.** 1998. Effect of low-osmolality nutrient media on growth and culturability of *Campylobacter* species. Appl Environ Microb **64:**4643-4649.

160. **Glunder G.** 1994. Antigenic Changes in *Campylobacter Spp* after Adaptation to Media with Increased Sodium-Chloride Concentrations. Berl Munch Tierarztl **107:**109-115.

161. **Fordtran JS, Locklear TW.** 1966. Ionic Constituents and Osmolality of Gastric and Small-Intestinal Fluids after Eating. Am J Dig Dis **11:**503-511.

162. **Stintzi A, Marlow D, Palyada K, Naikare H, Panciera R, Whitworth L, Clarke C.** 2005. Use of genome-wide expression profiling and mutagenesis to study the intestinal lifestyle of *Campylobacter jejuni*. Infect Immun **73:**1797-1810.

163. **Henggearonis R, Lange R, Henneberg N, Fischer D.** 1993. Osmotic Regulation of Rpos-Dependent Genes in *Escherichia coli*. J Bacteriol **175:**259-265.

164. **Mattick KL, Jorgensen F, Legan JD, Cole MB, Porter J, Lappin-Scott HM, Humphrey TJ.** 2000. Survival and filamentation of *Salmonella enterica* serovar Enteritidis PT4 and *Salmonella enterica* serovar Typhimurium DT104 at low water activity. Appl Environ Microb **66:**1274-1279.

165. **Aspedon A, Palmer K, Whiteley M.** 2006. Microarray analysis of the osmotic stress response in *Pseudomonas aeruginosa*. J Bacteriol **188:**2721-2725.

166. **Mclaggan D, Logan TM, Lynn DG, Epstein W.** 1990. Involvement of Gamma-Glutamyl Peptides in Osmoadaptation of *Escherichia coli*. J Bacteriol **172:**3631-3636.

167. **Rodriguez MB, Moyses LHC, Costa SOP.** 1990. Effect of Osmolarity on Aminoglycoside Susceptibility in Gram-Negative Bacteria. Lett Appl Microbiol **11:**77-80.

168. **Klasing KC, Adler KL, Remus JC, Calvert CC.** 2002. Dietary betaine increases intraepithelial lymphocytes in the duodenum of coccidia-infected chicks and increases functional properties of phagocytes. J Nutr **132:**2274-2282.

169. **Kempf B, Bremer E.** 1998. Uptake and synthesis of compatible solutes as microbial stress responses to high-osmolality environments. Arch Microbiol **170:**319-330.

170. **Mclaggan D, Naprstek J, Buurman ET, Epstein W.** 1994. Interdependence of K+ and Glutamate Accumulation during Osmotic Adaptation of *Escherichia coli*. J Biol Chem **269:**1911-1917.

171. **Sleator RD, Hill C.** 2002. Bacterial osmoadaptation: the role of osmolytes in bacterial stress and virulence. Fems Microbiol Rev **26:**49-71.

172. **Wood JM.** 1999. Osmosensing by bacteria: Signals and membrane-based sensors. Microbiol Mol Biol R **63:**230-267.

173. **Dubnau D, Losick R.** 2006. Bistability in bacteria. Mol Microbiol **61:**564-572.

174. **Graumann PL.** 2006. Different genetic programmes within identical bacteria under identical conditions: the phenomenon of bistability greatly modifies our view on bacterial populations. Mol Microbiol **61:**560-563.

175. **Veening JW, Smits WK, Kuipers OP.** 2008. Bistability, Epigenetics, and Bet-Hedging in Bacteria. Annual Review of Microbiology **62:**193-210.

176. **Guo BQ, Wang Y, Shi F, Barton YW, Plummer P, Reynolds DL, Nettleton D, Grinnage-Pulley T, Lin J, Zhang QJ.** 2008. CmeR functions as a pleiotropic regulator and is required for optimal colonization of *Campylobacter jejuni* in vivo. J Bacteriol **190:**1879-1890.

177. **Lin J, Michel LO, Zhang QJ.** 2002. CmeABC functions as a multidrug efflux system in *Campylobacter jejuni*. Antimicrob Agents Ch **46:**2124-2131.

178. **Pavlidis P, Noble WS.** 2003. Matrix2png: a utility for visualizing matrix data. Bioinformatics **19:**295-296.

179. **Schneider CA, Rasband WS, Eliceiri KW.** 2012. NIH Image to ImageJ: 25 years of image analysis. Nature methods **9:**671-675.

180. **Malik-Kale P, Raphael BH, Parker CT, Joens LA, Klena JD, Quinones B, Keech AM, Konkel ME.** 2007. Characterization of genetically matched isolates of *Campylobacter jejuni* reveals that mutations in genes involved in flagellar biosynthesis alter the organism's virulence potential. Appl Environ Microb **73:**3123-3136.

181. **Ritz M, Garenaux A, Berge M, Federighi M.** 2009. Determination of *rpoA* as the most suitable internal control to study stress response in *C. jejuni* by RT-qPCR and application to oxidative stress. J Microbiol Meth **76:**196-200.

182. **Wosten MMSM, Boeve M, Koot MGA, van Nuenen AC, van der Zeijst BAM.** 1998. Identification of *Campylobacter jejuni* promoter sequences. J Bacteriol **180:**594-599.

183. **Cools I, Uyttendaele M, Caro C, D'Haese E, Nelis HJ, Debevere J.** 2003. Survival of *Campylobacter jejuni* strains of different origin in drinking water. J Appl Microbiol **94:**886-892.

184. **Tholozan JL, Cappelier JM, Tissier JP, Delattre G, Federighi M.** 1999. Physiological characterization of viable-but-nonculturable *Campylobacter jejuni* cells. Appl Environ Microb **65:**1110-1116.

185. **Boulos L, Prevost M, Barbeau B, Coallier J, Desjardins R.** 1999. LIVE/DEAD BacLight : application of a new rapid staining method for direct enumeration of viable and total bacteria in drinking water. J Microbiol Meth **37:**77-86.

186. **MacKichan JK, Gaynor EC, Chang C, Cawthraw S, Newell DG, Miller JF, Falkow S.** 2004. The *Campylobacter jejuni* dccRS two-component system is required for optimal in vivo colonization but is dispensable for in vitro growth. Mol Microbiol **54:**1269-1286.

187. **Mukhopadhyay A, He ZL, Alm EJ, Arkin AP, Baidoo EE, Borglin SC, Chen WQ, Hazen TC, He Q, Holman HY, Huang K, Huang R, Joyner DC, Katz N, Keller M, Oeller P, Redding A, Sun J, Wall J, Wei J, Yang ZM, Yen HC, Zhou JZ, Keasling JD.** 2006. Salt stress in *Desulfovibrio vulgaris* Hildenborough: An integrated genomics a pproach. J Bacteriol **188:**4068-4078.

188. **Das G, Varshney U.** 2006. Peptidyl-tRNA hydrolase and its critical role in protein biosynthesis. Microbiol-Sgm **152:**2191-2195.

189. **Gunasekera TS, Csonka LN, Paliy O.** 2008. Genome-wide transcriptional responses of *Escherichia coli* K-12 to continuous osmotic and heat stresses. J Bacteriol **190:**3712-3720.

190. **Deuerling E, Mogk A, Richter C, Purucker M, Schumann W.** 1997. The ftsH gene of *Bacillus subtilis* is involved in major cellular processes such as sporulation, stress adaptation and secretion. Mol Microbiol **23:**921-933.

191. **Justice SS, Hunstad DA, Cegelski L, Hultgren SJ.** 2008. Morphological plasticity as a bacterial survival strategy. Nat Rev Microbiol **6:**162-168.

192. **Horwich AL, Low KB, Fenton WA, Hirshfield IN, Furtak K.** 1993. Folding in-Vivo of Bacterial Cytoplasmic Proteins - Role of GroEL. Cell **74:**909-917.

193. **Masters M, Blakely G, Coulson A, McLennan N, Yerko V, Acord J.** 2009. Protein folding in *Escherichia coli*: the chaperonin GroE and its substrates. Res Microbiol **160:**267-277.

194. **McLennan N, Masters M.** 1998. GroE is vital for cell-wall synthesis. Nature **392:**139-139.

195. **Schoemaker JM, Gayda RC, Markovitz A.** 1984. Regulation of Cell-Division in *Escherichia coli* - SOS Induction and Cellular Location of the SulA Protein, a Key to Lon-Associated Filamentation and Death. J Bacteriol **158:**551-561.

196. **Walker JR, Kovarik A, Allen JS, Gustafson RA.** 1975. Regulation of Bacterial-Cell Division - Temperature-Sensitive Mutants of *Escherichia coli* That Are Defective in Septum Formation. J Bacteriol **123:**693-703.

197. **Justice SS, Hung C, Theriot JA, Fletcher DA, Anderson GG, Footer MJ, Hultgren SJ.** 2004. Differentiation and developmental pathways of uropathogenic *Escherichia coli* in urinary tract pathogenesis. P Natl Acad Sci USA **101:**1333-1338.

198. **Wortinger MA, Quardokus EM, Brun YV.** 1998. Morphological adaptation and inhibition of cell division during stationary phase in *Caulobacter crescentus*. Mol Microbiol **29:**963-973.

199. **Spohn G, Scarlato V.** 1999. The autoregulatory HspR repressor protein governs chaperone gene transcription in *Helicobacter pylori*. Mol Microbiol **34:**663-674.

200. **Konkel ME, Kim BJ, Klena JD, Young CR, Ziprin R.** 1998. Characterization of the thermal stress response of *Campylobacter jejuni.* Infect Immun **66:**3666-3672.

201. **Karlyshev AV, McCrossan MV, Wren BW.** 2001. Demonstration of polysaccharide capsule in *Campylobacter jejuni* using electron microscopy. Infect Immun **69:**5921-5924.

202. **Sledjeski DD, Gottesman S.** 1996. Osmotic shock induction of capsule synthesis in *Escherichia coli* K-12. J Bacteriol **178:**1204-1206.

203. **Wai SN, Mizunoe Y, Takade A, Kawabata S, Yoshida S.** 1998. *Vibrio cholerae* O1 strain TSI-4 produces the exopolysaccharide materials that determine colony morphology, stress resistance, and biofilm formation. Appl Environ Microb **64:**3648-3655.

204. **Ingham CJ, Beerthuyzen M, Vlieg JV.** 2008. Population Heterogeneity of *Lactobacillus plantarum* WCFS1 Microcolonies in Response to and Recovery from Acid Stress. Appl Environ Microb **74:**7750-7758.

205. **Moyed HS, Bertrand KP.** 1983. HipA, a Newly Recognized Gene of *Escherichia coli* K-12 That Affects Frequency of Persistence after Inhibition of Murein Synthesis. J Bacteriol **155:**768-775.

206. **Hendrixson DR.** 2006. A phase-variable mechanism controlling the Campylobacter jejuni FlgR response regulator influences commensalism. Molecular microbiology **61:**1646-1659.

207. **Hitchen P, Brzostek J, Panico M, Butler JA, Morris HR, Dell A, Linton D.** 2010. Modification of the *Campylobacter jejuni* flagellin glycan by the product of the Cj1295 homopolymeric-tract-containing gene. Microbiology **156:**1953-1962.

208. **Bacon DJ, Szymanski CM, Burr DH, Silver RP, Alm RA, Guerry P.** 2001. A phase-variable capsule is involved in virulence of Campylobacter jejuni 81-176. Molecular microbiology **40:**769-777.

209. **van der Woude MW, Baumler AJ.** 2004. Phase and antigenic variation in bacteria. Clinical microbiology reviews **17:**581-611, table of contents.

210. **Blaser MJ.** 1997. Epidemiologic and clinical features of Campylobacter jejuni infections. The Journal of infectious diseases **176 Suppl 2:**S103-105.

211. **Ambur OH, Davidsen T, Frye SA, Balasingham SV, Lagesen K, Rognes T, Tonjum T.** 2009. Genome dynamics in major bacterial pathogens. Fems Microbiol Rev **33:**453-470.

212. **Mohawk KL, Poly F, Sahl JW, Rasko DA, Guerry P.** 2014. High frequency, spontaneous *motA* mutations in *Campylobacter jejuni* strain 81-176. PloS one **9:**e88043.

213. **Candon HL, Allan BJ, Fraley CD, Gaynor EC.** 2007. Polyphosphate kinase 1 is a pathogenesis determinant in Campylobacter jejuni. Journal of bacteriology **189:**8099-8108.

214. **Davis L, Young K, DiRita V.** 2008. Genetic manipulation of *Campylobacter jejuni*. Current protocols in microbiology **Chapter 8:**Unit 8A 2 1-8A 2 17.

215. **Kyle JL, Cummings CA, Parker CT, Quinones B, Vatta P, Newton E, Huynh S, Swimley M, Degoricija L, Barker M, Fontanoz S, Nguyen K, Patel R, Fang R, Tebbs R, Petrauskene O, Furtado M, Mandrell RE.** 2012. Escherichia coli serotype O55:H7 diversity supports parallel acquisition of bacteriophage at Shiga toxin phage insertion sites during evolution of the O157:H7 lineage. J Bacteriol **194:**1885-1896.

216. **Mittler G, Butter F, Mann M.** 2009. A SILAC-based DNA protein interaction screen that identifies candidate binding proteins to functional DNA elements. Genome research **19:**284-293.

217. **Cox J, Mann M.** 2008. MaxQuant enables high peptide identification rates, individualized p.p.b.-range mass accuracies and proteome-wide protein quantification. Nat Biotechnol **26:**1367-1372.

218. **Gaynor EC, Cawthraw S, Manning G, MacKichan JK, Falkow S, Newell DG.** 2004. The genome-sequenced variant of Campylobacter jejuni NCTC 11168 and the original clonal clinical isolate differ markedly in colonization, gene expression, and virulence-associated phenotypes. Journal of bacteriology **186:**503-517.

219. **Pang B, McFaline JL, Burgis NE, Dong M, Taghizadeh K, Sullivan MR, Elmquist CE, Cunningham RP, Dedon PC.** 2012. Defects in purine nucleotide metabolism lead to substantial incorporation of xanthine and hypoxanthine into DNA and RNA. Proc Natl Acad Sci U S A **109:**2319-2324.

220. **Hove-Jensen B.** 1988. Mutation in the phosphoribosylpyrophosphate synthetase gene (prs) that results in simultaneous requirements for

purine and pyrimidine nucleosides, nicotinamide nucleotide, histidine, and tryptophan in *Escherichia coli*. J Bacteriol **170:**1148-1152.

221. **Ames BN, Martin RG, Garry BJ.** 1961. The first step of histidine biosynthesis. J Biol Chem **236:**2019-2026.

222. **Galperin MY, Koonin EV.** 1997. Sequence analysis of an exceptionally conserved operon suggests enzymes for a new link between histidine and purine biosynthesis. Mol Microbiol **24:**443-445.

223. **Lieberman I, Kornberg A, Simms ES.** 1955. Enzymatic synthesis of pyrimidine nucleotides; orotidine-5'-phosphate and uridine-5'-phosphate. J Biol Chem **215:**403-451.

224. **Liechti G, Goldberg JB.** 2012. *Helicobacter pylori* relies primarily on the purine salvage pathway for purine nucleotide biosynthesis. J Bacteriol **194:**839-854.

225. **Keer J, Smeulders MJ, Williams HD.** 2001. A *purF* mutant of *Mycobacterium smegmatis* has impaired survival during oxygen-starved stationary phase. Microbiology **147:**473-481.

226. **Freese E, Heinze JE, Galliers EM.** 1979. Partial purine deprivation causes sporulation of *Bacillus subtilis* in the presence of excess ammonia, glucose and phosphate. Journal of general microbiology **115:**193-205.

227. **Bacon GA, Burrows TW, Yates M.** 1951. The effects of biochemical mutation on the virulence of *Bacterium typhosum*; the loss of virulence of certain mutants. British journal of experimental pathology **32:**85-96.

228. **Buchmeier NA, Libby SJ.** 1997. Dynamics of growth and death within a *Salmonella typhimurium* population during infection of macrophages. Can J Microbiol **43:**29-34.

229. **Chiang SL, Mekalanos JJ.** 1998. Use of signature-tagged transposon mutagenesis to identify *Vibrio cholerae* genes critical for colonization. Mol Microbiol **27:**797-805.

230. **Pechous R, Celli J, Penoske R, Hayes SF, Frank DW, Zahrt TC.** 2006. Construction and characterization of an attenuated purine auxotroph in a *Francisella tularensis* live vaccine strain. Infect Immun **74:**4452-4461.

231. **Faith NG, Kim JW, Azizoglu R, Kathariou S, Czuprynski C.** 2012. Purine biosynthesis mutants (purA and purB) of serotype 4b *Listeria monocytogenes* are severely attenuated for systemic infection in

intragastrically inoculated A/J Mice. Foodborne pathogens and disease **9:**480-486.

232. **Cersini A, Martino MC, Martini I, Rossi G, Bernardini ML.** 2003. Analysis of virulence and inflammatory potential of *Shigella flexneri* purine biosynthesis mutants. Infect Immun **71:**7002-7013.

233. **Ault-Riche D, Fraley CD, Tzeng CM, Kornberg A.** 1998. Novel assay reveals multiple pathways regulating stress-induced accumulations of inorganic polyphosphate in *Escherichia coli*. J Bacteriol **180:**1841-1847.

234. **Jung S, A Lee M-S, A Kim S-K, A Wanner B.** 2012. Effect of purine limitation caused by an amidophosphoribosyl transferase (purF) mutation on polyphosphate kinase 1 (ppk1) gene expression. Genes & Genomics **34:**27-34.

235. **Rallu F, Gruss A, Ehrlich SD, Maguin E.** 2000. Acid- and multistress-resistant mutants of *Lactococcus lactis* : identification of intracellular stress signals. Mol Microbiol **35:**517-528.

236. **Raphael BH, Pereira S, Flom GA, Zhang Q, Ketley JM, Konkel ME.** 2005. The Campylobacter jejuni response regulator, CbrR, modulates sodium deoxycholate resistance and chicken colonization. Journal of bacteriology **187:**3662-3670.

237. **Garavaglia M, Rossi E, Landini P.** 2012. The pyrimidine nucleotide biosynthetic pathway modulates production of biofilm determinants in *Escherichia coli*. PloS one **7:**e31252.

238. **Young KT, Davis LM, Dirita VJ.** 2007. Campylobacter jejuni: molecular biology and pathogenesis. Nature reviews. Microbiology **5:**665-679.

239. **Cools I, Uyttendaele M, Caro C, D'Haese E, Nelis HJ, Debevere J.** 2003. Survival of Campylobacter jejuni strains of different origin in drinking water. Journal of applied microbiology **94:**886-892.

240. **Chynoweth RW, Hudson JA, Thom K.** 1998. Aerobic growth and survival of *Campylobacter jejuni* in food and stream water. Lett Appl Microbiol **27:**341-344.

241. **Haddad N, Burns CM, Bolla JM, Prevost H, Federighi M, Drider D, Cappelier JM.** 2009. Long-term survival of *Campylobacter jejuni* at low temperatures is dependent on polynucleotide phosphorylase activity. Appl Environ Microbiol **75:**7310-7318.

242. **Hazeleger WC, Wouters JA, Rombouts FM, Abee T.** 1998. Physiological activity of *Campylobacter jejuni* far below the minimal growth temperature. Appl Environ Microbiol **64:**3917-3922.

243. **Schaaper RM.** 1988. Mechanisms of mutagenesis in the *Escherichia coli* mutator mutD5: role of DNA mismatch repair. Proc Natl Acad Sci U S A **85:**8126-8130.

244. **Horst JP, Wu TH, Marinus MG.** 1999. *Escherichia coli* mutator genes. Trends in microbiology **7:**29-36.

245. **Park C, Qian W, Zhang J.** 2012. Genomic evidence for elevated mutation rates in highly expressed genes. EMBO reports **13:**1123-1129.

246. **Bera AK, Chen S, Smith JL, Zalkin H.** 1999. Interdomain signaling in glutamine phosphoribosylpyrophosphate amidotransferase. J Biol Chem **274:**36498-36504.

247. **Zhou G, Smith JL, Zalkin H.** 1994. Binding of purine nucleotides to two regulatory sites results in synergistic feedback inhibition of glutamine 5-phosphoribosylpyrophosphate amidotransferase. J Biol Chem **269:**6784-6789.

248. **Shimaoka M, Takenaka Y, Kurahashi O, Kawasaki H, Matsui H.** 2007. Effect of amplification of desensitized *purF* and *prs* on inosine accumulation in *Escherichia coli*. Journal of bioscience and bioengineering **103:**255-261.

249. **Zhou G, Charbonneau H, Colman RF, Zalkin H.** 1993. Identification of sites for feedback regulation of glutamine 5-phosphoribosylpyrophosphate amidotransferase by nucleotides and relationship to residues important for catalysis. J Biol Chem **268:**10471-10481.

250. **Hochstadt J.** 1978. Adenine phosphoribosyltransferase from *Escherichia coli*. Methods in enzymology **51:**558-567.

251. **Sin IL, Finch LR.** 1972. Adenine phosphoribosyltransferase in *Mycoplasma mycoides* and *Escherichia coli*. J Bacteriol **112:**439-444.

252. **Hochstadt-Ozer J, Stadtman ER.** 1971. The regulation of purine utilization in bacteria. I. Purification of adenine phosphoribosyltransferase from *Escherichia coli* K12 and control of activity by nucleotides. J Biol Chem **246:**5294-5303.

253.	**Davidson CJ, Surette MG.** 2008. Individuality in bacteria. Annual review of genetics **42:**253-268.

254.	**Denamur E, Matic I.** 2006. Evolution of mutation rates in bacteria. Mol Microbiol **60:**820-827.

255.	**Bae J, Jeon B.** 2013. Increased emergence of fluoroquinolone-resistant *Campylobacter jejuni* in biofilms. Antimicrob Agents Chemother **57:**5195-5196.

256.	**Hanninen ML, Hannula M.** 2007. Spontaneous mutation frequency and emergence of ciprofloxacin resistance in *Campylobacter jejuni* and *Campylobacter coli*. The Journal of antimicrobial chemotherapy **60:**1251-1257.

257.	**Bayliss CD, Bidmos FA, Anjum A, Manchev VT, Richards RL, Grossier JP, Wooldridge KG, Ketley JM, Barrow PA, Jones MA, Tretyakov MV.** 2012. Phase variable genes of *Campylobacter jejuni* exhibit high mutation rates and specific mutational patterns but mutability is not the major determinant of population structure during host colonization. Nucleic Acids Res **40:**5876-5889.

258.	**Martincorena I, Seshasayee AS, Luscombe NM.** 2012. Evidence of non-random mutation rates suggests an evolutionary risk management strategy. Nature **485:**95-98.

259.	**Han J, Sahin O, Barton YW, Zhang Q.** 2008. Key role of Mfd in the development of fluoroquinolone resistance in *Campylobacter jejuni*. PLoS Pathog **4:**e1000083.

260.	**de Jong IG, Haccou P, Kuipers OP.** 2011. Bet hedging or not? A guide to proper classification of microbial survival strategies. BioEssays : news and reviews in molecular, cellular and developmental biology **33:**215-223.

261.	**Dubnau D, Losick R.** 2006. Bistability in bacteria. Molecular microbiology **61:**564-572.

262.	**Veening JW, Smits WK, Kuipers OP.** 2008. Bistability, epigenetics, and bet-hedging in bacteria. Annual review of microbiology **62:**193-210.

263.	**Thomas DK, Lone AG, Selinger LB, Taboada EN, Uwiera RR, Abbott DW, Inglis GD.** 2014. Comparative variation within the genome of *Campylobacter jejuni* NCTC 11168 in human and murine hosts. PloS one **9:**e88229.

264. **Jerome JP, Bell JA, Plovanich-Jones AE, Barrick JE, Brown CT, Mansfield LS.** 2011. Standing genetic variation in contingency loci drives the rapid adaptation of *Campylobacter jejuni* to a novel host. PloS one **6:**e16399.

265. **Holmes EC, Moya A.** 2002. Is the quasispecies concept relevant to RNA viruses? Journal of virology **76:**460-465.

266. **Biebricher CK, Eigen M.** 2006. What is a quasispecies? Current topics in microbiology and immunology **299:**1-31.

267. **Park SF.** 2002. The physiology of *Campylobacter* species and its relevance to their role as foodborne pathogens. International journal of food microbiology **74:**177-188.

268. **Reuter M, Mallett A, Pearson BM, van Vliet AH.** 2010. Biofilm formation by *Campylobacter jejuni* is increased under aerobic conditions. Appl Environ Microbiol **76:**2122-2128.

269. **Joshua GW, Guthrie-Irons C, Karlyshev AV, Wren BW.** 2006. Biofilm formation in *Campylobacter jejuni*. Microbiology **152:**387-396.

270. **Haddock G, Mullin M, MacCallum A, Sherry A, Tetley L, Watson E, Dagleish M, Smith DG, Everest P.** 2010. *Campylobacter jejuni* 81-176 forms distinct microcolonies on in vitro-infected human small intestinal tissue prior to biofilm formation. Microbiology **156:**3079-3084.

271. **Costerton JW, Stewart PS, Greenberg EP.** 1999. Bacterial biofilms: a common cause of persistent infections. Science **284:**1318-1322.

272. **Chang WS, van de Mortel M, Nielsen L, Nino de Guzman G, Li X, Halverson LJ.** 2007. Alginate production by *Pseudomonas putida* creates a hydrated microenvironment and contributes to biofilm architecture and stress tolerance under water-limiting conditions. J Bacteriol **189:**8290-8299.

273. **Matz C, McDougald D, Moreno AM, Yung PY, Yildiz FH, Kjelleberg S.** 2005. Biofilm formation and phenotypic variation enhance predation-driven persistence of *Vibrio cholerae*. Proc Natl Acad Sci U S A **102:**16819-16824.

274. **Elasri MO, Miller RV.** 1999. Study of the response of a biofilm bacterial community to UV radiation. Appl Environ Microbiol **65:**2025-2031.

275. **Flemming HC, Wingender J.** 2010. The biofilm matrix. Nat Rev Microbiol **8:**623-633.

276. **Tran CS, Rangel SM, Almblad H, Kierbel A, Givskov M, Tolker-Nielsen T, Hauser AR, Engel JN.** 2014. The *Pseudomonas aeruginosa* Type III Translocon Is Required for Biofilm Formation at the Epithelial Barrier. PLoS Pathog **10:**e1004479.

277. **Johnson TL, Fong JC, Rule C, Rogers A, Yildiz FH, Sandkvist M.** 2014. The Type II Secretion System Delivers Matrix Proteins for Biofilm Formation by *Vibrio cholerae*. J Bacteriol **196:**4245-4252.

278. **Berry AA, Yang Y, Pakharukova N, Garnett JA, Lee WC, Cota E, Marchant J, Roy S, Tuittila M, Liu B, Inman KG, Ruiz-Perez F, Mandomando I, Nataro JP, Zavialov AV, Matthews S.** 2014. Structural insight into host recognition by aggregative adherence fimbriae of enteroaggregative *Escherichia coli*. PLoS Pathog **10:**e1004404.

279. **Wan Z, Brown PJ, Elliott EN, Brun YV.** 2013. The adhesive and cohesive properties of a bacterial polysaccharide adhesin are modulated by a deacetylase. Mol Microbiol **88:**486-500.

280. **O'Toole G, Kaplan HB, Kolter R.** 2000. Biofilm formation as microbial development. Annu Rev Microbiol **54:**49-79.

281. **Stoodley P, Sauer K, Davies DG, Costerton JW.** 2002. Biofilms as complex differentiated communities. Annu Rev Microbiol **56:**187-209.

282. **Costerton JW, Lewandowski Z, Caldwell DE, Korber DR, Lappin-Scott HM.** 1995. Microbial biofilms. Annu Rev Microbiol **49:**711-745.

283. **Svensson SL, Davis LM, MacKichan JK, Allan BJ, Pajaniappan M, Thompson SA, Gaynor EC.** 2009. The CprS sensor kinase of the zoonotic pathogen Campylobacter jejuni influences biofilm formation and is required for optimal chick colonization. Molecular microbiology **71:**253-272.

284. **Whitchurch CB, Tolker-Nielsen T, Ragas PC, Mattick JS.** 2002. Extracellular DNA required for bacterial biofilm formation. Science **295:**1487.

285. **Marks LR, Reddinger RM, Hakansson AP.** 2012. High levels of genetic recombination during nasopharyngeal carriage and biofilm formation in *Streptococcus pneumoniae*. mBio **3**.

286. **Ma L, Conover M, Lu H, Parsek MR, Bayles K, Wozniak DJ.** 2009. Assembly and development of the *Pseudomonas aeruginosa* biofilm matrix. PLoS Pathog **5:**e1000354.

287. **Thomas VC, Thurlow LR, Boyle D, Hancock LE.** 2008. Regulation of autolysis-dependent extracellular DNA release by *Enterococcus faecalis* extracellular proteases influences biofilm development. J Bacteriol **190:**5690-5698.

288. **O'Toole GA, Kolter R.** 1998. Initiation of biofilm formation in *Pseudomonas fluorescens* WCS365 proceeds via multiple, convergent signalling pathways: a genetic analysis. Mol Microbiol **28:**449-461.

289. **Yao R, Alm RA, Trust TJ, Guerry P.** 1993. Construction of new *Campylobacter* cloning vectors and a new mutational cat cassette. Gene **130:**127-130.

290. **Wiesner RS, Hendrixson DR, DiRita VJ.** 2003. Natural transformation of *Campylobacter jejuni* requires components of a type II secretion system. J Bacteriol **185:**5408-5418.

291. **Vegge CS, Brondsted L, Ligowska-Marzeta M, Ingmer H.** 2012. Natural transformation of *Campylobacter jejuni* occurs beyond limits of growth. PloS one **7:**e45467.

292. **Kreth J, Merritt J, Shi W, Qi F.** 2005. Competition and coexistence between *Streptococcus mutans* and *Streptococcus sanguinis* in the dental biofilm. J Bacteriol **187:**7193-7203.

293. **Singh PK, Parsek MR, Greenberg EP, Welsh MJ.** 2002. A component of innate immunity prevents bacterial biofilm development. Nature **417:**552-555.

294. **Brady RA, Leid JG, Camper AK, Costerton JW, Shirtliff ME.** 2006. Identification of *Staphylococcus aureus* proteins recognized by the antibody-mediated immune response to a biofilm infection. Infect Immun **74:**3415-3426.

295. **Caldwell MB, Guerry P, Lee EC, Burans JP, Walker RI.** 1985. Reversible expression of flagella in *Campylobacter jejuni*. Infect Immun **50:**941-943.

296. **Konstantinidis KT, DeLong EF.** 2008. Genomic patterns of recombination, clonal divergence and environment in marine microbial populations. The ISME journal **2:**1052-1065.

297. **Simmons SL, Dibartolo G, Denef VJ, Goltsman DS, Thelen MP, Banfield JF.** 2008. Population genomic analysis of strain variation in *Leptospirillum group II* bacteria involved in acid mine drainage formation. PLoS biology **6:**e177.

298. **Claessen D, Rozen DE, Kuipers OP, Sogaard-Andersen L, van Wezel GP.** 2014. Bacterial solutions to multicellularity: a tale of biofilms, filaments and fruiting bodies. Nat Rev Microbiol **12:**115-124.

299. **Rosenberg SM.** 2009. Life, death, differentiation, and the multicellularity of bacteria. Plos Genet **5:**e1000418.

300. **Shapiro JA.** 1998. Thinking about bacterial populations as multicellular organisms. Annu Rev Microbiol **52:**81-104.

301. **Paganelli FL, Willems RJ, Jansen P, Hendrickx A, Zhang X, Bonten MJ, Leavis HL.** 2013. *Enterococcus faecium* biofilm formation: identification of major autolysin AtlAEfm, associated Acm surface localization, and AtlAEfm-independent extracellular DNA Release. mBio **4:**e00154.

302. **Wen Y, Behiels E, Devreese B.** 2014. Toxin-Antitoxin systems: their role in persistence, biofilm formation, and pathogenicity. Pathogens and disease **70:**240-249.

303. **Kobayashi K.** 2007. *Bacillus subtilis* pellicle formation proceeds through genetically defined morphological changes. J Bacteriol **189:**4920-4931.

304. **Perez-Nunez D, Briandet R, David B, Gautier C, Renault P, Hallet B, Hols P, Carballido-Lopez R, Guedon E.** 2011. A new morphogenesis pathway in bacteria: unbalanced activity of cell wall synthesis machineries leads to coccus-to-rod transition and filamentation in ovococci. Mol Microbiol **79:**759-771.

305. **Kuhl M, Rickelt LF, Thar R.** 2007. Combined imaging of bacteria and oxygen in biofilms. Appl Environ Microbiol **73:**6289-6295.

306. **Wessel AK, Arshad TA, Fitzpatrick M, Connell JL, Bonnecaze RT, Shear JB, Whiteley M.** 2014. Oxygen limitation within a bacterial aggregate. mBio **5:**e00992.

307. **Beery JT, Hugdahl MB, Doyle MP.** 1988. Colonization of Gastrointestinal Tracts of Chicks by *Campylobacter jejuni*. Appl Environ Microb **54:**2365-2370.

308. **Bronowski C, James CE, Winstanley C.** 2014. Role of environmental survival in transmission of *Campylobacter jejuni*. FEMS microbiology letters **356:**8-19.

309. **Miller WG, Yee E, Chapman MH, Smith TP, Bono JL, Huynh S, Parker CT, Vandamme P, Luong K, Korlach J.** 2014. Comparative genomics of the *Campylobacter lari* group. Genome biology and evolution.

310. **Kivisto RI, Kovanen S, Skarp-de Haan A, Schott T, Rahkio M, Rossi M, Hanninen ML.** 2014. Evolution and comparative genomics of *Campylobacter jejuni* ST-677 clonal complex. Genome biology and evolution **6:**2424-2438.

311. **Taveirne ME, Dunham DT, Miller WG, Parker CT, Huynh S, DiRita VJ.** 2014. Complete Genome Sequence and Annotation of a *Campylobacter jejuni* Strain, MTVDSCj20, Isolated from a Naturally Colonized Farm-Raised Chicken. Genome announcements **2.**

312. **Gajiwala KS, Burley SK.** 2000. Winged helix proteins. Current opinion in structural biology **10:**110-116.

313. **Tucker PA, Sallai L.** 2007. The AAA+ superfamily--a myriad of motions. Current opinion in structural biology **17:**641-652.

314. **Hanson PI, Whiteheart SW.** 2005. AAA+ proteins: have engine, will work. Nature reviews. Molecular cell biology **6:**519-529.

315. **Mogk A, Dougan D, Weibezahn J, Schlieker C, Turgay K, Bukau B.** 2004. Broad yet high substrate specificity: the challenge of AAA+ proteins. Journal of structural biology **146:**90-98.

316. **Ogura T, Yamada-Inagawa T.** 2002. [AAA family ATPases: ring-shaped chaperones which catalyze energy-dependent conformational changes of proteins]. Tanpakushitsu kakusan koso. Protein, nucleic acid, enzyme **47:**1182-1188.

317. **Snider J, Houry WA.** 2008. AAA+ proteins: diversity in function, similarity in structure. Biochemical Society transactions **36:**72-77.

318. **Snider J, Thibault G, Houry WA.** 2008. The AAA+ superfamily of functionally diverse proteins. Genome biology **9:**216.

319. **Vorwerk H, Mohr J, Huber C, Wensel O, Schmidt-Hohagen K, Gripp E, Josenhans C, Schomburg D, Eisenreich W, Hofreuter D.** 2014. Utilization of host-derived cysteine-containing peptides overcomes the restricted sulphur metabolism of *Campylobacter jejuni*. Mol Microbiol **93:**1224-1245.

320. **Zheng L, Baumann U, Reymond JL.** 2004. An efficient one-step site-directed and site-saturation mutagenesis protocol. Nucleic acids research **32:**e115.

321. **Miyazaki K, Arnold FH.** 1999. Exploring nonnatural evolutionary pathways by saturation mutagenesis: rapid improvement of protein function. Journal of molecular evolution **49:**716-720.

322. **Yao R, Guerry P.** 1996. Molecular cloning and site-specific mutagenesis of a gene involved in arylsulfatase production in *Campylobacter jejuni*. J Bacteriol **178:**3335-3338.

323. **Figurski DH, Helinski DR.** 1979. Replication of an origin-containing derivative of plasmid RK2 dependent on a plasmid function provided in trans. Proc Natl Acad Sci U S A **76:**1648-1652.

324. **Josefsen K, Nielsen H.** 2011. Northern blotting analysis. Methods in molecular biology **703:**87-105.

325. **Mann M.** 2006. Functional and quantitative proteomics using SILAC. Nature reviews. Molecular cell biology **7:**952-958.

326. **Auweter SD, Bhavsar AP, de Hoog CL, Li Y, Chan YA, van der Heijden J, Lowden MJ, Coombes BK, Rogers LD, Stoynov N, Foster LJ, Finlay BB.** 2011. Quantitative mass spectrometry catalogues *Salmonella* pathogenicity island-2 effectors and identifies their cognate host binding partners. J Biol Chem **286:**24023-24035.

327. **Ong SE, Foster LJ, Mann M.** 2003. Mass spectrometric-based approaches in quantitative proteomics. Methods **29:**124-130.

328. **Gagne JP, Pic E, Isabelle M, Krietsch J, Ethier C, Paquet E, Kelly I, Boutin M, Moon KM, Foster LJ, Poirier GG.** 2012. Quantitative proteomics profiling of the poly(ADP-ribose)-related response to genotoxic stress. Nucleic acids research **40:**7788-7805.

329. **Saeed AI, Sharov V, White J, Li J, Liang W, Bhagabati N, Braisted J, Klapa M, Currier T, Thiagarajan M, Sturn A, Snuffin M, Rezantsev A, Popov D, Ryltsov A, Kostukovich E, Borisovsky I, Liu Z, Vinsavich A, Trush V, Quackenbush J.** 2003. TM4: a free, open-source system for microarray data management and analysis. BioTechniques **34:**374-378.

330. **Blagoev B, Kratchmarova I, Ong SE, Nielsen M, Foster LJ, Mann M.** 2003. A proteomics strategy to elucidate functional protein-protein interactions applied to EGF signaling. Nat Biotechnol **21:**315-318.

331. **Vermeulen M, Hubner NC, Mann M.** 2008. High confidence determination of specific protein-protein interactions using quantitative mass spectrometry. Current opinion in biotechnology **19:**331-337.

332. **Rogers LD, Kristensen AR, Boyle EC, Robinson DP, Ly RT, Finlay BB, Foster LJ.** 2008. Identification of cognate host targets and specific ubiquitylation sites on the *Salmonella* SPI-1 effector SopB/SigD. Journal of proteomics **71:**97-108.

333. **Kelley LA, Sternberg MJ.** 2009. Protein structure prediction on the Web: a case study using the Phyre server. Nature protocols **4:**363-371.

334. **Saraste M, Sibbald PR, Wittinghofer A.** 1990. The P-loop--a common motif in ATP- and GTP-binding proteins. Trends in biochemical sciences **15:**430-434.

335. **Leipe DD, Wolf YI, Koonin EV, Aravind L.** 2002. Classification and evolution of P-loop GTPases and related ATPases. J Mol Biol **317:**41-72.

336. **Marchler-Bauer A, Lu S, Anderson JB, Chitsaz F, Derbyshire MK, DeWeese-Scott C, Fong JH, Geer LY, Geer RC, Gonzales NR, Gwadz M, Hurwitz DI, Jackson JD, Ke Z, Lanczycki CJ, Lu F, Marchler GH, Mullokandov M, Omelchenko MV, Robertson CL, Song JS, Thanki N, Yamashita RA, Zhang D, Zhang N, Zheng C, Bryant SH.** 2011. CDD: a Conserved Domain Database for the functional annotation of proteins. Nucleic acids research **39:**D225-229.

337. **Gao R, Mukhopadhyay A, Fang F, Lynn DG.** 2006. Constitutive activation of two-component response regulators: characterization of VirG activation in *Agrobacterium tumefaciens*. J Bacteriol **188:**5204-5211.

338. **Bobay BG, Thompson RJ, Hoch JA, Cavanagh J.** 2010. Long range dynamic effects of point-mutations trap a response regulator in an active conformation. FEBS letters **584:**4203-4207.

339. **Sanna MG, Swanson RV, Bourret RB, Simon MI.** 1995. Mutations in the chemotactic response regulator, CheY, that confer resistance to the phosphatase activity of CheZ. Mol Microbiol **15:**1069-1079.

340. **Dugar G, Herbig A, Forstner KU, Heidrich N, Reinhardt R, Nieselt K, Sharma CM.** 2013. High-resolution transcriptome maps reveal strain-specific regulatory features of multiple *Campylobacter jejuni* isolates. Plos Genet **9:**e1003495.

341. **Ho EC, Donaldson ME, Saville BJ.** 2010. Detection of antisense RNA transcripts by strand-specific RT-PCR. Methods in molecular biology **630:**125-138.

342. **Doherty NC, Shen F, Halliday NM, Barrett DA, Hardie KR, Winzer K, Atherton JC.** 2010. In Helicobacter pylori, LuxS is a key enzyme in cysteine provision through a reverse transsulfuration pathway. J Bacteriol **192:**1184-1192.

343. **Gibson KJ, Pelletier DA, Turner IM, Sr.** 1999. Transfer of sulfur to biotin from biotin synthase (BioB protein). Biochemical and biophysical research communications **254:**632-635.

344. **Berkovitch F, Nicolet Y, Wan JT, Jarrett JT, Drennan CL.** 2004. Crystal structure of biotin synthase, an S-adenosylmethionine-dependent radical enzyme. Science **303:**76-79.

345. **Roisin MP, Kepes A.** 1978. Nucleosidediphosphate kinase of *Escherichia coli*, a periplasmic enzyme. Biochimica et biophysica acta **526:**418-428.

346. **Parsot C, Cossart P, Saint-Girons I, Cohen GN.** 1983. Nucleotide sequence of thrC and of the transcription termination region of the threonine operon in *Escherichia coli K12*. Nucleic acids research **11:**7331-7345.

347. **Busch A, Richter AS, Backofen R.** 2008. IntaRNA: efficient prediction of bacterial sRNA targets incorporating target site accessibility and seed regions. Bioinformatics **24:**2849-2856.

348. **Eggenhofer F, Tafer H, Stadler PF, Hofacker IL.** 2011. RNApredator: fast accessibility-based prediction of sRNA targets. Nucleic acids research **39:**W149-154.

349. **Thomas SN, Wan Y, Liao Z, Hanson PI, Yang AJ.** 2011. Stable isotope labeling with amino acids in cell culture based mass spectrometry approach to detect transient protein interactions using substrate trapping. Analytical chemistry **83:**5511-5518.

350. **Trinkle-Mulcahy L, Boulon S, Lam YW, Urcia R, Boisvert FM, Vandermoere F, Morrice NA, Swift S, Rothbauer U, Leonhardt H, Lamond A.** 2008. Identifying specific protein interaction partners using quantitative mass spectrometry and bead proteomes. The Journal of cell biology **183:**223-239.

351. **Parey K, Demmer U, Warkentin E, Wynen A, Ermler U, Dahl C.** 2013. Structural, biochemical and genetic characterization of

dissimilatory ATP sulfurylase from *Allochromatium vinosum*. PloS one **8:**e74707.

352. **Leyh TS, Taylor JC, Markham GD.** 1988. The sulfate activation locus of *Escherichia coli* K12: cloning, genetic, and enzymatic characterization. J Biol Chem **263:**2409-2416.

353. **Kelly DJ.** 2001. The physiology and metabolism of *Campylobacter jejuni* and *Helicobacter pylori*. Symposium series**:**16S-24S.

354. **Weerakoon DR, Olson JW.** 2008. The *Campylobacter jejuni* NADH:ubiquinone oxidoreductase (complex I) utilizes flavodoxin rather than NADH. J Bacteriol **190:**915-925.

355. **Feder ME, Hofmann GE.** 1999. Heat-shock proteins, molecular chaperones, and the stress response: evolutionary and ecological physiology. Annual review of physiology **61:**243-282.

356. **Lemire JA, Harrison JJ, Turner RJ.** 2013. Antimicrobial activity of metals: mechanisms, molecular targets and applications. Nat Rev Microbiol **11:**371-384.

357. **Keyer K, Imlay JA.** 1996. Superoxide accelerates DNA damage by elevating free-iron levels. Proc Natl Acad Sci U S A **93:**13635-13640.

358. **Suzuki YJ, Carini M, Butterfield DA.** 2010. Protein carbonylation. Antioxidants & redox signaling **12:**323-325.

359. **Kertesz MA.** 2000. Riding the sulfur cycle--metabolism of sulfonates and sulfate esters in Gram-negative bacteria. Fems Microbiol Rev **24:**135-175.

360. **Kessler D.** 2006. Enzymatic activation of sulfur for incorporation into biomolecules in prokaryotes. Fems Microbiol Rev **30:**825-840.

361. **Klaassen CD, Boles JW.** 1997. Sulfation and sulfotransferases 5: the importance of 3'-phosphoadenosine 5'-phosphosulfate (PAPS) in the regulation of sulfation. Faseb J **11:**404-418.

362. **Sekowska A, Kung HF, Danchin A.** 2000. Sulfur metabolism in *Escherichia coli* and related bacteria: facts and fiction. Journal of molecular microbiology and biotechnology **2:**145-177.

363. **Geissmann T, Possedko M, Huntzinger E, Fechter P, Ehresmann C, Romby P.** 2006. Regulatory RNAs as mediators of virulence gene expression in bacteria. Handbook of experimental pharmacology**:**9-43.

364.   **Masse E, Majdalani N, Gottesman S.** 2003. Regulatory roles for small RNAs in bacteria. Current opinion in microbiology **6:**120-124.

365.   **Repoila F, Darfeuille F.** 2009. Small regulatory non-coding RNAs in bacteria: physiology and mechanistic aspects. Biology of the cell / under the auspices of the European Cell Biology Organization **101:**117-131.

366.   **Waters LS, Storz G.** 2009. Regulatory RNAs in bacteria. Cell **136:**615-628.

367.   **Labigne-Roussel A, Harel J, Tompkins L.** 1987. Gene transfer from *Escherichia coli* to *Campylobacter* species: development of shuttle vectors for genetic analysis of *Campylobacter jejuni*. J Bacteriol **169:**5320-5323.

368.   **Labigne-Roussel A, Courcoux P, Tompkins L.** 1988. Gene disruption and replacement as a feasible approach for mutagenesis of *Campylobacter jejuni*. J Bacteriol **170:**1704-1708.

369.   **Wang Y, Taylor DE.** 1990. Chloramphenicol resistance in *Campylobacter coli*: nucleotide sequence, expression, and cloning vector construction. Gene **94:**23-28.

370.   **Colegio OR, Griffin TJt, Grindley ND, Galan JE.** 2001. *In vitro* transposition system for efficient generation of random mutants of *Campylobacter jejuni*. J Bacteriol **183:**2384-2388.

371.   **Hendrixson DR, Akerley BJ, DiRita VJ.** 2001. Transposon mutagenesis of *Campylobacter jejuni* identifies a bipartite energy taxis system required for motility. Mol Microbiol **40:**214-224.

372.   **Golden NJ, Camilli A, Acheson DW.** 2000. Random transposon mutagenesis of *Campylobacter jejuni*. Infect Immun **68:**5450-5453.

373.   **Gritz L, Davies J.** 1983. Plasmid-encoded hygromycin B resistance: the sequence of hygromycin B phosphotransferase gene and its expression in *Escherichia coli* and *Saccharomyces cerevisiae*. Gene **25:**179-188.

374.   **Walton JR.** 1978. Apramycin, a new aminocyclitol antibiotic. I. In vitro microbiological studies. The Journal of antimicrobial chemotherapy **4:**309-313.

375.   **Brodersen DE, Clemons WM, Jr., Carter AP, Morgan-Warren RJ, Wimberly BT, Ramakrishnan V.** 2000. The structural basis for the action of the antibiotics tetracycline, pactamycin, and hygromycin B on the 30S ribosomal subunit. Cell **103:**1143-1154.

376. **Salauze D, Otal I, Gomez-Lus R, Davies J.** 1990. Aminoglycoside acetyltransferase 3-IV *(aacC4)* and hygromycin B 4-I phosphotransferase *(hphB)* in bacteria isolated from human and animal sources. Antimicrob Agents Ch **34:**1915-1920.

377. **Paget E, Davies J.** 1996. Apramycin resistance as a selective marker for gene transfer in mycobacteria. J Bacteriol **178:**6357-6360.

378. **Watanabe M, Sumida N, Murakami S, Anzai H, Thompson CJ, Tateno Y, Murakami T.** 1999. A phosphonate-induced gene which promotes penicillium-mediated bioconversion of *cis*-propenylphosphonic acid to fosfomycin. Appl Environ Microb **65:**1036-1044.

379. **Pardo JM, Malpartida F, Rico M, Jimenez A.** 1985. Biochemical basis of resistance to hygromycin B in *Streptomyces hygroscopicus*--the producing organism. Journal of general microbiology **131:**1289-1298.

380. **Magalhaes MLB, Blanchard JS.** 2005. The kinetic mechanism of AAC(3)-IV aminoglycoside acetyltransferase from *Escherichia coli*. Biochemistry-Us **44:**16275-16283.

381. **Ménard R, Sansonetti PJ, Parsot C.** 1993. Nonpolar mutagenesis of the *ipa* genes defines IpaB, IpaC, and IpaD as effectors of *Shigella flexneri* entry into epithelial cells. J Bacteriol **175:**5899-5906.

382. **Karlyshev AV, Wren BW.** 2005. Development and application of an insertional system for gene delivery and expression in *Campylobacter jejuni*. Appl Environ Microb **71:**4004-4013.

383. **Davis L, Young K, DiRita V.** 2005. Genetic manipulation of *Campylobacter jejuni*, Current protocols in microbiology. John Wiley & Sons, Inc.

384. **Lovdok L, Bentele K, Vladimirov N, Muller A, Pop FS, Lebiedz D, Kollmann M, Sourjik V.** 2009. Role of translational coupling in robustness of bacterial chemotaxis pathway. PLoS biology **7:**e1000171.

385. **Grabowska AD, Wandel MP, Lasica AM, Nesteruk M, Roszczenko P, Wyszynska A, Godlewska R, Jagusztyn-Krynicka EK.** 2011. *Campylobacter jejuni dsb* gene expression is regulated by iron in a Fur-dependent manner and by a translational coupling mechanism. BMC microbiology **11:**166.

386. **Lin AE, Krastel K, Hobb RI, Thompson SA, Cvitkovitch DG, Gaynor EC.** 2009. Atypical roles for *Campylobacter jejuni* amino acid ATP binding cassette transporter components PaqP and PaqQ in bacterial

stress tolerance and pathogen-host cell dynamics. Infection and immunity **77:**4912-4924.

387. **Moran NA.** 2002. Microbial minimalism: genome reduction in bacterial pathogens. Cell **108:**583-586.

388. **Fang FC, Casadevall A.** 2011. Reductionistic and holistic science. Infect Immun **79:**1401-1404.

389. **Noirot-Gros MF, Velten M, Yoshimura M, McGovern S, Morimoto T, Ehrlich SD, Ogasawara N, Polard P, Noirot P.** 2006. Functional dissection of YabA, a negative regulator of DNA replication initiation in *Bacillus subtilis*. Proc Natl Acad Sci U S A **103:**2368-2373.

390. **Winkler WC, Breaker RR.** 2005. Regulation of bacterial gene expression by riboswitches. Annu Rev Microbiol **59:**487-517.

391. **Kim DI, Birendra KC, Zhu W, Motamedchaboki K, Doye V, Roux KJ.** 2014. Probing nuclear pore complex architecture with proximity-dependent biotinylation. Proc Natl Acad Sci U S A **111:**E2453-2461.

392. **Manning G, Duim B, Wassenaar T, Wagenaar JA, Ridley A, Newell DG.** 2001. Evidence for a genetically stable strain of *Campylobacter jejuni*. Appl Environ Microbiol **67:**1185-1189.

393. **Gaynor EC, Cawthraw S, Manning G, MacKichan JK, Falkow S, Newell DG.** 2004. The genome-sequenced variant of *Campylobacter jejuni* NCTC 11168 and the original clonal clinical isolate differ markedly in colonization, gene expression, and virulence-associated phenotypes. J Bacteriol **186:**8159-8159.

394. **Stover CK, de la Cruz VF, Fuerst TR, Burlein JE, Benson LA, Bennett LT, Bansal GP, Young JF, Lee MH, Hatfull GF, Snapper SB, Barletta RG, Jacobs WR, Bloom BR.** 1991. New use of BCG for recombinant vaccines. Nature **351:**456-460.

395. **Burian J, Ramon-Garcia S, Sweet G, Gomez-Velasco A, Av-Gay Y, Thompson CJ.** 2012. The mycobacterial transcriptional regulator *whiB7* gene links redox homeostasis and intrinsic antibiotic resistance. J Biol Chem **287:**299-310.

396. **Guzman LM, Belin D, Carson MJ, Beckwith J.** 1995. Tight regulation, modulation, and high-level expression by vectors containing the arabinose PBAD promoter. J Bacteriol **177:**4121-4130.

397. **Rappsilber J, Mann M, Ishihama Y.** 2007. Protocol for micro-purification, enrichment, pre-fractionation and storage of peptides for proteomics using StageTips. Nature protocols **2:**1896-1906.

398. **Schaab C, Geiger T, Stoehr G, Cox J, Mann M.** 2012. Analysis of high accuracy, quantitative proteomics data in the MaxQB database. Molecular & cellular proteomics : MCP **11:**M111 014068.

APPENDIX A

APPENDIX A.1 TABLES OF STRAINS AND PLASMIDS

TABLE A.1.1 Bacterial strains and plasmids used in CHAPTER TWO.

Strain	Genotype or description	Source
Escherichia coli		
DH5α	F⁻, φ80d *deoR lacZΔM15 endA1 recA1 hsdR17*(r$_K$-m$_K$+) *supE44 thi-1 gyrA96 relA1 Δ(lacZYA-argF) U169.*	Invitrogen.
Campylobacter jejuni		
81-176	Wild type isolated from a diarrheic patient, undergone laboratory passage.	(33)
81-176 Δ*kpsM*	A site-insertional resistance marker mutant in *kpsM*, capsule negative strain, kanamycin^R.	(27)
Plasmids (maintained in *E. coli* strain)		
pSPI-GFP	Green fluorescent protein expressed by the *atpF`* promoter, in pMW10 backbone, kanamycin^R.	Erin Gaynor.

TABLE A.1.2 Bacterial strains and plasmids used in CHAPTER THREE.

Strain	Genotype or description	Source
Escherichia coli		
DH5α	F⁻, φ80d *deoR lacZΔM15 endA1 recA1 hsdR17*(r$_K$-m$_K$+) *supE44 thi-1 gyrA96 relA1 Δ(lacZYA-argF) U169.*	Invitrogen.
Campylobacter jejuni		
81-176	Wild type isolated from a diarrheic patient, undergone laboratory passage.	(33)
81116	Wild type, isolated from humans during a waterborne outbreak at a school in southeast England in 1981; undergone laboratory passage.	(392)
11168-O	Wild type, originally isolated from the feces of a diarrheic patient in 1977 by Martin Skirrow; minimal laboratory.	Newell, D and Skirrow, M. Veterinary Laboratories Agency.
11168-GS	Wild type, genome sequenced isolate, undergone laboratory passage.	(393)
81-176 Colony 1 *apt*I61T	Single colony isolate, whole genome sequenced.	This study.
81-176 Colony 2 *purF*A304G	Single colony isolate, whole genome sequenced.	This study.
81-176 Colony 3 *purF*G292S	Single colony isolate, whole genome sequenced.	This study.
81-176 Colony 4 *apt*I61T	Single colony isolate, whole genome sequenced.	This study.
81-176 Colony 5 *purF*G95delinsGV	Single colony isolate, whole genome sequenced.	This study.
81-176 Colony 1 *apt*I61T + pRRH-*apt*REF	Mutant single colony isolate with genome-integrated copy of operon containing reference sequence of *apt,* hygromycin[R].	This study.
81-176 Colony 2 *purF*A304G + pRRH-*purF*T91del	Mutant single colony isolate with genome-integrated copy of operon containing *purF*T91del, hygromycin[R].	This study.
81-176 Colony 3 *purF*G292S + pRRH- *purF*T91del	Mutant single colony isolate with genome-integrated copy of operon containing *purF*T91del, hygromycin[R].	This study.
81-176 Colony 5 *purF*G95delinsGV + pRRH: *purF*T91del	Mutant single colony isolate with genome-integrated copy of operon containing *purF*T91del, hygromycin[R].	This study.
81-176 + pRRH-*apt*A133T	81-176 with genome-integrated copy of *apt*A133T operon, hygromycin[R].	This study.
81-176 + pRRH-*purF*A304G	81-176 with genome-integrated copy of *purF*A304G operon, hygromycin[R].	This study.
81-176 + pRRH-*purF*G292S	81-176 with genome-integrated copy of *purF*G292S operon, hygromycin[R].	This study.
81-176 + pRRH-*purF*G95delinsGV	81-176 with genome-integrated copy of *purF*G95delinsGV operon, hygromycin[R].	This study.
81-176 Δ*apt::apr*[R]	Replacement deletion of *apt* with apramycin resistance cassette, apramycin[R].	This study.

Strain	Genotype or description	Source
81-176 96 Single colony isolates	96 single colony isolates – Sanger sequenced genotypes are shown in Figure 3A.	This study.
81-176 *purF*G95V	Single colony isolate 56, passaged 1X.	This study.
81-176 *apt*A133T	Single colony isolate 95, passaged 1X.	This study.
81-176 *purF*G292S	Single colony isolate 45, passaged 1X.	This study.
81-176 *apt*E154A	Single colony isolate 82, passaged 1X.	This study.
81-176 *purF*V336F	Single colony isolate 79, passaged 1X.	This study.
81-176 *apt*G135_136GinsGTANARVLLVDDLIATG	Single colony isolate 93, passaged 1X.	This study.
81-176 *purF*T91del	Single colony isolate 29, passaged 1X.	This study.
81-176 *purF*V93_D96del	Single colony isolate 88, passaged 1X.	This study.
81-176 *apt*P93_F94insFETFSCEYDLEYGSDK	Single colony isolate 27, passaged 1X.	This study.
81-176 DRH461	Strain 81-176 with an unmarked deletion of *astA* arylsulfatase reporter, streptromycin^R.	(79)
81-176 DRH461 + pRRA-RBS*astA*	Arylsulfatase deletion strain with genome-integrated *astA* reporter fused to reference RBS, apramycin and streptromycin^R.	This study.
81-176 DRH461 + pRRA-RBS**astA*	Arylsulfatase deletion strain with genome-integrated *astA* reporter fused to *apt* RBS sequence in colony 15, apramycin and streptromycin^R.	This study.
81-176 Δ*argH::cat*	Arginine auxotroph strain of *C. jejuni* for use in SILAC, chloramphenicol^R.	Dmitry Apel.
81-176 *purF*T91del Δ*cj1132c::apr*^{R}	Replacement deletion of cj1132c with apramycin resistance cassette in the *purF*T91del single colony background.	This study.
81-176 *purF*T91del Δ*cj1132c::apr*^{R} + pRRH-*cj1132c*	Complementation of the replacement deletion of *cj1132c* with genome-integrated copy of *cj1132c* in the *purF*T91del single colony background.	This study.
Plasmids (maintained in *E. coli* strain)		
pGEM-T	Linearized cloning vector, blue-white screening; ampicillin resistance.	Promega.
pAC1A	Vector containing the apramycin^R cassette.	(2)
pRRA	Genome-insertional gene delivery vehicle, apramycin^R.	(2)
pRRH	Genome-insertional gene delivery vehicle, hygromycin^R.	(2)
pGEM-*purF*	Cloning plasmid harboring *purF* and flanking regions, from PCR with oligos 6409 and 6410, ampicillin^R.	This study.
pGEM-*apt*	Cloning plasmid harboring *apt* and flanking regions, from PCR with oligos 6413 and 6414, ampicillin^R.	This study.

Strain	Genotype or description	Source
pGEM-*purF::apr*[R]	Plasmid containing replacement deletion of *purF* coding sequence, created via inverse PCR with oligos 6411 and 6412 and ligation to apramycin cassette, ampicllin and apramycin[R].	This study.
pGEM-*apt::apr*[R]	Plasmid containing replacement deletion of *apt* coding sequence, created via inverse PCR with oligos 6415 and 6416 and ligation to apramycin cassette, ampicillin and apramycin[R].	This study.
pRRH-*apt*REF	Genome-insertional gene delivery plasmid harboring *apt* reference sequence operon, insert created with oligos 2775 and 2776, hygromycin[R].	This study.
pRRH-*purF*T91del	Genome-insertional gene delivery plasmid harboring *purF*T91del operon, insert created with oligos 2777 and 2778, hygromycin[R].	This study.
pRRH-*apt*A133T	Genome-insertional gene delivery plasmid harboring *apt*A133T operon, insert created with oligos 2775 and 2776, hygromycin[R].	This study.
pRRH-*purF*A304G	Genome-insertional gene delivery plasmid harboring *purF*A304G operon, insert created with oligos 2777 and 2778, hygromycin[R].	This study.
pRRH-*purF*G292S	Genome-insertional gene delivery plasmid harboring *purF*G292S operon, insert created with oligos 2777 and 2778, hygromycin[R].	This study.
pRRH-*purF*G95delinsGV	Genome-insertional gene delivery plasmid harboring *purF*G95delinsGV operon, insert created with oligos 2777 and 2778, hygromycin[R].	This study.
pRRA-RBS*astA* (CGA**G**GCA)	Genome-insertional gene delivery plasmid harboring *astA* reporter fused to *apt* RBS reference sequence. Insert created with oligos 3812 and 3814, apramycin[R].	This study.
pRRA-RBS**astA* (CGA**A**GCA)	Genome-insertional gene delivery plasmid harboring *astA* reporter fused to *apt* RBS sequence in colony 15. Insert created with oligos 3813 and 3814, apramycin[R].	This study.
pGEM-*cj1132c*	Cloning plasmid harboring *cj1132c* and flanking regions, from PCR with oligos 0540 and 0541, ampicillin[R].	This study.
pGEM-*cj1132c::apr*[R]	Plasmid containing replacement deletion of *cj1132c* coding sequence, created via inverse PCR with oligos 0542 and 0543 and ligation to apramycin cassette, ampicillin and apramycin[R].	This study.
pRRH-*cj1132c*	Genome-insertional gene delivery plasmid harboring *cj1132c* with native promoter, insert created with oligos 8168 and 8169, hygromycin[R].	This study.

TABLE A.1.3 Bacterial strains and plasmids used in CHAPTER FOUR.

Strain	Genotype or description	Source/Reference
Escherichia coli		
DH5α	F⁻, φ80d *deoR lacZΔM15 endA1 recA1 hsdR17*(r$_K$-m$_K$+) *supE44 thi-1 gyrA96 relA1 Δ(lacZYA-argF) U169.*	Invitrogen.
Campylobacter jejuni		
81-176	Wild type isolated from a diarrheic patient, undergone laboratory passage.	(33)
81-176 *purF*V336F	Single colony isolate 79, passaged 1X.	Chapter 3.
81-176 *purF*T91del	Single colony isolate 29, passaged 1X.	Chapter 3.
81-176 *purF*D96G	Single colony isolate 55, passaged 1X.	Chapter 3.
81-176 *purF*V336F pRRH	Single colony isolate 79, with genome integrated pRRH, hygromycin^R.	This study.
81-176 *purF*V336F pRRA	Single colony isolate 79, with genome integrated pRRA, apramycin^R.	This study.
81-176 *purF*V336F pRRK	Single colony isolate 79, with genome integrated pRRK, kanamycin^R.	This study.
81-176 *purF*T91del pRRH	Single colony isolate 29, with genome integrated pRRH, hygromycin^R.	This study.
81-176 *purF*T91del pRRA	Single colony isolate 29, with genome integrated pRRA, apramycin^R.	This study.
81-176 *purF*T91del pRRK	Single colony isolate 29, with genome integrated pRRK, kanamycin^R.	This study.
81-176 *purF*D96G pRRH	Single colony isolate 55, with genome integrated pRRH, hygromycin^R.	This study.
81-176 *purF*D96G pRRA	Single colony isolate 55, with genome integrated pRRA, apramycin^R.	This study.
81-176 *purF*D96G pRRK	Single colony isolate 55, with genome integrated pRRK, kanamycin^R.	This study.
81-176 *purF*V336F + GFP	Single colony isolate 79, with pSPI-GFP, kanamycin^R.	This study.
81-176 *purF*V336F + RFP	Single colony isolate 79, with pRY112-Pdps-mRFP, chloramphenicol^R.	This study.

Strain	Genotype or description	Source/Reference
81-176 *purF*T91del + GFP	Single colony isolate 29, with pSPI-GFP, kanamycin^R.	This study.
81-176 *purF*T91del + RFP	Single colony isolate 29, with pRY112-Pdps-mRFP, chloramphenicol^R.	This study.
81-176 *purF*D96G + GFP	Single colony isolate 55, with pSPI-GFP, kanamycin^R.	This study.
81-176 *purF*D96G + RFP	Single colony isolate 55, with pRY112-Pdps-mRFP, chloramphenicol^R.	This study.
81-176 Δ*apt*	Δ*apt::apr*^R, Replacement deletion of *apt* with apramycin resistance cassette.	Chapter 3.
81-176 DRH461	Strain 81-176 with an unmarked deletion of *astA* arylsulfatase reporter, Streptomycin^R.	(79)
Plasmids (maintained in *E. coli* strain)		
pRRK	Genome-insertional gene delivery vehicle; kanamycin^R.	Brendan Wren.
pRRA	Genome-insertional gene delivery vehicle; apramycin^R.	(2)
pRRH	Genome-insertional gene delivery vehicle; hygromycin^R.	(2)
pSPI-GFP	Green fluorescent protein expressed by the atpF` promoter, in pMW10 backbone, kanamycin^R.	Erin Gaynor.
pRY112	Campylobacter shuttle plasmid, chloramphenicol^R.	(289)
pRK600	Triparental mating helper strain plasmid, *E. coli*, chloramphenicol^R.	(323)
pBca1020-R0040	Plasmid containing EX-Ptet-S-rbsRFP-P, (monomeric red fluorescent protein source), ampicillin^R.	iGEM part:BBa_J61002
pRY112-P*dps*	Insertion of *dps* (*cj1534c*) promoter into pRY112, chloramphenicol^R.	This study.
pRY112-P*dps*-mRFP	RFP expression plasmid, chloramphenicol^R.	This study.

TABLE A.1.4 Bacterial strains and plasmids used in CHAPTER FIVE.

Strain	Genotype or description	Source/Reference
Escherichia coli		
DH5α	F⁻, φ80d *deoR lacZΔM15 endA1 recA1 hsdR17*(r$_K$-m$_K$+) *supE44 thi-1 gyrA96 relA1 Δ(lacZYA-argF) U169*.	Invitrogen.
BL21(DE3)	*fhuA2 [lon] ompT gal (λ DE3) [dcm] ΔhsdS λ DE3 = λ sBamHIo ΔEcoRI-B int::(lacI::PlacUV5::T7 gene1) i21 Δnin5*.	New England Biolabs.
BL21(DE3) pET28a-Cj1533c-6XHIS	Expression construct, 6XHIS fusion to C-terminus of Cj1533c, kanamycin^R.	This study.
Campylobacter jejuni		
81-176	Wild type isolated from a diarrheic patient, undergone laboratory passage.	(33)
81-176 Δ*cj1533c*	Strain 81-176 with a deletion of cj1533c via replacement with *aph*A-2, kanamycin^R.	This study.
81-176 Δ*cj1533c+cj1533c*	Deletion strain complemented with *cj1533c* via pRRC genome-integration, kanamycin^R and chloramphenicol^R.	This study.
81-176 Δ*cj1533c+cj1533c*K K40,41GG	Deletion strain complemented with lysine-to-glycine site-directed mutant *cj1533c* via pRRC genome-integration, kanamycin^R and chloramphenicol^R.	This study.
81-176 Δ*cj1533c* pRY112-EPlibrary	Pooled (~10⁵) colony library of deletion strain complemented with high-copy replicative pRY112 containing error prone PCR directed evolution of *cj1533c* amplicons, kanamycin^R and chloramphenicol^R.	This study.
81-176 Δ*cj1533c* pRY112-*putative sRNA*	NaCl-enriched clone containing putative sRNA in high-copy replicative pRY112, kanamycin^R and chloramphenicol^R.	This study.
81-176 Δ*cj1533c+putative sRNA*	Deletion strain with genome-integrated putative sRNA after transfer into pRRC gene delivery plasmid, kanamycin^R and chloramphenicol^R.	This study.
81-176 Δ*fur*	Deletion of *fur* via replacement with *aph*(7''), hygromycin^R.	This study.
81-176 Δ*perR*	Deletion of *perR* via replacement with *aac*(3)IV, apramycin^R.	This study.
81-176 *cosR*^{OE}	Overexpression of *cosR* via fusion to the atpF' promoter in high-copy replicative plasmid pRY112, chloramphenicol^R.	This study.
81-176 Δ*dps*	Deletion of *dps* via replacement with *aac*(3)IV, apramycin^R.	This study.
81-176 Δ*cj1533c*Δ*dps*	Double deletion of *cj1533c* and *dps*, kanamycin^R and apramycin^R.	This study.
81-176 Δ*argH*	SILAC arginine auxotroph, chloramphenicol^R.	Dmitry Apel.
81-176 Δ*argH*Δ*cj1533c*	SILAC arginine auxotroph with a deletion of *cj1533c*, kanamycin^R and chloramphenicol^R.	This study.

Strain	Genotype or description	Source/Reference
81-176 Δ*argH* Δ*cj1533c*+*cj1533c*	SILAC arginine auxotroph *cj1533c* deletion strain complemented with *cj1533c* via pRRA genome-integration, kanamycin[R], apramycin[R] and chloramphenicol[R].	This study.
81-176 Δ*argH* Δ*cj1533c*+*putative sRNA*	SILAC arginine auxotroph *cj1533c* deletion strain complemented with *putative sRNA* via pRRA genome-integration, kanamycin[R], apramycin[R] and chloramphenicol[R].	This study.
Plasmids (maintained in *E. coli* strain)		
pRRA	Genome-insertional gene delivery vehicle; apramycin[R].	(2)
pRRC	Genome-insertion gene delivery vehicle, chloramphenicol[R].	(382)
pRY112	*Campylobacter* shuttle plasmid, chloramphenicol[R].	(289)
pRK600	Triparental mating helper strain plasmid, *E. coli*, chloramphenicol[R].	(323)
pGEM-T	Linearized cloning vector, blue-white screening; ampicillin[R].	Promega.
pGEM-*cj1533c*	Cloning plasmid harboring *cj1533c* and flanking regions, from PCR with oligos 5712 and 5713, ampicillin[R].	This study.
pGEM-*cj1533c*::*kan*[R]	Plasmid containing replacement deletion of *cj1132c* coding sequence, created via inverse PCR with oligos 5714 and 5715 and ligation to *aphA-2* cassette, ampicillin and kanamycin[R].	This study.
pGEM-*cj1533c*KK40,41GG	*Dpn*I-mediated site directed KK40,41GG mutation of pGEM-cj1533c using inverse PCR with oligos 9223 and 9224.	This study.
pGEM-*fur*	Cloning plasmid harboring *cj1533c* and flanking regions, from PCR with oligos 95711 and 95712, ampicillin[R].	This study.
pGEM-*fur*::*hyg*[R]	Plasmid containing replacement deletion of *cj1132c* coding sequence, created via inverse PCR with oligos 95713 and 95714 and ligation to *aph*(7") cassette, ampicillin and hygromycin[R].	This study.
pGEM-*perR*	Cloning plasmid harboring *perR* and flanking regions, from PCR with oligos 95715 and 95716, ampicillin[R].	This study.
pGEM-*perR*::*apr*[R]	Plasmid containing replacement deletion of *perR* coding sequence, created via inverse PCR with oligos 95718 and 95719 and ligation to *aac*(3)IV cassette, ampicillin and apramycin[R].	This study.
pGEM-*dps*	Cloning plasmid harboring *dps* and flanking regions, from PCR with oligos 2429 and 2430, ampicillin[R].	This study.
pGEM-*dps*::*apr*[R]	Plasmid containing replacement deletion of *dps* coding sequence, created via inverse PCR with oligos 2431 and 2432 and ligation to *aac*(3)IV cassette, ampicillin and apramycin[R].	This study.

Strain	Genotype or description	Source/Reference
pET28a	IPTG-inducible *lac* promoter expression plasmid, kanamycin[R].	Promega.
pET28c-Cj1533c-6XHIS	C-terminal 6XHIS-tagged Cj1533c, from insert amplified with oligonucleotides 3523/7208 and cloned into pET28a.	This study.
pRRC-*cj1533c*	Genome-insertional gene delivery complementation plasmid harboring *cj1532c* with native promoter, insert created with oligos 8610 and 8613, chloramphenicol[R].	This study.
pRRA-*cj1533c*	Genome-insertional gene delivery complementation plasmid harboring *cj1532c* with native promoter, insert created with oligos 8610 and 8613, apramycin[R].	This study.
pRRC-*putative sRNA*	Genome-insertional gene delivery complementation plasmid harboring *putative sRNA* with native promoter, insert created with oligos 8610 and 4382, chloramphenicol[R].	This study.
pRRA-*putative sRNA*	Genome-insertional gene delivery complementation plasmid harboring *putative sRNA* with native promoter, insert created with oligos 8610 and 4382, apramycin[R].	This study.
pRY112-*putative sRNA*	Multi-copy replicative plasmid harboring putative sRNA insert created by error-prone PCR with oligos 8881 and 8882, chloramphenicol[R].	This study.
pRRC-*cj1533c*KK40,41GG	Genome-insertional gene delivery complementation plasmid harboring site-directed KK40,41GG mutant with native promoter, insert created with oligos 8610 and 4382, chloramphenicol[R].	This study.
pRY112-*atpF'*	Multi-copy replicative plasmid harboring *atpF'* promoter insert created by PCR with oligos 7633 and 7644, chloramphenicol[R].	This study.
pRY112-*atpF'-cosR*	Multi-copy replicative plasmid harboring *atpF'* promoter and a *cosR* insert created by PCR with oligos 9438 and 9434, chloramphenicol[R].	This study.

TABLE A.1.5 Bacterial strains and plasmids used in CHAPTER SIX.

Strain or plasmid	Genotype or description	Source
Escherichia coli		
DH5α	F⁻, φ80d *deoR lacZΔM15 endA1 recA1 hsdR17*(r$_K$-m$_K$+) *supE44 thi-1 gyrA96 relA1 Δ(lacZYA-argF) U169.*	Invitrogen.
Campylobacter jejuni		
81-176	Wild type isolated from a diarrheic patient.	(33)
81-176 pRRH	Strain 81-176 with genome-integrated pRRH, hygromycin^R.	This study.
81-176 pRRA	Strain 81-176 with genome-integrated pRRA, apramcyin^R.	This study.
81-176 pRRC	Strain 81-176 with genome-integrated pRRC, chloramphenicol^R.	This study.
81-176 pRRK	Strain 81-176 with genome-integrated pRRK, kanamycin^R.	This study.
81-176 Δ*astA::hyg*^{R}	Deletion of *astA* with *aph*(7"), hygromycin^R.	This study.
81-176 Δ*astA::apr*^{R}	Deletion of *astA* with *aac*(3)IV, apramycin^R.	This study.
DRH461	Strain 81-176 with an unmarked deletion of *astA,* streptomycin^R.	(79)
DRH461 pRRH+*astA*	DRH461 with integrated pRRH and polycistronic promoterless *ast,* streptomycin^R and hygromycin^R.	This study.
DRH461 pRRA+*astA*	DRH461 with integrated pRRA and polycistronic promoterless *astA,* streptomycin^R and apramycin^R.	This study.
DRH461 pRRH+*astA* (reverse)	DRH461 with integrated pRRH and reverse orientation promoterless *astA,* streptomycin^R and hygromycin^R.	This study.
DRH461 pRRA+*astA* (reverse)	DRH461 with integrated pRRA and reverse orientation promoterless *astA,* streptomycin^R and apramycin^R.	This study.
DRH461 pRRH+(p)*astA* (reverse)	DRH461 with integrated pRRH and reverse orientation endogenous promoter and *astA,* streptomycin^R and hygromycin^R.	This study.
DRH461 pRRA+(p)*astA* (reverse)	DRH461 with integrated pRRA and reverse orientation endogenous promoter and *astA,* streptomycin^R and apramycin^R.	This study.
Plasmids (maintained in *E. coli* strain)		
pMV261.hyg	Source of *aph*(7"), hygromycin^R.	(394, 395)
p261comp.apra	Source of *aac*(3)IV, apramycin^R.	(395)
pGEM-T	Linearized cloning vector, blue-white screening, ampicillin^R.	Promega.
pBAD24	Low-copy arabinose-inducible expression vector, and ampicillin^R.	(396)
pAC1H	pBAD24 ligated to *aph*(7") amplified with 5631 and 5632; hygromycin^R and ampicillin^R.	This study.
pAC1A	pGEM-T ligated to *aac*(3)IV amplified with 5633 and 5634, apramycin^R and ampicillin^R.	This study.
pRRC	Genome-insertional gene delivery vehicle, chloramphenicol^R.	(382)

Strain or plasmid	Genotype or description	Source
pRRK	Genome-insertional gene delivery vehicle, kanamcyin^R.	Brendan Wren.
pRRH	Genome-insertional gene delivery vehicle, hygromycin^R	This study.
pRRA	Genome-insertional gene delivery vehicle, apramycin^R.	This study.
pGEM-T+*astA*	pGEM-T ligated to *astA* amplified with 5707 and 5708, ampicillin^R.	This study.
pGEM-T+*astA*::*hyg^R*	pGEM-T with *astA* interrupted with *aph*(7") from pAC1H, hygromycin^R and ampicillin^R.	This study.
pGEM-T+*astA*::*apr^R*	pGEM-T with *astA* interrupted with *aac*(3)IV from pAC1, apramycin^R and ampicillin^R.	This study.
pRRH+*astA*	pRRH ligated to *astA* amplified with 0688 and 0689, hygromycin^R.	This study.
pRRA+*astA*	pRRA ligated to *astA* amplified with 0688 and 0689, apramycin^R.	This study.
pRRH+*astA* (reverse)	pRRH ligated to *astA* amplified with 0690 and 0691, hygromycin^R.	This study.
pRRA+*astA* (reverse)	pRRA ligated to *astA* amplified with 0690 and 0691, apramycin^R.	This study.
pRRH+(p)*astA* (reverse)	pRRH ligated to *astA* amplified with 0692 and 0691, hygromycin^R	This study.
pRRA+(p)*astA* (reverse)	pRRA ligated to *astA* amplified with 0692 and 0691, apramycin^R	This study.

APPENDIX A.2 TABLES OF OLIGONUCLEOTIDES

TABLE A.2.1 Oligonucleotides used in CHAPTER TWO.

Oligo Ref. No	Name	Sequence 5'-3' (Restriction sites bolded)	Purpose / Notes
2456	AC gyrA qPCR CODE	CTTTGCCTGACGCAAGAGATGGTT	For quantitative RT-PCR via SYBR-Green. Target: *gyrA*.
2457	AC gyrA qPCR COMP	AGCACCCACTATACGGGCTGATTT	For quantitative RT-PCR via SYBR-Green. Target: *gyrA*.
2458	AC groEL qPCR CODE	GAAGCAATTGGCGCAGCTATCGTT	For quantitative RT-PCR via SYBR-Green. Target: *groEL*.
2459	AC groEL qPCR COMP	CCACACCTGCATCAAATC CTGCAT	For quantitative RT-PCR via SYBR-Green. Target: *groEL*.
2460	AC dnaK qPCR CODE	CGCGGTATGCCACAAATCGAAGTT	For quantitative RT-PCR via SYBR-Green. Target: *dnaK*.
2461	AC dnaK qPCR COMP	TCTCTTGAGCCCTACCTGTTGCTT	For quantitative RT-PCR via SYBR-Green. Target: *dnaK*.
2462	AC kpsM qPCR CODE	GGTTAACTCCTCGTCCTTTACTTGA	For quantitative RT-PCR via SYBR-Green. Target: *kpsM*.
2463	AC kpsM qPCR COMP	TGCCGCCGTTAGAGCTTGTCTATT	For quantitative RT-PCR via SYBR-Green. Target: *kpsM*.
2464	AC katA qPCR CODE	TCAACAGTAGCAGGTGAAGCAGGT	For quantitative RT-PCR via SYBR-Green. Target: *katA*.
2465	AC katA qPCR COMP	ATCGCGGATGAAGAATGTCGGAGT	For quantitative RT-PCR via SYBR-Green. Target: *katA*.

TABLE A.2.2 Oligonucleotides used in CHAPTER THREE.

Oligo Ref. No	Name	Sequence 5'-3' (Restriction sites bolded)	Purpose / Notes
6409	AC purF CODE	GCAAAGTGCTAGTGAAGTGATGCC	For insertion of *purF* and flanking sequence into pGEM-T.
6410	AC purF COMP	CCAATCGCCGATCAAAGTCGTTCT	For insertion of *purF* and flanking sequence into pGEM-T.
6411	AC purF InvCOMP	ACAC**GGTACC**CTGCACACATTTTAAATTCCTAAAAAAT	Introduces *KpnI* for ligation to resistance cassette.
6412	AC purF InvCODE	ACAC**TCTAGA**CTCAAAGCATAGGCGATGAAAGG	Introduces *XbaI* for ligation to resistance cassette.
6413	AC apt CODE	GCATTAGGCGGAAGATTAATCGGG	For insertion of *apt* and flanking sequence into pGEM-T.
6414	AC apt COMP	AGTGATTGATGCCCAAACCCAAGC	For insertion of *apt* and flanking sequence into pGEM-T.
6415	AC apt InvCOMP	ACAC**GGTACC**CATAATAATGCCTCGATTTTTGCTTC	Introduces *KpnI* for ligation to resistance cassette.
6416	AC apt InvCODE	ACAC**GGATCC**GTGTTTTAGAAATTTAAAACTATAGAAAGG	Introduces *BamHI* for ligation to resistance cassette.
6417	AC purF SEQ CODE	GGCTTAGCAAGCAAGAAGCA	For amplification/sequencing of *purF* from 96 single colonies.
6418	AC purF SEQ COMP	TGCAAGTGCAACCTTGCCTAATCC	For amplification/sequencing of *purF* from 96 single colonies.
6419	AC apt SEQ CODE	CAGACCTTACATCTTTAAGAACTAGAA	For amplification/sequencing of *apt* from 96 single colonies.
6420	AC apt SEQ COMP	GCTAGATCTTTGTATTGGTAAAGT	For amplification/sequencing of *apt* from 96 single colonies.
0790	AC prsA SEQ CODE	ATATAAGCTTTTTAAATTTACAGCAG	For amplification/sequencing of *prsA* from 96 single colonies.
0791	AC prsA SEQ COMP	ATATGTTTTTTGTTTCTTTAAGTAGC	For amplification/sequencing of *prsA* from 96 single colonies.
2775	AC apt-operon CODE	ACAC**CAATTG**AAGCACACTTCACTAAAAGCTTC	For complementation of mutant alleles. Introduces an *MfeI* site upstream of the promoter of the first gene in the *apt* operon.
2776	AC apt-operon COMP	ACAC**GGATCC**CTCAAGTTCTATTGCAAGCGTAG	For complementation of mutant alleles. Introduces a *BamHI* site upstream of the promoter of the first gene in the *apt* operon.
2777	AC purF-operon CODE	ACAC**CAATTG**GCTATAAAAGTTCTACCAAATACCG	For complementation of mutant alleles. Introduces an *MfeI* site upstream of the promoter of the first gene in the *purF* operon.

Oligo Ref. No	Name	Sequence 5'-3' (Restriction sites bolded)	Purpose / Notes
9439	AC purF-operon COMP#2	ACAC**GGATCC**TCAAAATATAAATGTAGGAAGTGC	For complementation of mutant alleles. Introduces a *Bam*HI site upstream of the promoter of the first gene in the *purF* operon.
3812	AC RBSapt-astA CODE	ACAC**TCTAGA**CGAGGCATTATTATGAGACTTAGCAAAAC	For reporter fusion. Introduces an XbaI site, and the WT *apt* RBS in context with *astA*. Cloned into pRRA.
3813	AC RBSapt15-astA CODE	ACAC**TCTAGA**CGAAGCATTATTATGAGACTTAGCAAAAC	For reporter fusion. Introduces an *Xba*I site, and the *apt*15 mutant RBS in context with *astA*. Cloned into pRRA.
3814	AC astA COMP	ACAC**CAATTG**TTATTGTTATTTTTTAGGATTGAATGC	For reporter fusion. Introduces an *Mfe*I site after *astA*. Cloned into pRRA.
1413	AC AmpSEQ purF CODE	CGATTAAAATCGCTATTTGGCTTAG	To generate *purF* amplicon for Illumina sequencing.
1414	AC AmpSEQ purF COMP	TATAAATGTAGGAAGTGCAAGTGC	To generate *purF* amplicon for Illumina sequencing.
1415	AC AmpSEQ apt CODE	AAGAACTTAATAAAATCAAAGCAGACC	To generate *apt* amplicon for Illumina sequencing.
1416	AC AmpSEQ apt COMP	ATATAAGCTAGATCTTTGTATTGGTAAAG	To generate *apt* amplicon for Illumina sequencing.
1417	AC AmpSEQ prsA CODE	AGCTTTTTAAATTTACAGCAGTTTTTAAC	To generate *prsA* amplicon for Illumina sequencing.
1418	AC AmpSEQ prsA COMP	AATATATGTTTTTTGTTTCTTTAAGTAGC	To generate *prsA* amplicon for Illumina sequencing.
2351	AC purF Biotin-TEG 350 CODE	/5BiotinTEG/<u>CAAAAA</u>**CTGCAG**ATGTGTGCAGTTGTAGGAG	Biotinylated oligo to create probe for protein pulldown. Contains *Pst*I site for elution from streptavidin, and a <u>spacer</u> region.
2352	AC purF 350 COMP	TGAATAAGTCTTGATCTTACCTCTTC	To create probe for protein pulldown.
2353	AC prsA 350 CODE	ATGCGAGGTTATAAAATTTTTTCAG	To create probe to clear DNA binding proteins prior to pulldown with the biotinylated probe.
2354	AC prsA 350 COMP	TGAATCAAATTAGCCACAAGTTTAG	To create probe to clear DNA binding proteins prior to pulldown with the biotinylated probe.
0540	AC Cj1132c FlkCODE	GTCTTTTAAGGGTAGGGCATAG	For introduction of *cj1132c* and flanking regions in pGEM-T.
0541	AC Cj1132c FlkCOMP	AATAGCGTCAAATTTTTCTCTCTC	For introduction of *cj1132c* and flanking regions in pGEM-T.
0542	AC Cj1132c InvCOMP	ACAC**GGTACC**TATAACCTTCATTTTTTGCCATTTTTAACC	Introduces *Kpn*I for ligation to resistance cassette.
0543	AC Cj1132c	ACAC**TCTAGA**AGTGAAATTTCAAAAGT	Introduces *Xba*I for ligation to

Oligo Ref. No	Name	Sequence 5'-3' (Restriction sites bolded)	Purpose / Notes
	InvCODE	TCGATCTTAAG	resistance cassette.
8168	AC Cj1132 pRRCODE	ACAC**TCTAGA**GTCTTTTAAGGGTAGGG CATAG	For complementation of mutant. Introduces an *Xba*I site upstream of the promoter of *cj1132c*. Cloned into pRRH.
8169	AC Cj1132 pRRCOMP	ACAC**GGATCC**CACCACCGCTAATAAGA ATTTTC	For complementation of mutant. Introduces a *Bam*HI site at the end of *cj1132c*. Cloned into pRRH.

TABLE A.2.3 Oligonucleotides used in CHAPTER FOUR.

Oligo Ref. No	Name	Sequence 5'-3' (Restriction sites bolded)	Purpose / Notes
1413	AC AmpSEQ purF CODE	CGATTAAAATCGCTATTTGGCTTAG	To generate *purF* amplicon for Illumina sequencing.
1414	AC AmpSEQ purF COMP	TATAAATGTAGGAAGTGCAAGTGC	To generate *purF* amplicon for Illumina sequencing.
1415	AC AmpSEQ apt CODE	AAGAACTTAATAAAATCAAAGCAGACC	To generate *apt* amplicon for Illumina sequencing.
1416	AC AmpSEQ apt COMP	ATATAAGCTAGATCTTTGTATTGGTAAAG	To generate *apt* amplicon for Illumina sequencing.
1417	AC AmpSEQ prsA CODE	AGCTTTTTAAATTTACAGCAGTTTTTAAC	To generate *prsA* amplicon for Illumina sequencing.
1418	AC AmpSEQ prsA COMP	AATATATGTTTTTTGTTTCTTTAAGTAGC	To generate *prsA* amplicon for Illumina sequencing.
6417	AC purF SEQ CODE	GGCTTAGCAAGCAAGAAGCA	For amplification/sequencing of *purF* from 96 single colonies.
6418	AC purF SEQ COMP	TGCAAGTGCAACCTTGCCTAATCC	For amplification/sequencing of *purF* from 96 single colonies.
3212	AC Cj1534c (364-)CODE	ACAC**GGTACCTCTAGA**TCTTCACGAACTTTTAAACGCTC	For amplification of *dps* promoter for insertion into pRY112. Restriction sites: *Kpn*I, *Xba*I.
3213	AC Cj1534c(-RBS)COMP	ACAC**CTCGAGCCCGGG**<u>ACTCC</u>TTTTTTTAATTTTTAAAATTA	For amplification of *dps* promoter for insertion into pRY112. Restriction sites: *Xho*I, *Sma*I. Other: <u>RBS</u>.
3214	AC RFPCODE	ACAC**CCCGGG**ATGGCTTCCTCCGAAGACG	For amplification of mRFP for insertion into pRY112-Pdps. Restriction sites: *Sma*I.
3215	AC RFPCOMP	ACAC**ACTAGTCAATTG**TTATTAAGCACCGGTGGAGTGA	For amplification of mRFP for insertion into pRY112-Pdps. Restriction sites: *Spe*I, *Mfe*I.

213

TABLE A.2.4 Oligonucleotides used in CHAPTER FIVE.

Oligo Ref. No	Name	Sequence 5'-3' (Restriction sites bolded)	Purpose / Notes
5712	AC Cj1533c FlkCODE	AAAAAACTCAATGAAGCAGCAG	For introduction of *cj1533c* and flanking regions into pGEM-T.
5713	AC Cj1533 FlkCOMP	TTTTTGGAGAATGGACTTGGG	For introduction of *cj1533c* and flanking regions into pGEM-T.
5714	AC Cj1533c InvCOMP	ACAC**GGTACC**TTTTTACCACAAAATCGTGGG	Introduces *Kpn*I for ligation of *cj1533c* deletion construct to resistance cassette. Also for DIG-labeled probe generation.
5715	AC Cj1533c InvCODE	ACAC**TCTAGA**TTTATCACTCTTTCAAGCGAGG	Introduces *Xba*I for ligation of *cj1533c* deletion construct to resistance cassette.
8610	AC Cj1533c 75CODE	ACAC**TCTAGA**GCAAAATGTAATTTAAGGGGCT	For complementation of Δcj1533c in gene-insertional plasmid with *Xba*I.
8613	AC Cj1533c COMP	ACAC**CAATTG**AAACAACACCTAAAATCCAAGTG	For complementation of Δcj1533c in gene-insertional plasmid with *Mfe*I
4382	AC Cj1533c EPTrunc	ACAC**CAATTG**CGATCAGTTTTTTCAATTCCGGT	For complementation of Δcj1533c with putative sRNA in gene-insertional plasmid with *Mfe*I
3523	AC Cj1533c-HIS pET28a	ACAC**CTCGAG**AAATCCAAGTGAAAATTTATCAAAAGATATG	For protein purification with *Xho*I site for introduction into pET28a.
7208	AC Cj1533c-HIS pET28a.1	ACAC**CCATGG**GCAAAGTACTTAATTTTTTTTATGAAAACC	For protein purification with *Nco*I site for introduction into pET28a.
2429	AC cj1534c FlkCODE	ACTATGCACGCTTTAATCGC	For introduction of *dps* and flanking regions into pGEM-T.
2430	AC cj1534c FlkCOMP	TTTCATTCAGAAAATCAGCAAGTC	For introduction of *dps* and flanking regions into pGEM-T.
2431	AC cj1534c InvCOMP	ACAC**GGTACC**TTGTAACTGACATGATTGACTCC	Introduces *Kpn*I for ligation of *dps* deletion construct to resistance cassette.KpnI
2432	AC cj1534c InvCODE	ACAC**TCTAGA**GTAATTTAAGGGGCTTTATGCC	Introduces *Xba*I for ligation of *dps* deletion construct to resistance cassette. Also for DIG-labeled probe generation.
5711	AC fur flkCODE	TTAGTTTTTTGTGTAGCAAGAATCG	For introduction of *fur* and flanking regions into pGEM-T.

Oligo Ref. No	Name	Sequence 5'-3' (Restriction sites bolded)	Purpose / Notes
5712	AC fur FlkCOMP	TTGTATCCTCATCTTCAATGTTTGC	For introduction of *fur* and flanking regions into pGEM-T.
5713	AC fur invCOMP	ACAC**GGTACC**CACATTTTCTATCAGCATATCACTC	Introduces *Kpn*I for ligation of *fur* deletion construct to resistance cassette.
5714	AC fur invCODE	ACAC**GGATCC**TGATTGTAATAATCAAAAAGCAAAGG	Introduces *Bam*HI for ligation of *fur* deletion construct to resistance cassette.
5715	AC perR flkCODE	TTGAACATGGAAAAACAAGTGAGG	For introduction of *perR* and flanking regions into pGEM-T.
5716	AC perR flkCOMP	TCTTTCCTATAATCTTTTTTCGAGC	For introduction of *perR* and flanking regions into pGEM-T.
5717	AC perR invCOMP	ACAC**GGTACC**TAATTCCATTTTATTTATTCCTTGC	Introduces *Kpn*I for ligation of *perR* deletion construct to resistance cassette.
5718	AC perR invCODE	ACAC**GGATCC**AAAAGTGTCATTAAGCAAAATAAGG	Introduces *Bam*HI for ligation of *perR* deletion construct to resistance cassette.
2435	AC Cj1534c cDNA	ATTACAAATGCAAGCAGATGCTC	For detection of *dps-cj1533c* polycistron.
2436	AC cj1533c cDNA	CCTCGCTTGAAAGAGTGATAAA	For detection of *dps-cj1533c* polycistron.
6185	AC sRNA-cj1533c-CODE	TTTTGAAATTTGATTTTTTCTTTC	For generation of sRNA probe.
6186	AC sRNA-cj1533c-COMP	TCCTTTTTTTAAAGGATAAAATTGAAAG	For generation of sRNA probe.
8881	AC Cj1533c 75CODEpRY112	ACAC**GGTACC**GCAAAATGTAATTTAAGGGGCT	For introduction of cj1533c into pRY112 with *Kpn*I. Used for error-prone PCR.
8882	AC Cj1533c COMP pRY112	ACAC**TCTAGA**AAACAACACCTAAAATCCAAGTG	For introduction of cj1533c into pRY112 with *Xba*I. Used for error-prone PCR.
9223	AC K40A-K41A SDM COMP	AAAAATAAGTGTAGCAGCACCACAAATCGTGGGCC	For site-directed mutagenesis of the *cj1533c* complement.
9224	AC K40A-K41A SDM CODE	GGCCCACGATTTTGTGGTGCTGCTACACTTATTTTT	For site-directed mutagenesis of the *cj1533c* complement.
7633	AC atpF CODE	TC**GGGCCC**AAGATGAAATAAAAAAATTAAAACAAA	For introduction of the *atpF'* promoter into pRY112 with *Apa*I site.
7634	AC atpF COMP	TC**CTCGAG**ATAGTAGCAAGCATTATGGAAGGAT	For introduction of the *atpF'* promoter into pRY112 with *Xho*I site.
9438	AC 0379 CODE	AC**CCCGGG**ATTTTTCTTAATAAGGATAG	For introduction of *cosR* into

Oligo Ref. No	Name	Sequence 5'-3' (Restriction sites bolded)	Purpose / Notes
		AACAAATGAGAATTTTAGG	pRY112-*atpF'* with *Eco*RV/*Sma*I.
9434	AC 0379 COMP	AC**CTGCAG**CACCGAAGGTGCAAAATTGTTAAGA	For introduction of *cosR* into pRY112-*atpF'* with *Pst*I.

TABLE A.2.5 Oligonucleotides used in CHAPTER SIX.

Oligo Ref. No	Name	Sequence 5'-3' (Restriction sites underlined)	Purpose / Notes
5631	AC hygCODE	ACACCAATTGGGTACCCGGGTGACTAACTAGGA GGAATAA**ATGACACAAGAATCCCTGTTAC**	*aph*(7''), sense, start codon changed to ATG. *Mfe*I, *Kpn*I, *Sma*I
5632	AC hygCOMP	GTGTGCATGCCTGCAGCATATGTCTAGAGGATC CCCGGGTCATTATTCCCTCCAGGTA**TCAGGCGC CGGGGGCGGTGTCC**	*aph*(7''), antisense. *Sma*I, *Bam*HI, *Xba*I, *Nde*I, *Pst*I, *Sph*I
5633	AC aacCODE	ACACCAATTGGGTACCCGGGTGACTAACTAGGA GGAATAA**ATGCAATACGAATGGCGAAAAG**	*aac*(3)IV, sense, start codon changed to ATG. *Mfe*I, *Kpn*I, *Sma*I
5634	AC aacCOMP	GTGTGCATGCCTGCAGCATATGTCTAGAGGATC CCCGGGTCATTATTCCCTCCAGGTA**TCAGCCAA TCGACTGGCGAGCG**	*aac*(3)IV, antisense. *Sma*I, *Bam*HI, *Xba*I, *Nde*I, *Pst*I, *Sph*I
5705	AC pRRC InvCOMP	ACACGGTACCTCCTCCGTAAATTCCGATTTG	pRRC *cat,* antisense. *Kpn*I
5706	AC pRRC InvCODE	TGGATGAATTACAAGACTTGCTG	pRRC *cat,* sense.
5707	AC astA FlkCODE	TATAGGCGAACCAAAAAATCC	Flanking *astA,* sense.
5708	AC astA FlkCOMP	AAATGTAAATTTGGAAAAGCTTCTC	Flanking *astA,* antisense.
5709	AC astA InvCOMP	ACACGGTACCGATCAATCCTTTAAAATTATTTA A	5'-internal *astA,* antisense. *Kpn*I
5710	AC astA InvCODE	ACACTCTAGACAATAAGCCCAAAAATAAATTTG G	3'-internal *astA,* sense. *Xba*I
0688	AC pRRXastA-P CODE	ACACTCTAGATAAAGGATTGATCATGAGACTTA G	Promoterless *astA,* sense. For polycistronic expression. *Xba*I
0689	AC pRRXastA COMP	ACACCAATTGATAAGCCCAAATTTATTTTTGGG C	*astA,* antisense. For polycistronic expression. *Mfe*I
0690	AC pRRXastA-P CODE	ACACTCTAGATAAAGGATTGATCATGAGACTTA G	Promoterless *astA,* sense. For reverse expression. *Mfe*I
0691	AC pRRXastA COMP	ACACCAATTGATAAGCCCAAATTTATTTTTGGG C	*astA,* antisense. For reverse expression. *Xba*I.
0692	AC pRRXastA+P CODE	ACACTCTAGATATAGGCGAACCAAAAAATCC	Upstream *astA,* sense. For reverse expression. *Mfe*I.

APPENDIX A.3 ADDITIONAL METHODS AND MATERIALS

A.3.1 SILAC labeling of *C. jejuni*

C. jejuni Δ*argH* auxotroph was metabolically labeled with either 400uM L-arginine (Sigma-Aldrich, Oakville, ON) for "light" or $^{13}C_6^{15}N_4$ L-Arginine (Cambridge Isotope Laboratories, Andover, MA) for "heavy" in modified DMEM (Lys/Arg -/-) media containing 4500 mg/L glucose, 4 mM L-glutamine (ThermoFisher Scientific) supplemented with added 20mM glutamine and 10uM iron ascorbate). Cells were grown overnight in SILAC media and subcultured (OD 1.0) into fresh media for 4 hours prior to harvesting to ensure complete labeling. *C. jejuni* was lysed on ice with 0.4 mg mL^{-1} lysozyme within 50 mM Tris pH 8.0, 150 mM NaCl, 0.1 mM Triton X-100 containing Complete protease inhibitor cocktail without EDTA (Roche). Lysates were pre-cleared at 16,000 x g. for 10 min prior to affinity purification.

A.3.2 DNA affinity chromatography experiments

These modified procedures were based on published supplemental methodology (216). Biotinylated *purF* dsDNA bearing a spacer sequence (5'CAAAA3' at the sense strand) followed by a PstI restriction site (5'CTGCAG3') (~5 mg) was diluted in buffer DW (20 mM Tris-HCl, pH 8.0, 2 M NaCl, 0.5 mM EDTA, 0.03% NP-40) to give a final volume of 0.4 ml and incubated (rotary wheel, 3 hours, room temperature) with 100 mg of agarose-streptavidin bead resin (Invitrogen) equilibrated with two washes (0.4 ml each) of TE buffer containing 0.01 % (v/v) NP40 and two washes of buffer DW (0.75 ml each). After the binding step the beads were washed 1X time in 0.4 ml TE (containing 0.02 % NP40), 3X in 0.4 ml DW buffer, and re-suspended in 0.1 ml of buffer DW. Beads-dsDNA were next incubated for 1 hour in 1 mL blocking buffer (20 mM HEPES, pH 7.9, 0.05 mg/ml BSA, 0.05 mg/ml glycogen, 0.3 M KCl, 0.02 % NP40, 2.5 mM

DTT, 5 mg/ml polyvinylpyrrolidone) at RT on a rotary wheel using. Blocking buffer was removed by washing with 1 ml of 1x restriction endonuclease buffer (New England Biolabs buffer 3) containing 0.02 % NP40 and two times with 2.67 ml buffer G (20 mM Tris-HCl, pH 7.3, 10 % (v/v) glycerol, 0.1 M KCl, 0.2 mM EDTA, 10 mM potassium glutamate, 0.04 % NP40, 2 mM DTT, Complete Protease Inhibitors).

Pre-cleared lysates (~10 mg/ml) were adjusted to 10 mM potassium glutamate and diluted with one volume of buffer G and separately subjected to a pre-clearing step (one hour, rotating wheel, 4°C) employing agarose-streptavidin beads (washed with TE/0.02% NP40, buffer DW and equilibrated in buffer G) at a final concentration of 100 mg/ml.

The beads were removed and the differentially labeled extracts were mixed separately with the blocked *purF* probe and the control DNA (5 mg of amplified *prsA* DNA) beads at a final concentration of 100 mg/ml, followed by incubation (3 hr, rotating wheel, 4°C,). Beads were recovered, washed 4X with buffer G (1.8 ml each) and one wash (0.5 ml) with restriction endonuclease buffer (NEB buffer 3; adjusted to 0.02% (v/v) NP40, 2.5% (v/v) glycerol, 1 mM DTT, Complete protease inhibitors). The probe and control beads were combined in 0.5 mL restriction endonuclease buffer, and 15 ul of PstI was added (New England Biolabs) for 1 hr incubation at 25°C.

A.3.3 ArgC digestion of peptides

Eluted samples were then precipitated in 5 volumes of ethanol within 50 mM $NaCH_3COO$ and 20ug glycogen/ml overnight. The resulting precipitation was solubilized in 6 M urea, 2 M thiourea, 40 mM NH_4HCO_3 and reduced for one hour with 10mM Dithiothreitol (DTT) followed by alkylated with 25mM iodoacetamide for one hour in the absence of light. Excess IAA was removed by

the addition of 100 mM DTT and samples incubated for a further hour prior to digestion. Samples were diluted 5-fold with ArgC digestion buffer (50mM Tris-HCl pH 8.0, 10mM $CaCl_2$, 5mM EDTA, 50mM DTT) and digested with 2ug of ArgC overnight at 25°C. Digestion was terminated with the addition of 1% trifluoroacetic acid and peptide digests were purified using C_{18} EMPORE (Sigma-Aldrich) Stop And Go Extraction (STAGE) tips (397).

A.3.4 Identification of peptides using reversed-phase LC-MS

Purified peptides were resuspended in Buffer A (0.5% acetic acid) and analyzed on a two-column EASY-nLC1000 system set up coupled to a Q-exactive (Thermo Scientific, San Jose CA). Samples were loaded onto a trap column, an in-house packed 2 cm, 100 μm inner diameter, 360 μm outer diameter column containing Aqua 5 μm C18 (Phenomenex, Torrance, CA), at 5 μL/min prior to gradient separation on a packed in-house 30 cm, 75 μm inner diameter, 360 μm outer diameter, ReproSil – Pur C_{18} AQ 1.9μm (Dr. Maisch, Ammerbuch-Entringen, Germany) at 250 nL/min. A 180 min gradient was run from 0% buffer B (80% ACN, 0.5% acetic acid) to 32% B over 140 min, then from 32% B to 40% B in the next 5 min, then increased to 100% B over 2.5 min period, held at 100% B for 2.5 min, and then dropped to 0% B for another 20 min. The instrument were operated using Xcalibur v2.2 (Thermo Scientific) with a capillary temperature of 250°C using a top 10 data-dependent approach switching between MS (resolution 70k, AGC target of $1x10^6$), and HCD MS-MS events (resolution 17.5k AGC target of $1x10^6$ with a maximum injection time of 60ms, NCE 28 with 20% stepping).

A.3.5 SILAC peptide data analysis

MaxQuant (v1.3.0.5)(217) was used for identification and quantification of the resulting experiments, with the resulting two biological replicates searched

together to ensure a global false discovery rate of less than 1% in accordance with the to the work of Schaab *et al* (398). Database searching was carried out against the NCBI *C. jejuni* 81-176 database (Accession: PRJNA58503, downloaded 27/08/ 2013) (total 1758 protein sequences) with the following search parameters: carbamidomethylation of cysteine as a fixed modification; oxidation of methionine, acetylation of protein N-terminal ArgC/P cleavage with a maximum of 2 missed cleavages. A multiplicity of two was used, with each multiplicity denoting one of the SILAC amino acid combinations (light and heavy respectively). The precursor mass tolerance was set to 7 ppm and MS/MS tolerance 20 ppm in with a maximum false discovery rate of 1.0% set for protein identifications. The resulting protein group output was processed within the Perseus (v1.2.0.17) analysis environment to remove reverse matches and common proteins contaminates prior to analysis and calculate the Significant B values with a Benjamini-Hochberg false discovery rate of 0.05.